PART 1: EMPLOYING CONVENTIONAL DEFOAMER EMULSIONS TO ENHANCE THE FLOTATION REMOVAL OF FLEXOGRAPHIC NEWS INKS

PART 2: SINGLE FIBER MODIFICATION VIA THE ADDITION OF EXOGENOUS EXPANSIN

A Dissertation

Presented to

The Academic Faculty

by

Greg DeLozier

In Partial Fulfillment

Of the Requirements for the Degree
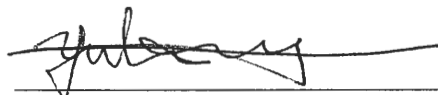
Doctor of Philosophy in Paper Science

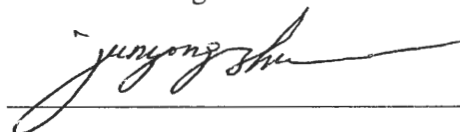Institute of Paper Science and Technology

December, 2003

PART 1: EMPLOYING CONVENTIONAL DEFOAMER EMULSIONS TO ENHANCE THE FLOTATION REMOVAL OF FLEXOGRAPHIC NEWS INKS

PART 2: SINGLE FIBER MODIFICATION VIA THE ADDITION OF EXOGENOUS EXPANSIN
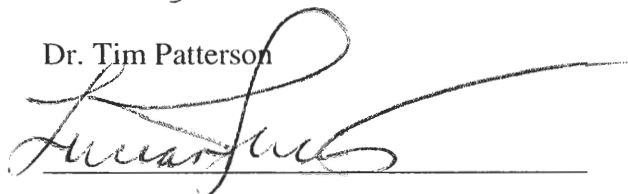
Approved by:

Dr. Yulin Deng

Dr. J.Y. Zhu

Dr. David White

Dr. Tim Patterson

Dr. Lucian Lucia

Date Approved 4/6/04

ACKNOWLEDGEMENT

To simply thank my wife, Esther, for understanding the late nights, weekends and "holidays" that were unceremoniously sacrificed over the past four years of this dissertation would be analogous to an award-winning actor expressing gratitude to a producer for simply "fronting the money" for his film. Unlike the producer, she was drafted on more than one occasion as a source of cheap labor during particularly intensive (i.e. tedious and/or grimy) phases of the investigation. For her continuous support, contribution and understanding, I am extremely fortunate and grateful.

Dr. Yulin Deng, in addition to providing a constant sounding-board for my thought or idea of the moment, was always able to challenge me with the "next step" of my research. His ability to seamlessly shift from a discussion into the fundamentals of calcium carbonate precipitation to my initial highly-speculative mechanisms of flexographic ink collection ensured that my research remained on track and with a clear goal. As if his advisor-role was not enough, ultimately, Dr. Deng would provide the lead that would cement the beginning of my career in the industry. My gratitude to Dr. Deng for facilitating both my academic and career ambitions cannot be overstated.

TABLE OF CONTENTS

LIST OF FIGURES

LIST OF EQUATIONS

SUMMARY

Paper mills will adjust, ink manufacturers will advance, pressrooms will adopt and, unfortunately, recycling mills must adapt. Variation in paper grades, inks and printing processes, designed to meet industry specifications, customer expectations, environmental considerations and economic sustainability, is reflected in the quality and heterogeneity of waste paper channeled back into recycling operations. In most instances, design and optimization of novel printing techniques, ink chemistries and substrate are pursued with minimal concern for the recyclability of a final product. Development of fiber reconditioning technology (e.g. secondary fiber modification, novel deinking chemistries, etc.) capable of contending with an inherently difficult component of a secondary fiber-containing furnish is usually initiated only upon recognition the problem. This system of retrospective innovation has, out of necessity, become an acceptable pattern within the fiber recovery industry.

This thesis documents the conceptualization, development and assessment of two separate mechanisms to facilitate the recycling of wastepaper resources. The first approach documents and attempts to elucidate the mechanism by which colloidally-stable flexographic ink particles are effectively "floated" away from the fiber fraction by incorporating a commercial defoamer within an aerated pulp. In the second phase, the ability of an exogenously applied protein to recover virgin fiber attributes within secondary fiber is quantified. Neither technology is expected to necessitate investment of extensive capital and either, when optimized, can be considered an environmentally-friendly and/or a more efficient alternative to current deinking systems.

GENERAL INTRODUCTION

Paper mills can expect to produce more, pressrooms can expect to print more and, unfortunately, recycling mills can expect to receive more. As paper grades and printing processes evolve to meet industry specifications, customer expectations, environmental considerations and economic sustainability, the adjustment is reflected in the quality and heterogeneity of waste paper channeled back into recycling operations. In most instances, the development and optimization of novel printing techniques, ink chemistries and substrate is pursued with minimal concern for the recyclability of a final product incorporating one or more of the "advances". Development of fiber reconditioning technology (e.g. secondary fiber modification, novel deinking chemistries, etc.) capable of contending with an inherently difficult component of a secondary fiber-containing furnish is usually initiated only upon recognition the problem. This system of retrospective innovation has, out of necessity, become an accepted pattern within the industry. Although industrial chemical suppliers are content to introduce new products on an annual basis, their ability to consistently provide effective solutions to the problems at hand is beginning to flag in the face of increasingly variable printed paper wastes.

This thesis was initiated in an attempt to envision, develop and provide assessment of two separate mechanisms to facilitate the recycling of wastepaper resources. The initial approach documents and attempts to elucidate the mechanism by which colloidally-stable flexographic ink particles are effectively "floated" away from the fiber fraction by incorporating a commercial defoamer within an aerated pulp. In the

second phase, the ability of an exogenously applied protein to recover virgin fiber attributes within secondary fiber is quantified. Neither technology is expected to necessitate investment of extensive capital and either, when optimized, can be considered an environmentally-friendly and/or a more efficient alternative to current deinking systems. Due to the exclusivity of each approach and the specific grade of waste paper for which the technology is intended, separate introductions and backgrounds are provided for each.

INTRODUCTION TO DEINKING FLEXOGRAPHIC ONP

The intransigence of dispersed flexographic ink to conventional alkaline flotation deinking operations is well-documented within the fiber recovery industry. In addition to diminutive sizes that preclude adhesion at the air bubble surface, dispersed flexographic ink particles are characterized by remarkable electrosteric colloidal stabilities that resist the formation of more floatable aggregates[1].

In an effort to maintain required brightness levels in recovered pulp, recycling operations must exercise vigilance to ensure that the feed stream contains extremely small percentages of flexographically printed material ($\leq$5%)[2]. Most flexographic printing of newspapers is confined to North America, Italy and England[3]. However, within these countries, conversion to flexo printing is anticipated to increase as photopolymer plates become more accessible and affordable. In fact, in late 2002, News International, the UK-based publisher of such wide circulation dailies as The Sun, The News of the World and The Times, was assessing the feasibility of flexography within its pressrooms (paperloop.com).

Numerous attempts to improve the floatability of flexo ink with varying degrees of success are described within current literature. One particularly promising approach involves neutral or slightly acidic flotation of the pulp followed by a traditional alkaline flotation stage[4] [5]. Unionized flexo ink is effectively removed during the former stage while oil-based offset inks are preferentially floated during the latter. Unfortunately, this two-pronged approach would appear to necessitate significant modification to existing operations.

Revision of traditional flotation chemistry appears to be a more popular means to augment flexo flotation. Addition of polymeric flexo "collectors"[6][7], flexo adsorbing organoclays[8][9][10], and lignosulphonates[11] to the pulper and/or flotation cell have been purported to enhance ink removal. A hybrid technology employing both equipment modification and novel chemistry may exploit the benefits afforded by both.

Surfactant spray deinking technology was recently patented as an economical means to moderate the substantial loss of fiber and water during conventional operations[12]. The technique involves delivery of the frothing agent onto the surface of the active cell rather than pre-mixed with the pulp prior to flotation. The concentration of the frother at the surface of the cell minimizes instances in which fiber hydrophilicity and contaminant hydrophobicity are compromised through nonspecific adsorption of amphiphilic frothing agent. Although not as detrimental as physical entrainment, such interactions contribute to the amount of floated fiber within reject streams[13][14]. With furnishes composed of oil-based offset ONP and OMG, surfactant spray flotation has been shown to significantly reduce fiber loss, water loss and frother consumption while maintaining brightness gain levels comparable to those obtained through conventional flotation.

Unfortunately, like conventional flotation, pulp brightness using surfactant spray technology is adversely affected when the percentage of flexo ONP within the feed exceeds 5%. However, under the proper conditions, a siloxane-based defoaming agent was found to boost flotation deinking efficiency of furnishes comprised of 100% flexo

ONP. Such technology may enable flotation deinking operations to increase the proportion of flexographically-printed material within their feed.

This latter phase of the thesis begins with the confirmation of this phenomenon within laboratory flotation trials. In addition, a series of subsequent experiments conducted to elucidate the fundamental mechanisms leading to the flotation of flexo by this system are presented

LITERATURE REVIEW – DEINKING FLEXOGRAPHIC ONP

OVERVIEW

Before attempting to define the intransigency of flexographically-printed old newsprint (ONP) to conventional deinking procedures, the deinking procedures themselves as well as the specific inks for which they have been developed will be provided. To this end, the review begins with comparison between the more traditional offset news inks and the relatively new flexographic news inks. Since the interactions between an ink and the actual newsprint influences, to a large extent, the dispersion behavior of ink particles within the pulper, paper-ink interactions will be summarized following the descriptions of the oil-based and flexographic inks. Next, an abbreviated review of the principles of flotation deinking will facilitate conceptualization of specific factors that contribute to efficient ink removal. Initially, the concept of flotation deinking will be introduced with respect to oil-based inks. A fundamental understanding of the physicochemical mechanisms involved will allow an appreciation of the basic premise of a recently patented variation of traditional flotation chemistry, surfactant spray deinking, to be elaborated in the subsequent section.

The review will conclude by presenting the rationale behind the intransigence of flexographic ink to removal through either of the aforementioned flotation technologies. The physicochemical and morphological attributes of a typical dispersed flexographic ink particle will be conveyed with the objective of defining the associated colloidal stability and exemption from flotation. This final section of the literature

review will include a synopsis of recent technologies developed to contend with flexographic ink within mills incorporating flotation deinking operations.

OFFSET LITHOGRAPHY

Although flexography is predicted to emerge in the coming decade as the premier technique for printing newsprint, lithography or offset printing is currently the most common printing procedure. Approximately 41% of uncoated paper is printed by offset lithography. This equates to a large amount of offset printed newsprint being produced and eventually contributing to waste paper reserves annually[15].

Offset lithography exploits the incompatible interactions between hydrophobic oil-based ink and water to form an image that may be transferred to a substrate. The surface of the printing plate or roller consists of hydrophilic, non-image regions that are covered with a thin film of water. Small amounts of isopropanol or alkyd resins may be included within the water to lower the surface tension and allow the aqueous film to spread across the hydrophilic surface. Ink transferred to the roller or plate will immediately confine itself to the hydrophobic, image regions of the surface. In this fashion, the separation of ink and water will form an image on the surface of the plate. The image is subsequently transferred to a second rubber-coated plate or roll. In a basic system, the rubber coat or blanket, bearing the reverse inked image, contacts the paper surface and transfers the image. By using a series of offset roll configurations, different layers of ink may be sequentially transferred to the moving paper web to develop colored images.

Offset inks are classified as either coldset or heatset depending on the mechanism of ink fixation to the printed surface. The common denominator of these inks is the inclusion of large amounts of hydrophobic oils during manufacture. Two primary subclasses of oil-based inks destined for newsprint applications are coldset and heatset offset inks. Coldset inks are affixed to the paper surface via penetration and evaporation phenomena whereas heatset inks, as the name implies, rely on heat-mediated polymerization for setting and adherence.

Printing inks such as offset, are composed of four basic constituents: a pigment, a binder, a vehicle and a solvent. In some instances, additives may be included for such purposes as buffering, chelating metal ions or providing biocidal effects. Black, by far the most important color within the newspaper industry, is obtained by using carbon black as a pigment. This pigment is characterized by high specific surface area (80 – 110 m^2/g) and small particle size (15 – 60 nm diameter). The actual pigment has little affinity for either the hydrophobic ink medium or the cellulosic newsprint. Therefore a binder molecule is included to complex with the pigment to form a stable colloid within the ink and anchor the pigment to the surface of the newsprint sheet upon printing.

The binder in coldset inks prepared for newsprint is usually a hydrocarbon resin or oil (e.g. napthenic petroleum oils)[16] whereas alkyd resins are the most widely employed binder system in heatset-offset litho printing applications. Alkyd resins may also be found within coldset news inks but usually at much smaller quantities. Coldset inks contain 0.2 to 0.6% binder which comprises 20 to 60% of heatset inks[17][18].

Alkyd resins are produced through esterification reactions between natural fatty acid triglycerides (e.g. soy derived oil) with polyhydric alcohols (e.g. glycerol) and polyacids (e.g. dibasic phtalic acid)[18]. The ultimate resin structure can be easily engineered in the polymer molecule by varying reactant species and quantity. Therefore, alkyd resins can be designed for optimal printing performance within any number of ink formulations. Fortunately, the wide variety of resins available to the offset ink manufacturer does not present an equal number of problems to the recycler[a].

Another notable difference between the inks is the type of vehicle employed. Coldset offset inks contain extremely small quantities of drying vegetable oils and resins (0.5-2.5% and 0.2-0.6% respectively). The primary ink vehicle in coldset ink is low viscosity mineral oil (70-84%). Heatset inks are based upon slightly more expensive drying vegetable oil vehicles. Vegetable oil vehicles are prepared through esterification of 16 and 18 carbon fatty acid chains of various degrees of saturation to glycerols. These semi-drying triglyceride oils, in addition to providing a supporting medium for the pigment-binder complexes, may also chemically interact with the resin binder during affixation of ink to the paper surface. Offset ink vehicles are, in turn, dispersed in a mineral oil solvent to complete the liquid ink formation. An easily discernable difference between vegetable oil-based inks and mineral oil-based inks is

---

[a] Although the presence of certain resin chemistries has been linked with enhancing the severity of the "summer effect" in aged ONP furnishes.

the final appearance of the printed material. Images printed with vegetable oil-based inks exhibit greater gloss and color intensity than mineral oil-based images.

The exact amount and chemistry of each component within the ink depends upon the anticipated end-use requirements of the ultimate product. Newspapers have relatively short lifetimes as a printed medium. Therefore, there is a tendency to use inexpensive, low-quality inks rather than those used to print more permanent papers. These inks tend to contain small percentages of expensive binders (e.g. alkyd resin) and vehicles (e.g. vegetable oil) and relatively large amounts of pigment. Fortunately, these inks are also more amenable to removal via flotation.

Offset Ink-Paper Interaction

Effective offset ink transfer is a function of phase separation and selective absorption of one of the phases. Since ink mobility in the z-direction is only significant at the point of contact with the blanket[19], the separation of phases should be as rapid as possible to minimize pigment penetration into the fiber matrix. Pigments within the paper, rather than located at the surface, cannot contribute to overall print quality. The other extreme condition involves excessively slow or incomplete phase separation that also leads to poor quality print that may rub off or remain sticky and damage downstream conversion equipment. The lower viscosity phase containing the solvent and the vehicle is designed to rapidly penetrate the porous newsprint via capillary action. This causes the less mobile pigment and binder complexes to remain at the paper surface and form an extremely viscous substance. This viscosity limits but does not completely eliminate lateral migration of the ink across the paper surface. Ink remaining

at the surface contributes to the ultimate type or image. At this point, most coldset offset newspapers printed today are considered ready for circulation. Some low rub newsprint inks, contain slightly elevated levels of alkyd resins and unsaturated vegetable oils, undergo post-print oxidative polymerization. This allows some amount of mechanical affixation to the paper surface.

In heatset-offset lithography, ink is transferred to the paper surface in an identical fashion to the coldset version. However, the mechanism of ink affixation to the fiber surface is the main difference between the two ink types. As mentioned previously, coldset ink dries by rapid penetration of the ink vehicle into the fiber web leaving pigment and binder at the surface. Although penetration of the vehicle into the fiber web occurs during heatset offset printing as well, the printed image must be subjected to a post-print thermal "curing" event.

Raising the temperature of the printed sheet is essential for drying the vegetable oil vehicle and alkyd binder to the paper surface. In addition, the heat promotes polymerization between the oils and the binder as double bonds are oxidized and cross-linked. The resulting three-dimensional matrix anchors pigment to paper components either by chemical bridging or by physical entrapment[20].

Chemical interactions between ink components and the cellulosic substrata of newsprint are few and not expected to contribute to print permanency. Carboxylic acid constituents within certain resin binders have been postulated to interact with basic constituents within cellulose[21]. However, inks intended for newsprint are often characterized by very low amounts of these particular polar resins. Since the

hydrophobic, hydrocarbon ink vehicles of newsprint offset inks are relatively incompatible with cellulosic surfaces[6], the primary means of offset ink affixation to the cellulose surface will be through van der Waals intermolecular forces. This may account for the exceptional adherence to groundwood furnish of newsprint in which lignin and extractive content may augment hydrocarbon/fiber interactions.

FLEXOGRAPHY

Flexographic printing can be loosely considered a modernized version of traditional letterpress printing. Like letterpress, flexography utilizes a raised surface bearing the image and/or print to be transferred to a specific substrate. Extending the similarity between the two processes, both tend to require a water-based ink incorporating certain rheological properties that favor rapid and complete transfer during printing operations. The primary difference between the two printing techniques lies in the image-bearing plate. While the standard letterpress plate can range from moveable type to light-sensitive photopolymer into which the image is laser-etched, the basic geometry remains that of a two-dimensional slab that impacts the entirety of the substrate as a single unit. Expectedly, the process is relatively slow and is typically reserved for printing books and other materials for which print-quality and longevity are of paramount importance. Flexography, however, requires that the image-bearing plate be wrapped around a cylinder. During a printing run, a series of rollers and doctor blades continuously meter ink onto the raised surfaces on one side of the cylinder while the opposite side continuously impacts upon and transfers the ink to a web-fed substrate racing through the press nip. The advantage of this technology over letterpress resides

13

in the sheer quantity of material that may be printed in a short time. This quality has proven particularly attractive to the house-hold consumables industry in which a constant supply of labeled packages, bags, boxes and similar image-bearing containers is essential.

One of the most attractive qualities of flexographic printing within the packaging industry is the capacity for efficiently transferring ink to a wide range of substrates (e.g. metal foils, coated and uncoated board, polymeric films, etc.) with little or no loss of print quality. Other benefits purportedly correlated with flexographic printing, besides being a more environmentally-sound procedure, include superior print and image quality, greater image permanence and relatively easy equipment clean-up. Inevitably, the adaptability, productivity and print quality inherent to the technology will lead to newsroom conversions from traditional lithography to flexography.

Flexographic Inks

Flexographic ink composition is relatively devoid of the complexity required within oil-based inks. Flexographic inks are characterized as water-based due to the aqueous nature of their vehicles. Replacing the volatile solvents inherent to offset ink formulations with water serves to limit the quantity of VOC emissions from the pressroom[22].

Carbon black pigment particles are aggregated and stabilized within the alkaline aqueous phase by adsorbed polymeric binders containing ionizable acrylic functional groups[1]. The high pH required to promote dispersion of the pigment-binder complexes

is obtained by adding an amine such as ammonia to the vehicle. Although closely guarded as proprietary compounds, a generic chemical structure of a polyelectrolyte binder may include styrene and vinyl acetate monomers. These unionizable monomers provide the main constituents of the binder backbone. The presence of ionizable monomers such as acrylate and methacrylate, imparts colloid stabilizing capacity to the binder.

Flexographic Ink-Paper Interactions

When taking into account all of the steps that must occur for an oil-based offset ink to properly "set" onto the paper surface, the interaction between flexographic ink and the paper surface appears relatively simple. Transfer of the ink to the paper is straightforward and once on the paper, "setting" of the ink occurs rapidly. This partially accounts for the small amount of material that a flexographic printer must generate before the mass-printed image meets customer standards. Conversely, offset print jobs often produce significant amounts of substandard material before the ink transfer produces an acceptable image. These abbreviated "ramp-up" periods are one of the factors driving the conversion from offset to flexography.

Upon transfer to the paper, evaporation of the aqueous alkaline flexographic ink vehicle triggers protonation of the ionized acrylic moieties. The corresponding reduction of stabilizing charged groups leads to precipitation of the binder onto the fiber. Noncovalent interactions between the cellulosic surface and the film forming monomers of the binder backbone (e.g. styrene and/or vinyl acetate) effectively affix the binder-pigment aggregate to the paper. This chemical "anchoring" of the pigment to

the fiber surface prevents rubbing of the ink from the surface. Ink removal during rubbing is more prevalent with oil-based offset inks since these tend to deposit pigment at the paper surface as a consequence of simple phase separation rather than actual chemical affixation. Since the rate of vehicle evaporation is often greater than that from offset inks, the pigment-binder complexes will not penetrate as deeply into the fiber web thereby leaving significantly more pigment at the paper surface. The resulting image quality is yet another advantageous facet of flexographic printing. In addition, immediate "setting" of the ink precludes lateral migration across the paper surface and preserves print and image clarity.

FLOTATION DEINKING

Overview

Ink removal from printed waste paper is generally considered a two-stage process. In the first stage, the ink particles are detached from the fibrous substrate and dispersed into an aqueous bulk phase. This phase is conducted largely within the pulper unit. The second stage involves the selective separation and removal of ink contaminants from the actual fiber. Technologies incorporating forced aeration of the ink-containing pulp, or flotation, are currently operating world-wide and provide this second phase of deinking. The following review of deinking operations that include flotation will be based on a furnish composed of the more traditional offset printed ONP.

Pulping

Disintegration of waste paper within a batch or drum pulper provides enough mechanical shear and turbulence to account for most of the ink detachment that will occur throughout the entire deinking process. Bennington *et al* have associated ink detachment with three mechanical forces: fiber-rotor interactions, interfiber friction, and fiber-medium interactions[23]. It is worth noting that these defined interactions are unique to batch pulpers. The increasingly popular drum pulpers are expected to possess a slightly different set of interactions (i.e. fiber-rotor interactions will be absent while interfiber friction-based interactions are expected to dominate).

The final quality of the deinked pulp depends largely upon the ability of the pulper to separate ink from fiber. If a combination of ink and/or substrate variables precludes detachment of an ink particle from the fiber under a defined set of operating conditions within the pulper, the remainder of the deinking regime will be incapable of completing ink removal resulting in a inferior recovered furnish. This inevitably leads to increased bleach usage and/or the addition of dyes or brighteners to counteract the decreased brightness. Factors that must be considered when optimizing a specific pulper to contend with the furnish on hand are presented below. Again, these factors and the relation of each to ink detachment proficiency within the pulper are discussed within the framework of oil-based inks. These conditions, considered capable of being optimized for efficient removal of offset inks do not necessarily pertain to water-based inks or toners.

Pulper Chemistry

An area of constant debate within the literature concerns the contribution of individual chemical components to actual detachment of affixed ink within the pulper. With exceptions, three chemical additives provide the foundation of a pulper cocktail designed to facilitate detachment of ink particles from the fiber: sodium hydroxide, sodium silicate, and hydrogen peroxide. An additional fourth component is comprised of a specific surfactant or surfactant system designed to augment ink particle release from the fiber, stabilize liberated particles, aggregate dispersed particles and/or modify the surface properties of released ink particles. These four components are routinely used in deinking operations with a wide spectrum of waste paper compositions (e.g.

ONP, OMG, SC, MOW, etc.). Slight adjustments to addition levels, repulping equipment, non-chemical pulping parameters, and/or the surfactant system appear to be the only points of divergence between furnishes. The contribution of each chemical additive to repulping operation will be discussed below.

Sodium hydroxide provides essential alkali to the pulper for swelling of individual fibers. Fibers have been observed to increase in cross-sectional diameter by up to 50% in the presence of alkali[24]. Swelling of a fiber occurs as extensive hydrogen bonding within and between bonded fibers is disrupted within the alkaline environment. Hydrated fibers become more flexible and interfiber bonded area decreases to augment disintegration of the waste paper. A combination of the swelling and enhanced flexibility of the fiber physically disrupts the ink-fiber interface thereby liberating previously affixed particles. The degree to which a particular ink-fiber interface can be disrupted by alkali action alone depends upon a number of physicochemical variables inherent to specific ink-fiber interactions. For example, fiber swelling may physically disrupt the bond between an offset ink particle and the fiber surface. However, should that ink particle actually surround and/or penetrate the fiber surface, simple swelling of the interface will be less likely to liberate the particle. This physical attachment is especially problematic when attempting to remove thermoplastic toner particles from MOW furnishes.

Although NaOH is primarily seen as a pH-maintaining additive, its addition also serves to hydrolyze ester bonds within offset ink binder resins. Therefore, a small amount of alkali-mediated chemical softening of affixed ink particles may compliment

particle detachment from the fiber. In the same fashion, NaOH saponifies fatty acids often present within the surfactant component and extractives released from the pulp to provide other benefits to the deinking process. Saponification of ester bonds within triglyceride additives is a critical step in some deinking formulations.

Unfortunately, should the level of alkali become too high, the secondary furnish will have a tendency to yellow[25]. This is especially common in pulps containing significant portions of groundwood (i.e. high concentrations of lignaceous material). Therefore, it is essential that a level be selected to promote fiber swelling, ester hydrolysis and fatty acid saponification without precipitating a yellowing effect. Laboratory and mill-scale investigations have been conducted with 0.3 to 1% dry weight NaOH additions per unit weight of oven dry fiber with relatively good results[26] [27 28 29 24].

Sodium silicate is not directly involved with the liberation of ink from the fiber surface. Instead, the silicates are able to complex with detached ink particles within the pulper and prevent their redeposition onto the fiber[25]. Silicates have been suggested to provide a system buffering effect that maintains the initial pH. This effect keeps the system from alkaline environments that stimulate pulp darkening (i.e. yellowing). In addition, silicates perform a protective task by complexing with heavy metal ions that may otherwise inactivate hydrogen peroxide. Chelating agents such as EDTA and DTPA may also be included for additional metal ion complexing. Like NaOH, silicate dosages should be optimized. Moe *et al* found that high levels of silicate addition

actually hampered deinking efficiency[28b]. Silicate addition levels within the laboratory pulper and at the mill are roughly 1 to 2.5%[26 27 28 29 30].

Peroxide addition to the repulper is primarily a proactive means of fiber bleaching. Modest levels of peroxide discourage the tendency of a pulp to yellow after exposure to alkaline conditions. In concert with peroxide, NaOH levels can be adjusted to provide a deinking favorable pH that would usually promote yellowing. High levels of peroxide can lead to increased fragmentation of the ink particle. However, by a presumed increase in system buffering capacity, silicate addition to the pulper counteracts this trend[31]. Peroxide levels within the repulper are typically between 0.3 and 3%[16 27 28 29]. It is easy to recognize the convoluted interplay that exists between these three chemical additives as a deinking system proceeds towards optimization.

Surfactant addition to the repulper is generally considered to improve the overall deinking performance of a flotation line. Surfactant systems added directly to the pulper are not generally credited with improving ink detachment form the fiber. In the stead, the surfactants serve to stabilize, disperse and modify the surface chemistry of detached ink particles. Some surfactants, however, have been implicated as being capable of directly disrupting the ink-fiber interface, effectively displacing the attached

---

[b] The exact mechanism has yet to be defined but Moe *et al* postulate that silicates may complex with calcium ions within the water thereby reducing hardness and, therefore, the tendency to form calcium soaps.

ink or softening the attached ink particle for subsequent removal by shear forces. However, most are added to the pulper primarily to facilitate downstream ink separations.

Rao *et al* suggest that non-ionic surfactants are capable of assisting the detachment of coldset offset ink particles from newsprint[27]. The mechanism appears to be a function of ink topography and the rates of ink detachment a function of surfactant penetration. Uneven ink particle topography presents a landscape of various ink projections and areas of thin ink film coverage. These are expected to quickly soften in the presence of even low levels of surfactant. This should enhance detachment rates in response to mechanical shear. Deeper, coherent layers of the ink particle are rather inaccessible to low levels of surfactant. Increased surfactant dosages displayed the ability to increase detachment rates by deeper penetration into the coherent layer. To this end, surfactant penetration into the ink particle is proposed to be the rate-determining factor behind coldset offset ink particle release.

Most newsprint deinking mills employ non-ionic surfactants as dispersants. Nonionic surfactant addition (e.g. ethoxylated linear alcohols, ethoxylated alkyl phenols, ethoxylated fatty acids, oligoethylene-oxide alkyl ether, polyethyleneoxide alkyl ether, etc.) lowers the surface tension of the repulping medium thereby increasing the wettability of ink-coated fiber. This indirectly assists in fiber swelling and the corresponding detachment of ink particles alluded to earlier. The non-ionic surfactant is proposed to solubilize the detached ink particle and create a stable emulsion that does not readily redeposit onto the fiber. Rao *et al* concluded that the nonionic surfactants

either augment particle detachment or flotation efficiency with respect to the hydrophile-lipophile balance (HLB) of the molecule[27]. He suggests that surfactants with high HLB values (more water soluble) increase brightness and that low HLB surfactants (with an increased capability to penetrate the hydrophobic offset ink particle) actually assist ink detachment from the fiber. Accordingly, Pirttinen and Stenius found the size and geometry of detached ink particles to be directly influenced by the dosage of non-ionic surfactant[24]. High surfactant concentrations encourage fragmentation of large ink particles. This may be a function of ink penetration into affixed ink particles as put forth by Rao *et al*[27c]. However, Moe *et al* question the value of the hydrophilization of the ink particle with a non-ionic surfactant[28]. According to these researchers, providing the ink particle with a hydrophilic surface chemistry as the surfactant adsorbs will adversely affect favorable interactions with hydrophobic calcium soap complexes and result in poor flotation efficiency.

Fatty acids are often employed as collector chemicals due to their ability to form ink-affinitive soaps with calcium ions. These 16 to 18 carbon chain amphoteric molecules are produced during NaOH-mediated ester hydrolysis (i.e. saponification) of triglyceride additives. The acidic end groups readily complex with calcium ions present within the repulper to form calcium soap precipitates. These soaps will eventually associate with detached ink particles thereby rendering them hydrophobic. Additional

----

[c] Ink penetration is, expected to be inversely related to the HLB of the non-ionic surfactant and directly related to the amount of non-ionic surfactant added.

calcium ions within the repulping medium contribute to charge neutralization of the ink particles. These ink-soap complexes will heterocoagulate with similar complexes and can ultimately form ink particle aggregates within the floatable size range. However, the overall size of the heterocoagulated aggregate is a function of the shearing forces present within the repulper. These forces serve to disrupt larger aggregates and, thereby, establish an average particle size within a particular system. This fatty acid-calcium soap system is considered to be the most prevalent collector system in industry today and most commercially available deinking agents are founded upon this chemistry.

An emulsion of fatty acid and non-ionic surfactant has been implicated by Haynes as the most effective means of ink detachment and protection against redeposition within the repulper[32]. The Norske Skog Skogn DIP mill in Norway has operated successfully with a mixture of fatty acids and ethoxylated fatty acids added directly to their drum repulpers[28]. However, the efficiency of surfactant addition, either as soap, fatty acids, non-ionic surfactants or a combination thereof, is likely to be as variable between recovery operations as the material they process.

Water Hardness

Although the full influence of calcium ion concentration within process waters of a deinking mill is not appreciated until the flotation stage (i.e. the formation of calcium-fatty acid soap collectors), water hardness within the repulper may directly influence ink particle detachment and fragmentation. Røring *et al* found high calcium ion concentrations to encourage ink particle fragmentation under standard alkali conditions within the repulper[31]. The justification for this phenomenon appears to lie

within interfiber shearing interactions. High calcium ion concentration was found to reduce fiber swelling. Therefore, ink particle detachment was prone to occur by fragmentation of the ink from the fiber surface rather than release as a complete, large particle. Silicates, through a complexation reaction, appear to counteract water hardness-mediated fragmentation. However, the addition level should not be extreme to avoid adversely affecting the formation of calcium-fatty acid soaps and the subsequent collection of dispersed ink particles.

pH

Clearly, maintaining an optimal pH within the pulping unit is essential for maximum fiber swelling and the consequent ink detachment. The sodium hydroxide component, in concert with the silicate, is responsible for raising the pH to acceptable levels. A pH between 8 and 10 is considered appropriate to promote optimal swelling and, when applicable, complete fatty acid saponification. In addition to disrupting hydrogen bonds within the fiber wall and within interfiber bonded area, the alkaline environment promotes ionization of organic acids on the surface of ink particles and hydrolysis of ester bonds within the resin binders and ink vehicles. As a result, ink particles become more dispersible, soluble, flexible and more susceptible to detachment in response to shearing forces.

Temperature

Temperature within the pulper affects a number of the interactions responsible for ink detachment. The extensive hydrogen bonding within and between fiber is

rapidly hydrated at higher temperatures. In addition, the resulting increase in the thermal energy of the system augments disruption of instances of chemical bonding between ink and the fiber surface. Elevated pulper temperatures approaching the T_g of certain polymeric ink constituents (e.g. synthetic resin binders) may soften the ink particles thereby rendering them more liable to shear-mediated detachment without fragmentation. However, should the temperature become too high, these same ink particles may assume a tacky, viscous consistency that readily redeposits onto the fiber or is fragmented into unfloatable dimensions. High temperatures may also solubilize certain chemicals within the incoming waste stock that may adversely affect downstream flotation efficiency. Laboratory scale and mill pulpers generally operate at 40 to 60°C to minimize detriments caused by temperature extremes[16 25 29 32].

Retention Time

The actual time that the printed waste remains within the repulper has a rather significant influence on detached particle size distribution and geometry as well as the degree of actual ink detachment. Generally, longer retention times within the pulper generate smaller liberated ink particles in response to the increased mechanical action. Short pulping times avoid promoting comminution of liberated ink particles. Pirttinen and Stenius proposed that the greatest amount of coldset offset ink detachment occurs within the first ten minutes of repulping[24]. Additional mechanical activity beyond this time results in increased ink particle fragmentation. Consequently, high temperatures and brief retention periods within the repulper generate free ink particles that appear highly amenable to downstream flotation operations[32].

Detached Particle Dimensions

The shape and size distribution of detached ink particles is primarily determined within the pulper. Particles released from the fiber have specific volumes and shapes. Particle dimensions are dictated by the specific combination of ink chemistry, thermal exposure and the intensity and duration of mechanical agitation within the repulper. Water-based flexographic inks are notoriously difficult to remove on account of extremely small, liberated pigmented particles ($< 1\mu m$) either redepositing on or within a fiber or resisting removal by flotation. On the other hand, ink particles may assume shapes (e.g. plates) that also disfavor removal by flotation through increased drag. Other inks may not release fiber within the repulper but rather physically retain fiber or fiber fragments (also difficult to remove by flotation and contribute to fiber loss when they are effectively separated). Fortunately, coldset offset ink particles tend to possess a size distribution, shape and release pattern that promote efficient deinking.

The size and geometry of ink particles detached within the repulper are intimately linked with the efficiency of subsequent ink removal operations. Washers, cleaners, screens and flotation cells have individual requirements for maximum ink particle separation from the fiber. The pulper is burdened with the task of detaching ink particles from the fiber in a size and shape preferred by downstream operations.

PRE-FLOTATION

After the pulping stage, the furnish is submitted to a series of high density cleaners and coarse screens designed to remove heavier contraries (e.g. staples, glass,

etc.) and less dense but significantly large particles (e.g. shives, plastic, etc.), respectively. To avoid large losses of yield across the coarse screens, the rejected streams may be subjected to secondary and tertiary screens to recover fiber. Shearing forces generated within these particular units are mild compared to the pulper. However, one can imagine that some detachment and/or fragmentation of ink occurs as the slurry is subjected to hydrodynamic shear due to centrifugal forces within cleaners and spontaneous acceleration behind screen foils. As the slurry exits these pre-flotation stages, ink detachment from the fiber is presumed to be complete. This finite degree of detachment represents the deinking operation's best effort to detach ink from the fiber prior to flotation.

FLOTATION

Overview

Flotation deinking technology has emerged as the premier technique for ink removal from OMG and ONP grades. Practical understanding of the actual chemiphysicomechanical phenomena that serve as the foundation of the flotation deinking process is essential before disparities between deinking offset-printed ONP and deinking flexographically-printed can be highlighted and addressed. To this end, relevant components of this particular stage of the deinking process will be discussed in more depth.

Although the mechanical agitation of the repulper liberates ink from the fiber, the ink particles largely remain within the pulp throughout washing and screening.

Therefore, the flotation cells must efficiently remove large volumes of dispersed ink particles in a spectrum of configurations and dimensions. Flotation technology exploits divergent physicochemical properties of the various components of a hydrated secondary pulp to selectively separate fiber from contaminants. In brief, air bubbles are percolated upwards through an ink-containing furnish. Under the proper conditions, dispersed ink particles and aggregates tend to collect at the liquid-air interface of the rising bubbles. The air bubble then transports the attached ink to the surface of the flotation unit. Eventually, a stable foam, comprised of the air bubbles and entrained ink particles is created at the surface of the flotation cell. This foam serves to retain "floated" ink particles at the cell surface and is subsequently skimmed to effectively separate contaminant from furnish. Although this procedure appears relatively straightforward, there are numerous factors within a particular system that can influence the efficacy of any or all of the essential steps toward successful ink flotation. Fortunately, dispersed oil-based ink particles tend to possess a combination of surface chemistries and morphologies that favors flotation with minimal or no modification of the above stages.

Dispersed Oil-Based Ink Particles

Once liberated from the fiber surface, an ink particle may be treated as an individual entity with a unique set of physico-chemical properties. Since the newly dispersed oil-based ink particle will almost never consist of a single particle of carbon black pigment, the term "entity" is used here to describe an agglomerated body of numerous pigment particles held together via the polymeric binder resins and residual

oil vehicles employed during their manufacture. Although some sources of surface charge may exist (e.g. from organic acids that have avoided complete oxidation during the combustion-derived preparation of the pigment) on the carbon black, these do not contribute significantly to the overall charge of the ink particle. In the stead, within the alkaline environment experienced within the repulper, acidic functional groups within the aforementioned binder resins tend to ionize and are implicated as the primary source of dispersed ink particle surface charge[33]. However, even with total dissociation of all ionizable components, the surface of the offset ink particle will remain somewhat hydrophobic on account of the presence of residual oil vehicle. This slight hydrophobicity tends to destabilize offset inks released from the fiber during repulping. Ideally, thermodynamic forces will promote aggregation of the destabilized ink particles. However, total colloidal destabilization is prevented via the hydration of ionized surface components. By hydrophobizing the particles via chemical means, colloidal destabilization can be carried to completion and the ink particles will be drawn into agglomerated assemblies. In this manner, dispersed ink particles may be simultaneously stripped of any solubilizing surface charge and combined into aggregates with more floatable dimensions.

The hydrophobization and formation of ink-containing aggregates outlined above will be discussed within the framework of a system currently employed within world-wide flotation deinking operations. Although deinking agent manufacturers readily market their products as a generation or two beyond the simple addition of fatty

acid chemistry to the repulper, most rely, to some extent, on the undeniable ability of calcium-fatty acid soaps to effectively increase brightness across a flotation cell.

Although it has been established that a relationship exists between fatty acid and calcium ion for effective flotation deinking, the specific nature of that association has yet to be clearly elucidated. A common theme to practically all proposals is the initial conversion of sodium salts of fatty acids to calcium salts (i.e. soaps). This conversion, whether performed *in situ*, on site or at the manufacturer, involves the alkaline-mediated saponification of protonated fatty acid additives into water-soluble sodium soaps[34] [35]. The manner and site in which the sodium-fatty acid soaps interact with calcium ion to ultimately promote ink particle flocculation followed by adhesion to an air bubble remains speculative.

Over the last few decades, the fundamental mechanism behind the ability of calcium-soap to initiate ink particle aggregation and enhance flotation has been the focus of exhaustive investigation. In the interest of brevity, and since calcium-soap chemistry has not demonstrated the same proficiency with flexo ink (i.e. the focus of this thesis), the most recent, complete and reasonably accepted hypotheses will be presented.

Larsson *et al* forward a mechanism that begins with dispersive adsorption of hydrophobic carbon chains of the ionized fatty acids onto the hydrophobic regions of the oil-based ink particle[36]. Adsorption of the fatty acid onto the ink particle contributes to the anionic surface charge already in place as a consequence of ionization of ink components. At this point, the electrostatic repulsion between ink particles as well as

the colloidal stability of the individual particle will increase relative to an ink particle that has not adsorbed fatty acid. Although increasing the negative charge of the particle surface does not appear to favor enhanced floatability, it does guarantee that a significant amount of fatty acids have been retained at the particle surface. The importance of this localization becomes apparent upon the addition of calcium ion. The bivalent ion is proposed to associate with the ionized carboxylic hydrophilic regions of the adsorbed fatty acids thereby serving the dual purpose of neutralizing or reducing the anionic surface charge of the ink particle and forming a water-insoluble calcium-fatty acid soap that precipitates back onto the particle surface. In either case, the colloidal stability of the particle is compromised leading to the formation of aggregates of ink and calcium-soap. The collective hydrophobicity of this complex may readily adhere to a passing air bubble for transport to the cell surface.

Another mechanism postulated by Putz *et al* is also dependent upon the adsorption of the hydrophobic alkyl portion of the ionized fatty acid to the hydrophobic ink particle regions[37]. In addition to associating with the ink particle, excess, ionized fatty acid will adsorb at the air-water interface of a bubble. The molecule should orient itself so that the hydrophobic carbon chain terminus is protruding into the air phase while the hydrophilic region remains solvated within the bulk aqueous phase. Instead of serving as a "charge-neutralizing" agent, dissolved calcium ions are suggested to form a bridge between hydrophilic fatty-acid carboxylic groups at the particle surface and those located at the air bubble surface. This sort of "indirect" association of an ink particle or aggregate with the air bubble through calcium ion-bridging has been

contemplated in earlier attempts to define the ink-electrolyte-air bubble interaction but this particular mechanism discounts the contribution of particle charge to colloidal stability. In the stead, ink particle adhesion to a passing air bubble is simply a function of the adsorption of fatty acid.

By whatever means that aggregation and/or hydrophobization of dispersed ink particles occurs in the presence of calcium ion and fatty acid, the requisite that the two be present is obvious. Subsequent ink interactions with air bubbles within the aerated pulp are heavily influenced by the final particle shape, size and surface chemistry imparted by the association with calcium-fatty acid soap precipitates.

Ink-Air Bubble Collision, Adhesion, Retention and Removal

For the most part, a dispersed ink particle or an agglomeration of ink particles has little affinity for a passing air bubble. An air bubble rising through an aqueous medium is characterized by fluid streamlines established as liquid flows around the bubble's periphery. These "streamlines" effectively provide a boundary between an ink particle and the actual air-liquid interface of the bubble surface. For ink-bubble contact to occur, the particle must be large enough and possess the inertia to penetrate this barrier rather than follow the flow lines around the bubble. Overly fragmented oil-based inks and submicron water based inks are unlikely to possess the kinetic energy to cross the boundary layer and therefore must be "collected" or aggregated into larger particle agglomerates. Offset ink particles in the size-range from 10 to 150 μm have been accepted as the most floatable of the dispersed ink species.

The ability to penetrate the boundary layer represents only one of the two obstacles to successful air bubble-ink interactions. Although containing significant residue of the hydrophobic oil vehicle, offset ink particles may still undergo surface ionization upon dispersion in alkaline medium. In addition to carboxyl units on the carbon black pigment itself, binders retained within the ink aggregate will ionize and contribute to the overall solubilizing surface charge. This charge provides the particle some amount of colloidal stability and this stability, in turn, resists physical interactions with the air-liquid interface of the bubble. Fortunately, dispersed offset ink particles retain a significant portion of hydrophobic surface area for interaction with the alkyl chains of fatty acids. Simply precipitating the adsorbed fatty acids with calcium ion and/or neutralizing the slight surface charge of the ink particle with calcium ion is sufficient to generate the entropic driving force behind air bubble-ink particle interactions.

Once in contact with the air-liquid interface, actual adhesion of the ink particle to the passing bubble is not guaranteed. Should the particle remain largely within the aqueous phase with relatively little projecting into the air phase, hydrodynamic shearing forces within the former phase may dislodge the particle before it can be transported to the flotation unit surface. Calcium ion bridging interactions between fatty acid carboxylate groups adsorbed at the particle surface and their counterparts adsorbed at the air bubble surface may provide a certain amount of resistance to shear-mediated detachment. However, actual adsorption into the interface is presumed to physically isolate the particle from the shearing forces.

To increase the instances of ink-air bubble collisions that result in successful ink particle adhesion, more air bubbles may be percolated through the recovered pulp. By reducing the average bubble diameter while maintaining a constant rate of air flow into the flotation cell, the total interfacial surface area available for interaction with dispersed ink particles may be increased. A 1:6 ink aggregate-air bubble ratio has been forwarded as optimal for successful interaction[34]. Care must be taken to ensure that the air bubble size does not become too small to avoid nonselective floating of valuable furnish components such as fines and filler[d]. In either case, the goal is to maximize the number of productive collisions so as to ultimately remove the most amount of ink from the fiber fraction as possible.

At the surface of the aerated cell, an ink particle-air bubble complex is incorporated within a layer of foam comprised of similar bubbles. This layer should be sufficiently stable to isolate the ink particle from the bulk phase within the cell to avoid allowing the particle to return to the pulp. The entrained, floated ink is then removed via the action of rotor-mounted paddles pushing the foam towards a weir or vacuum suction at the cell surface.

------

[d] Dissolved air flotation exploits the tendency for extremely small bubbles to float practically every colloid-sized particle suspended within an aqueous medium. This technology finds extensive use within water-reclamation and treatment operations.

POST-FLOTATION

Accepts from the flotation portion of the deinking line are then subjected to any variation of forward and reverse cleaners and fine screens. The cleaners are designed to centrifugally separate furnish components through density dissimilarities. The screens provide a physical boundary consisting of minute slots engineered to permit the passage of fibers and fines while rejecting larger particles (e.g. glass, large ink particles, stickies, etc.). After this phase of "cleaning", the pulp may then be passed through a gamut of disc thickeners, deckers, and/or screw presses to concentrate the pulp into a pad and thereby remove a large portion of the supporting medium in which dispersed ink particles may still remain. This thickened pulp represents the culmination of the collective effort of the individual units comprising the deinking line. Since the pulp may then be subjected to bleaching chemistry to meet a final mill determined target brightness, the efficiency of the deinking operation should be evaluated upstream from this point.

DEINKING OF FLEXOGRAPHIC NEWSPRINT

Dispersed Flexo Ink Particles

For all the purported benefits that may be obtained by substituting flexography for lithography in the pressroom, the presence of flexo-printed material within the feed to flotation deinking operations can only be considered detrimental to deinking efficiency and, ultimately, end-product quality. Unlike oil-based offset inks that are largely released from the fiber surface through the concerted action of mechanical

shearing forces and interfacial swelling, flexo inks are released from the fiber surface via ionization of the associated binder under alkaline pulping conditions. The resultant colloidally-stable flexo ink particles tend to have similar characteristics to the carbon black and binder agglomerate found in fresh, unprinted flexographic ink. That is to say, the pigments are provided colloidal stability through the hydration of ionized moieties of the adsorbed carboxylated binder. In addition, the ionized binder confers electrostatic repulsion between individual ink particles thereby ensuring that larger aggregates will not form. An additional steric component to colloidal stabilization of dispersed flexo ink particles has also been identified as the "loops" and "tails" of the adsorbed polymeric binder disfavor direct particle-particle contact[1] [38]. This "electrosteric" stabilization of the dispersed flexo ink particle under alkaline conditions ensures that liberated particles will have a high surface charge combined with a submicron aggregate diameter. These are both properties found to effectively diminish the removal efficiency of a contaminant through flotation.

The importance of particle size during flotation deinking cannot be overstated. Larger particles such as dispersed oil-based inks within the size range of 10 to 150 microns are considered amenable to first required instances for effective flotation: the ability to penetrate the fluid flow lines established around a rising air bubble and the air-water interface of the bubble itself. Since the inertia of a rising air bubble is finite, only larger ink particles will possess sufficient mass to avoid following the slip planes around the bubble. Particles that are too large may effectively penetrate the boundary layers and even the air-liquid interface. However, the particles will be readily stripped

from the air bubble as it rises upwards through the bulk medium. Particles that are too small, regardless of their surface chemistry, will not be able to approach the air bubble surface but will assume a projective course that carries them around and away from the rising bubble. Dispersed flexo ink particles fall into this latter category and, therefore, do not satisfy even the first condition for effective flotation.

Once having penetrated the boundary established around the air bubble, the surface charge of the ink particle assumes a dominant role in the effectiveness of particle-bubble interactions. Offset ink particles are imparted with residual vehicle oil-enriched hydrophobic surface regions. To this end, the particles are amphiphilic and are readily inserted into the air-liquid interface. Unfortunately, flexo ink particles, with the ionized adsorbed binder are highly anionic and not likely to adsorb to the bubble surface even in the improbable event that they successfully navigate the fluid boundaries around the rising bubble.

Flexo in Conventional Deinking Operations

The tendency of flexo particles to be released from the fiber in sizes and with surface chemistries that do not respond to conventional flotation deinking practices is responsible for the limits most mills place on the amount of flexographic printed material within their raw feed. Mills incorporating single-loop flotation technology may be able to tolerate flexo ONP at concentrations of 5% of the total furnish but, if possible, strive to avoid the grade altogether.

The colloidal stability of flexographic ink particles liberated during alkaline pulping makes them highly susceptible to removal within wash deinking operations. Simple displacement of the dispersed ink from the fiber via washing results in the generation of an inky filtrate. Flexographic ink is subsequently separated from the filtrate through conventional dissolved air flotation and/or ultrafiltration[39 40 41 42] before the wash water may be recycled within the mill. It is not uncommon for recovered waste containing substantial amounts of flexographic print to be routed to mills employing washing technology even at the expense of increasing costs to defray any additional shipping expenses. Although the primary drawbacks of wash deinking are considered to be the loss of fiber yield across the washer units and the massive amounts of water involved in the actual washing, flexo ink presents yet another disadvantage in that it has been shown to readily redeposit onto the fiber surface during the formation of fiber mats[43]. The resultant drop in the optical qualities of the final pulp diminishes the advantage of washing technology over flotation technology when faced with significant amounts of flexo printed material within the feed furnish.

Deinking Flexo Literature

Numerous attempts to augment the efficiency of flotation operations faced with ever-increasing amounts of flexo within their feed streams are documented. At this point, a brief review of these endeavors will be provided. For simplicity, the review will begin with trials conducted with novel chemistries earmarked for enhanced flotation removal of flexo and other water-based inks and conclude with trials involving manipulation of conventional process itself.

39

Ironically, although conventional flotation deinking operations incorporating calcium-fatty acid chemistry are apparently incapable of removing dispersed water-based inks, laboratory trials have demonstrated that the resultant soap precipitates readily "collect" flexo ink particles in fiber-free suspensions. McLennan *et al* found the rate and extent of deposition on flexo ink onto precipitated soap particles to be a function of excess calcium ion in the bulk aqueous phase[44]. The spontaneous deposition appears to occur as the net surface charge of the flexo ink particles is reduced during complexation interactions with divalent calcium ion. A reduced surface charge facilitates heterocoagulation between the flexo ink and soap particles rather than through the formation of calcium ion "bridges" between the two components.

McLennan's results would appear to indicate that "collection" of flexo ink can be readily accomplished via deposition of ink onto pre-formed, precipitated calcium soap particles. Such a mechanism to concomitantly reduce the hydrophilicity of dispersed flexo and incorporate the particles into larger aggregates would appear to enhance the floatability of the water-based ink. This stands in contrast to the proposed "microencapsulation" mechanism in which precipitating calcium soap onto the surface of oil-based ink particles increases hydrophobicity and aggregate size. Although the addition of calcium alone was found to promote the aggregation of flexo particles into large, potentially floatable flocs, the loose, expanded architecture of the homocoagulates would rapidly disintegrate within the hydrodynamic conditions of an

aerated flotation unit[e]. All results provided during these trials tend to point towards effective "collection" of flexo ink via conventional calcium soap chemistry. However, this capacity is not reflected in mills incorporating similar chemistry within their flotation operations.

The discrepancies between the response of dispersed flexo ink in controlled laboratory conditions and the familiar intransigence of the ink at the industrial-scale were confirmed and investigated in a series of papers. Although indicating that flexo ink collection involves calcium soap-mediated microencapsulation rather than deposition upon pre-formed soap particles, Dorris *et al* advance the concept of efficient flexo collection using conventional calcium soap chemistry[45]. However, the assertion is made with the proviso that fiber or any similar interfering substance be absent in the aerated suspension. The authors speculate that some component of the furnish may be physically and/or chemically responsible for the inability of ink particle-calcium soap complexes to form in flotation units. In a follow-up article, Chabot *et al* were able to demonstrate that increasing the amount of fiber within a floated pulp effectively reduced the floatability of dispersed flexo ink[46]. The authors conclude that the excessive hydrodynamic conditions within the flotation unit and the physical presence of fibers adversely influence the kinetics of aggregate formation and/or microencapsulation.

---

[e] Although increasing the concentration of calcium did correspond with the formation of denser, more shear-resistant flocs, the calcium levels typically encountered in flotation deinking operations were found to promote the looser flocs.

Although system variables such as bubble size, air flow rate and impeller rotational speed were found to affect the floatability of dispersed flexo ink, the presence of fiber was determined primarily responsible for inhibiting ink-soap aggregate formation. Rather than mechanically disintegrating aggregates, the fibers, by reducing the overall turbulence within the system, may indirectly reduce the number of ink particle-ink particle and ink particle-soap particle collisions. Another possibility stems from the notion that process water entrained within a fiber floc, is relatively static. The diffusional constants of ink particles suspended within this relatively quiescent pool, both within the floc and between the floc and the aqueous bulk phase, are severely limited leading to reduced aggregation kinetics. In effect, as the density of the fibrous matrix increases, the probability of collision between ink and soap particles will decrease.

In light of the conclusions drawn from the above investigations, calcium-soap chemistry, although capable of enhancing the floatability of flexo ink particles in fiber free suspensions, is rendered ineffective in deinking mill operations involving actual pulps. To contend with the same physicochemical conditions presumed to exist within an aerated flotation unit that disrupt the formation of floatable heteroaggregates of flexo ink and soap, alternate chemistries and deinking agents have been designed.

Revision of traditional flotation chemistry appears to be a popular means to augment flexo flotation. Philippe describes a mechanism, borrowing from both micropolymer and microparticle technology, to effectively collect dispersed flexo ink[7]. The agent, defined as possessing the characteristics of dispersed flexo ink particles,

complexes in some manner with the ink. The particulate nature of the agent-ink complex confers amenability to flotation removal. Various proportions of flexographically-printed ONP within the 70:30 ONP:OMG furnish were selected to replicate expected feed compositions entering conventional flotation deinking mills. A furnish containing 30% flexo ONP was taken to represent the most extreme case. When used in concert with traditional calcium soap chemistry, the addition of the novel chemistry at the pulper was purported to enhance flexo removal at both flotation stages and at the washer units of a pilot-scale deinking operation. In addition, ash removal rates were increased and TAPPI dirt counts were reduced. These benefits were afforded with little or no impact upon the final yield of the freshly deinked pulp relative to that treated with pure calcium soap chemistry. Unfortunately, due to the proprietary nature of the product, Philippe makes no attempt to define the mechanism by which the flexo ink particles are "collected" onto the microparticle surface.

Sain *et al* adopt an empirically-rooted approach to develop a single agent capable of deinking mixed furnishes containing significant proportions of flexo-printed material[6]. During their investigations, the authors evaluate the efficacy of traditional calcium soap chemistry, alkoxylated-fatty acid collector systems and a series of four novel copolymers constructed from 2,5 furandione (i.e. maleic anhydride) and aromatic hydrocarbon monomer units. By manipulating the ratio of the polar furandione to aromatic hydrocarbon, each copolymer is imparted with a unique HLB value and acidity. The great variation in molecular mass was apparently designed into the copolymer series during synthesis. The ultimate description of the synthetic copolymers

indicated submicron particles with a narrow size distribution and furandione concentration-dependent acid-values.

From the investigation, the fatty acid-alkoxy derivatives were found to promote the flotation of flexo ink to a greater extent than calcium soap chemistry. However, the brightness gain obtained through the use of the derivatives was still not large enough to merit classification as an efficient flexo ink collector. On the other hand, the copolymer system appeared to facilitate the aggregation of dispersed flexo ink particles thereby enhancing the efficiency of the flotation separation process. A proposed mechanism for the collector-like behavior is similar to the manner in which flexo ink-calcium soap complexes form according to Dorris et al[45]. Briefly, the carboxylic acid functionalities at the surface of the copolymer particle, ionized in the alkaline conditions of the pulper, are neutralized via addition of divalent calcium ion or lowering of the pH. The particles lose solubility and begin to precipitate. Precipitation leads to heterocoagulation with similarly neutralized flexo ink particles and other aggregates of copolymer and ink. The resulting complex possesses the morphology and surface hydrophobicity that enables successful adhesion to passing air bubbles. Additional conditioning time before aeration of the flotation unit was hypothesized to allow larger aggregates to form with more shear-resistant densities. When considered within the framework of the purported factors preventing the formation of floatable calcium soap-flexo ink aggregates[45,46], the formation of floatable aggregates of copolymer and ink via the same pathway of precipitation appears questionable.

Heise *et al* found that flotation deinking of furnishes containing up to 30% flexo ONP can be effectively accomplished with a commercial deinking agent based upon organoclay technology[10]. The preparation of organoclays involves the modification of smectite-type clay particles with quarternary amines[8]. The most optimal clays are those having considerable cation exchange capacities to maximize retention of the amine upon the particle surface. By varying the composition of the amine, the organoclay may be tailored to facilitate either washing or flotation removal of water-based inks[f]. Modification of the clay particle surface can either be conducted prior to addition to the pulper or may actually be carried out *in situ* to exploit fillers and clays released from dissolved OMG coatings[9]. The deinking agent used by Heise *et al* was of the former variety. Their investigation included a closed-loop pilot-plant trial in which the organoclay additive was introduced to the pulper. To estimate the capacity of the reagent to enhance the flotation efficiency of the operation, the investigators monitored the optical quality of the recirculated process water as well as the brightness of the floated accepts. Trial results indicated that the organoclay technology was capable of enhancing the brightness of the accept stream in addition to promoting the flotation of the ash component of the furnish.

---

[f] Hydrophilic organoclays, earmarked to enhance wash deinking, may be prepared by reacting the clay with ethoxylated quarternary ammonium salts while hydrophobic clays may contain di- and trialkylated versions of the ammonium salt.

An approach to enhance the flotation removal of flexo ink using a combination of new deinking chemistry in concert with modifications to the deinking process was recently provided by Alesse *et al*[11]. Again, the furnish was prepared to replicate feed streams to Italian flotation deinking mills. To truly test the value of their approach, the investigators selected a flexographic ONP concentration of 40% of the total furnish. In addition to novel pulper chemistry, the post-flotation thickening stage included a shower of process water designed to enhance the rate and extent of displacement of dispersed flexo ink from the forming fiber mat. Rather than enhance the floatability of flexo ink, this procedure was engineered to enhance the washability of flexo ink. Of particular relevance to flexo ink, they found that the incorporation of lignosulfonate within the pulper resulted in enhanced detachment of the ink from the fiber and a reduction in redeposition of the ink back onto the fiber. This two-pronged approach of both reducing the ability of flexo ink to redeposit onto the fiber and improving the displacement of dispersed ink at the washer stage provided significant brightness gains with an 80% yield.

Continuing with the idea of restructuring the flotation process, Galland *et al*, forward the concept of a neutral stage in series with the traditional alkaline stage[4,5]. By pulping a mixed furnish containing significant amounts of flexo ONP under neutral conditions, the authors suggest that extensive ionization of the flexo ink binder can be minimized. Instead of gradual dispersion via surface ionization of the attached flexo ink particles into the aqueous phase, mechanical detachment is the primary means of particle detachment. The resultant size distribution and surface charge of flexo ink

particles released from the fiber during neutral pulping is far more favorable to flotation removal than the dispersed ink particles liberated during alkaline pulping operations.

To avoid further comminution of the flexo ink particles, neutral pulping is followed by neutral flotation. In this stage, flexo ink particles, and other sources of alkaline-induced anionicity, are preferentially floated. On account of the neutral pulping, oil-based inks largely remain attached to the fiber or are too large to effectively float. To contend with this particular component of the furnish, the floated pulp must be subjected to an ensuing alkaline flotation stage. This second flotation effectively separates the residual oil-based inks. Although expected to be capital-intensive, the two-stage approach is the most referenced method to deink mixed furnishes by flotation. Single-loop flotation mills generally do not have the luxury of modification of or addition to existing operations. In the stead, the mill may attempt to lower the pH of the available pulping and flotation stages. However, this must be accomplished while remaining attentive to the alkalinity-induced removal of oil-based inks from the fiber. In general, the amount of flexo ONP that can be tolerated by a mill running at a lower pH without adversely affecting its ability to remove conventional oil-based inks is 2-3% of the total furnish[47].

Recently, Vernac *et al* provided an overview of a concerted effort to improve the deinkability of flexographic inks[47]. Concerned parties with a vested interest in improving this particular aspect of water-based inks ranged from ink manufacturers and printers to paper manufacturers and recyclers. Two independent approaches to contend with small but potent proportions of flexo printed material within flotation operations

were investigated. In the first case, unique flexographic inks with characteristics highly amenable to conventional flotation processes were developed and assessed. The second case involved educated modification to the process and/or chemistry of existing flotation operations.

The authors summarize the first phase of the research in which two major ink manufacturers attempt to provide a deinkable flexographic ink. Although, in both cases, the formulations could not be deemed absolutely "recycler-friendly", the results of laboratory and pilot-scale flotation deinking trials were promising. According to Vernac, an ink manufacturer indicated that the primary obstacle to creation of a deinkable flexo ink formulation is the lack of commonality with chemistries considered favorable to pressroom runnability and print quality. Despite this issue, some European pressrooms are currently experimenting with the modified versions of flexographic ink.

The remainder of the paper deals with adaptation at the recycling operation end of the chain. The authors initially revisit the concept of neutral pulping as a means to limit fragmentation of flexo ink particles yet include the disclaimer that the modification comes at the expense of detachment of more conventional oil-based inks. Enhanced rates of flexo flotation obtainable via lowering the pH of the pulper and/or flotation unit are overshadowed by tempered brightness gains as a consequence of residual, undetached offset inks.

Although three separate chemistries were forwarded by the respective manufacturer for agglomerating dispersed flexo ink into floatable conformations, laboratory and pilot plant trials were not able to produce acceptable brightness gains in

pulps containing flexo ONP. These chemistries included a poly-aluminum-chloride/ aluminum soap-based collector, a series of silicates with varying ratios of SiO_2 to Na_2O, and even the aforementioned organoclay of Heise *et al*[10]. A proprietary blend of fatty acid and "surfactant" provided by one particular company did enhance the brightness of pulps containing 30% flexo ONP to within 4% of that obtained from flexo-free pulps. Unfortunately, the merit of this particular system is tempered by the concomitant increase in chemical dosage and cost. In addition the chemistry tends to adversely affect yield across the flotation unit.

Although not directly pertaining to enhancement of the floatability of flexo ink, means to improve the brightness of flotation accepts in recycle mills include process water treatments, accessory post-flotation washing stages and incorporation or modification of a post-bleaching stage. At this point, two stage flotation deinking is mentioned as a viable alternative to contend with up to 30% flexo ONP in the feed stream. However, conversion to the technology is hypothesized to incur additional yield losses and bleach requirements in addition to the initial capital expenditure.

Notwithstanding the purported benefits supported by bench- and pilot-scale trials, technologies specifically designed to contend with flexographic material within the feed furnish, whether they be of the chemical or process variety, have yet to be exploited at the industrial level. For the most part, recyclers must resign themselves to fluctuations in the quality of the incoming feed and absorb the additional costs associated with increased bleach usage with higher than average flexo ONP levels. Unfortunately, this complacency may ultimately cease to be an economically viable

option should flexography continue to be adopted within global pressrooms. To this end, the search continues for a practical solution to the deinkability issues surrounding furnishes containing flexographic news inks.

QUANTIFYING DEINKING EFFICIENCY

Overview

In order that paper manufacturers recognize and faithfully replicate products of customer-accepted brightness, standards have been developed to provide qualitative descriptions of this particular optical property. These standards have been adopted by deinking mills so that the brightness of their recovered DIP may be gauged against customer expectations. Proper measurement of brightness has traditionally been one of relativity. Samples proposed to be brighter than a control sample would be analyzed and results of that particular experiment compared. However, collating these results to those of other experiments proved impracticable due to the ambiguous nature of the measuring apparatus. Determination of brightness is relative to the illuminant, filters, apparatus, and the dimensions of the sampling aperture. Therefore, a system of analytical equipment (i.e. lamps, photocells, optic lenses and filters, and the dimensions, interior lining, and gloss traps of the sampling chamber) enabling the best reproduction of sampling conditions is necessary. Usually, a spectrophotometer is offered based on the fact that all essential components within the apparatus are standardized. Proper calibration to extreme brightness values measured by a master instrument will provide measurements comparable to reported values extraneous to the experiment at hand[48] [49] [50] [51] [52].

A general procedure to calculate a numerical value for brightness, based on TAPPI Standard T452, "Brightness of pulp, paper, and paperboard (directional reflectance at 457 nm)" requires that a sample be analyzed by a geometry of 45°/0°. This means that an illuminant will project radiation onto the sample at a 45° angle and the reflection be viewed by positioning the effective wavelength detecting photocell directly above the sample (0°). Incident light of wavelength 457 nm is reflected from the sample surface, through a filter, and detected by the photocell to provide a numerical estimate of reflectance. However, this directional approach is sensitive to machine-direction induced patterns within the paper as well as surface non-uniformities. This necessitates a large number of measurements across the sample to obtain statistical significance.

Another procedure for brightness assessment is provided by ISO Standard T 525 om-92. This method incorporates diffuse viewing geometry referred to as d/0°. The position of photocell remains in a 0° geometry relative to the sample and actively detects reflection of 457 nm light. Although initially employed to measure the brightness of pulp, accurate brightness values of paper samples may be obtained as well[50]. This value appears to be an essential one within the deinking industry. The most conspicuous component of a diffuse measuring apparatus is the hollow, lined, integrated sphere into which illumination is cast parallel to the sample. The interior of the sphere acts to diffuse the light in all directions prior to contact with the sample surface. In this manner, incident light, simulating natural illumination, will come from all directions

and surface aberrations will have negligible effect on reflection. This advantage over directional geometry enables fewer measurements of the sample to obtain statistically significant average values.

An explanation concerning the decision to use an effective wavelength of 457 nm as a standard of brightness is founded upon a user interface. Based on the fact that the human eye interprets subtle shades of blue light superimposed upon yellow as white and that a "white" paper or pulp emitting blue light is psychologically interpreted as brilliant white, brightness can be measured in terms of percent reflection of incident 457 nm blue light. In fact, brightness, according to the paper industry, is directly related to the reflectance of blue light. Higher blue light reflectance is manifested as a whiter product[50]. The degree of brightness is given a numerical value according to the absolute reflectance of blue light from the sample. For example, an ideal sample reflecting all incident light of wavelength 457 nm will have a brightness value of 1.0. If 45% of incident 457 nm radiation is absorbed, 55% will be reflected to the photocell and recorded as 0.55 (An ISO Brightness value of 55%). Although brightness values obtained in this manner may not completely account for the radiance of a paper sample, the rough estimates of absolute blue reflectance values provided when comparing pulps of similar composition are usually sufficient.

Ink particles remaining within the pulp sheet will absorb the incident light and reduce reflectance to lower brightness values. Depending upon their number, large ink particles or aggregates remaining within the pulp will decrease brightness to a certain degree. However, on a weight basis, small ink-derived particles (<10 μm), with a

greater specific surface area than large particles, will absorb more light and decrease brightness levels significantly more than large particles. ISO brightness values are generally taken from post-flotation recovered pulps but values obtained by post-repulper hyperwashed pulps may provide the deinking mill with an idea of ink particle detachment efficiency within the repulper.

Yield

Optical parameters such as brightness and ERIC values have traditionally served as the means to evaluate the efficiency of a particular deinking process. Numerous papers have been published extolling the virtues of a novel deinking chemistry and/or deinking unit design based exclusively on these values. A third parameter, neglected within these investigations, allows a more accurate appraisal of their innovations. Often considered the core of "fiber recovery" operations, ironically, the deinking process was rarely evaluated in terms of its ability to recover fiber. Recently, due to the increasing costs of both raw feed and landfill space, the impact of specific chemistries and fiber recovery procedures on the amount of fiber actually recovered (i.e. fiber yield[g]) has gained weight during process evaluations.

---

[g] This value is idealistically obtained as the ratio of oven dry fiber recovered to the amount that was initially fed into the system. The system may be as complex as an entire deinking operation from waste yard to finished product or as simple as a single flotation cell.

53

Although significantly higher yield losses can be expected with wash deinking technology, the amount of fiber within reject streams from conventional flotation deinking mills is considerable. Two separate camps of thought regarding the loss of fiber during flotation deinking exist yet are not considered to completely exclude the possibility of the other.

Figure 1 depicts the postulated mechanisms leading to fiber yield loss during conventional flotation deinking operations. Ajersch *et al* advance the concept of "hydraulic entrainment" of fiber within rising air bubbles as the dominant factor behind yield loss[14]. In this mechanism, fibers and fines are incorporated within the hydrodynamic flow patterns established around and between rising air bubbles (e.g. around and between bubbles "A" and "B" in the figure). Although the fluid dynamic drag forces generated by a single bubble are insufficient to carry a single fiber, the forces established by the upward movement of numerous bubbles readily carry fiber to the cell surface. In addition, fiber flocs in which rising air bubbles become entrapped will be lifted to the cell surface via buoyancy forces (e.g. the scenario present in the figure around air bubble "A"). At the surface, the fibers are carried along with the process water, into the lamellae of the froth. The inherent stability, structure and fluid dynamics of the froth dictate the critical amount of fiber that may be entrained. These properties are, in turn, related to pulp consistencies, gas flow rates, bubble sizes and the duration of the flotation trial. Froths characterized by large bubbles, thick interlamellar spaces and slow draining rates are more likely to entrain fiber. Conversely, froths containing smaller bubbles with thin films (ideally stabilized via direct electrostatic

repulsion between the hydrophilic end groups of the frothing agents rather than through entrainment of process water) and high rates of draining will permit entrained fibers to be washed back into the bulk slurry.
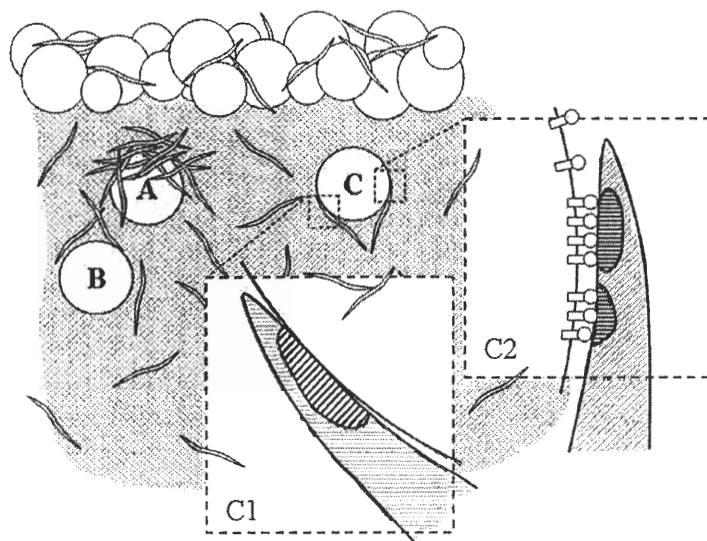
Figure 1: Postulated mechanisms leading to fiber loss during conventional deinking operations. Fibers entrained within the hydrodynamic drag currents established within and around bubbles "A" and "B" is expected to be the major contribution to yield loss. However, fiber flocs may also be lifted to the cell surface due to additional buoyancy imparted by entrapped air bubbles ("A"). Instances of true flotation of the fiber involve actual adhesion to the air-water interface (C). Adhesion may be driven through interactions with hydrophobic regions of the fiber surface (C1) or may be facilitated by the inactivation of hydrophilic regions of the fiber surface (C2) through nonspecific adsorption of surfactant (i.e. frothing agent).

The authors discount the role of true flotation (i.e. actual adhesion between the air bubble and fiber) since the high "wettability" of all fibers assayed suggests a surface hydrophilicity that does not favor air bubble-fiber interactions. To further support this claim, the investigators pretreated the pulp with sodium dodecyl sulfate to "hydrophilize" any hydrophobic regions of the fiber surface. The extremely hydrophilic

fibers, having absolutely no attraction to the air-liquid interface of a bubble, were incorporated into the froth and providing yield losses comparable to unmodified fibers.

Deng revisited the subject of yield loss during flotation deinking and was able to confirm the dominant role of entrainment[13]. However, he was also able to identify some true flotation of the wood fiber as a consequence of chemical deactivation of the fiber surface. His hypothesis is founded upon receding and advancing contact angles of fibers in aqueous solutions. The receding contact angle provides a measure of the ability of a suspended solid (e.g. wood fiber) to adhere to the air-liquid interface of a passing air bubble. A receding contact angle of zero suggests an extremely wettable, hydrophilic surface. Numerous publications have concluded that the receding contact angle of zero for a wood fiber in an aqueous solution precludes any true flotation of the fiber[14]. However, Deng points out that a definitive assessment of the physicochemical attributes of a fiber surface must also account for the advancing contact angle of the wood fiber in aqueous solution. Although supporting the notion that thermodynamically favorable adhesion between the suspended fiber and the air bubble is unlikely, he notes that the intense agitation within the aerated flotation unit may still favor bubble-fiber interactions. Collisions between the fiber and the air bubble surface may possess sufficient energy to surmount energy barriers that prohibit physical contact under more quiescent conditions. In effect, the fibers may be capable of "piercing" the air-liquid interface. Just as adhesion of a solid particle to an air-liquid interface is predicted by receding contact angles, detachment of the very same particle is a function of the advancing contact angle. With this in mind, release of the fiber from the "pierced" air

bubble becomes advancing contact angle-dependent. The portion of the fiber residing in the bulk air must be drawn back into the bulk aqueous medium for effective detachment.

At this point, the relevance of including the advancing contact angle as a means to reveal true flotation of fiber comes into play. Variations within the advancing contact angles taken from a series of both sized and unsized chemically bleached fibers and mechanically pulped secondary fibers corresponded to different rates of true flotation of the fibers. The more hydrophobic fibers (i.e. sized bleached fibers and mechanically pulped fibers) with larger advancing contact angles were prone to float more readily than the others sampled. However, under certain conditions, reducing the hydrophobicity of the fiber surface through the adsorption of surfactants reduces the advancing contact angle thereby facilitating release of the fiber from the air bubble. Deng demonstrates that the advancing contact angle is highly sensitive to a variety of surfactants typically found within deinking operations. He concludes with the suggestion that true flotation is occurring within a flotation cell but that physical entrainment remains the primary cause of fiber loss.

Loss of fiber, either via entrainment, true flotation or some combination of the two is expectedly a major concern in the European fiber recovery industry where mills employing flotation far outnumber wash deinking mills. Any technology capable of maintaining or, more favorably, increasing the optical properties of a deinked pulp while simultaneously reducing the amount of valuable fiber within the reject stream is welcome.

By plotting the brightness gain against the fiber yield loss incurred during a flotation trial, a relatively quick means to gauge deinking efficiency can be obtained from the slope of the resulting curve. **Figure 2** is a hypothetical example of two separate processes designed to float oil-based inks. "A" and "B" represent two separate collector chemistries used at manufacturer recommended dosages. Assuming that the flotation conditions, other than the chemistries, remained static, the slopes of the trend lines indicate that "B" promotes the flotation of ink with less reduction in final yield than "A". Chemistry "B" is capable of reducing the yield loss by 50% relative to chemistry "A" while maintaining a similar brightness gain. Based on these results, the most optimal chemistry for the mill would obviously be "B". This approach to determining the efficiency of the deinking process is adopted during the course of pilot flotation trials conducted during the current research.

Brightness Gain f(Yield Loss)
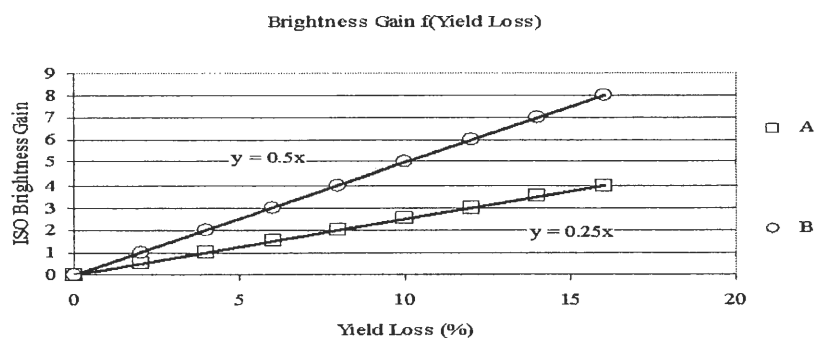
Figure 2: Evaluation of flotation deinking chemistry by assessing brightness gain as a function of fiber yield loss. The slope of the resulting trend line enables comparison between products/processes.

SURFACTANT SPRAY FLOTATION DEINKING

Fundamental Mechanism

A potential means to reduce yield loss without adversely affecting the optical qualities of the deinked pulp was recently introduced by Deng *et al*[12]. As the name implies, surfactant spray flotation deinking involves delivery of an aerosolized aqueous suspension directly onto the surface of the flotation cell. As a result, two unique but complementary mechanisms leading to a reduction in the amount of fiber entrained within the foam are envisioned.

The first mechanism involves retroactive recovery of fiber from the foam. Droplets of the aqueous spray expectedly modify the structure and stability of the foam at the surface of the cell. This ability to recover entrained fiber from froths by "washing" the foam with spray water was documented by Robertson *et al*[53]. As bubbles within the foam break and/or coalesce in response to mechanical disruption, fibers entrained within the interlamellar spaces may be returned to the underlying bulk suspension. In addition, sprayed liquid flowing downward through lower, unmodified regions of the foam may carry previously entrained fiber back into the slurry. Recovery of fiber from the foam in either of these scenarios is presumed to occur without dislodging hydrophobic oil particles actively adhering to bubbles within the foam.

The second mechanism to reduce yield loss via surfactant spray technology is preventative in nature. As described previously, chemical addition during conventional deinking operations is conducted primarily within the pulper. The major components of

the deinking agent formulation (i.e. caustic, silicate, and surfactants) are added directly to the pulper to ensure adequate mixing and contact times for optimal deinking efficiency. In practically all instances, the formulae may contain an additive(s) that promotes foam stabilization upon reaching the flotation cell. The inclusion of this particular component appears rather absolute considering that a prerequisite for efficient flotation deinking is the establishment of a stable froth layer. Most frothing agents are low molecular weight, amphiphilic compounds specifically mixed into the furnish with the sole purpose of providing foam stability. Unfortunately, through nonspecific adsorption, these agents may alter the surface chemistry of furnish components. More specifically, the hydrophobicity of ink particles (**Figure 3**) and the hydrophilicity of fines and fibers may be compromised as the frothing agent deposits onto their respective surfaces. Consequently, the probability of adhesion between ink particles and passing air bubbles will diminish while that between fibers and the air bubbles will increase.
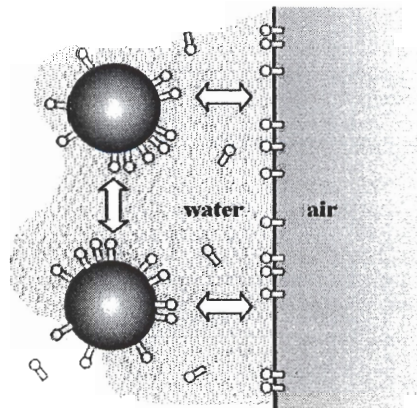
Figure 3: Nonspecific adsorption of amphiphilic surfactants onto the hydrophobic regions of suspended ink particles increases colloidal stability. The additional surface charge does not favor interactions with passing air bubbles.

60

The key premise of surfactant spray flotation deinking is the relocation of the frothing agent from the pulper to the spray (**Figure 4**). Zhu *et al* have demonstrated that surfactant delivered in this manner tends to remain at the interface between the actual froth and the aqueous pulp slurry[54]. By segregating the agent from the rest of the chemistry, instances in which the frother adsorbs onto furnish components will be limited. Ideally, ink particles carried to the surface of the cell will be subsequently entrained within a foam prepared completely from the surfactant spray. By this method, some amount of control over the consistency and volume of the froth may be maintained by adjusting the flow rate, pattern and/or consistency of the surfactant spray.
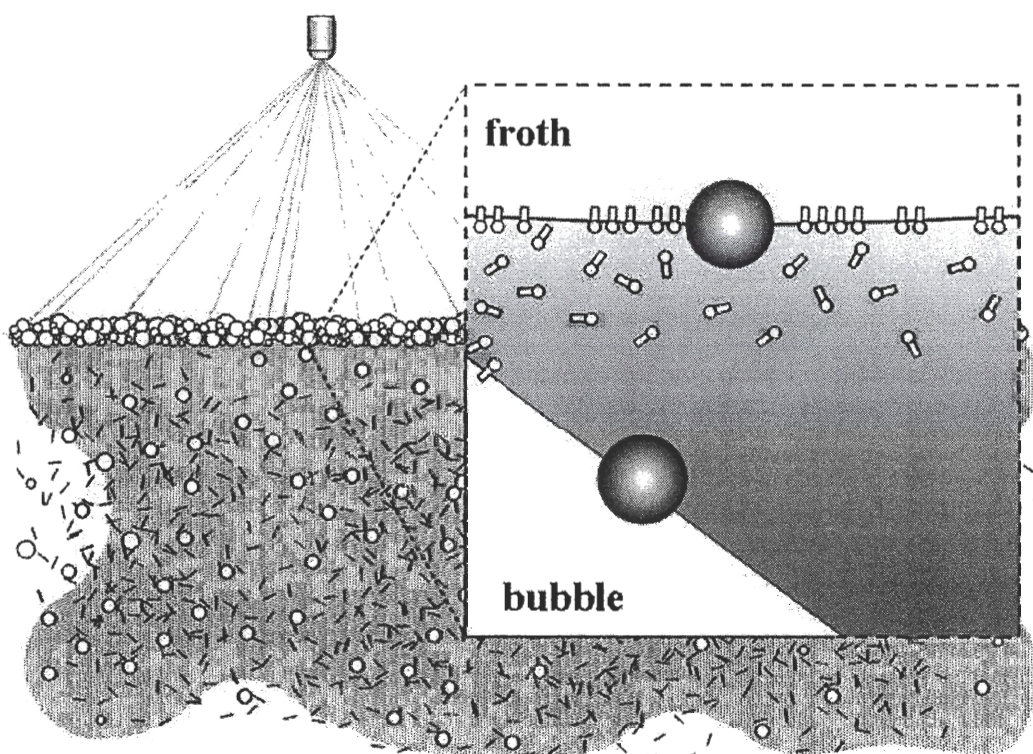
Figure 4: By delivery of frothing agent via surfactant spray, the surfactant tends to remain within the vicinity of the froth-water interface. This limits instances of nonspecific adsorption of the surfactant onto fibers and ink particles. Ink-laden bubbles are only stabilized by frothing agent upon reaching the cell surface.

In addition to reducing fiber yield loss, pilot trials incorporating spray deinking technology, indicate that a significantly smaller volume of process water is entrained within the foam. This appears to benefit flotation operations in which water loss is both environmentally and economically undesirable. Also, by concentrating frothing agent at the surface layer of the cell and thereby avoiding counterproductive, chemical consuming interactions within the bulk suspension, a much smaller amount can provide comparable foam stabilities.

Defoamer Addition

During control trials in which neither conventional frothing agents nor surfactant spray are incorporated into the flotation process, the formation of a stable foam will still be observed. Surface active agents released from either the wood fiber itself (i.e. resins, fatty acids, lignin-derived phenyl propanoids, etc.) or from other components of the repulped, printed material readily adsorb at the air-liquid interface of rising bubbles. To neutralize the self-foaming behavior of recovered furnishes, a siloxane-based defoamer may be mixed with the pulp prior to aeration. Through careful interplay between frother addition via surfactant spray and defoamer addition directly within the feed furnish, an additional element of control over the ultimate froth properties can be established.

PROBLEM ANALYSIS

In the final decade of the 20th century, flexographic printing of newsprint emerged as a practical alternative to traditional offset printing. The primary stimuli driving newspapers to adapt the novel technology were shorter start-up times, improved print quality and reduced rub-off. In addition, since flexographic inks are suspended in water rather than organic solvents, VOC emissions from the pressroom were greatly reduced. At the end of 2001, the number of global newspapers operating flexographic presses had increased to 49 and continued growth was forecast[3].

Unfortunately, the flexographic renaissance of the 90's would prove disastrous to the fiber recovery industry. Gradually, flotation deinking mills would come to realize that extremely small percentages of flexographic material within the raw feed corresponded to dramatic reductions in deinked pulp brightness. The small size and inherent colloidal stability of dispersed flexographic ink effectively resisted separation during traditional flotation operations. Initially, the relatively small number of flexographically-printed newspapers allowed the deinking mills to avoid the grade altogether. Flexo-ONP was conveniently diverted to land fills or mills outfitted with wash deinking technology. As the popularity of flexographic printing increased, flotation mills were no longer afforded the luxury of flexo-free raw feeds. Instead, fiber recovery operations merely absorbed the additional bleaching costs required to maintain a target brightness when processing small amounts of flexo in the feed stream.

Once established, the cyclical nature of the flexo-bleach relationship guaranteed that as long as the amount of flexo-ONP continued to mount, so did bleach

requirements. At some point, the economic sustainability of mill operations will be subject to diminishing returns stemming from the increased chemical usage. With this in mind, flotation deinking mills have been forced to modify their chemistries and processes in an attempt to stay abreast of the increase in flexo-ONP.

In anticipation of a continuously depreciating quality of raw furnishes, process chemical manufacturers became involved. In the literature review section, an attempt was made to introduce some chemistries and procedural modifications designed to assist flexo ink separation within flotation operations. Common to all, however, is the absence of industrial acceptance. One particular reason for this commonality is the difficulty encountered when attempting to develop a single deinking agent formulation or process to contend with the absolute heterogeneity of the actual raw feed. In some cases, the flotation of flexo ink comes at the expense of a reduction in offset (oil-based) ink particle removal. In others, the cost of the reagent designed to collect and float dispersed flexo ink effectively outweighs the cost of additional bleaching. In spite of these drawbacks, process chemical manufacturers still seek the "magic bullet" with which mixed furnishes can be successfully deinked.

As of late 2003, the rate of conversion from lithographic (i.e. offset) to flexographic printing in worldwide pressrooms has been tempered by the lackluster economy. Suffering from a loss in advertising revenue, newspapers have become more hesitant to shoulder the initial capital expenditure associated with flexography. The reduced conversion rate may have granted recyclers and chemical suppliers a temporary reprieve during which they have been able to optimize their operations and chemistries

to contend with current levels of flexographic printed wastepaper. Unfortunately, as recyclers learn to deal with small volumes of flexo-ONP, investigations into novel flexo-deinking additives have become rare. Soon, the fallibility of this complacency may be exposed as signs emerge that an economic recovery is imminent. It is simple to imagine such a recovery, ensuring an increase in newspaper-based advertising, restoring the pre-depression, pro-flexography trend. Instances in which large-circulation newspapers appear poised to adopt flexography within the pressroom include the recent decision of News International to convert *The Sun*'s presses to flexography[55] and Italy's *La Republica* to increase the number of pages in its flexographically-printed daily.

The problem is expected to be especially severe in the European fiber recovery industry where mills employing flotation deinking far outnumber those based solely upon washing. Ironically, the environmental benefits afforded by flotation (e.g. reduced water consumption and increased yields) stand to be negated by the incidentals of increased bleach usage and landfill space demand associated with high levels of flexo-ONP in the raw feed. Although Germany has resorted to a preemptive moratorium on flexographic printing of newsprint, the United States, the United Kingdom and Italy appear especially vulnerable to an increase in the amount of flexo-ONP in the waste stream.

The initial purpose of the current thesis was to investigate the amenability of flexographic ink to spray surfactant flotation deinking. Having established the fact that the dispersed ink particles cannot be effectively separated by conventional flotation, the surfactant spray application was hypothesized to exploit the unique separation of

chemistries upon which the technology is founded. Designing a method to enhance or facilitate a specific process around an existing concept originally engineered to improve an unrelated process is not uncommon[h]. When investigations into the fundamental mechanisms of the initial concept are incomplete, it becomes virtually impossible to predict the outcome of experiments stemming from the provisional technology. This is especially the case when the objective of the new experiment significantly differs from that of the original investigation. The incorporation of surfactant spray flotation technology within a process designed to enhance the flotation of dispersed flexo ink provides an ideal example of the above observation.

Surfactant spray deinking technology was patented as a means to reduce fiber yield loss across a conventional flotation unit without affecting final pulp optical qualities. However, hydrodynamic conditions inherent to the system design permitted speculation that the technology may be employed to enhance flexo flotation (i.e. improve brightness as well). **Figure 5** presents the idealized mechanism of flexo ink "collection" via surfactant spray technology. Although conventional cationic polyelectrolytes are readily capable of collecting anionic flexo ink particles and

---

[h] The patented process by which *Sildenafil citrate*, a developmental hair-loss preventative, was originally synthesized (i.e. the innovative concept) has been extended to the development of a slightly more lucrative product with a function quite unrelated to balding (i.e. the new mechanism). The wisdom of sudden shifts in the focus of research and development will be revisited in the decision to abandon efforts to enhance flexo flotation via modification of the composition of the surfactant spray.

similarly charged contaminants, addition of these agents directly to a raw feed is tantamount to a clinic in counter productivity. Cationic collector escaping instantaneous consumption by the fiber fraction of the furnish may actually anchor flexo particles to fines, fibers, fillers, etc. Consequently, the use of cationic collectors within the pulp and paper industry is primarily limited to fiber-free unit operations in which the ability of the reagent to initiate the nonselective agglomeration of anionic contaminants is of benefit (i.e. process water clarification units incorporating dissolved air flotation, DAF, technology).
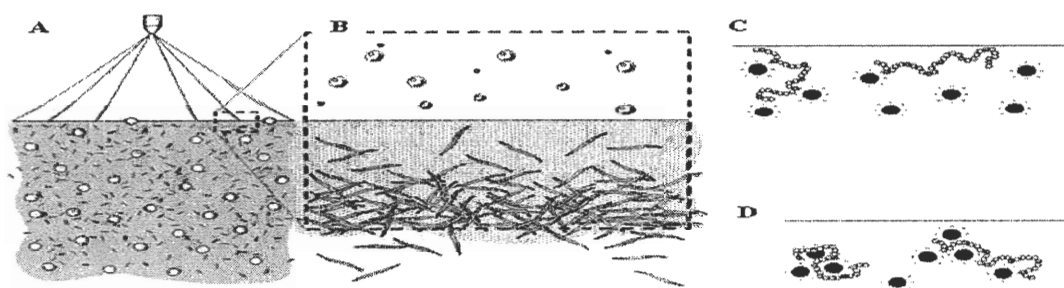
Figure 5: A potential mechanism to enhance flotation deinking of flexo ink via surfactant spray technology: **A.** Surfactant spray containing cationic collector is applied to the surface of an aerated flotation cell containing dispersed flexo ink. **B.** The droplets deliver the collector to the fiber-deficient interface. **C-D.** Without nonspecific adsorption of the collector onto the fiber, aggregation of dispersed flexo ink particles into floatable dimensions and surface chemistries is more probable.

As the figure indicates, the issue of unfavorable interactions between the collector and fiber, fines, fillers, etc. may be addressed by including the collector within the surfactant spray. Surfactants delivered onto the surface of an aerated cell in such a

manner were found to remain within the vicinity of the interface between the bulk aqueous phase and the froth layer[54]. Ideally, cationic collectors would behave in similar fashion. Surfactant spray technology, designed to reduce the amount of fiber brought to the cell surface, and the concomitant localization of the collector within this region were hypothesized to minimize undesirable collector-fiber interactions. In addition, boundary effects at the surface of the aerated suspension were predicted to establish a concentration gradient of fiber near the interface. Such a gradient would allow for a thin surface layer of relatively fiber-free liquid. Flexo ink particles, suspended within the aqueous medium, would remain within the thin layer. The probability of successful interaction between cationic collector sprayed onto the surface of the cell and flexo ink particles suspended within the interfacial layer will be greater than that of a collector simply mixed into the furnish. The resulting aggregates of flexo ink and collector may adhere to rising bubbles to be floated. As ink particles within the top layer are removed, diffusion of additional particles from the bulk medium restores the concentration equilibrium.

Although the postulated mechanism to float flexo ink is founded upon delivery of cationic collector within the surfactant spray, the inclusion of frothing agent within the spray cannot be discontinued. Flexo ink carried to the surface of the flotation unit will simply return to the bulk phase through gravitational and excessive hydrodynamic forces. Frothing agent application ensures that a foam capable of retaining floated ink aggregates is established at the cell surface. In effect, the concept of collector addition to the spray cannot be uncoupled from frother addition.

The experimental phase of the investigation began with confirmation of the inability of conventional flotation operations to contend with furnishes in which offset ONP was replaced with flexographically printed ONP. A potential cationic collector was subsequently included within the surfactant spray and the flotation efficiency evaluated with respect to brightness gains and yield loss reductions.

Investigations designed to optimize the probability of maximum flexo-collector interactions provided surprising results. Enhanced flotation efficiency, although confirmed, was not a sole consequence of collector addition but, in the stead, involved a subtle modification of the furnish properties. In fact, the contribution of collector to the overall brightness gain/yield loss reduction was minimal compared to that of the unlikely discovery. Accordingly, the focus of the investigation was shifted to the new mechanism to augment the flotation of flexo ink. The remainder of the thesis-related research would revolve around the elucidation of this mechanism by which dispersed flexo ink is rendered amenable to conventional flotation.

Since the value-added contribution of the new chemistry to the process of deinking flexo was greater than that of the original approach involving collector within the surfactant spray, the decision to realign the investigation was considered reasonable. Moreover, avoiding the costs associated with an additional deinking reagent (i.e. the cationic collector) by utilizing a pre-existing furnish component always presents a

favorable situation. This unconventional, reactionary approach to applied research is not uncommon within commercial research and development operations[i].

---

[i] Once again, see Pfizer's contribution to hair-loss prevention.

EXPERIMENTAL PROCEDURES

SURFACTANT SPRAY TRIALS

General

Flotation deinking trials, conducted during the initial phase of the investigation, were grouped into three general categories: Conventional fatty acid-calcium soap flotations, surfactant spray flotations in which collector was incorporated into the spray solution, and surfactant spray flotations without the benefit of a surface-applied collector. In the second and third categories, incorporating surfactant spray technology, the spray always contained a frothing agent. For simplicity, the experimental methods common to all three categories of flotation trials will be addressed first. When applicable, variations in experimental parameters/conditions will be highlighted and discussed with respect to the affected trial(s).

Furnish Preparation

Regardless of the variables adopted during individual flotation trials, the preparation of the furnish remained relatively constant. Pulping was conducted within a Lamort pulper (Kadant Lamort, Vitry-le-François, France) equipped with a helical rotor. Pulp consistency was maintained at 8% on an oven dry basis. OMG constituted 30% of the furnish during initial trials while the remaining 70% was ONP. During the remainder of this exploratory phase, the composition of the ONP fraction would vary from 100% offset printed material (Atlanta Journal Constitution) to 100% flexographically printed material (Knoxville News Sentinel). A series of trials was also

conducted with furnish prepared from 30% OMG, 60% offset ONF and 10% flexo ONP. Great care was taken to ensure that material placed into the pulper was free of contraries such as staples, inserts, magazine spines, etc.

Prior to the pulping of the OMG:ONP blends, the OMG fraction was allowed to soak to facilitate disintegration of the coating. The coated paper was placed in a 5 gallon plastic container to which 8 liters of 50°C tap water was added. After covering, the container was allowed to stand for 2 hours during which time the temperature returned to ambient conditions. At the end of the soaking period, the appropriate amount of ONP was placed into the container with the OMG and a volume of 50°C tap water was added to obtain the 8% oven dry consistency required for pulping. The prepulped furnish was allowed to stand for an additional 10 minutes to ensure complete saturation of the ONP fraction. During this final stage, all soaking material within the container was hand-torn into ~5 cm wide strips to facilitate pulping.

At the end of the raw feed preparation, the contents of the container were transferred to the Lamort pulper. To avoid the addition of extra variables within the system, chemical addition to the pulper was streamlined to include only caustic and silicate. Sodium hydroxide (50% solution in water, Aldrich) and sodium silicate (~14% NaOH, ~27% SiO_2, Aldrich) were added directly to the pulper to establish respective charges of 0.8 and 1.0% based on dry paper weight. After pulping for 1 minute, the pH was adjusted to 10 with caustic. The furnish was then pulped for an additional 9 minutes with an average temperature of approximately 50°C.

Barring a few variations in composition, all furnishes prepared during the first phase of the investigation were prepared in the above manner. However, furnishes in which the OMG fraction was omitted, were prepared without the benefit of the 2 hour soaking period. 100% ONP furnishes were simply pre-soaked for 10 minutes prior to pulping.

FLOTATION TRIALS

All flotations were conducted within an 18 liter scaled version of the Voith E-cell common to industrial flotation operations. The Plexiglas laboratory flotation unit, termed the E-18, is pictured in **Figure 6**. Aeration within the cell is achieved by way of a closed-circuit "injector-like" system that blends air with pulp within the recirculation loop. A manual gas flow valve enables control over the total volume of air pulled via vacuum pressure into the pulp stream. Complete closure of the valve permits thorough mixing of the pulp within the cell without aeration. At a pre-determined time, the valve may be opened to initiate air flow into the pulp at a specified rate. As in full-scale E-cell varieties, froth generated during the flotation cascades over a relatively lower area of the cell wall into a reject trough. At the end of the flotation period, the contents of the trough (i.e. flotation rejects) can be removed through an opening in the bottom of the trough. Likewise, the pulp remaining within the cell (i.e. flotation accepts) is removed via a drain port affixed to the cell bottom. Analyses of flotation efficiency involving evaluation of rejects and accepts were conducted from these "stream" samples. To obtain data regarding the feed stream, aliquots of the pulp were simply removed immediately after pulping.

Although primarily used in laboratory trials during investigations of novel deinking chemistries, the E-18 design was found to be invaluable during the evolution of surfactant spray deinking technology. Retrofitting the unit with the necessary equipment was a simple matter. **Figure 6** clearly displays the two-nozzle "bank" design from which the surfactant spray was delivered during relevant trials. The flow to the nozzles was provided from a pressurized canister containing pre-made surfactant solution (seen to the left of the flotation cell in the first image).
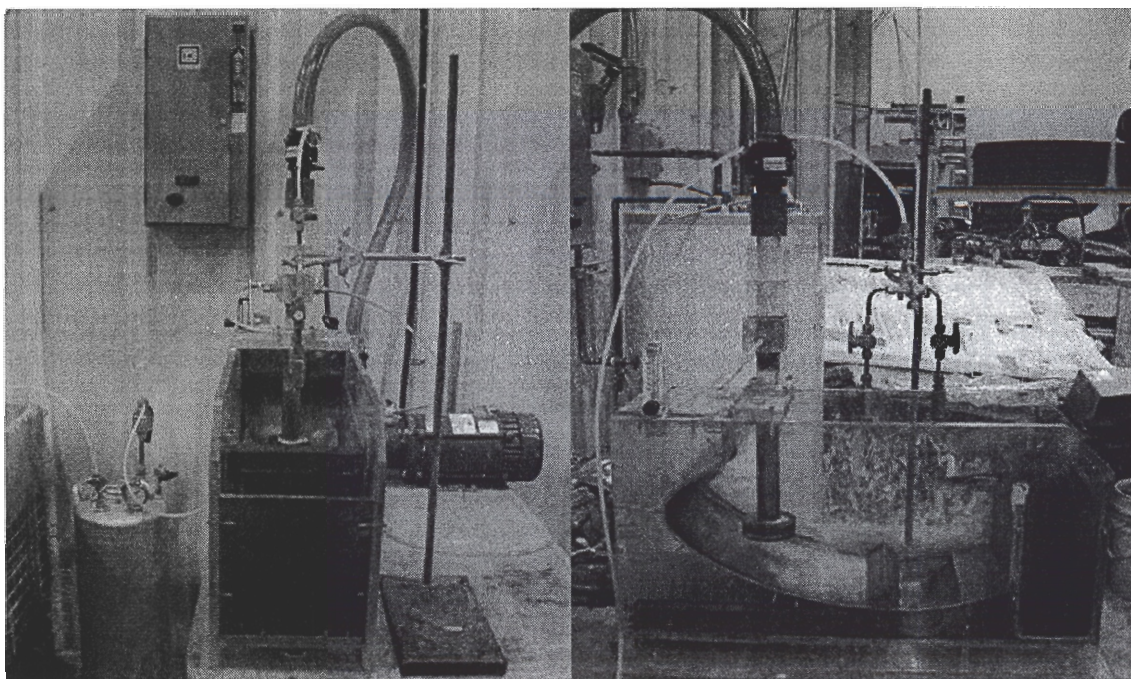
Figure 6: E-18 flotation cell.

Conventional flotation trials, employing calcium-soap collection chemistry, would be conducted throughout the course of the entire investigation. Results obtained were compared to those yielded from trials in which a novel chemistry and/or process was substituted. To ensure that the equipment was functioning in a manner consistent with earlier trials, the initial trials were conducted with furnishes composed from the 70:30 blend of offset printed ONP and OMG. As the furnishes evolved in line with the investigation, flexographically printed ONP replaced offset ONP and would eventually replace the OMG fraction. Although actual flotation times decreased during this evolution, the procedure by which furnishes were floated remained constant.

A sample of 8% consistency pulp containing 180 oven dry grams of solids (2250 g wet weight) was transferred to a separate 5 gallon bucket. 1.8 grams of reagent grade sodium oleate (J.T. Baker Inc.) and 3.6 grams of calcium chloride (Sigma-Aldrich) were added directly to the pulp. The fatty acid and calcium chloride levels within the final pulp were 100 and 200 ppm respectively. The pulp was mixed by hand in the bucket before being placed within the flotation unit. The pulp was diluted to 1% consistency within the flotation unit with distilled water warmed to 45°C. A fill level line within the unit served to ensure that the working volume remained at 18 liters. With the aeration valve closed, the circulation pump was used to mix the pulp for 5 minutes during which time the pH was adjusted to 8.5 with 1 M NaOH. After the mixing period, air was

introduced into the cell at a flow rate of 30 scfm during a specified flotation period[j].
Temperature and pH variations, monitored throughout the trial, were slight and,
therefore, presumed to be of minimal consequence to final observations. With the
exception of furnish composition, conventional trials throughout the reported
investigation were carried out in this fashion.

Unmodified Spray Surfactant (first set of trials)

As an extension of initial trials designed to replicate published accounts of
surfactant spray deinking efficacy, all furnishes floated via conventional chemistry were
also subjected to the new technology. Given that surfactant spray technology was
designed to avoid the nonspecific interactions associated with surfactants in the feed,
calcium chloride and the fatty acid salt were not added to the pulp prior to flotation. In
the stead, the frothing agents were delivered via the spray. As would be the case for the
remainder of the investigation, the surfactant spray contained 100 ppm Triton X-100
(analytical grade, J.T. Baker Inc.) as the frothing agent. Immediately after the 5 minute
mixing period, the nozzle bank was opened to allow spray flow. When operated at 40
psi, the surfactant spray system delivered ~410 ml of liquid onto the aerated pulp during
the 6 minutes of flotation. **Figure 7** shows a front view of the spray as it is applied to
the cell surface.

---

[j] Actual flotation periods would vacillate between 6 and 10 minutes. The former period was
eventually adopted as the standard during the investigation in the interest of time.
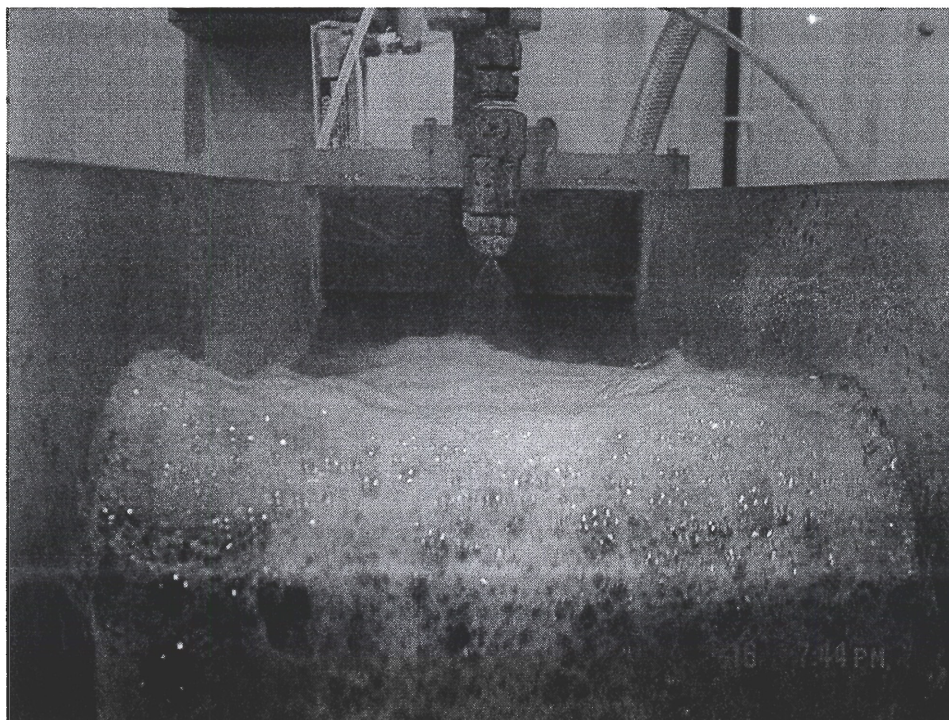
Figure 7: Front view of the E-18 flotation unit operated with surfactant spray. By premixing an excess of defoamer within the pulp prior to flotation, all foam generated in this picture is a consequence of frothing agent within the spray.

As mentioned previously, constituents within the raw feed possessed the ability to stabilize foam. This inherent foaming potential within the incoming pulp made it difficult to isolate and quantify surfactant spray-mediated foam generation and stabilization. To counteract the pulp-derived foam, a nonionic, siloxane-based defoamer emulsion, TDA-32 (Taylor Chemicals, Lawrenceville, Georgia) was mixed with the pulp prior to aeration. Various concentrations of the defoamer were assayed to determine the optimal level to effectively neutralize all instances of foam regardless of furnish composition. By ensuring that all foam generated during the flotation originates

from frothing agent supplied within the surfactant spray, the technology provides a certain amount of process control.

Unmodified Spray Surfactant (second set of trials)

The original trials conducted to reveal the applicability of surfactant spray technology to the flotation of furnishes containing high concentrations of flexo ink were faulty owing to a drawback in the pad preparation procedure. The tendency of flexo to follow the filtrate from the forming pad will be addressed in the "Brightness Pad Preparation" section. With the solution to the dilemma firmly in place, the trials outlined above were repeated exactly as before.

Cationic Demand

Before conducting trials incorporating a cationic collector within the surfactant spray, an intimate knowledge of furnish characteristics was required. Continuing with the assumption that flexo ink, diffusing into the relatively fiber-free froth-liquid interface would be preferentially consumed by cationic collector applied as a spray, an attempt was made to elucidate the distribution of charge throughout the whole furnish. Ideally, to avoid unfavorable interactions between fiber and the collector, the fiber fraction of the furnish could be neutralized via the addition of multivalent electrolyte to the furnish prior to flotation. Consumption of the electrolyte by furnish components was expected to proceed in random fashion. Should the dispersed flexo ink fraction possess a greater cationic demand than the fiber fraction, complete neutralization of the fiber

fraction would still find the flexo ink fraction with an exploitable, residual anionic charge.

A modified version of conventional back titration was employed to determine the cationic demand of the furnish. Briefly, this technique requires that an excess of cationic polyelectrolyte (e.g. poly-diallyldimethylammonium chloride) be added to the sample in question. After thorough mixing to ensure that that cationic demand of the sample is satisfied, the sample is filtered. The filtrate, containing the excess cationic polymer, is "back titrated" with an anionic polyelectrolyte (e.g. polyvinyl sulfate potassium) to an endpoint of zero charge[k]. Incorporation of an indicator dye within the filtrate, allows the neutralization point to be revealed by a color change. Previously conducted standardization allows the volume of anionic polyelectrolyte required to reach endpoint to be correlated with a specific amount of cationic polyelectrolyte within the filtrate. By subtracting the amount of cationic polyelectrolyte within the filtrate from the amount originally added to the sample, the cationic demand within the sample is given.

Since the main point of this phase of the investigation was to isolate the cationic demand of the flexo ink from that of the remainder of the furnish, the two components were separated via a series of fractionation stages. A sample of 100% flexo ONP

---

[k] Prior to the actual assay, the amount of anionic polyelectrolyte required to "neutralize" and equivalent amount of cationic polyelectrolyte must be determined through simple titration.

furnish was diluted to 0.1% consistency and adjusted to a pH of 8.5. A liter of this diluted furnish was filtered across a dynamic drainage jar equipped with a 76 micron screen. The filtrate, representative of the < 76 μm fraction of the furnish, was assumed to contain the flexo ink among other contaminants. Cationic demand measurements would be conducted on this fraction as well as the whole furnish, diluted to 0.1% consistency, to obtain approximate values.

To determine the cationic demand of the whole pulp, 50 ml of the 0.1% consistency furnish, pH 8.5, was transferred to a 100 ml beaker. To the furnish, 5 ml 0.001 N poly-diallyldimethylammonium chloride (poly-DADMAC) (Nalco, Chicago, IL) was added to provide the excess cationic polyelectrolyte. The furnish was then allowed to mix for 30 minutes. After the mixing period, the furnish was then filtered across an 0.2 μm GTTP Isopore membrane (Millipore, Billerica, MA) within a nitrogen pressurized Amicon 8050 50 ml stirred cell filtration vessel (Millipore, Billerica, MA). The filtrate, containing unconsumed poly-DADMAC, was transferred to a clean 100 ml beaker. To ensure that all of the residual poly-DADMAC was washed from the pulp, another 50 ml distilled water, adjusted to pH 8.5, was added to the stirred filtration unit and allowed to mix for 5 minutes. The washing filtrate was again collected and then combined with the first filtrate. Ten drops of the indicator dye, o-Toluidine Blue (TBO) were added to the filtrate and allowed to mix for 1 minute. The filtrate was then back titrated with 0.001 N polyvinyl sulfate potassium (PVSK) (Nalco, Chicago, IL) to an endpoint indicated by a color change. Unfortunately, the reproducibility of the assay was difficult due to the subtle color changes involved. Therefore, a spectrophotometer

(Hewlett Packard 8453, Germany) operating at a wavelength of 620 nm was used to accurately gauge the back titration endpoint. **Figure 8** shows a graph of absorption at this wavelength as a function of PVSK addition. The endpoint was determined as the midpoint within the slope generated as the color change occurs. From the microequivalents of PVSK required to reach endpoint, the microequivalents of poly-DADMAC within the filtrate were determined. A simple subtraction allowed the cationic demand, in microequivalents of poly-DADMAC, to be determined. This procedure was repeated with the < 76 µm fraction of the 0.01% consistency pulp to provide the cationic demand of the pulp fraction containing the flexo ink. From the cationic demand determined for the whole pulp, the fraction attributed to the < 76 µm fraction could be subtracted to yield the cationic demand of the > 76 µm, or fiber/fines, fraction.
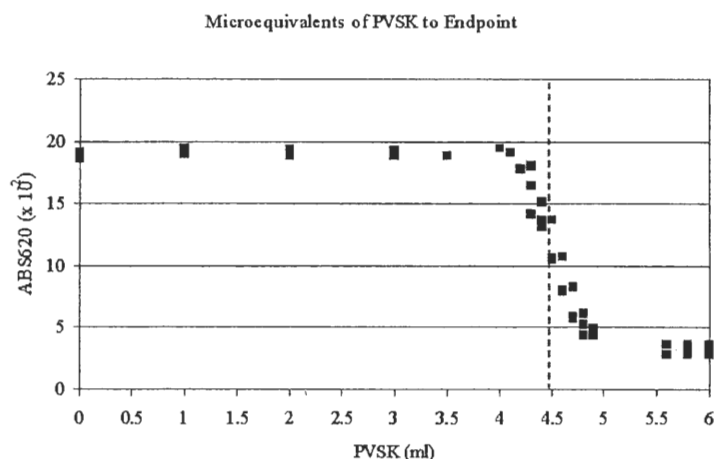
Figure 8: Determination of endpoint while back titrating the whole furnish with PVSK. The true endpoint is indicated by the dotted line. By observing absorption reduction at 620 nm wavelength, the method ensures reproducibility and accuracy.

Cationic demand measurements taken from the fractionated 100% flexo ONP furnish served to justify the next phase of the investigation. Four sets of trials were designed to reveal any increase in deinking efficiency using surfactant spray technology incorporating cationic collector. All trials were performed with a 100% flexo ONP furnish adjusted to 1% consistency, pH 8.5 and 45°C. In the first set, flotation trials were conducted with increasing concentrations of calcium (measured in ppm $CaCl_2$). The calcium chloride was added directly to the pulp prior to dilution to a 1% consistency within the E-18. As usual, the surfactant spray contained 100 ppm TX-100. During these initial trials, no defoamer was employed.

The second set of trials, an extension of the first set, was carried out to provide a base line deinking efficiency value before cationic collector was added to the surfactant spray. In essence, the first set of trials was repeated with the exception of 200 ppm TDA-32 defoamer mixed with the pulp along with the various amounts of calcium chloride. The concentration of 200 ppm defoamer was selected simply because it was determined to sufficiently repress foam generation from the 100% flexo furnish.

The third and fourth set of trials were conducted with cationic polyacrylamide (CPAM) incorporated within the surfactant spray. The concentration of CPAM within the spray was 20 ppm and 40 ppm respectively. Although the trials were conducted with

varying levels of calcium chloride, the concentration of TDA-32 remained constant at 200 ppm.

Spray Surfactant (with Defoamer)

With the revelation that interactions between the defoamer, calcium chloride and dispersed flexo ink favor increased deinking efficiency, flotation trials to empirically define the relationship were designed. Of utmost importance, validation of the observed phenomenon was essential before attempting to define, elucidate or optimize the exact mechanisms involved. To this end, the trials incorporating solely TDA-32 and calcium chloride were repeated. Again, the concentration of the defoamer within the E-18 was held constant at 200 ppm. Both calcium chloride and defoamer were mixed with the pulp prior to dilution. During the 5 minute mixing period prior to aeration, the pH was adjusted to 8.5 while the temperature remained approximately 45°C. The surfactant spray contained only 100 ppm TX-100 and was applied for the duration of the 6 minute flotation period following mixing.

To evaluate the system in light of existing chemistries, two commercial agents, purported to enhance the flotation rate of flexo ink, were mixed with the 100% flexo ONP pulp. Vinings A (Vinings Industries, Inc., now Kemira) and Sansink® (BASF Corp.) were obtained directly from the manufacturer. Vinings A was added to achieve a concentration of 25 ppm within the flotation unit. Sansink was assayed at concentrations of 25 and 50 ppm. Although calcium chloride and defoamer were

generally absent from the furnish during these flotation trials, one trial was conducted with 50 ppm Sansink and 100 ppm $CaCl_2$.

Having established the value of defoamer within the system for flexo ink removal, the importance of defoamer composition was examined. Since TDA-32 is classified as an organically-modified polydimethylsiloxane emulsion, a mineral oil-based defoamer was substituted. Laboratory trials designed to quantify the defoaming capacity of various antifoam agents found that 100 ppm ECCO P-048 was as effective as 200 ppm TDA-32. Flotation trials were then conducted with 100 ppm ECCO P-048 in the presence of 0, 100 and 200 ppm calcium chloride under the same conditions as before. A single trial was performed in which the level of ECCO P-048 was raised to 200 ppm at a calcium chloride concentration of 100 ppm.

Brightness Pad Preparation

The initial stages of the investigation included the evolution of a procedure for preparing pulp brightness pads. Considering that, in most cases, estimation of deinking efficiency stems from qualitative analyses of brightness pads, the importance of this particular phase of the investigation is virtually impossible to overemphasize. For a procedure to be suitable, a high degree of repeatability was essential. In addition to this proviso, the procedure must account for significant variations in furnish composition. Acceptable pads prepared from 70:30 blends of offset ONP and OMG must also be prepared from 100% flexographically printed ONP. By avoiding deviations within the preparation procedure, qualitative comparisons between pads derived from different furnishes became possible.

Before launching into details of the actual procedure, the definition of an "acceptable pad" is necessary. An acceptable pad is one that accurately reflects the concentration of ink within the furnish in question. Qualitative measurements taken from both sides of a brightness pad should exhibit exceptional similarity. Two detriments associated with pad preparation are ink washing-effects and pad sidedness. In the former case, ink washed from the pad during formation tends to cause overestimation of the efficiency of a deinking process. Some paper manufacturers contend that the contribution of washing-effects during pad preparation is permissible since a similar scenario unfolds as the pulp drains at the forming table. However, this perception is flawed since the washed ink tends to build-up in the mill process waters and must be addressed eventually. Accurate measurement of flotation deinking efficiency must take care to avoid washing-effects during pad formation in order that all unfloated ink particles are retained within the pad.

The issue of sidedness is also a consequence of drainage during pad formation. Sidedness arises when ink is unevenly distributed across the thickness of the forming pad. Larger ink particles tend to be retained near the top of the pad while smaller particles may accumulate within the bottom fiber layers. The resulting z-directional, ink gradient ensures that optical measurements taken from one side of the pad will be significantly different from those taken from the opposite side.

The degree of washing and the severity of sidedness are a direct function of the geometry, size and surface chemistry of the ink particles dispersed throughout the pulp. The following description of pad preparation begins with the initial procedure adopted

for the 70:30 blends of offset ONP and OMG. When flexo ONP was substituted for offset ONP and the limitations of the original procedure became evident. Therefore, a series of exploratory investigations were conducted to find an alternate means by which to prepare an acceptable brightness pad. Once the effectiveness of a particular technique was confirmed, pads would be prepared by this method for the remainder of the flotation trials.

The initial brightness pad preparation technique borrowed heavily from TAPPI standard T218 sp-97. Minor modifications, made for convenience, were determined to have minimal influence upon the final optical properties of the pulp pad. When applicable, deviations from the TAPPI procedure are noted.

Following flotation, a consistency measurement was taken from the "deinked" pulp. A volume of pulp containing 4 oven-dry grams of solids was then transferred to Hamilton Beach milkshake blender and mixed for 60 seconds. No pH adjustment was made to the pulp which tended to have a post-flotation pH of 8.1 ± 0.2 regardless of composition[l]. During the mixing, a Whatman 4 filter (150 mm dia., 20-25 μm pore size), placed in a Büchner funnel, was saturated with a small amount of distilled water[m].

---

[l] According to T218 sp-97, the pulp pH should be adjusted to ~6.5 to minimize pH-related color swings.

[m] T218 sp-97 suggests that the Büchner funnel be equipped with a fritted glass filtering disk to facilitate even drainage during pad formation.

The funnel was placed into the neck of a 4 liter Erlenmeyer flask with tubulation connected to an adjustable vacuum system. The mixed pulp was then poured into the flask and a vacuum of 25 psig was immediately applied. Just before the pad began to show spots of "dryness", the vacuum was terminated. The final pad was recovered and stored in a dark, airtight plastic bag during formation of the remainder of the pads. Two pads containing 4 oven-dry grams of solids were prepared from the pulps following each flotation trial.

To press the pads, each pad, complete with attached filter paper, was sandwiched between 2 sheets of blotter paper. The stack of blotter paper and wet brightness pads was then pressed at 50 psig for 10 minutes. To avoid introducing additional variation, the stack always contained 7 pads. Following the pressing, the filter paper was peeled away from and then brought back together with each pad. This step served to facilitate separation of the pad from the filter after drying. All pads were arranged, filter paper side up, on a Speed Dryer (Emerson Model 130, Portland, Maine) set at 105°C and allowed to dry for 10 minutes[n]. The final pads were allowed to cool for an hour and then submitted to optical analysis.

---

[n] Speed drying the pads is another point of significant diversion from T218 sp-97 which requires that the pads be air-dried under restraint. Although the speed drying technique did introduce some surface irregularities, brightness values taken from speed dried sheets and from restraint dried sheets were not significantly different.

Analysis of pulp pad brightness was conducted according to TAPPI T 525 om-92. The selection of a method incorporating diffuse geometry over directional geometry stemmed from the desire to reduce the number of measurements required for statistical significance. In addition, by allowing the incident light to strike the sample surface from an infinite number of directions and angles, subtle surface irregularities resulting from drying the pad without restraint would be less likely to influence the measured brightness.

From each side of the pad, 5 separate fields were subjected to brightness and ERIC measurements with a Technibrite Micro TB-1C Brightness tester (Technidyne Corp., New Albany, IN) with diffuse viewing geometry. The 10 values reported for both sides were averaged to generate representative values. This was repeated with the second pad prepared from the same furnish and the results averaged with those from the first pad. In addition to brightness, the Technibrite tester was used to measure the effective residual ink concentration (ERIC) within the pads according to the method of Jordan and Popson[56]. ERIC measurements were restricted to pads prepared during the initial TDA-32/calcium chloride and ECCO P-048/calcium chloride trials rather than taken from every pad created during the investigation.

To determine whether or not results from the sheets were acceptable, standard deviation within the results was calculated. When this value exceeded 1, the pad was considered to suffer from substantial sidedness and was discarded. All brightness measurements conducted during the course of the investigation followed this procedure.

When preparing and analyzing brightness pads from furnishes comprised of offset ONP and OMG, the above techniques could be employed with great success. However, when flexo ONP began to be substituted for the offset ONP the shortcomings of the technique became evident. While oil-based offset ink particles liberated during the pulping tended to be large enough to limit their ability to move within the draining pulp pad, the submicron size and hydrophilic nature of the dispersed flexo ink particles allowed them the freedom of movement during pad formation. The filtrate obtained during pad formation was as dark as the pre-filtered pulp suspension indicating that a substantial portion of the non-floated ink simply passed directly through the filter paper. In addition, flexo ink particles that did not pass through the filter would tend to concentrate on the lower side of the forming pad. Dark annuli in regions corresponding to perforations within the Büchner funnel would appear on the lower face of the pad. Between the extensive washing and the extreme sidedness patterns, it was impossible to obtain qualitative optical data from pads formed from furnishes containing flexo-printed material. Before the investigation could proceed further, the pad preparation technique would have to be adjusted to contend with the furnish variation.

Retention of dispersed flexo ink particles within a forming pad has been accomplished with varying degrees of success. Ben and Dorris assay a number of published methods for creating brightness pads with even ink distribution across the pad thickness[57]. They conclude that homogenous and complete retention of both oil- and water-based inks within forming pads can be accomplished through the addition of

fixation aids. The addition of cationic polyacrylamide (CPAM) and alum as pulp conditioners prior to pad formation was shown to affix ink particles to the fiber mat without altering ink particle dimensions. The exact ratio of CPAM to alum depends on the furnish since variations in ink types and pH appeared to influence the efficacy of the concerted retention. Rather than forward a specific formulation of the fixation aids as a blanket solution to the sidedness or washing problems, the authors stress that the most optimal ratio of fixation agent addition must be empirically determined.

To evaluate the value of these two agents as retention aids during pad formation in the present investigation, 4.0 g pads were prepared from pre-conditioned, post-flotation, 70:30 flexo ONP:OMG furnishes. For convenience, the conditioning was either conducted with CPAM or with alum but not with a mixture of the two. The aid was pipetted into the pulp sample immediately before mixing. Following formation, the pads were pressed and dried in the usual fashion. Standard deviation between ISO brightness values taken from both sides of the sheet were used to determine sidedness. Results would stand to indicate whether or not fixation aid addition to the pulp immediately before pad formation was feasible.

After confirming that the addition of fixation aids would not be acceptable during this investigation, an alternate method to ensure complete retention of flexo within the pad was adopted. Acidification of pulp prior to pad formation has been described in the literature as an effective means to affix flexo ink[43 46]. Lowering the pH to 3 allows the adsorbed binders to protonate and, thereby, precipitate the ink. For the remainder of the investigation, brightness pads would be formed from acidified pulps.

The reject trough within the E-18 flotation unit made collection of the froth straightforward and simple. Following a flotation, the reject stream was collected from the trough and vacuum filtered across a pre-weighed VWR 415 filter pad placed in the Büchner funnel. No attempt to adjust the pH was made due to the excessive volumes of froth generated during some flotations relative to others. The volume of the resultant filtrate was recorded. The weight of the wet pad was taken and then the pad was allowed to dry overnight at 105°C. The fraction of solids rejected during flotation was calculated by subtracting the weight of the filter paper from that of the oven dry reject pad and dividing the result by 180 (i.e. the original weight, in oven dry grams, of the total solids in the flotation unit prior to flotation). Assuming a density of 1 g/ml, the mass of water evaporated from the pad was converted to volume and added to the volume of filtrate produced during pad formation. This allowed the determination of water loss during the flotation. **Figure 9** is the worksheet prepared to assemble and quantify all brightness gains and fiber/water losses generated during 6 flotations.

	CaCl2 (ppm)	TDA-32 (ppm)	Pluronic L-61	Pluronic L-51	ECCO P-048	Sanuzink	Vinlage A	Flotation pH	Na-Oleate	Flotation Time (min)
3T.1	50.00				200.00			8.50		5.00
3T.3						250.00		8.50		6.00
3T.5					200.00			8.50		6.00
3T.7	100.00				200.00			8.50		6.00
3T.9	100.00	200.00						8.50		6.00
3T.11	200.00				200.00			8.50		12.00
3T.13	100	200						8.5		2nd Flot = 6 min
Standard										

Pad #	3T.1	3T.2	3T.3	3T.4	3T.5	3T.6	3T.7	3T.8	3T.9	3T.10	3T.11	3T.12	3T.13	3T.14	STD
Top ISO	24.60	23.80	19.70	19.20	20.90	20.50	24.70	24.70	26.30	27.60	27.30	26.70	32.90	32.30	18.80
	24.20	23.90	19.90	19.50	21.60	21.30	24.90	25.40	27.30	27.60	27.30	27.00	33.00	32.50	17.90
	24.10	23.60	19.70	19.60	21.70	21.30	24.60	25.10	27.40	27.60	27.60	27.20	32.90	32.40	18.10
	24.30	24.00	19.60	20.00	21.20	21.20	25.20	26.20	27.30	27.60	25.90	27.20	32.40	32.00	17.70
	24.50	23.90	19.00	20.00	21.10	20.80	25.00	25.10	27.50	27.40	27.20	25.90	32.60	31.90	18.50
Bottom ISO	23.30	23.50	18.80	18.20	20.90	20.40	24.20	24.40	26.90	27.30	27.30	26.00	31.30	30.40	17.40
	23.20	23.30	18.10	18.30	20.20	20.70	24.40	24.50	27.30	27.20	27.10	25.80	31.50	29.20	17.70
	23.00	23.00	18.90	18.10	20.10	20.40	24.40	24.40	26.80	27.60	25.90	25.20	31.70	29.20	17.20
	23.40	22.60	18.90	18.60	20.10	19.90	24.00	24.10	26.50	25.80	25.40	26.10	31.40	30.10	17.60
	22.90	22.50	18.20	18.60	20.20	20.30	24.00	24.40	26.70	27.20	25.80	25.90	31.40	29.50	18.10
Average ISO	23.75	23.40	19.05	19.00	20.80	20.59	24.53	24.73	27.00	27.36	27.05	26.50	32.11	30.99	17.89
STDEV	0.65	0.56	0.63	0.76	0.62	0.47	0.41	0.44	0.42	0.25	0.34	0.66	0.71	1.43	0.50
Combined Average ISO	23.58		19.04		20.76		24.63		27.19		26.79		31.55		17.90
Combined STDEV	0.62		0.67		0.54		0.43		0.39		0.54		1.24		0.40
Filtrate Vol	830.00		1910.00		640.00		716.00		1160.00		1320.00		1260.00		
Wet Pad	24.74		109.16		16.16		16.84		46.05		39.39		63.03		
Dry Pad	6.34		17.98		4.72		6.44		11.45		10.50		10.96		
Filter	1.22		1.24		1.25		1.25		1.25		1.25		1.43		
H2O loss (%)	4.71		11.12		3.62		4.04		6.58		7.49		7.12		
Fiber loss (%)	2.84		9.30		1.93		2.33		5.67		5.13		5.31		
Brightness Gain	6.68		1.15		2.85		6.73		9.30		8.90		13.56		

Figure 9: Spreadsheet into which results from brightness, fiber and water loss measurements were entered to determine the efficacy of a particular set of flotation variables.

FLEXO INK ANALYSIS

Having successfully documented the ability of defoamer and calcium chloride inclusion within the flotation cell to augment deinking performance, the investigation entered a more fundamental phase. During this final phase, an attempt was made to elucidate the mechanisms responsible for the interactions between defoamer, calcium chloride and dispersed flexo ink that facilitate flotation removal. This would commence with characterization of the flexo ink particles suspended within the furnish at the conditions employed during the flotation trials.

Pressate Preparation

To obtain a fiber-free suspension of flexo ink particles, the actual furnish used during flotation trials appeared to be the most convenient, and appropriate, starting point. A 100% flexo ONP furnish was prepared according to the established protocol. An aliquot of the furnish was then diluted to 1% consistency and filtered across a dynamic drainage jar equipped with a 76 μm screen. Finally, the filtrate was, itself, vacuum filtered across a VWR 415 filter (20-25 μm pore size) to yield the "pressate" or fiber-free flexo ink suspension. This pressate would be used during subsequent analyses performed to determine the inherent nature of flexo ink particles released during the pulping of the flexo ONP.

Particle Size and Zeta Potential

Fortunately, measurements to determine the average ink particle size as well as the zeta potential of the suspended ink particles could be conducted concurrently through the use of a Zetasizer 4 (Malvern Instruments, Southborough, MA). In brief, the Zetasizer converts laser light scattering patterns within a colloidal suspension into particles velocities. Since laser light is inherently of singular frequency, shifts occurring within the frequency of light scattered by the particles relative to the laser are indicative of movement towards or away from the laser source. This Doppler shift in frequency, as particles undergo simple Brownian displacement, provides an average particle diffusion coefficient within the suspension. This process to define particle motion is collectively referred to as photon correlation spectroscopy (PCS). The resulting particle diffusion coefficient is converted to an average hydrodynamic particle radius via the Stokes-

Einstein equation. Expectedly, particle size measurements taken from flexo ink suspensions will be overestimated values due to adsorbed binder at the particle surface which tends to increase the hydrodynamic radius.

$$R = \frac{kT}{6\pi\eta D}$$

Equation 1: Stokes-Einstein equation employed by the Zetasizer to determine the average hydrodynamic radius of suspended particles (R) from a measured translational diffusion coefficient (D). k is the Boltzmann constant, T is the absolute temperature and η is the viscosity of the supporting medium.

A liter of the flexo ink pressate was heated to 45°C and adjusted to a pH of 8.5. After taking particle size measurements from the unmodified pressate, calcium chloride stock was slowly added to the stirred sample. At predetermined calcium chloride concentrations, aliquots were submitted for particle size measurements. All measurements were conducted at while maintaining the sample cell temperature within the Zetasizer at 45°C. After obtaining particle size measurements with pure pressate, the experiment was repeated with 200 ppm TDA-32 present within the pressate.

Within the same instrument, the zeta potential of suspended flexo ink particles was conducted from the same sample employed during particle size measurements. In brief, the system generates an electric field across the sample. Electrophoretic mobility of the particles in response to the applied field is determined from light scattering dynamics as the particles migrate across a fringe created by a pair of laser beams. The light is absorbed by a photo-multiplier within the system which correlates the scattering dynamics with an average particle velocity. Through the use of the Smoluchowski

equation, the zeta potential of the particle can be determined from the calculated particle velocity.

DEFOAMER ANALYSIS

Concluding that flexo ink-calcium chloride interactions were not solely responsible for the observed brightness gains during flotation trials, the focus shifted to possible calcium-mediated modification of the defoamer. TDA-32 is marketed as an organically-modified polydimethylsiloxane defoamer emulsion. The exact formulation (i.e. emulsifiers, emulsion stabilization agents (e.g. carboxy methyl cellulose, CMC), etc.) remains proprietary. For enhanced defoaming capabilities, the emulsion droplets contain particles of hydrophobic fumed silica.

Microscopy

Direct measurement of emulsion droplet size was accomplished via conventional light microscopy. A 200 ppm suspension of TDA-32 was prepared in distilled water. After adjusting the suspension to a pH of 8.5, a 50 µl aliquot was transferred to a hemacytometer with precisely calibrated boundary lines within the counting chamber (Bright Line, Hausser Scientific, Horsham, PA). A charged coupled device (CCD) camera attached to the microscope was used to generate digital photomicrographs of the emulsion droplets. Separate images were taken of the boundary line pattern within the counting chamber at the same magnification and resolution as that used to generate images of the droplets. Through the use of image analysis software (Scion Image – Beta 4.02, Scion Corp.), the known distances between

adjacent boundaries were used to determine the diameter of individual emulsion droplets. An advantage of the Scion program is its ability to simultaneously measure the diameters of numerous objects within the image. The output, taken from 10 separate fields within the hemacytometer counting chamber, was combined to yield an average diameter of TDA-32 emulsion droplets.

Surface Charge

The surface charge of TDA-32 emulsion droplets was determined as a function of pH. One liter of 200 ppm TDA-32 was prepared with distilled water. Since determination of the zeta potential via electrophoretic mobility measurements requires the presence of counterions within the supporting medium, 25 ppm calcium chloride was included within the TDA-32 suspension. While stirring, the pH of the suspension was gradually increased by slowly adding 0.5 N NaOH. At randomly selected pH values, aliquots of the suspension were submitted to analysis within the Zetasizer 4.

Conductivity

To determine whether suspended TDA-32 emulsion droplets were capable of consuming calcium ion, an indirect approach employing conductivity measurements was adopted. A suspension of 2000 ppm TDA-32 was adjusted to 8.5 pH and

thermostatted at 45°C°. A stock solution of calcium chloride was slowly added to the stirred suspension and the conductivity recorded.

Cationic Demand

The cationic demand of the 200 ppm suspension of TDA-32 emulsion droplets was conducted with a PCD03 particle charge analyzer from Mutek. To generate the appropriate concentration of defoamer, 1 ml of a 25 g/L stock solution of TDA-32 was added to 100 ml of distilled water warmed to 45°C. When applicable, calcium chloride stock was added to establish pre-selected concentrations. The resulting suspension was allowed to mix for 5 minutes. During the mixing period, the pH of the suspension was adjusted to 8.5. These conditions were believed to loosely represent those prior to actual flotation trials with the exception of furnish components. From the mixed suspension, 10 ml was pipetted into the chamber of the autotitrator and titration initiated immediately. From each 100 ml suspension, a total of three cationic demand measurements were made and the results averaged.

Cationic Demand in the Presence of Polyvinyl Sulfate Potassium

Cationic demand measurements were also performed in the presence of an anionic polymer. Due to an approximate 1:1 charge neutralization ratio with poly-

---

° The 10 fold increase in TDA-32 concentration was selected in order to amplify the amount of calcium consumed relative to the expected miniscule amounts consumed by 200 ppm TDA-32.

DADMAC, PVSK was selected as a convenient representation of ionized flexo binder. After preparing the 200 ppm suspension of TDA-32 as described above and adding the calcium chloride, 5 ml of 0.001 n PVSK was pipetted into the 100 ml sample. After allowing the sample to mix at 45°C and adjusting the pH to 8.5, 10 ml of the mixture was transferred to the autotitrator and titrated to the endpoint with 0.001 n poly-DADMAC. Since 5 ml of 0.001 n PVSK was initially added to the mixture, 5 ml of 0.001 n poly-DADMAC required to reach the endpoint would indicate that no "binder" was adsorbed onto or across the oil/water interface of the emulsion droplet. If increasing calcium chloride levels are responsible for biphasic transfer of the binder onto or into the emulsion droplet, the overall cationic demand of the system was expected to reduce.

Analysis of TDA-32/CaCl$_2$ Films

Continuing with the investigation into potential interactions between calcium chloride and TDA-32, the physicochemistry of films formed from the two components was then analyzed. Fourier transform infrared spectroscopic analysis of the films (FT-IR) was employed to elucidate potential calcium induced modification of the chemistry of the oil phase. Since the 200 ppm TDA-32 suspension was perceived as too dilute to permit the formation of confluent films for FT-IR analysis, 1 liter of a 25 g/L TDA-32 suspension was prepared with distilled water. The suspension was adjusted to 8.5 pH with 0.5 N NaOH and heated to 45°C. While stirring the suspension, a 72 g/L stock solution of calcium chloride was slowly added. The addition amounts were selected to correspond to 0, 25, 100, 200 and 400 ppm calcium chloride additional levels when using a 200 ppm TDA-32 suspension (i.e. all calcium chloride additions were multiplied

by 125). After each calcium chloride addition, the suspension was allowed to mix for 5 minutes. After this period, 400 µl of the suspension was pipetted onto the polyethylene support matrix of a disposable, 5 x 10 cm IR card (3M, St. Paul, MN). After transferring aliquots of the suspension to 5 separate IR cards (each representative of a TDA-32 film formed with varying calcium chloride levels), the cards were allowed to dry overnight within a laboratory desiccator to ensure the removal of all water from the films. A 200 Nicolet Avatar 360 FT-IR E.S.P. equipped with a KBr beamsplitter, Ever Glo radiation source and a deuterated triglycine sulfate (DTGS) detector was used to measure mid IR adsorption across the films. Adsorption spectra recorded for the polyethylene film were subtracted from the overall spectra to correct the values recorded for the TDA-32/$CaCl_2$ films.

Contact angle measurements provided insight into the ability of calcium to influence the ultimate surface chemistry of the film surface. A liter of pressate and a separate liter of distilled water were heated to 45°C. Once thermostatted, TDA-32 was added to each liter to obtain concentrations of 200 ppm. After stirring for five minutes, during which time the pH was adjusted to 8.5, a 100 mg/ml stock solution of calcium chloride was added incrementally to achieve final suspension concentrations of 0, 25, 50, 100 and 200 ppm within each of the suspensions. After each increment, the suspension was allowed to mix for 2 minutes thereby enabling the adjustment of the pH to 8.5. After the mixing period, six 750 µl aliquots of suspension were pipetted onto a pre-cleaned, 75 x 50 x 1 mm microscope slide (Fisher Scientific). The slides were allowed to dry overnight to form 6 individual minifilms. With the use of a FTA200

(First Ten Ångstroms. Portsmouth, VA), digital images were obtained of a drop of Millipore-pure water placed on the surface of the film. Image analysis software allows calculation of the contact angle of the droplet upon the film. The results obtained from all 6 mini-films were averaged to yield the reported contact angle.

Films were also prepared from suspensions of pressate in the absence of TDA-32. Again, the pressate was heated to 45°C and adjusted to a pH of 8.5 before any calcium chloride was added to the suspension. Films were formed as before. The primary difference during the contact angle measurements taken from these films was in the composition of the actual droplet. Contact angles were determined for drops of pure water on the film as well as drops of an 8.5 pH, 200 ppm TDA-32 suspension.

Surface Tension of TDA-32 Suspensions

Initial experiments were designed to monitor surface tensions of water, an aqueous suspension of 200 ppm TDA-32 and pressate both with and without 200 ppm TDA-32 at various calcium chloride levels. A liter of each suspension was prepared, thermostatted at 45°C and adjusted to 8.5 pH. A volume of 50 ml was transferred from the bulk suspension to a water-jacketed 100 ml beaker. The beaker, connected to a heating unit (Brinkman RM6 Lauda), was preheated to 45°C. The beaker was placed onto the stage of a dynamic contact angle analyzer (Series 300 DCA, Cahn) and allowed to equilibrate for 3 minutes without agitation. The surface tension of the liquid was then determined according to Wilhelmy plate methods. Only the receding contact angles were reported from the investigation. Calcium chloride was added to the bulk

100

suspension to achieve a concentration of 25 ppm. After allowing a mixing period of 5 minutes, 50 ml were transferred to the jacketed beaker to repeat the surface tension measurement process. Ultimately, the surface tension for each of the four suspensions (i.e. water, water + TDA-32, pressate, pressate + TDA-32) would be determined at calcium chloride concentrations of 0, 25, 50, 100, 200 and 400 ppm calcium chloride.

To determine whether the temperature of the suspension affects interactions between calcium chloride and defoamer, surface tension measurements were taken from a 200 ppm TDA-32 suspension while increasing the temperature. A one liter suspension of TDA-32 was prepared with distilled water and adjusted to 8.5 pH. The suspension was slowly stirred at room temperature (~22°C). While the suspension was mixed, the water jacketed beaker was heated to a predetermined temperature of 25, 30, 35, 40, 45, 50, 55, 60 or 65°C. From the suspension, 50 ml was transferred to the heated beaker and allowed to equilibrate for 5 minutes on the DCA stage. The receding surface tension was then determined via the Wilhelmy plate method as before. The results from seven cycles were averaged to yield a final value. After obtaining values from the 200 ppm TDA-32 suspension, another 200 ppm TDA-32 suspension was prepared with 100 ppm calcium chloride. The measurements of surface tension as a function of temperature were repeated with aliquots from this suspension.

Defoaming Power of TDA-32

An indirect means to observe the impact, if any, that calcium chloride has on spreading behavior of the TDA-32 defoamer droplets across the air bubble involved

foam stability measurements. 0.5 L of frothing liquid was prepared with 200 ppm TX-100 and either 0 or 100 ppm calcium chloride. TDA-32 was added to the solution to establish a defoamer concentration gradient. The mixture of defoamer, frothing agent (i.e. TX-100) and calcium chloride was slowly poured into a 2 L graduated cylinder so as not to generate any premature foam. An air stone mounted at the bottom of the cylinder was used to generate 1-2 mm air bubbles. At time zero, air was introduced into the cylinder at a rate of 2.00 SLPM. After 1 minute of aeration, the height of the foam layer was recorded and the air flow terminated. The time for the foam to collapse to ½ the initial height was used as in index of foam stability (measured in seconds). Foam stability was plotted against TDA-32 concentration (in ppm) for solutions both with and without 100 ppm calcium chloride.

Surface Excess Concentration of TDA-32

To gauge the ability of TDA-32 emulsion droplets to adsorb at the air/water and air/pressate interfaces, the Gibbs equation was employed to determine the surface excess concentration, Γ, of the defoamer (**Equation 2**).

$$\Gamma = -\frac{c}{RT} \cdot \frac{d\gamma}{dc}$$

Equation 2: The Gibbs Equation used to calculate surface excess concentration, Γ, of a nonionic surfactant.

Since Γ is a function of the surface tensions, γ, obtained for various concentrations, c, of surfactant (i.e. TDA-32), a number of separate trials were performed in which both the TDA-32 and calcium chloride concentrations were varied.

All suspensions were prepared with distilled water, adjusted to pH 8.5 and thermostatted, as before, at 45°C. The Wilhelmy plate technique was then used to measure the surface tension of the various suspensions. The curves generated from the receding surface tensions as a function of calcium chloride concentration for a variety of TDA-32 suspensions, were then used to calculate Γ in mg/m^2 at any of the assayed conditions.

INTERFACIAL KINETICS

PDMS-water/pressate Emulsions

Since direct observation of the TDA-32 emulsion droplet/water interface was impractical, a mimetic system was developed. In this system, an interface was created by layering an oil phase onto an aqueous phase. The dispersed phase within the TDA-32 emulsion consists of an organomodified polydimethylsiloxane (PDMS). Accordingly, a hydroxyl-terminated, unmodified version of PDMS (Q1-3563, Dow Corning, Midland, MI, 55-90 cP) was selected to represent this dispersed phase. Twelve 15 ml borosilicate test tubes were cleaned with 1:1 H_2SO_4/HNO_3 followed by thorough washing with Millipore pure water. All tubes were placed into a thermostatted water bath held at 45°C. To each tube, 5 ml of Q1-3563 were added and allowed to equilibrate to 45°C over 1 hour. One liter of Millipore pure water and another of pressate were adjusted to pH 8.5 with 0.5 N NaOH and warmed to 45°C. A 5 ml aliquot from each aqueous suspension was layered onto the top of the preheated PDMS in two separate tubes. The tubes were then vortexed for 10 seconds and then returned to the thermostatted bath.

Calcium chloride was added to the remaining aqueous suspension to establish a concentration of 25 ppm. After each calcium chloride addition, the pH was readjusted to 8.5. Again, 5 ml were transferred from each suspension to a PDMS-containing tube followed by mixing via vortex. In this manner, PDMS-water and PDMS-pressate emulsions were prepared with increasing concentrations of calcium chloride within the aqueous phase.

The stability of the emulsified phase was correlated with the volume fraction of the emulsified phase as a function of time. To determine this, digital images taken of the tubes immediately upon mixing and at various intervals afterwards were analyzed via image analysis software (Scion Image – Beta 4.02, Scion Corp.). The volume fraction of the emulsified layer at each time point was taken to be the layer height divided by the total height of the liquid within the tube.

Creation of a Mimetic Oil-Water Interface

A simulation of the TDA-32 droplet-pressate interface was developed to maximize observable interfacial area within a single microscopic plane of view. A drop of neat PDMS (100 μl) was placed on a microscope slide. A separate drop of pressate (100 μl), adjusted to pH 8.5 and predetermined calcium chloride concentration was placed ~0.5 cm from the oil drop. A glass cover slip was gently lowered onto both drops thereby causing the drops to flow into one another. The resulting interface was readily observable under magnification. Photomicrographs were taken at 5 and 10 minutes after formation of the interface.

RESULTS AND DISCUSSION

FLOTATION TRIALS

Exploratory Trials

The initial trials were simply repetitions of the experiments conducted to validate the advantage of spray surfactant deinking over conventional flotation deinking. **Figure 10** presents the results obtained from trials conducted with a 70:30 blend of offset ONP and OMG. These results further underscore the ability of surfactant spray technology to reduce fiber loss. Although the brightness gain is adversely affected somewhat, the 1 to 2 point loss may be negated by a longer flotation period and/or a series of flotations.
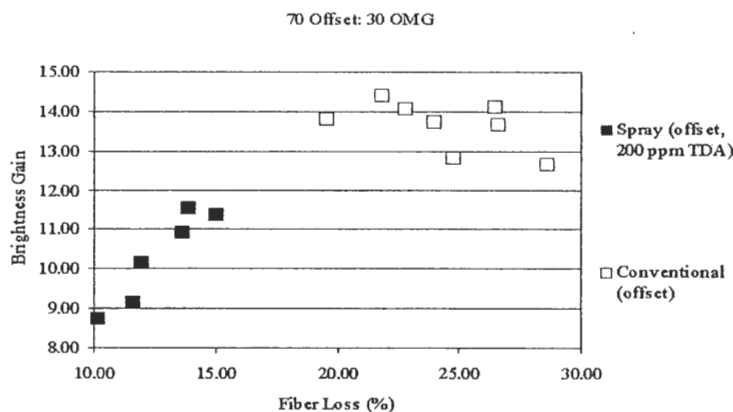
Figure 10: Deinking efficiency of a traditional blend of offset ONP and OMG. The data indicates that the surfactant spray technology does reduce fiber yield loss, however, with a slight detriment to brightness gain.

Rather than spend time optimizing the surfactant spray technology to contend with the offset ONP and OMG furnish, flexo ONP was then substituted for offset ONP without adjusting the actual flotation process (**Figure 11**). The problems encountered by mills when flexo enters with the feed furnish was immediately evident. Neither conventional nor surfactant spray deinking was able to effectively brighten the pulp. Fortunately, the ability of the latter technology to reduce fiber yield loss persisted. Inclusion of TDA-32 defoamer during the surfactant spray trials may have further reduced fiber yield losses but was not assayed to minimize variables during these initial investigations. A slight increase in brightness gain relative to that obtained through conventional chemistry (the opposite of that seen during flotation of offset ONP:OMG furnishes) suggested that the dispersed flexo ink was interacting with components of the surface application and was, thereby, retained to some degree within the froth layer. This provided hope that inclusion of a cationic collector within the spray may enhance the retention of flexo ink at the cell surface speculated in **Figure 5**.
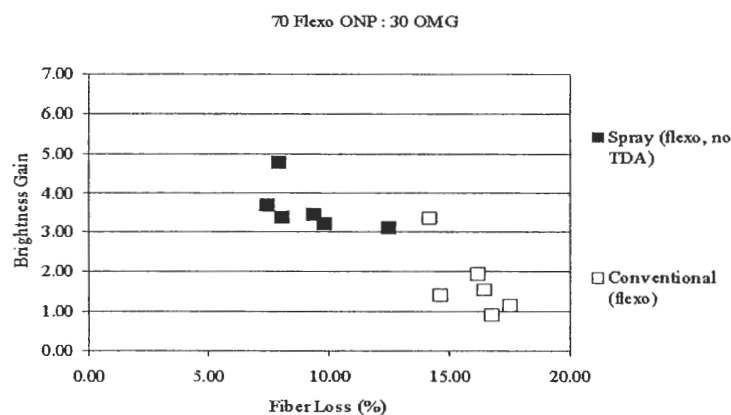
Figure 11: Flotation trials conducted with flexo ONP substituted for offset ONP.

The inclusion of flexographically-printed material within the feed furnish caused excessive foaming. Foam stabilization was presumed to be a function of the charged flexo binder within the pulp. To neutralize the inherent foaming capacity of the furnish prior to surfactant spray addition, primary flotations were conducted with varying levels of the defoamer, TDA-32. **Figure 12** suggests that froth-mediated yield losses can be reduced via defoamer addition while still maintaining comparable brightness gains. Based on these observations, surfactant spray trials for the remainder of the investigation would be conducted with 200 ppm TDA-32.
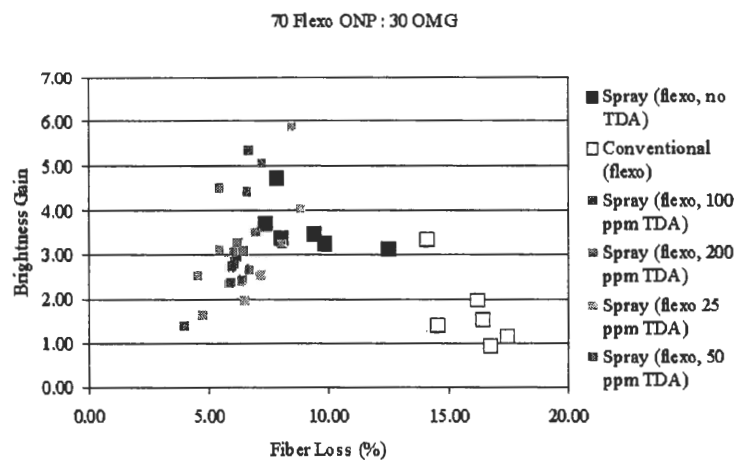
Figure 12: Flotation deinking efficiencies generated through variations in the defoamer levels within the 70:30 flexo ONP to OMG furnish.

During flotation trials involving flexo ONP, brightness pad preparation did not reveal sidedness issues. However, the filtrate from forming pads was notably dark suggesting that a considerable amount of ink was washed from the pad. At this point,

the results from an accessory investigation into means to retain flexo ink within the forming web are provided.

Pad Preparation

The results from the fixation aid trials incorporating alum are presented in **Figure 13**. From the figure, it is apparent that increasing the addition of alum to the pulp prior to pad formation actually resulted in an initial increase in pad sidedness (i.e. the standard deviation between sides increases). At the addition level of 250 ppm, the sidedness decreased. Unfortunately, the corresponding decrease in pH to neutrality made it difficult to isolate the ability of alum to affix ink to the fiber from simple precipitation of the ink onto the fiber surface in response to the reduced alkalinity. At every alum concentration used, the filtrate remained dark suggesting that a significant amount of the ink was still being washed from the pad.
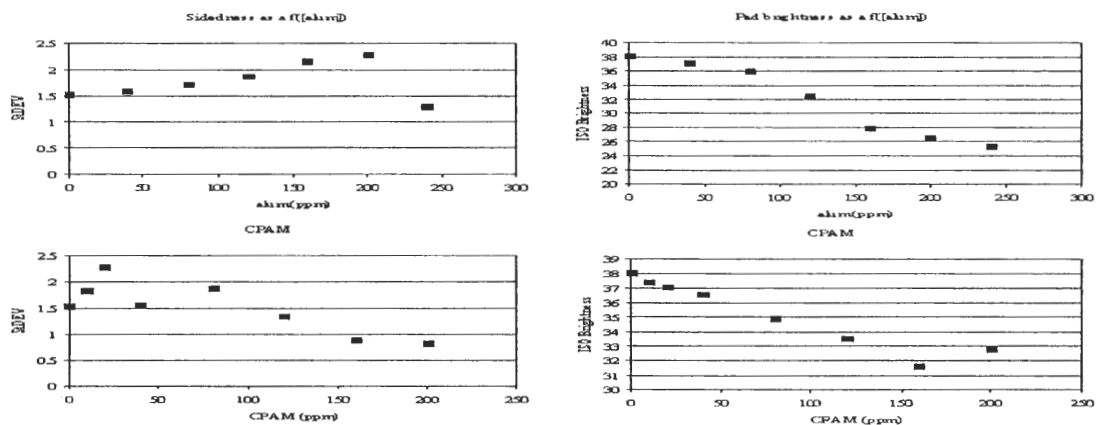
Figure 13: Results from trials designed to reduce the sidedness of pulp pads by preconditioning the pulp with alum. The standard deviation values represent the difference in values taken from one side of the pad relative to the opposite side. A decrease in pad ISO brightness was assumed to indicate enhanced retention of ink within the forming pad.

Figure 14 presents the results taken from pads preconditioned with various addition levels of CPAM. After an initial increase in sidedness, the polyelectrolyte retention aid was able to effectively reduce the sidedness to a value not obtainable via alum addition. However, the final pad brightness values remained higher than those reported during alum addition suggesting that comparably more ink was washed away with the filtrate. The dark color of the filtrate confirmed that washing was still a problem at the CPAM levels selected.
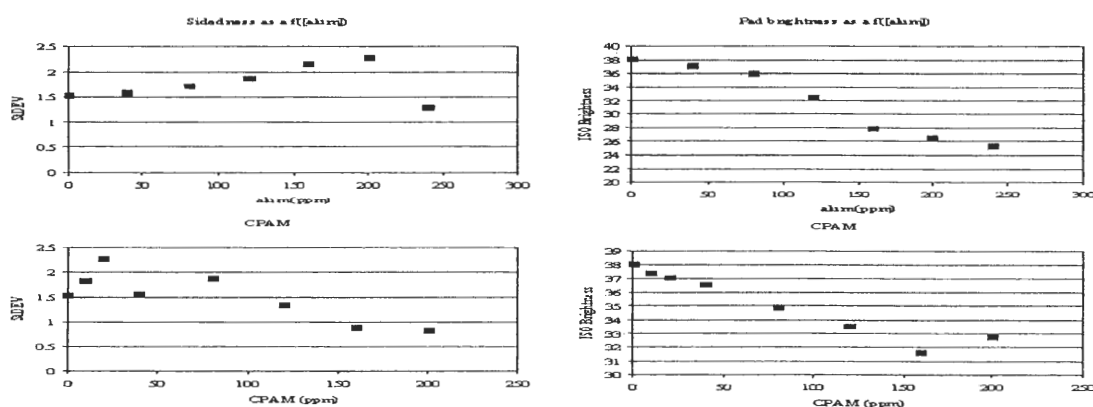
Figure 14: CPAM, although capable of reducing pad sidedness at lower addition levels than alum, does not retain as much ink in the forming pad.

Unfortunately, neither alum fixation nor cationic polyelectrolyte retention appeared to efficiently resolve the sidedness issue during pad formation. To this end, a simple retention mechanism, exploiting the ionized flexo ink binder moieties, was adopted. By simply lowering the pH of the pulp to 3 prior to pad formation, the ionized binder protonates and, thereby, precipitates onto the surface of the nearest fiber. Obviously this technique raises some additional considerations. A sudden drop in pH is

expected to affect the physical nature of ink aggregates within the sheet. Practically instantaneous precipitation of the ink onto the fiber surface precludes the formation of ink-ink complexes. Consequently, ink particles will tend to be smaller and characterized with greater surface area available for interaction with impinging light during brightness/ERIC measurements. The end result of this immobilization technique is noticeably darker pads. The probable discrepancy between pads formed both with and without classical retention aides and those formed under acidic conditions was considered negligible due to the relative, rather than absolute, nature of the investigation.

Flotation Trials

Once the technique by which to form brightness pads was optimized, the trials designed to determine the best concentration of defoamer to effectively neutralize the furnish-derived foam were repeated. The results are presented in **Figure 15**. In all instances, the detriment associated with flexo is apparent. Of significance is the fact that the addition of defoamer to the furnish prior to flotation did not reduce brightness gains in response to the reduced froth volume. In fact, the excessive use of defoamer actually appeared to augment flexo removal relative to defoamer-free conditions. Another interesting revelation is that the concurrent addition of defoamer with conventional chemistry results in the largest brightness gain (however, the yield loss remains high). At this point, a synergistic mechanism between the defoamer and either component of the calcium-fatty acid soap complex could be hypothesized to facilitate the flotation of flexo ink.

110
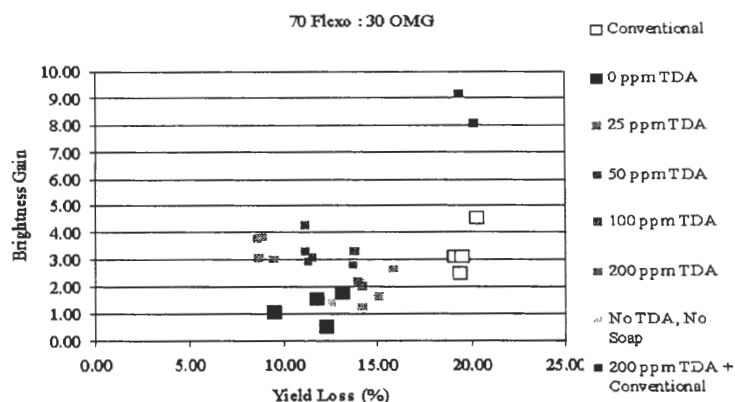
Figure 15: Deinking efficiencies determined for 70:30 flexo ONP to OMG furnish with various defoamer concentrations.

From the results of trials in which the unmodified surfactant spray technology was applied, the flotation of flexo appeared minimal. When the trials were repeated to allow brightness pad preparation by the new technique, the results indicated that the surfactant spray technology was not able to remove flexo to the same degree as conventional flotation. Notwithstanding results that indicate that the ink is not interacting with surfactants within the topmost layers of the flotation unit, the decision to include cationic polymeric collectors in the surfactant spray was upheld. Before blindly spraying such an agent onto the top of the cell, the furnish would have to undergo further analyses.

Cationic Demand

Cationic demands measured for the whole, the > 76 μm and the < 76 μm fractions of the furnish are presented in **Figure 16**. According to the results, the < 76

111

μm fraction, presumed to contain all of the dispersed flexo ink, was capable of consuming approximately 85% of the added poly-DADMAC while the > 76 μm fraction consumed the other 15%. Addition of the measured cationic demands of the two fractions resulted in a demand very close to that of the whole furnish. This served to support the significance of the measurements. The results appeared to suggest that the fiber component may be effectively neutralized via calcium addition while the flexo component still retains significant anionic charge. At this point, attempts to exploit this envisioned residual charge commenced.
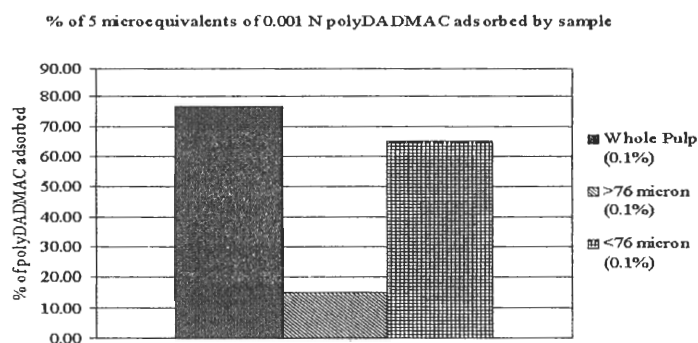
Figure 16: Cationic demand for the 100% flexo ONP furnish.

Surfactant Spray Incorporating Cationic Collector

Before adding cationic collector to the surfactant spray, a series of trials was conducted to reveal the deinking efficiency of the E-18 at various calcium chloride addition levels. The addition of calcium to secondary furnishes is known to generate considerable froth and, thereby, adversely affect yield. The multivalent ion readily

112

complexes with materials released from the paper during pulping operations. Soap-like complexes between various extractives and calcium ion may precipitate onto the surface of fibers and, thereby, reduce fiber hydrophilicity. In addition, the complexes may act as surface active agents adsorbed at the air-liquid interface and capable of lowering surface tension. The lowered surface tension favors foam stability. **Figure 17A** shows that increasing the concentration of calcium increases yield losses within the foam with minimal brightness gains. Clearly, simply neutralizing the fiber component with calcium is not a mechanism to improve the floatability of flexo ink.
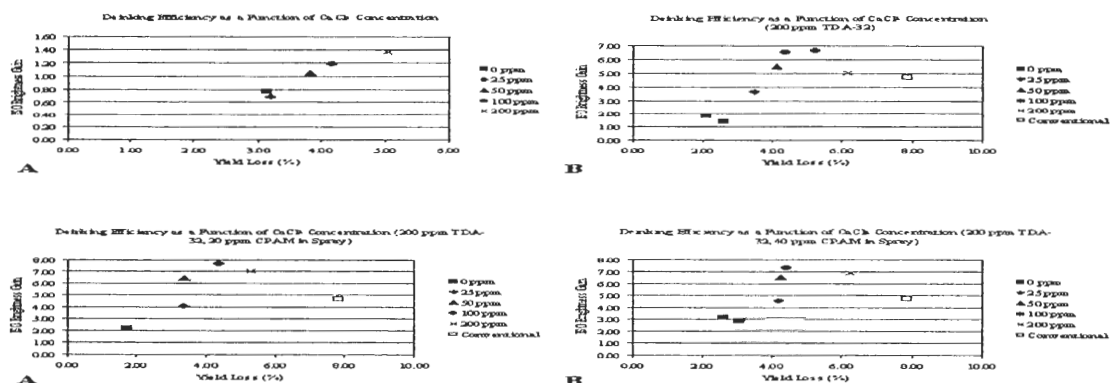
Figure 17: A. Surfactant spray flotation deinking efficiencies at various calcium chloride concentrations. B. Deinking efficiencies obtained at various calcium chloride concentrations when 200 ppm TDA-32 defoamer was included within the pulp.

When 200 ppm TDA-32 (2.0% based on the oven-dry weight of the furnish) was mixed into the 100% flexo ONP pulp prior to flotation to counteract the calcium-mediated foam, some notable results were obtained (**Figure 17B**). At this specific concentration of TDA-32, increasing the calcium levels appeared to enhance brightness gains relative to those obtained without the defoamer. The significance of this increase

was underscored by performing a flotation with the conventional calcium-soap chemistry. Expectedly, the inclusion of defoamer, by reducing froth generation, kept yield losses below those of conventional flotation (~50% less). Surprisingly, the defoamer, at 100 ppm $CaCl_2$, was able to generate an approximately 2 ISO brightness point gain beyond that of conventional chemistry. The results from these trials suggest that the selectivity within the flotation unit increases in response to a synergetic mechanism existing between the defoamer and the calcium. However, before final conclusions stemming from the above observations were drawn, flotation trials incorporating cationic collector into the surfactant spray were conducted.

Figure 18 presents the results from flotation trials conducted with CPAM included within the surfactant spray. Again the increase in brightness to yield loss ratios relative to conventional chemistry was apparent. In addition, the optimal hardness for maximum ink flotation remained 100 ppm calcium chloride.
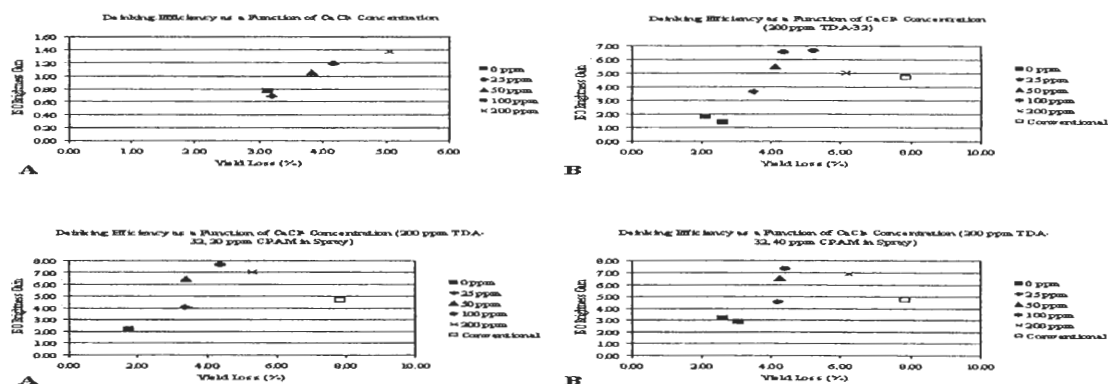
Figure 18: A. Deinking efficiencies obtained via application of surfactant spray incorporating 20 ppm CPAM. B. Similar data obtained with 40 ppm CPAM within the spray.

Since the trials to determine the effectiveness of cationic collector applied as a spray were conducted in random order, the significance of the findings would not be determined until the results were condensed into a single graph (**Figure 19**). Initially, the brightness increase obtainable via the addition of collector-containing spray permitted speculation that the original hypothesis was accurate: collection of flexo ink into floatable aggregates was occurring near the froth-liquid interface. However, further examination of the results led to the conclusion that indefinite interactions between the defoamer, calcium chloride and the dispersed flexo ink were, in fact, responsible for the brightness increase. The addition of CPAM onto the surface of the cell appeared superfluous. However, neither TDA-32 nor calcium chloride alone could generate the brightness increases obtained when both were present. The existence of an optimal combination of the two for maximum ink removal was reflected in all trial sets in which the defoamer was present.
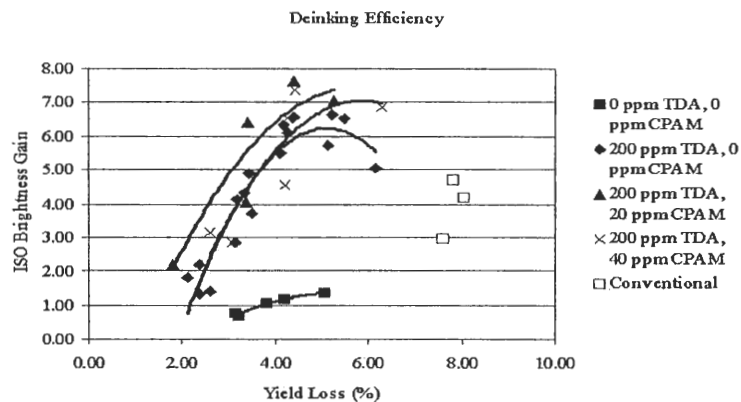
Figure 19: Superimposition of the results from trials designed to detect improvement in deinking efficiency of 100% flexo ONP by inclusion of cationic collector (CPAM) within the surfactant spray.

Confirmation of the phenomenon was achieved by repeating the flotation trials conducted with calcium chloride and defoamer. **Figure 20** presents the results from these trials combined with the initial results. The data appear to leave little doubt that the system does improve the deinking efficiency of the E-18. The initially observed optimal calcium chloride concentration (i.e. 100 ppm) for optimal deinking performance with 200 ppm TDA-32 was repeatedly confirmed during these trials.
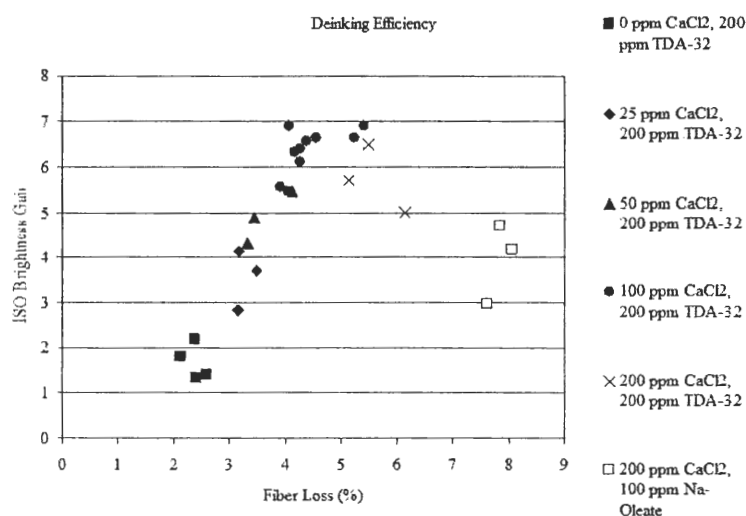
Figure 20: Deinking efficiencies from flotation trials conducted in the presence of 200 ppm TDA-32 and various concentrations of calcium chloride. Results from conventional flotation trials are included for comparison.

Currently, the most widely accepted means by which to gauge deinking efficiency is through the measurement of residual ink remaining within brightness pads formed from floated pulp. By comparison of the effective residual ink concentration (ERIC) between pre-floated and post-floated pulps, efficiencies can be ascribed to various deinking conditions, processes, and/or chemistries. **Figure 21** presents the

results from pads formed from pulps floated with various proportions of TDA-32 and calcium chloride as well as by conventional calcium soap chemistry. The unfloated pulp was determined to have ERIC values in excess of 5000 ppm. At values of this magnitude, the measurement of ERIC becomes far less accurate. Nonetheless, some interesting results are evident as the concentration of calcium increases.
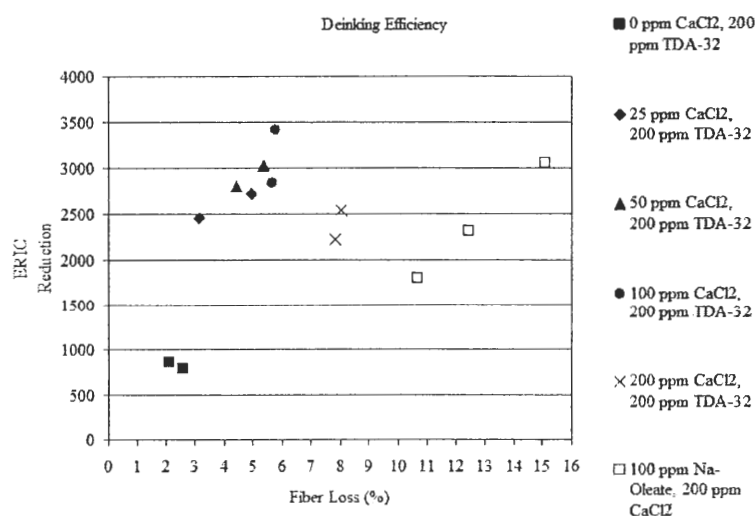
Figure 21: ERIC values obtained from pads prepared from post-floated pulps. Values are expressed as a measure of the decrease or reduction in ERIC during the flotation relative to the unfloated furnish.

Immediately evident is the tendency for large reductions in measurable ERIC as a function of calcium chloride concentration. In this case, ERIC reduction is closely linked to the brightness gains reported in **Figure 20**. In fact, the observed relatedness between ISO brightness and ERIC values taken from these pads appears to contradict reports that the two cannot be used interchangeably to quantify deinking efficiency. This observation can be explained by considering that the boundary conditions within

117

which ERIC measurements are believed a more accurate measure of deinking efficiency than brightness measurements. A nonlinear relationship exists between reflectance (i.e. brightness) and ink concentrations (i.e. ERIC) typically encountered in deinking mill furnishes. At these low levels of ink, even slight variations in concentration can significantly affect the measured brightness/ERIC values. However, at higher ink concentrations (i.e. > 1000 ppm), a linear, inverse relationship between brightness and ink concentration begins to emerge. The resultant slope closely parallels that obtained by plotting ERIC values as a function of ink concentration. Since the model furnish used during the entire investigation was composed of 100% flexo ONP, the ERIC values of the unfloated pulp were expectedly high (>5000 ppm). Even under the most optimal deinking conditions employed (i.e. 200 ppm defoamer, 100 ppm calcium chloride) the final ERIC values remained greater than 1000 ppm. To this end, ISO brightness gain determined from the analysis of brightness pads was determined to be an acceptable means to gauge deinking efficiency. No additional ERIC values would be taken for the remainder of the investigation.

Before adapting the investigation to elucidate the fundamental mechanisms behind the observed flexo-defoamer-calcium chloride interaction, additional trials were conducted to evaluate the system with respect to commercial deinking additives purported to contend with flexo ink. **Figure 22** presents the results from flotation trials conducted with manufacturer recommended doses of their respective deinking agent. For comparison, the results from the calcium-defoamer trials are included. Immediately evident is the inability of either commercial chemistry to replicate the brightness

gain/yield loss reductions of the new system. In fact, both chemistries assayed appeared to preferentially float fiber resulting in an unacceptable loss of yield across the cell. Increasing the calcium concentration did little more than enhance the volume of foam generated during the trial.
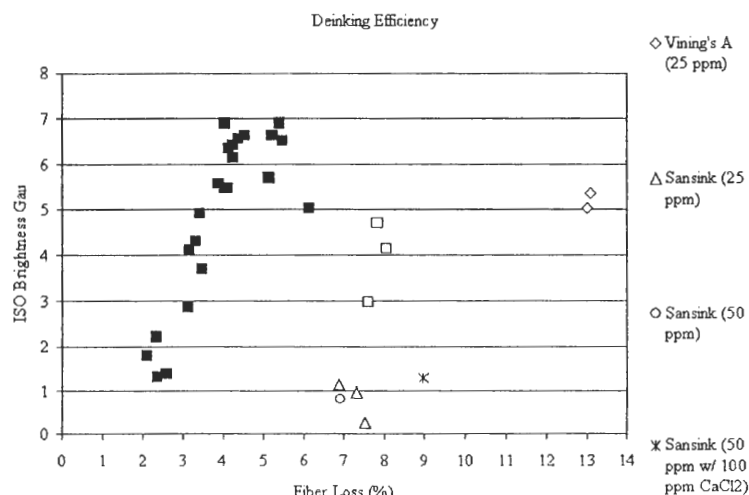
Figure 22: Deinking efficiencies obtained with commercial deinking agents compared to the TDA-32/calcium chloride chemistry (■).

Agents specifically designed to enhance the flotation rate of commercial inks were not capable of achieving the same value-added benefits afforded by the apparent defoamer/calcium chloride synergy. The composition of the defoamer and the corresponding contribution to the observed deinking behavior was then brought into question. **Figure 23** presents the results from trials conducted with a non-siloxane defoamer, ECCO P-048 substituted for the siloxane-based defoamer, TDA-32. Comparable brightness gains/yield loss reductions indicate that the phenomenon may not be unique to TDA-32 addition. Rather, the observed "collecting" behavior may be

119

primarily dependent upon the presence of an adequate liquid-liquid interface upon which the flexo ink particles can interact. Further investigation into the fundamental physicochemistry of the interface existing between various oils and aqueous suspensions of dispersed flexo ink was considered necessary before a feasible mechanism could be forwarded.
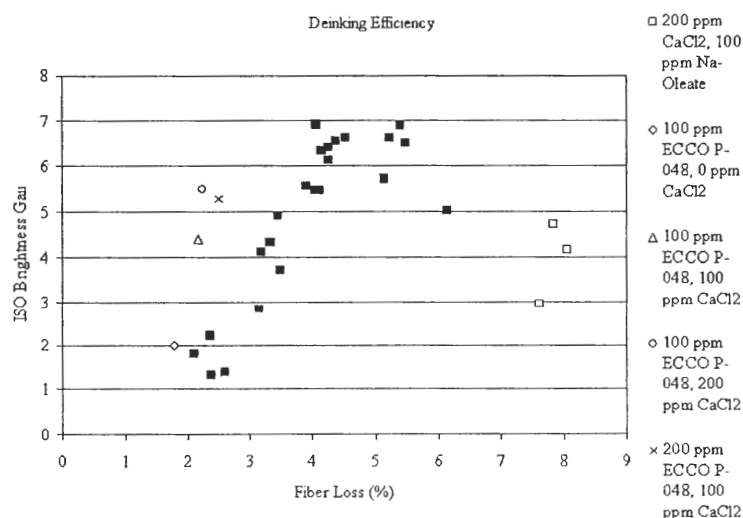
Figure 23: Deinking efficiencies obtained by substituting a non-siloxane defoamer, ECCO P-048, for the siloxane-based defoamer, TDA-32. Results from trials incorporating TDA-32 at various calcium addition levels are included for comparison (■).

DISPERSED FLEXO INK CHARACTERIZATION

Before any attempt to define the mechanism by which the 100% flexo ONP furnish is brightened via defoamer and calcium chloride addition, a fundamental approach was adopted to define the individual components of the system. Possibly the most important of these components is the suspended flexo ink particle and its *in situ* behavior during the flotation trials. Numerous accounts are present within the literature linking the general unfloatability of the ink to its diminutive size and robust colloidal stability. A common theme to all published accounts is the indifference of dispersed flexo ink to increased calcium levels in the presence of fiber. This is not to say that aggregates are not forming. Rather, the ultimate aggregate size, dictated by shearing forces inherent to the aerated flotation unit, remains too small to be effectively floated.

The inability of calcium alone to enhance flotation was supported during the original flotation trials (see **Figure 19**). The results from particle size measurements presented in **Figure 24** clearly indicate that aggregation is not occurring at calcium chloride levels employed during the flotation trials (even within fiber-free conditions). The inclusion of 200 ppm TDA-32 within the pressate actually appeared to hinder the formation of aggregates at the high calcium chloride addition levels. Justification for this observation was provided following detailed analysis of the defoamer.
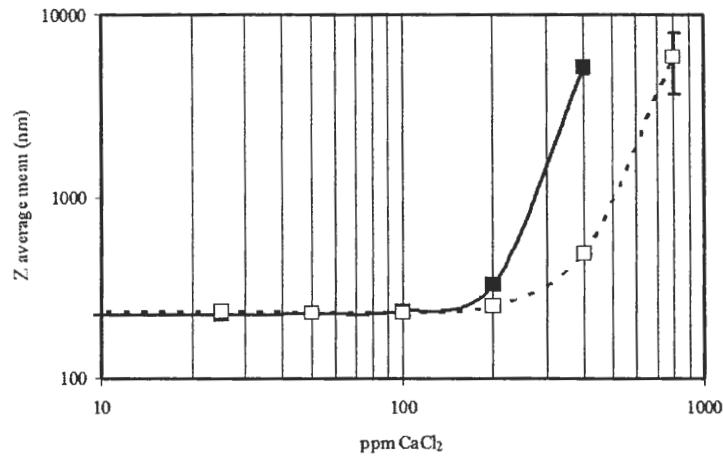
Figure 24: The calculated hydrodynamic diameter of dispersed flexo ink particles as a function of calcium chloride concentration within the pressate (■) and within the pressate containing 200 ppm TDA-32 (□).
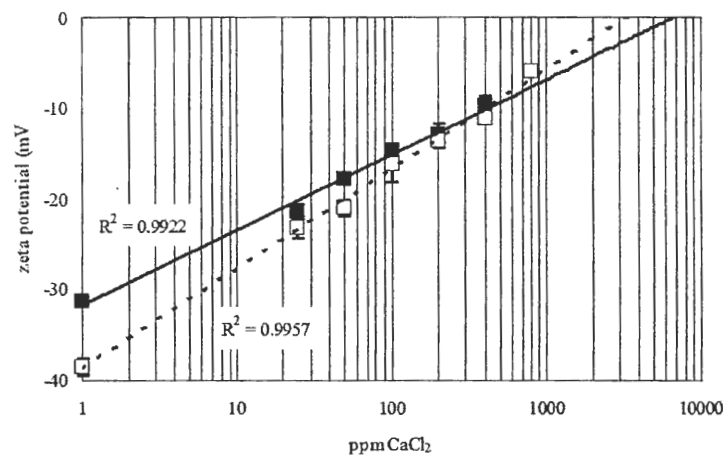
Figure 25: Zeta potential of flexo ink particles suspended within the pressate both without (■) and with (□) the inclusion of 200 ppm TDA-32.

The results from the zeta potential measurements taken from pure pressate and pressate containing 200 ppm TDA-32 are presented in **Figure 25**. Although not realized during the measurements, extrapolation of the trend line indicated that the point of zero

charge (pzc) for flexo particles in the absence of defoamer would require a concentration of more than 6000 ppm or 54 mM calcium chloride. The addition of TDA-32 to the pressate lowered the calcium chloride concentration required to reach the pzc to approximately 3000 ppm or 27 mM.

At first, the results from the particle size measurements and the zeta potential measurements appear counterintuitive. At calcium chloride concentrations that promote aggregation of flexo ink particles (i.e. 200 ppm), the particles continue to possess significant surface charge (i.e. a zeta potential of > -10 mV). Surface charges of this magnitude would be expected to resist aggregation through simple electrostatic repulsion. This discrepancy may be explained within the framework of factors that contribute to colloidal stability.

Stabilization of colloidal particles with complex, dynamic geometries (i.e. ink particles with adsorbed polymeric binders) is defined by two components: electrostatic and steric repulsion. Compression of the electrostatic double layer of dispersed flexo ink particles is a simple matter of increasing concentration and/or valence of the counterion within the bulk suspension. However, as this component to colloidal stability is tempered, the flexo ink particles may continue to resist aggregation due to steric repulsion between polymeric resins adsorbed at the particle surface[1]. Conversely, the steric component to colloidal stability may be neutralized via the addition of sufficient counterion. In this latter case, the ink particle may still retain residual surface charge while, simultaneously, lose colloidal stability. Electrosterically stabilized particles such as dispersed flexo inks tend to require high electrolyte concentrations to neutralize both

123

components and promote aggregate formation. The ability of flexo ink to form aggregates while still maintaining considerable surface charge implies that the steric component plays a key role in maintaining colloidal stability of the particles. However, notwithstanding the mechanism by which flexo ink particles were aggregated via calcium chloride addition, the levels required were much greater than those experienced during the flotation trials. Floatable aggregates were not forming within the unit during the trials.

In short, the results obtained during spray surfactant flotation trials with calcium chloride as the only additive are reasonable. Calcium-mediated formation of flexo-ink aggregates with surface chemistries and/or dimensions amenable to flotation is not occurring within the aqueous bulk phase of an aerated pulp during the trials.

DEFOAMER CHARACTERIZATION

Concluding that specific interactions between calcium chloride and dispersed flexo ink particles were unlikely to enhance the flotation rate seen during trials, the investigation then addressed the defoamer. Marketed as a nonionic, siloxane-based defoaming agent, the chemistry of TDA-32 emulsion droplets was not expected to be influenced by increased levels of calcium chloride. In fact, the manufacturer-purported conveniences associated with the defoamer include a general indifference to pH level and water hardness. However, in view of the apparent interaction between flexo ink, defoamer and calcium chloride documented during the trials, the possibility of calcium-mediated defoamer modification could not be immediately rejected.

Microscopy

Before tailoring the investigation to reveal calcium-defoamer interactions, direct observation of emulsion droplets was conducted through conventional light microscopy. Analysis of the resulting digital stills taken of the emulsion yielded the bin results seen in **Figure 26**. Diameters from 7 to 25 μm with an average of 13.26 μm were measured from a total sample number of 390 droplets. Direct microscopic examination of the defoamer droplets revealed the presence of "vesicles" within the oil phase. Although the composition of the dispersed phase within the "continuous" phase of the oil droplet is not known, personal conversation with the manufacturer permits speculation that they are aqueous in nature. As is revealed later, the existence of aqueous droplets within the TDA-32 droplets (w/o emulsion) may be used to justify one of the potential mechanisms for flexo ink collection.

TDA Droplet Size
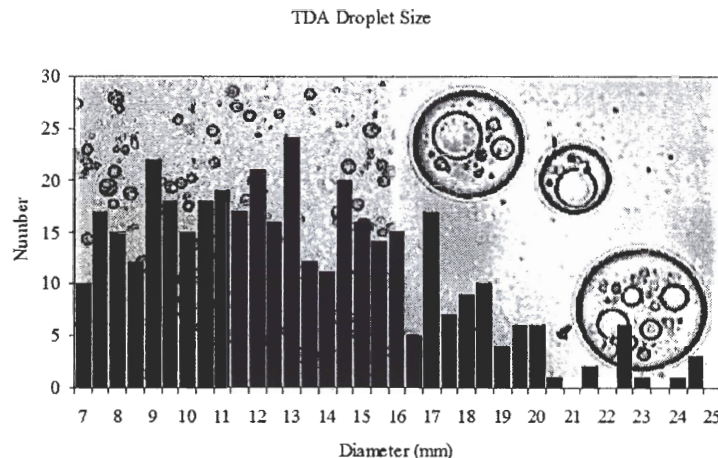
Figure 26: Analysis of digital images taken of a 200 ppm suspension of TDA-32 emulsion provided these droplet diameter bin results. The inset provides two separate magnifications of the droplets.

Charging of the Emulsion Droplet

Although TDA-32 is purportedly nonionic, the ability of an oil droplet to carry a surface charge within an alkaline environment has been demonstrated[58]. The observed charging of hydrocarbon oil droplets at high pH values is attributed to hydroxyl ions, generated during normal dissociation-association events within the continuous water phase. Hydroxide anions tend to be less hydrated than hydrogen or hydronium cations. Thus, the preferential migration of hydroxide from the bulk aqueous phase towards the interface is viewed as thermodynamically favorable. Since the flotation trials were conducted at a pH of 8.5, the potential exists for electrostatic interactions between divalent calcium ion and the anionic oil/water interface. Adsorbed calcium ion on the surface of emulsion droplets could, conceivably, affix anionic flexo ink particles

126

through a "bridging" effect. Not only would such a scenario require demonstrated pH-mediated surface charging, the consumption of calcium by an aqueous suspension of TDA-32 would have to be confirmed.

Figure 27 presents the results from zeta potential measurements taken from a 200 ppm TDA-32 suspension as a function of pH. Immediately apparent is the tendency of the emulsion droplets to become more anionic as the alkalinity of the system increases. Although the ultimate surface charge as a result of the increase is slight compared to the overall anionic charges of other components within the furnish, the results do not completely negate the possibility of electrostatic interactions between calcium ion and the defoamer surface. Having confirmed charging of the oil droplet surface, the potential for consumption of calcium by the defoamer was examined.

Zeta Potential of 200 ppm TDA-32 w/ 25 ppm CaCl₂ as a Function of pH
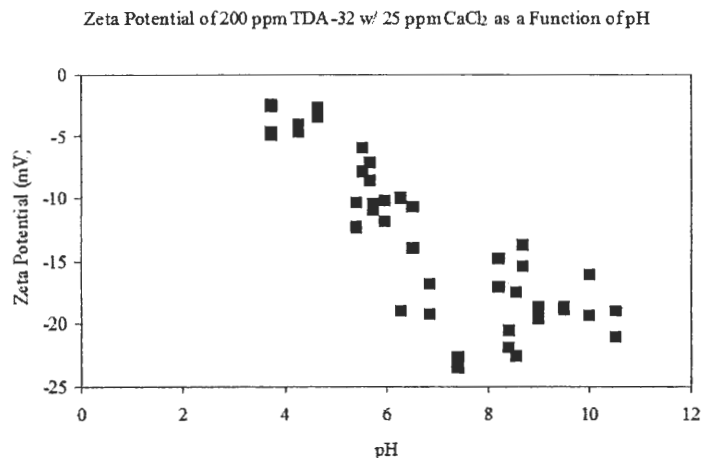
Figure 27: Zeta potentials calculated for TDA-32 emulsion droplets as a function of suspension pH.

Presumably, adsorption of calcium ion at the oil/water interface would reduce the amount of electrolyte within the bulk phase capable of contributing to overall conductance. Gradually increasing the calcium ion concentration while monitoring system conductivity should indirectly yield the amount of calcium consumed (i.e. removed from the aqueous bulk phase) per given concentration of TDA-32. At calcium levels below the amount required to screen the available surface charge of the emulsion, the conductivity should remain relatively constant. The point at which the calcium ion addition leads to an excess was presumed to be marked by a significant increase in conductivity. **Figure 28** presents the results from the first trial in which calcium levels went from 0 to 160 ppm. Unfortunately, the electrolytic strength of the calcium chloride stock solution was too high to reveal what appeared to be an extremely slight change in conductivity at low levels. Immediately evident, however, is that the calcium consumption by the 2000 ppm TDA-32 suspension is small if not nonexistent.

Conductivity f([CaCl$_2$]) w/ 2000 ppm TDA-32
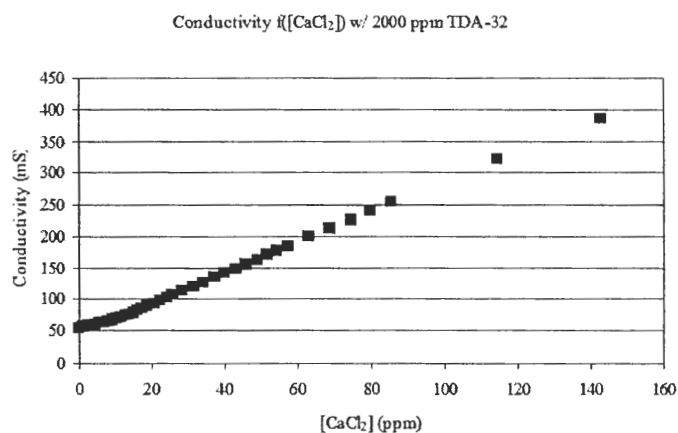
Figure 28: Conductivity of 2000 ppm TDA-32 suspension as a function of calcium chloride concentration.

Although more academic than relevant to the investigation, the strength of the calcium chloride stock was reduced in order to detect the presence of extremely slight changes in conductivity. **Figure 29** shows that there does appear to be a calcium chloride concentration (~9 ppm) above which the conductivity of the suspension begins to increase rapidly. Considering that the suspension contains 2000 ppm TDA-32, this minor consumption of calcium cannot be used to support the concept of specific interactions occurring between calcium and defoamer. However, the results do not completely negate the possibility of such an interaction. The ability of calcium ion, theoretically adsorbed on the surface of the emulsion droplets, to contribute to conductivity remains unknown.
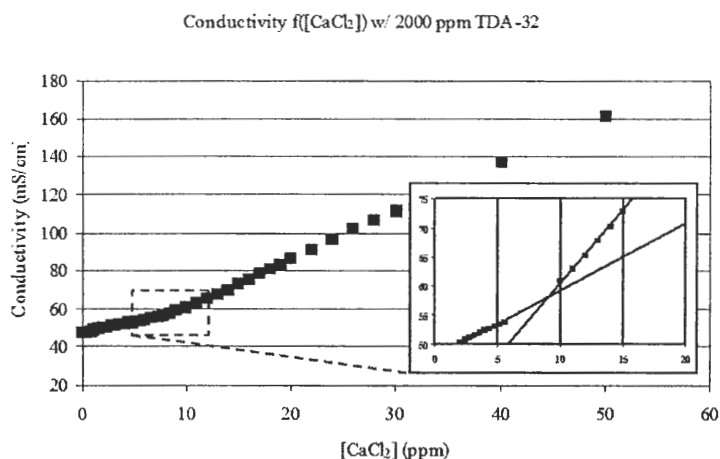
Figure 29: Conductivity of a 2000 ppm suspension of TDA-32 as a function of calcium chloride concentration. The inset provides a magnified view of the point at which the conductivity begins to apparently increase.

In light of the results from the calcium consumption experiments, the possibility of flexo ink particle affixation to the emulsion droplet surface via divalent ionic bridge formation appears remote. However, since TDA-32 droplets were shown to gain some amount of anionic character under alkaline conditions, cationic demand measurements were performed on suspensions of the defoamer. **Figure 30** presents the cationic demand of the 200 ppm TDA-32 suspension as a function of calcium chloride. Increasing the charge-screening calcium chloride levels was expected to reduce the amount of cationic polyelectrolyte required to reach the end point of neutrality. Ironically, cationic demand actually increases with calcium chloride concentration. Although the results appeared counterintuitive at first, a potential explanation for the observed response stems from consideration of mechanical shearing action within the autotitrator.
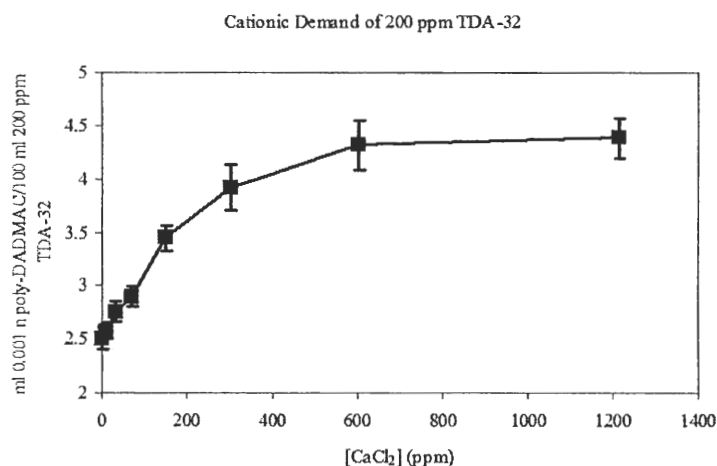
Figure 30: Cationic demand of a 200 ppm TDA-32 suspension (pH 8.5) as a function of calcium chloride concentration.

To make the cationic demand measurements more applicable to the present investigation, anionic polymer (PVSK) was added to the 200 ppm TDA-32 suspension to mimic desorbed flexo ink binder. **Figure 31** shows that the addition of the anionic polymer expectedly increases the amount of cationic polyelectrolyte required to satisfy the cationic demand. However, of immediate note is the apparent surge in cationic demand at a calcium chloride concentration of 200 ppm. The reason for this observation is not clear.

Cationic Demand of 200 ppm TDA-32 in 5 ml of 0.001 n PVSK
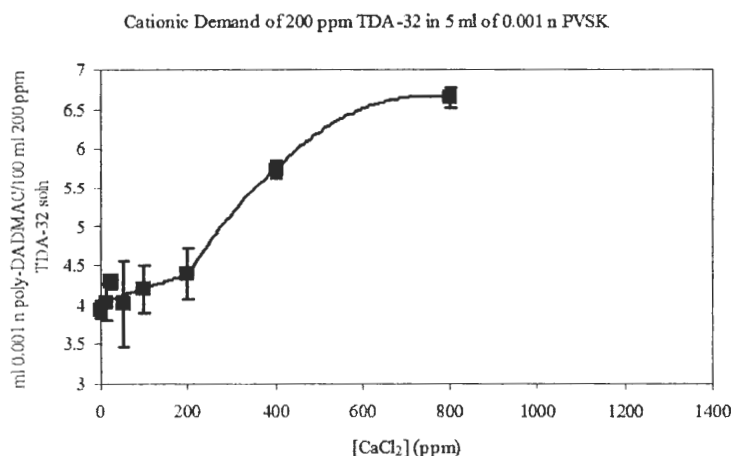
Figure 31: Cationic demand of a 200 ppm TDA-32 suspension as a function of calcium chloride concentration. 5 ml of 0.001 n PVSK was premixed with the suspension prior to titration to represent desorbed flexo binder.

Analysis of Films Formed from TDA-32/Calcium Chloride/Pressate

Another means to ascertain calcium chloride-mediated modification of the physicochemistry of the TDA-32 emulsion droplet was through direct analysis of films containing the two components. **Figure 32** presents the IR adsorption spectra taken from a film prepared from TDA-32 suspensions with varying concentrations of calcium

chloride. Although care was taken to ensure the removal of all water from the film prior to adsorption measurements, the presence of a strong band at 3412 cm⁻1 indicated considerable water-derived hydroxyl functionalities. Rather than chemically alter the polydimethylsiloxane structure of the oil, increasing the calcium levels only appeared to enhance the ability of the film to adsorb ambient moisture[p]. This observation, once again, appears to support the lack of specific interactions between the defoamer and calcium.
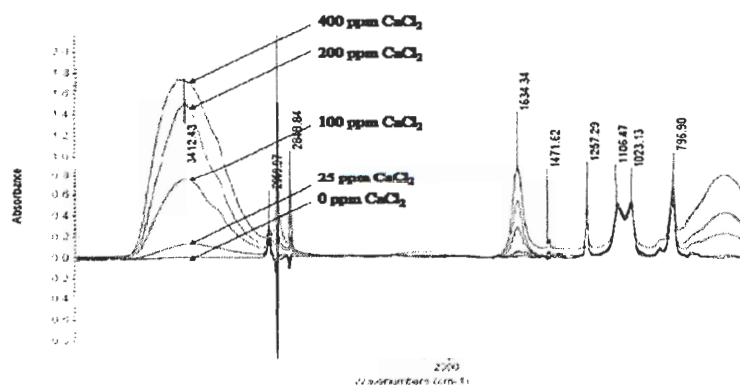
Figure 32: FT-IR adsorption spectra taken from TDA-32 films prepared with varying concentrations of calcium chloride.

---

[p] A subtle change in absorbance at 1634 cm-1 in response to increased calcium chloride levels may arise from C=O deformation oscillations. This may indicate that carbonyl groups are formed from some component of TDA-32 but, due to the proprietary nature of the defoamer, the exact component responsible is not known.

In the event that increasing calcium chloride concentrations influence the film forming characteristics of TDA-32 emulsions, contact angle measurements were taken from the resultant film surface. The results, presented in **Figure 33**, are in agreement with the observations made during FT-IR analysis of the film. The reduced contact angle obtained from TDA-32 films as electrolytic strength of the initial suspension increases is a consequence of readily hydratable, dissociated calcium and chloride ions dispersed within the film. As an inert salt, the calcium chloride simply increases the wettability of the TDA-32 film.
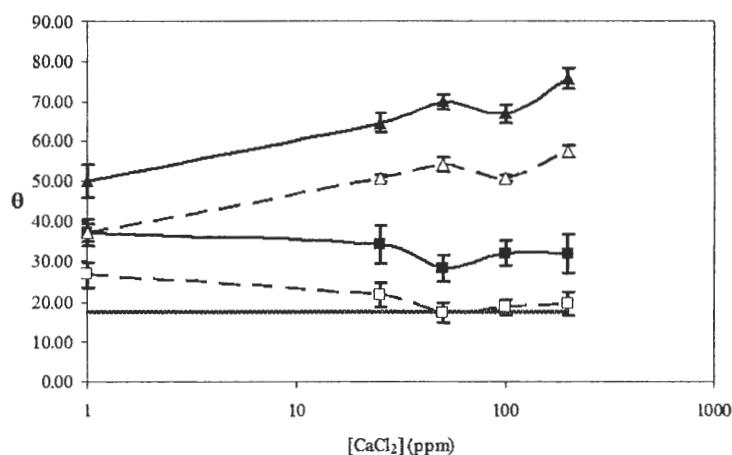
Figure 33: Contact angle measurements taken from films as a function of calcium chloride concentration. The bold, horizontal line is the average contact angle taken from a water droplet on the glass microscope slide. ■ and □ represent contact angles obtained from films prepared from aqueous suspensions of 200 ppm TDA-32 at 0 and 5 seconds after initial contact with the droplet, respectively. ▲ and △ represent contact angles taken from pressate containing 200 ppm TDA-32 at the respective 0 and 5 second time intervals.

When TDA-32 was included within pressate films, the contact angle actually increased with calcium chloride addition. Immediately, this was presumed to indicate that all three components (i.e. defoamer, calcium chloride and flexo ink particles) were

essential before high contact angles could be obtained. Increasing the contact angle of an ink-containing aggregate (presumed to constitute the bulk of the film) corresponds with an enhanced probability for successful aggregate-air bubble interactions.

To confirm the requisite that all three components be present in order to generate aggregates (i.e. film) with relatively high contact angles, contact angles were taken from films prepared from pressate and calcium chloride. In the first set of trials, contact angles of water droplets against the pressate/calcium chloride films were measured. In the second set, a 200 ppm TDA-32 suspension was substituted for the water droplet. Should the contact angle of water against the film reduce with increasing calcium chloride levels (as seen in **Figure 33**), perhaps the inclusion of the defoamer within the droplets would reduce the apparent wettability of the film.

dH2O or 200 ppm TDA-32 onto film formed from pressate and CaCl2
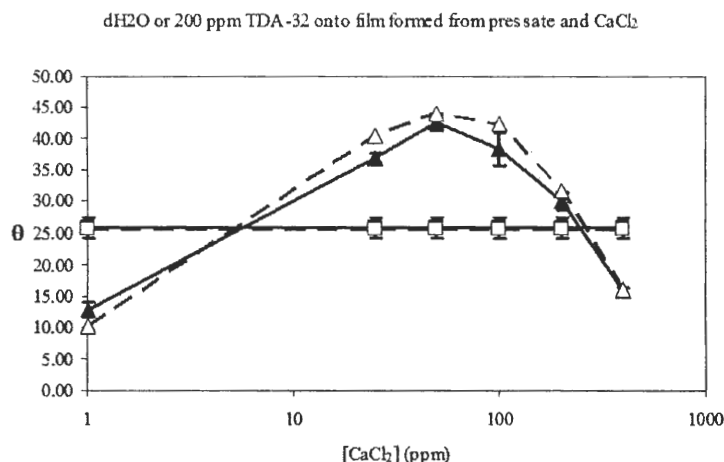
Figure 34: Contact angles obtained from films prepared from pressate and various concentrations of calcium chloride. ■ and □ represent drops of water and 200 ppm TDA-32, respectively, on the glass microscope slide. The contact angles determined from the film surface are represented by ▲ (pure water) and △ (200 ppm TDA-32).

However, **Figure 34** indicates contact angles taken with water droplets were not significantly different than those taken with the 200 ppm TDA-32 droplet. Unfortunately, the maximum contact angles taken from the pressate/calcium chloride films were still lower than those taken from the pressate/TDA-32/calcium chloride films. Although the defoamer within the film is not absolutely necessary for increasing the contact angle, its presence does result in a greater increase in the angle relative to defoamer-free films.

An apparent optimum concentration of calcium chloride exists to achieve maximum contact angle values. The significance of this revelation stems from the fact that a similar "optimum concentration" of calcium chloride for maximum deinking efficiency was encountered during the initial flotation trials. An explanation for this observed maximum draws from the charge screening action of the divalent calcium ion. At low calcium levels, 100% of the ion is adsorbed by the pressate components (i.e. dispersed flexo ink particles). This serves to reduce the surface charge and, therefore, the wettability of the film surface. At the optimum calcium concentration, all potentially hydratable groups within the pressate film are "shielded" by adsorbed calcium ion. At this point, contact angles taken from the film surface are greatest. Above this calcium addition level, the divalent electrolyte begins to impart a cationic charge to the aggregates which tends to increase wettability.

Superposition of **Figure 33** and **Figure 34** suggests that some manner of film modification, both with and without TDA-32, occurs at a calcium chloride concentration of 50 ppm (**Figure 35**). The discrepancy between this optimal

concentration and the optimal concentration of 100 ppm observed during the flotation trials is expected. Fiber and fines, consuming a certain amount of calcium ion in a whole furnish, were expected to decrease the amount of calcium chloride available to interact with the pressate fraction of the furnish.
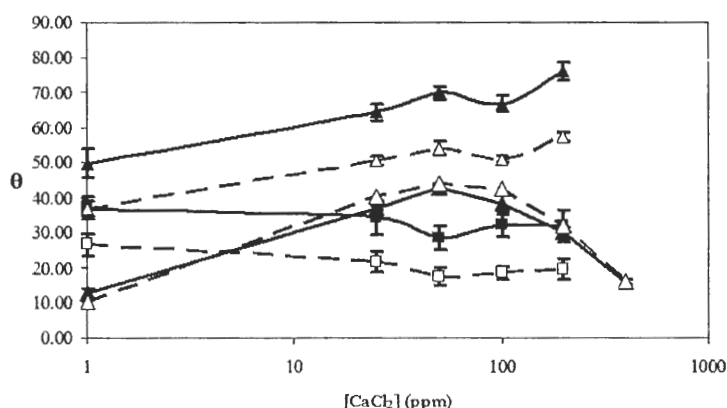
Figure 35: Superposition of **Figure 33** and **Figure 34** reveals calcium-dependent maxima/minima during contact angle measurements of films.

Defoamer Kinetics

The primary activity of defoamer when suspended within a medium is to rapidly spread across the surface of an air bubble. If chemical interactions between calcium and the defoamer exist, the kinetics of spreading behavior may be modified. TDA-32 emulsion droplets are formulated to efficiently adsorb onto and rapidly spread across the typical air-water interface. While the requisite for maximum interfacial adsorption is patently obvious, the need for rapid lateral diffusion of the defoamer across the air-water interface must be explained within the framework of foam stabilizing phenomena. In brief, certain surface active materials adsorbed at the air-water interface may stabilize

136

an air bubble rising through the medium against coalescence with other air bubbles. Usually the stabilization effect is a result of electrostatic repulsion existing between similarly-charged hydrophilic head groups located at the surface of both air bubbles. The magnitude of repulsion dictates the ultimate thickness of lamellae within a foam generated from the air bubbles. Water drainage from the lamellae is finite since a specific volume must remain within the film to hydrate the ionized head groups. Through water-based cohesive forces, hydration and electrostatic repulsion, thinning of the lamellae is limited and the foam is stabilized against collapse.

Following adsorption, rapid lateral diffusion of the defoamer across the air-water interface physically displaces these foam-stabilizing agents. Due to the nonionic nature of the defoamer, no electrostatic repulsion exists between air bubbles or within the lamellae of the ultimate foam. Coalescence of air bubbles coated with the defoamer occurs readily and the foam either collapses or does not form at all. Unfortunately, defoamer droplets, as a consequence of spreading across an interface, cannot return to the bulk phase. For continued defoaming action, the level of defoamer must be constantly refreshed.

Although spreading behavior may be expected to change in response to chemical modification of the defoamer, the rate and extent of spreading may be influenced by other factors as well. For example, rather than chemically interact with the TDA-32 droplet, dissociated calcium and chloride ions may modify the physicochemical properties of the medium in which the droplet is suspended. According to Harkins' equation to determine the *initial spreading coefficient* (S) of an oil droplet at

an air/water interface (**Equation 3**), the kinetics associated with spreading are a function of three separate surface free energies present within the system: at the air/"water" interface (γ_{aw}), at the oil/air interface (γ_{oa}) and at the oil/"water"[q] interface (γ_{ow})[59]. When S is positive, spreading will occur spontaneously while a negative value indicates that the droplet simply forms a "lens" at the interface with minimal to no spreading.

$$S = \gamma_{aw} - (\gamma_{oa} + \gamma_{ow})$$

Equation 3: Harkins' equation to predict the interfacial spreading behavior of an oil droplet

According to the Harkins' equation, calcium chloride can enhance spreading behavior without directly affecting the chemistry and, therefore, the surface free energy of the oil droplet (γ_{ow} and/or γ_{oa}) by increasing γ_{aw}. This revelation is significant since no evidence of chemical modification of the defoamer in the presence of calcium chloride has been documented during the investigation. Electrolytes have been known to actually increase the surface tension of aqueous mediums (γ_{aw}) by interacting with solvating molecules (e.g. water) within the medium more strongly than the solvent molecules can interact between themselves[60]. Since the electrolytes tend to remain within the bulk of the medium, attractive forces drawing solvating molecules back into

---

[q] "Water" refers to the aqueous phase of the system rather than pure water.

the bulk are more extreme than in the absence of electrolyte. Consequently, the shrinking forces (i.e. surface tension) at the air-solvent interface are greater than in the absence of electrolyte.

Notwithstanding the means by which it occurs, an increase in γ_{aw} correlates with an enhanced spreading coefficient with the proviso that γ_{oa} and γ_{ow} remain relatively constant or even decrease. Since no data was collected by this point in the investigation that would suggest a change in either of these properties as a function of calcium chloride concentration, they were presumed constant during the initial surface tension analyses.

The results presented in **Figure 36** suggest that the ability of calcium and chloride ion to affect the surface free energy of an air-water interface is largely concentration dependent. Increasing the calcium chloride concentration from 0 to 50 ppm gradually increased the measured surface tension. Interestingly, a sharp increase in surface free energy was observed as the calcium chloride concentration increased from 50 to 100 ppm. A possible explanation for these observations stems from the concept of solvation-mediated "molecular ordering" within the bulk aqueous phase. The gain in surface free energy (i.e. increased surface tension) at low ionic strengths may be attributed to water molecules preferentially solvating electrolytes within the bulk aqueous phase. However, as the ionic strength of the aqueous phase increases, more water molecules are required to solvate the additional electrolytes. As water molecules orient themselves to solvate the electrolytes, the order within the system begins to increase. From a thermodynamic perspective, the resultant decrease in the entropy of

the system ($\Delta S < 0$) corresponds with an increase in system free energy (G). This increase in free energy may manifest as an increase in surface and/or interfacial tension. Below a calcium chloride concentration of 50 ppm, the contribution of solvation-mediated ordering of water molecules to the ultimate surface free energy is probably insignificant. However, above this concentration, the entropically unfavorable ordering of water molecules is amplified by the ordering of solvated ions. As the ionic strength increases, repulsion between similarly charged electrolytes limits spatial mobility within the medium resulting in a structured lattice of solvated ions. At 50 ppm calcium chloride concentration, the decreased entropy begins to significantly affect the surface free energy. Above 100 ppm, calcium and chloride ions may disrupt the balance between water molecules and electrolyte required for optimal order within the bulk phase. The reduced order lowers the free energy and, therefore, the surface tension of the aqueous phase.

Surface Tension as a Function of [CaCl₂]
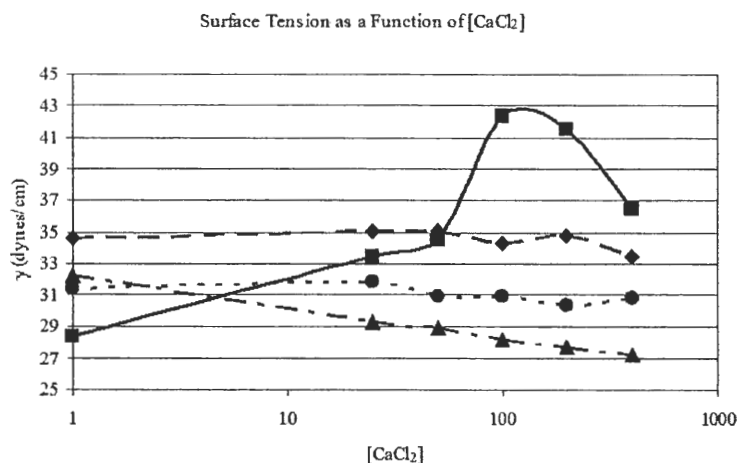
Figure 36: Surface tensions of various suspensions as a function of calcium chloride concentration. All suspensions were maintained at 45°C and 8.5 pH and all reported surface tensions are receding. The suspensions are: distilled water (■), 200 ppm TDA-32 in distilled water (▲), pressate (♦) and pressate with 200 ppm TDA-32 (●).
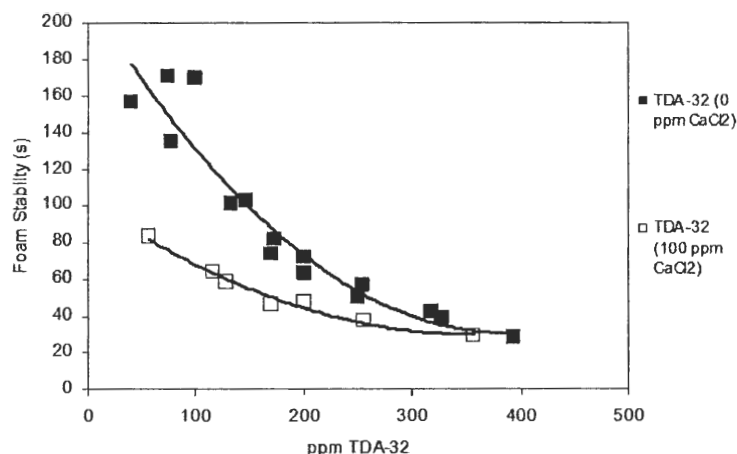
Figure 37: Stability of a model foam as a function of TDA-32 defoamer concentration. In addition to various levels of defoamer, the foaming liquid contains 200 ppm TX-100 and either 0 or 100 ppm CaCl$_2$.

The postulated enhanced spreading coefficient in response to increasing calcium chloride concentrations in suspensions of distilled water was supported by trials designed to gauge the strength of TDA-32 as a defoamer. **Figure 37** shows that the ability of TDA-32 to destabilize and collapse foam exhibits limited calcium chloride dependency. At low TDA-32 concentrations, increasing the calcium concentration to 100 ppm promotes the rapid collapse of foam. Although the foam becomes increasingly unstable as defoamer concentration increases, the calcium chloride dependency observed at low defoamer levels becomes less pronounced. As the amount of defoamer in the foaming liquid approaches 300 ppm, the ability of calcium chloride to enhance the defoaming power of TDA-32 is minimal. However, at 200 ppm TDA-32, a calcium

chloride concentration of 100 ppm remains capable of accelerating foam collapse. This observation may indicate that the defoamer spreads more effectively across the air bubble for enhanced foam control in the presence of calcium chloride. This explanation supports the impression that calcium chloride additions improve the spreading behavior of the defoamer by increasing the tension of the air/water interface.

Unfortunately, the above speculation was rendered immaterial when the suspensions contained TDA-32 and/or pressate. Returning to **Figure 36**, the increase in surface tension in response to calcium chloride additions observed with pure water was not present in a defoamer suspension, a suspension of pure pressate or a mixed suspension of defoamer and pressate. On the contrary, 200 ppm TDA-32, when present within both the water and pressate suspensions, actually appeared to lower surface tension in response to increasing calcium chloride levels. According to the Harkins' equation, a reduction in surface tension is indicative of diminished spreading behavior[59]. Calcium and chloride ions may be consumed by pressate components and, thereby, unable to participate in interactions that may affect the surface tension. With this in mind, it is difficult to envision enhanced spreading of the defoamer across air bubbles within the whole furnish. Rather than by increasing γ_{aw}, enhanced rates of spreading at air/"water" interfaces under actual flotation conditions must involve reducing γ_{ow} and/or γ_{oa}.

When 200 ppm TDA-32 was included within the pure water and pressate suspensions, the ultimate surface tensions became similar. However, in each case, the

142

defoamer's ability to affect γ_{aw} appeared relatively independent of calcium chloride concentration. Of note is the initial surface tension of the 200 ppm TDA-32 suspension relative to that of pure water. The higher value obtained from the former suspension indicates that the TDA-32 reduces the susceptibility of the surface tension of aqueous solutions to thermal influence (at least at 45°C).

Having determined the spreading behavior of defoamer droplets at air/pressate interfaces to be relatively independent of calcium chloride concentration, the rate of diffusion of the droplets to the interface as a function of ionic strength was examined. An indirect yet convenient means to quantify surface adsorption of a surfactant was availed through the use of the Gibbs adsorption equation.

$$\Gamma = -\left(\frac{C}{RT}\right) \cdot \left(\frac{d\gamma}{dc}\right)$$

Equation 4: Gibbs adsorption isotherm

Assuming that the TDA-32 acts as a nonionic surfactant, the surface excess concentration (Γ), or the amount of defoamer located at the quiescent air/water interface at equilibrium was determined. To reveal any calcium chloride-mediated variations in the ability of TDA-32 to adsorb at the interface, a separate value of Γ had to be determined for several different suspensions of TDA-32. This effectively provided the relationship between the concentration of surfactant (i.e. TDA-32), c, and the measured surface tension, γ. **Figure 38** presents the surface tensions, γ_{aw}, obtained from various

suspensions of TDA-32 as a function of calcium chloride concentration. Although increasing the concentration of TDA-32 in the suspension significantly reduced the surface tension, the magnitude of the reduction was generally independent of calcium chloride concentration.
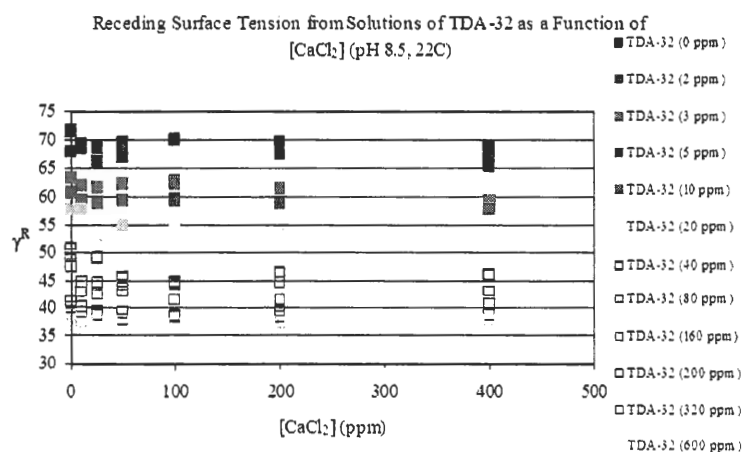
Figure 38: Surface tensions obtained from various suspensions of TDA-32 as a function of calcium chloride concentration. All samples were thermostatted at 45°C and adjusted to pH 8.5 prior to assay.

From the figure, the ability of TDA-32 to lower the surface tension appears to be limited. The data were recast to reflect the tendency of surface tension to decrease with increasing levels of TDA-32 at various ionic strengths (**Figure 39**). Interestingly, the TDA-32 concentration at which the ability to lower the surface tension reaches a plateau, 200 ppm, was the same as that found to completely collapse foam generated during the flotation trials. However, once again, the tendency for a specific

concentration of TDA-32 to reduce the surface tension is not significantly affected by calcium chloride.
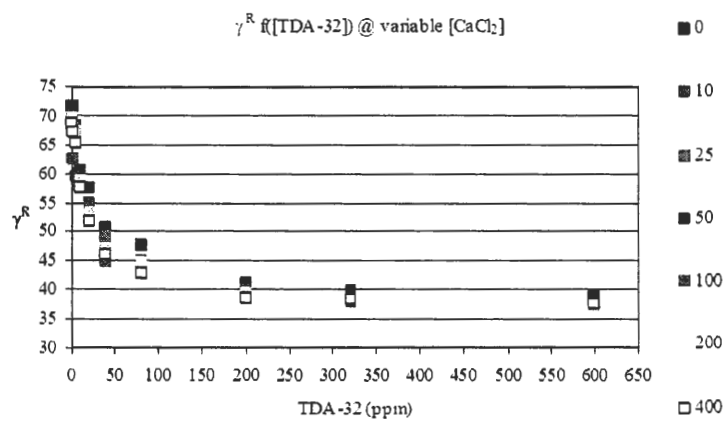
Figure 39: Surface tension measurements rearranged to reflect the influence of calcium chloride on the surface energy reductions associated with specific concentrations of TDA-32.
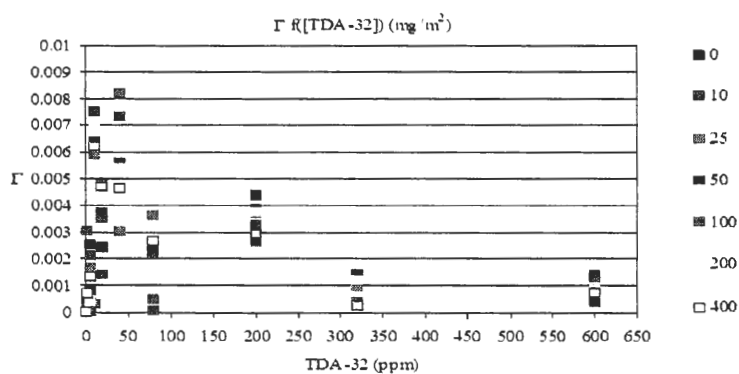
Figure 40: Surface excess concentrations of surfactant (i.e. TDA-32) as a function of both surfactant and calcium chloride (ppm values listed in the legend) concentration.

The various combinations of TDA-32 concentration and calcium chloride addition and their resultant surface tension values were used to determine the surface excess concentrations via the Gibbs adsorption equation. The results, presented in **Figure 40** indicate that, in all cases, extremely minute quantities (< 0.01 mg/m^2) of the defoamer actually locate near the air/water interface regardless of the calcium chloride concentration. The variations in Γ between suspensions were considered too insignificant to support an influence of calcium chloride concentration on rates of diffusion of TDA-32 to the air/water interface.

The results from **Figure 40** were recast to provide the surface excess concentrations as a function of calcium chloride concentration for various suspensions of TDA-32 (**Figure 41**). Again, calcium chloride has relatively little impact on the surface excess concentrations. The amount of TDA-32 adsorbed at the air/water interface appears to be independent of the concentration of the surfactant in the bulk. The apparently small quantities of TDA-32 adsorbed at the interface may be readily explained by the film forming properties of polydimethylsiloxane (PDMS).
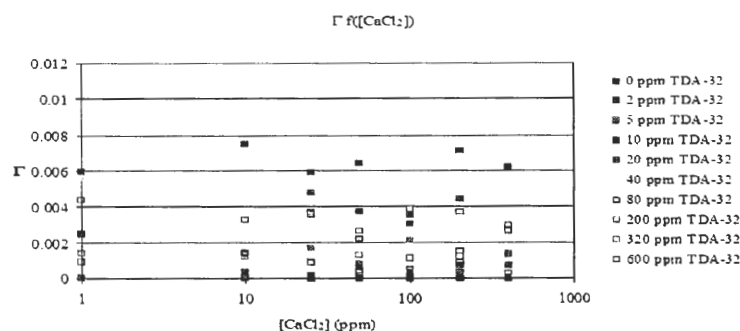
Figure 41: Surface excess concentration as a function of calcium chloride concentration for various suspensions of TDA-32.

In conclusion, calcium chloride does not appear to enhance the rate and magnitude of adsorption of TDA-32 at the air/liquid interface. In addition, the inability of calcium chloride to increase the surface tension of a suspension of pressate and TDA-32 indicates that spreading behavior is independent of ionic strength according to the Harkins' equation (Error! Reference source not found.).

Emulsions

Rather than by increasing γ_{aw}, calcium-mediated modification of defoamer kinetics at air/"water" interfaces within the pressate must involve reducing γ_{ow} and/or γ_{oa}. To determine whether calcium chloride influences the interfacial tension between the TDA-32 emulsion droplets and an aqueous continuous phase, a model system was developed. As in most siloxane-based defoamers, the dispersed phase of TDA-32 is polydimethylsiloxane (PDMS) with proprietary organomodifications within the

147

siloxane backbone. Since direct monitoring of the interfacial kinetics at the emulsion droplet surface was impractical, an artificial PDMS/aqueous phase interface was developed by combining equal parts of both phases in a standard test tube. In addition to providing a relatively large continuous and planar interface between the two phases, the two phase system would isolate calcium chloride-dependent, interfacial kinetics from the influence of excessive variables associated with the emulsified defoamer (e.g. emulsifying agents, emulsion stabilizing agents, hydrophobic silica, etc.). The type and stabilities of emulsions prepared by vigorously mixing the two phases were used as indirect means to ascertain the effect of calcium chloride on PDMS/water and PDMS/pressate interfacial properties.

Figure 42 presents the results obtained by emulsifying PDMS with distilled water and with pressate containing various concentrations of calcium chloride. In all instances, the emulsified layer consisted of water/pressate-in-oil (w/o) droplets. A possible explanation for this latter observation may draw from the concept of phase inversion temperature, PIT. For an emulsified system of approximately equal volumes of oil and water, the PIT represents the temperature at which the emulsion will spontaneously invert from o/w to w/o or vise versa[61]. Deviation between the system temperature and the PIT correlates with an increase in emulsion stability. In general, below the PIT, emulsions tend to be o/w. Conversely, above the PIT, w/o emulsions are more likely to form. This phenomenon appears to be relatively independent of the oil type when homogenized with a pure water phase. To this end, the observations made

during the emulsification trials suggest that the PDMS-water system is above the PIT at 45°C.
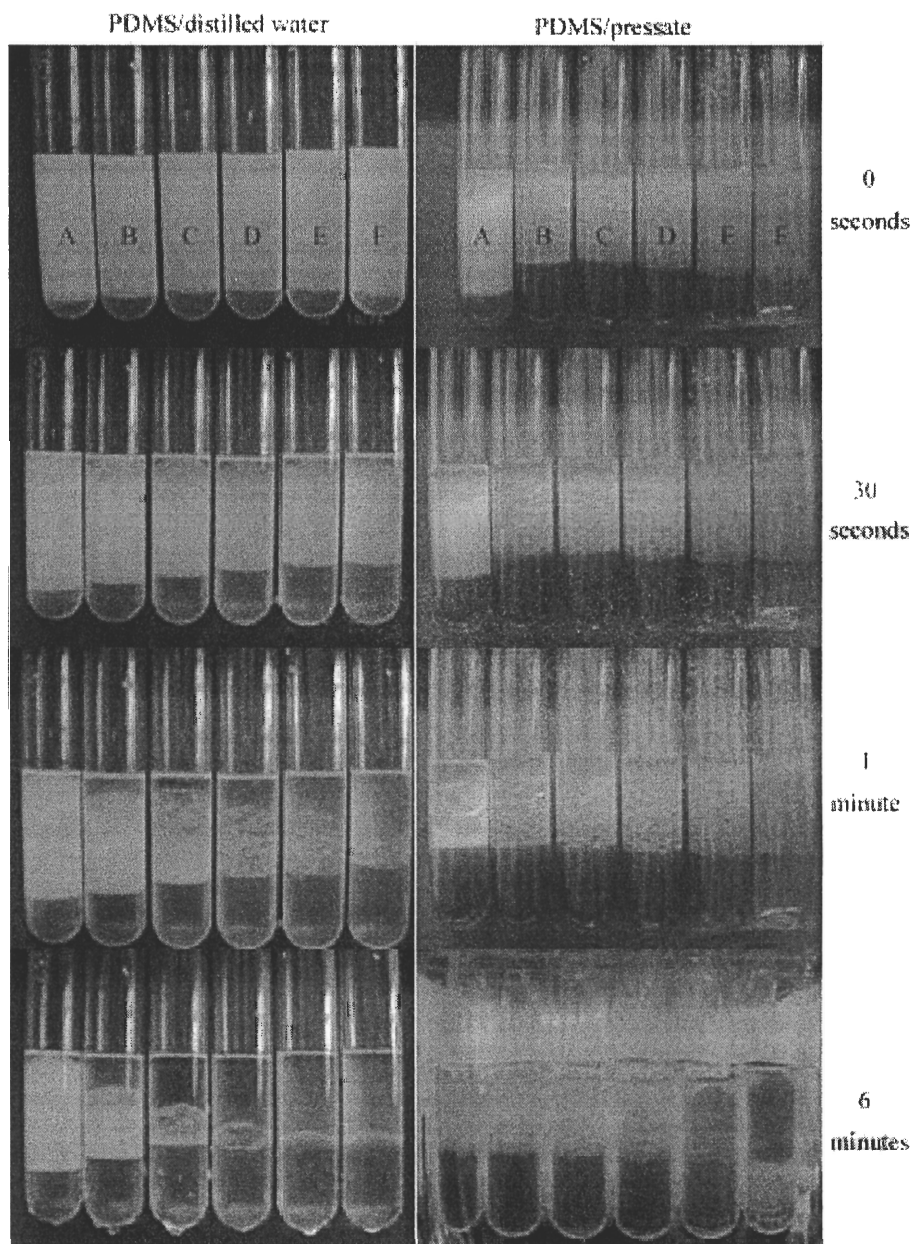
Figure 42: PDMS/water (left) and PDMS/pressate (right) emulsion stability as a function of calcium chloride concentration within the aqueous phase. CaCl$_2$ concentrations are: A. 0 ppm, B. 25 ppm, C. 50 ppm, D. 100 ppm, E. 200 ppm and F. 400 ppm. After formation, all emulsions were allowed to equilibrate at 45°C.
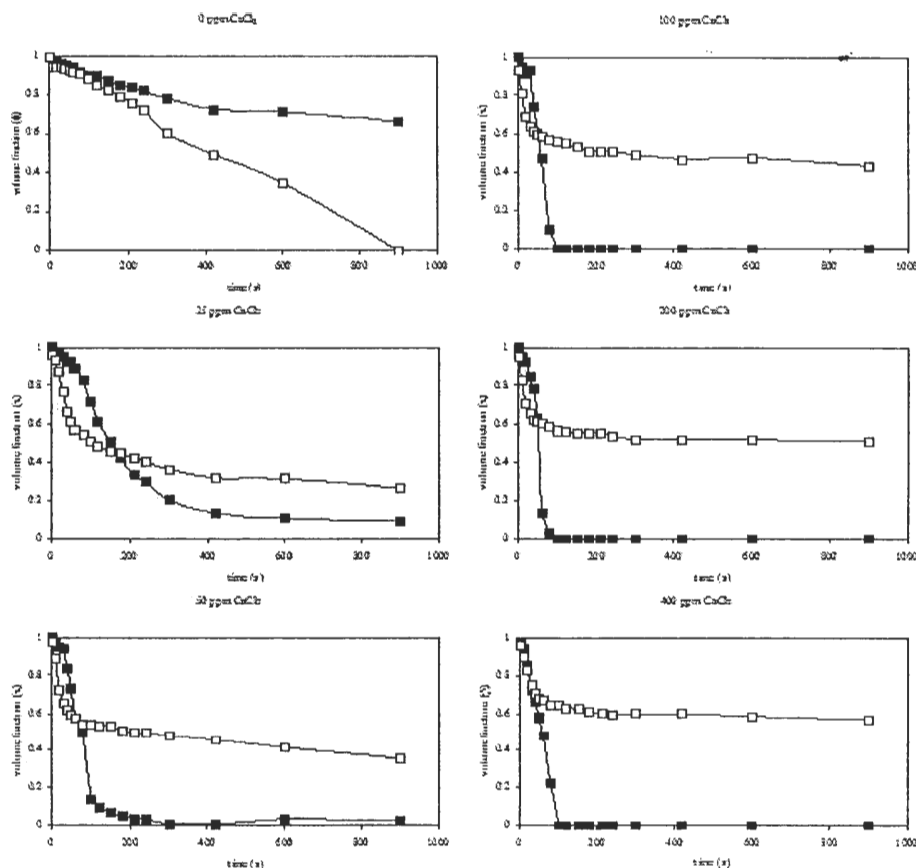
Figure 43: Emulsion stability as a function of calcium chloride concentration. Each graph represents the stabilities over time for both water-in-PDMS (■) and pressate-in-PDMS (□) emulsions.

Before forwarding an explanation for the observed behavior involving pressate, the emulsification dynamics with the simple two phase water-PDMS system will be discussed. This system was assumed to be binary in nature (i.e. consisting of only neat oil and Millipore-pure water). To understand the thermodynamic nature of an emulsion, the difference in surface free energy relative to the two, pre-homogenized continuous phases must be considered. Emulsion formation and stability is heavily dependent upon the interfacial tension that originally exists between two immiscible phases: PDMS (*o*) and water (*w*). The magnitude (and direction) of the free energy of the system, ΔG,

150

associated with emulsion formation provides an idea as to whether the emulsification process will occur spontaneously or will require energetic input by the equation in **Equation 5**.

$$\Delta G_{form} = \Delta A \cdot \gamma_{ow} - T\Delta S_{disp}$$

Equation 5: Equation to calculate the free energy change associated with emulsion formation. ΔS_{disp} accounts for the entropy change associated with the dispersion of emulsified droplets of one phase within the other.

The correlation between high interfacial tension (γ_{ow}) and ΔG requires the change in interfacial area (ΔA) within the system (i.e. emulsion) to be as minimal as possible. Generally, this corresponds to a complete separation of the two immiscible phases. To this end, high interfacial tensions are associated with greater rates of emulsion coalescence (i.e. collapse) and the inability of a stable emulsion to form. Low interfacial tensions are more conducive to emulsion formation and stability since the free energy change upon a similar increase in interfacial area is relatively small[62]. The fact that a transient emulsion forms following homogenization suggests that the PDMS-water interfacial tension is relatively small (again, this is a requirement for a successful defoamer to spread across an air-water interface according to Harkins' equation).

Although interfacial tension (γ_{ow}) can be directly measured within the laboratory, a more accurate and less time consuming approach involves a relatively simple calculation based upon the surface active forces inherent to each phase. The surface tension of each phase is presumed to be the cumulative result of a number of

unique components. The surface tension of water is defined by two primary components: dispersion forces (γ_w^d) and polar forces (γ_w^p) such as the unique intermolecular hydrogen bonding interactions associated with water. Although the definition of the "surface" of water is actually an "interface" with gas (usually air), the contribution of similar components (e.g. γ_a^d and γ_a^p) within air to the interfacial/surface tension is negligible. Consequently, the surface tension of water is simply:

$$\gamma_{wa} = \gamma_w^d + \gamma_w^p$$

Equation 6: The surface tension of water (usually measured against air) can be expressed as the sum of individual dispersion forces and polar forces.

In similar fashion, the surface tension of an oil phase against air (γ_{oa}) can be determined. With regard to nonpolar oils, such as alkanes, the second term within the equation can be discounted since all surface energy arises from dispersion forces within the liquid phase. However, the surface tension of polar oils, such as the polydimethylsiloxane used during the emulsification trials, is defined by both components: γ_o^d and γ_o^p. For a 50 cS PDMS oil, these values have been calculated, at 25°C, to be 20.12 mJ m^{-2} and 0.88 mJ m^{-2}, respectively, yielding a γ_{oa} of 21.0 mJ m^{-2} [63].

Once the surface tensions and the magnitude of the individual contributions from each component for the two immiscible liquids are known, the interfacial tension between the two phases can be calculated according to the equation[64]:

152

$$\gamma_{ow} = \gamma_{oa} + \gamma_{wa} - 2\sqrt{\gamma_o^d \gamma_w^d} - 2\sqrt{\gamma_o^p \gamma_w^p}$$

Equation 7: Fowkes' equation to determine interfacial tension as a function of the various forces existing within two separate immiscible phases.

In the case of nonpolar oils, the fourth term can be omitted. However, for polar oils (e.g. PDMS), this term is included and the resultant interfacial energy, γ_{ow}, can be anticipated to be lower than with nonpolar oils. The tendency for interfacial energies of polar oils against water to be lower than those between nonpolar oils and water has been demonstrated by Binks and Clint[63]. Polar forces acting across the interface, between the two phases, are largely responsible for the reduced interfacial energy. The calculated γ_{ow} can be used as a means to predict the stability of an emulsion consisting of the two phases by considering the resultant ΔG.

The documented transient emulsification, occurring upon homogenization of water and PDMS, supports the relatively low interfacial tension that exists between the two phases. However, the tendency for increasing calcium chloride concentrations within the aqueous phase to promote rapid coalescence of emulsion droplets (i.e. reduce emulsion stability) must be addressed. Since no additional surface active agents existed within the two-phase system, destabilization of the emulsion (i.e. increasing the ΔG of the system) must wholly dependent upon increasing interfacial tension. Increasing calcium chloride concentrations in water have already been shown to increase γ_{wa} (**Figure 36**). Similarly, interfacial tension, directly related to the surface tension of water, can be expected to increase as well according to **Equation 6**. Increasing the calcium chloride concentration within the aqueous phase, by increasing the interfacial

tension, promotes the rapid collapse of the water-PDMS emulsion. The tendency of the system to minimize interfacial area as it proceeds towards thermodynamic equilibrium is reflected in the size of the emulsion droplets at higher calcium chloride concentrations (**Figure 44**). The ability of high aqueous phase salt concentrations to influence the diameter of droplets in binary emulsions was noted almost 100 years ago[65].
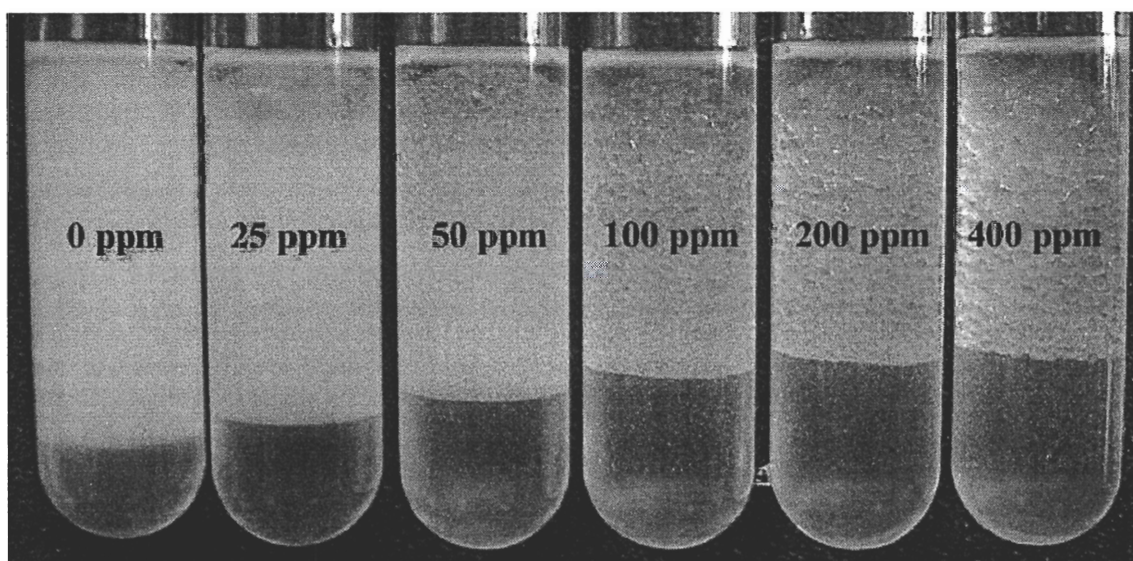
Figure 44: PDMS-water emulsions 1 minute and 30 seconds following homogenization. Calcium chloride concentrations within the aqueous phases prior to emulsification are presented as ppm. The lower continuous phase is aqueous.

Returning to **Figure 42** and **Figure 43**, the impact of increasing concentrations of calcium chloride on emulsion stability seen in PDMS-water systems is exactly opposite to that seen in PDMS-pressate systems. Apparently, rather than increase the interfacial free energy, γ_{ow}, between the two phases as predicted in the former system, γ_{ow} in the latter system appears to decrease in response to increasing electrolytic

strength. Since it has been previously determined that increasing the calcium chloride concentration within pressate does not affect γ_{aw} (**Figure 36**) and is not expected to affect γ_{oa}, the demonstrated ability to minimize ΔG by lowering γ_{ow} within the system must be attributed to another factor.

A possibility, not expected within the PDMS-water system, is that components inherent to the pressate may assume the role of surfactants capable of reducing interfacial tension and extending the life of the emulsified phase. Although this material includes desorbed binder, dyes, filler particles, and natural extractives (e.g. fatty acids, triglycerides, resin, etc.) from the repulped waste paper, the primary component of interest was dispersed flexo ink (presumed to comprise the majority of the dispersed material). The question was asked: Could this particular component assume the role of a surfactant?

Ternary emulsion systems, consisting of an oil phase, an aqueous phase and a surfactant have often demonstrated salt-dependent kinetics[66][67]. These emulsions are generally much more stable than the simple binary system consisting of only water and oil since the surfactant, by adsorbing at the interface, significantly lowers the interfacial tension. However, similarities between flexo ink particles (i.e. ~200 nm aggregates of carbon black pigment and adsorbed polyacrylate binder) and conventional molecular emulsifying agents are expectedly few. In addition to the size difference, emulsifiers are generally characterized by their amphiphilic nature which makes their localization at the interface energetically favorable. Conversely, under alkaline conditions, dispersed flexo inks are uniformly anionic owing to the random distribution of adsorbed, ionized

binder. By all accounts, dispersed flexo ink, or any other similarly charged colloidal substance, should exhibit absolutely no affinity for the interface and remain comfortably hydrated and stable within the aqueous phase. However, this is not always the case.

Finely divided solids, acting as colloidal substances, are routinely used to stabilize emulsions of industrial and commercial importance. Adsorption and assembly of colloidal particles at a liquid-liquid interface has been extensively investigated and numerous descriptions of the thermodynamic driving forces involved are availed within current literature[68] [69]. Known as Pickering emulsions[70], the type, emulsion droplet size and stability are always a function of the characteristics of the emulsifying agent (i.e. particle) and the composition of the two phases[71]. Inter-particle interactions, wettability, size, etc. determine the direction of the interfacial curvature upon particle adsorption and, consequently, the predisposition of freshly homogenized immiscible phases to separate into w/o or o/w emulsions or even emulsify at all[63] [72] [73] [74] [75]. Numerous attempts to exploit the preferential adsorption of these colloidal solids upon a liquid-liquid interfacial "template" during the construction of spherical "supra-particles" have been documented[76] [77] [78]. Binks and Lumsdon provide an excellent summary of numerous investigations concerning the ability of solids to stabilize emulsions[79]. Although clays[80], metal sulfates, silica, and iron oxide are proven colloidal emulsifiers, the demonstrated ability of carbon black to adsorb at the interface is of particular relevance to the present study. Moreover, adsorption of carbon black at the interface favors the formation of w/o emulsions[65] [81] [82]. Unfortunately, since the system temperature is above the PIT, the PDMS-aqueous phase emulsions tend to be w/o even

156

in the absence of aggregates of carbon black (i.e. flexo ink). An additional complication arises from the fact that polar oils, regardless of the system PIT and adsorbing colloidal species, are more likely to form w/o Pickering emulsions[63] [83]. Clearly, correlation between the observed emulsion type and the adsorption of flexo ink at the interface cannot be justified by simple observation of the resultant emulsion alone. However, the ability of flexo ink to adsorb at the interface and stabilize the emulsion as a function of calcium chloride concentration cannot be refuted (**Figure 45**). The fact that the emulsion stability appears to be a function of the electrolytic strength of the aqueous phase strongly supports the idea of formation of surface active complexes between ions and pressate components (i.e. flexo). Since the ability of flexo to act as a surfactant apparently depends on the availability of calcium ion, the effective surfactant concentration within the PDMS-pressate system can be fine-tuned merely by adjusting the level of calcium chloride within the pressate.
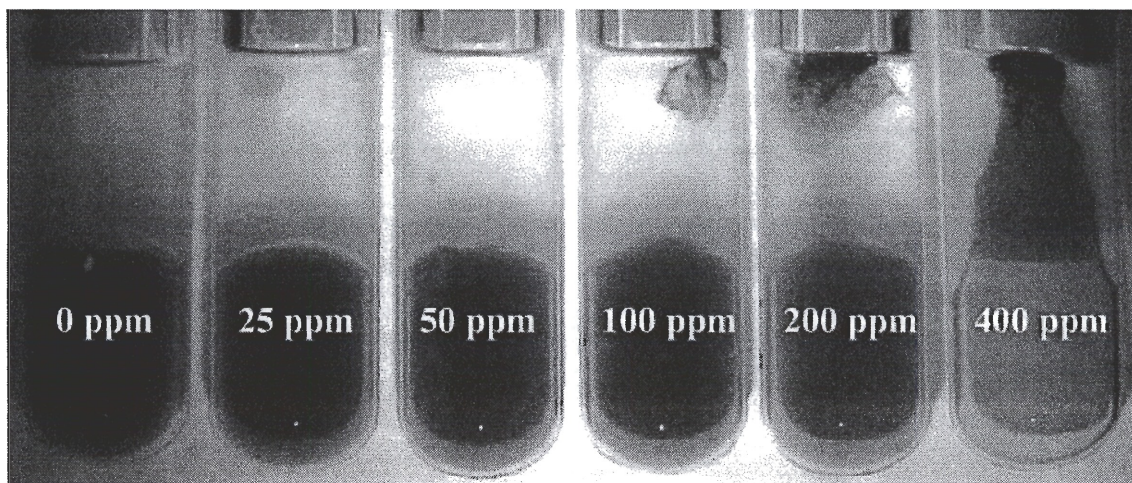
Figure 45: Emulsion tubes following a 1.5 hour separation period. Prior to emulsification via vortexing, the lower, aqueous pressate phase contained the calcium chloride concentration indicated as "ppm".

An analysis of the total carbon, TC, within the aqueous phase following emulsification plainly shows that the corresponding concentration of flexo ink decreases (presumably through interfacial adsorption) as calcium chloride levels rise (**Figure 46**). This calcium chloride-mediated adsorption, presumably, is responsible for the enhanced emulsion stability by lowering the interfacial tension.
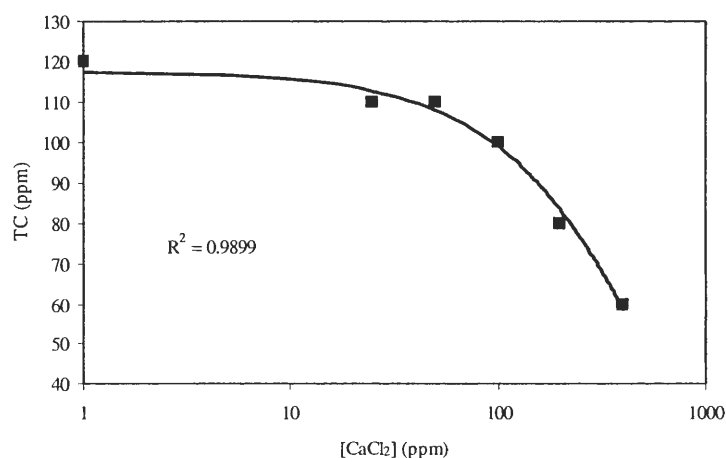
Figure 46: Total carbon contained within the aqueous pressate phase as a function of initial calcium chloride concentration following emulsification with equal parts PDMS.

Unfortunately, comparisons drawn between the PDMS-pressate emulsion results and the observed ability of TDA-32 to enhance the flotation of flexo ink are difficult. Unlike actual trials, there did not appear to be an optimal calcium chloride concentration promoting the adsorption of flexo at the oil-pressate interface. In the stead, interfacial adsorption appeared to increase at all salt concentrations employed.

With the correlation between calcium chloride concentration and flexo adsorption at a model emulsion droplet surface established, the actual PDMS-pressate interface of the model was examined. Continuing with the assumption that the interface generated with polydimethylsiloxane oil was similar to the TDA-32 interface *in situ*, a mimetic system was developed to provide a cross-sectional perspective of the defoamer-pressate interface. As the calcium concentration within the pressate increased, dark bodies were observed to form within the oil phase (**Figure 47**). Rather than adsorb at the immediate interface, flexo ink particles appear to materialize as ~0.5 μm aggregates within the PDMS bulk phase. This trend intensifies with calcium addition up to a maximum concentration of 100 ppm. Beyond this value, biphasic transfer of flexo appears to cease. This observation is of immediate relevance since it corresponds to results obtained during flotation trials.

A similar phenomenon was noted during experiments conducted to elucidate the mechanism of reversed micelle formation as a function of electrolyte concentration[66]. Increasing the concentration of monovalent cation tended to suppress incorporation of a molecular solute into a reversed micelle[r]. However, when calcium ion was substituted

---

[r] A reversed micelle is expected to be much smaller than the "dark bodies" formed within the PDMS. However, mechanisms leading to reverse micelle formation are anticipated to be similar to those governing dark body formations.

for the monovalent species, solvation of the solute into the bulk oil phase was observed to increase. Electrolyte-induced mass transfer of the solute from the aqueous phase to the continuum, reversed micellar interfaces and micellar pools of the bulk oil phase was concluded. Interestingly, the reported solubilization exhibited an optimum calcium concentration analogous to the observations presented in **Figure 47**. Increasing the calcium level beyond the optimal range resulted in an immediate decrease in the stability of the solute. Similar stabilization of flexo ink particles is presumed to occur at the TDA-32 emulsion droplet surface. Unfortunately, the thermodynamic model developed to describe interface partitioning behavior could not be extended to systems incorporating multivalent cations. Consequently, rationale behind reduced solubility at high calcium levels was not offered.
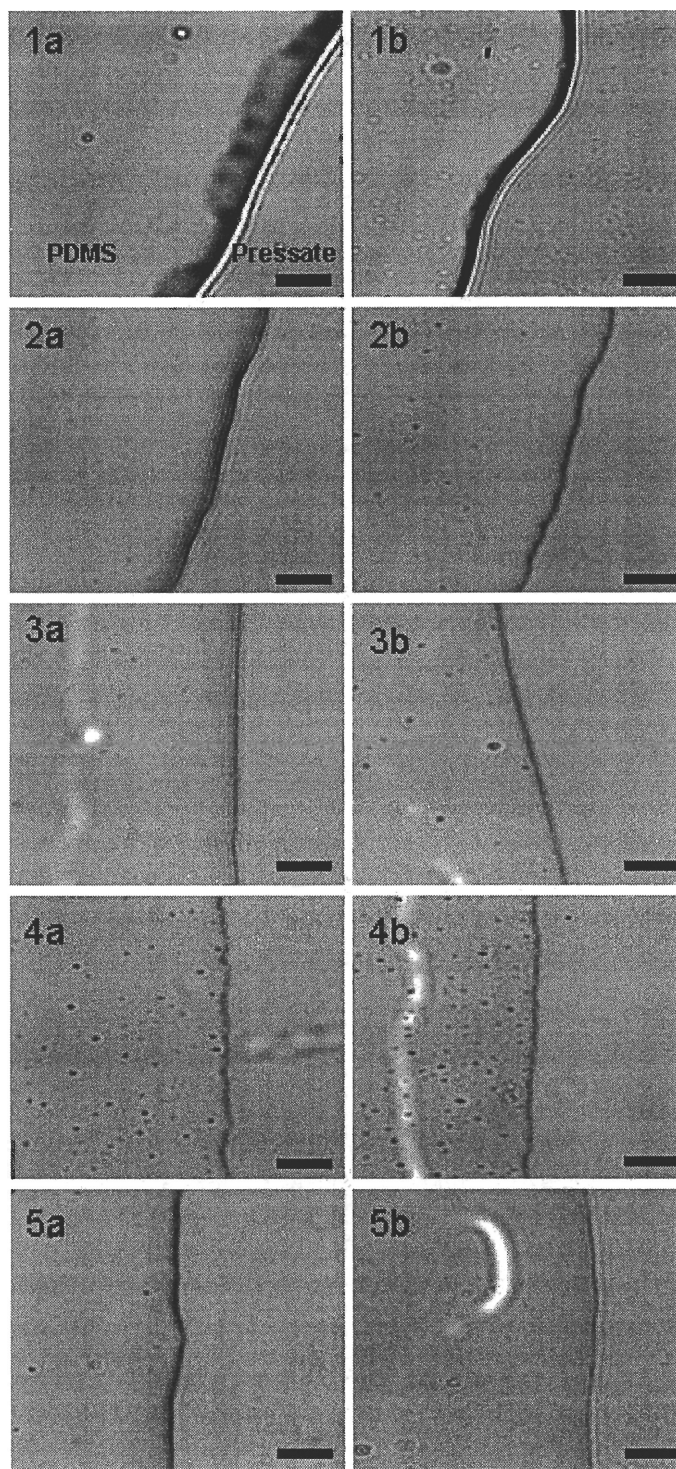
Figure 47: The polydimethylsiloxane-pressate interface as a function of calcium chloride concentration. 1= 0 ppm, 2 = 25 ppm, 3 = 50 ppm, 4 = 100 ppm and 5 = 200 ppm CaCl$_2$. (a = after 5 min, b = after 10 min). Bar = 10 μm.

161

COLLOIDS AT LIQUID-LIQUID INTERFACES

To account for the observations, mechanisms governing the transfer and subsequent adsorption of colloidal materials at liquid-liquid interfaces must be considered. For convenience and clarity, these two fundamental dynamics will be addressed separately. Since most of the fundamental studies with regard to interfacial adsorption involve latex particles with well-defined surface chemistries and dimensions[63 74 77 78 84], comparisons between the model colloids and flexo ink particles are drawn only when applicable. Although most forwarded mechanisms can be applied equally to particles initially located within the bulk oil continuum, the following discussion assumes that particles (i.e. flexo ink) originate from the aqueous phase.

Diffusion to the Interface

The efficiency by which a particle adsorbs at an interface is wholly dependent upon the ability of the particle to arrive at the interface. In other words, the rate limiting step within the process of adsorption is simple diffusion from the bulk medium. In most instances, relatively little long-range attractive or repulsive forces exist between the particle in question and the interface. Consequently, in relatively quiescent systems, such as in the mimetic interfacial trials, the rate of particle flux to the interface is likely to be a function of simple Brownian motion within the pressate[68]. This accounts for the relatively long periods required before flexo particles become discernable aggregates during the mimetic interface trials (5-10 minutes). Conversely, during the homogenization step immediately preceding the emulsion trials, the rate of particle diffusion to the interface was dramatically enhanced through convection. During

flotation trials, the rate of flexo ink particle interactions with the surface of TDA-32

droplets or films on rising air bubbles was expected to fall between these two extremes.

Interfacial Adsorption of Colloidal Particles
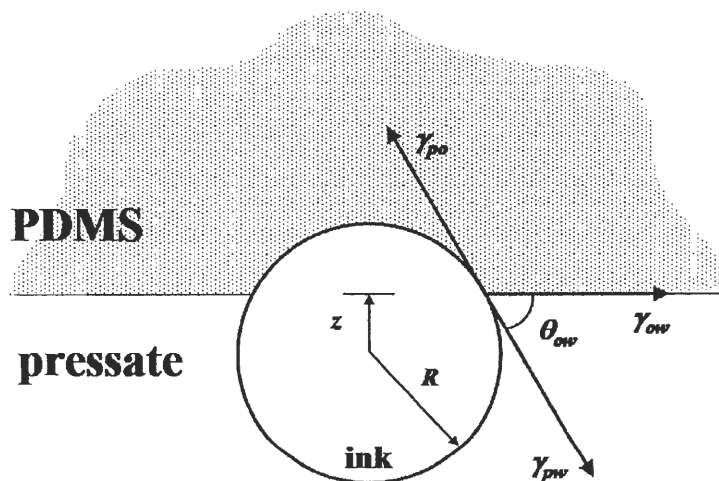
Figure 48: A diagram of a flexo ink particle/aggregate adsorbed at the PDMS-pressate interface. R is the particle radius while z is equal to R minus the penetration depth into the PDMS phase. The vectors ascribed to each of the three resultant interfacial/surface energies are labeled, γ_{po}, γ_{ow} and γ_{pw}. The contact angle, measured through the water phase, of the attached particle is denoted by θ.

Figure 48 presents an idealized diagram of a flexo ink particle (i.e. an aggregate

of carbon black pigments and adsorbed polyacrylate binder) located at the PDMS-water

interface. Once the flexo ink particle initiates physical contact with the interface, the

potential for actual insertion into the interface is dictated by the inherent

physicochemical nature of the particle surface and the resultant perturbation to the

thermodynamic equilibria of the total system. Transfer of the flexo ink particle (p) from

the bulk aqueous phase to the PDMS-water interface leads to the formation of a new

163

interface and, therefore, a new contribution to the total free energy of the system: γ_{op}. The change in free energy accounting for the formation of the new interface can be approximated via the equation[85]:

$$\Delta E = -\frac{\pi R^2}{\gamma_{ow}} \cdot [\gamma_{ow} - (\gamma_{pw} - \gamma_{po})]^2$$

Equation 8: Equation to determine the change in the Helmholtz free energy (ΔE) as a function of particle (p) adsorption at an oil (o)-water (w) interface. R is the effective radius of the particle.

Another way of evaluating the affinity of a particle for an oil-water interface is by quantifying the energy of interfacial attachment[71]. The energy of attachment, E, of a spherical colloid of radius R to an oil-water interface is related to both the interfacial tension between the two phases, γ_{ow}, and the contact angle that characterizes the interfacially adsorbed particle by the equation:

$$E = \pi R^2 \gamma_{ow} (1 \pm \cos\theta)^2$$

Equation 9: Energy of attachment of a particle to a typical oil-water interface. For $\theta < 90$, the sign within the bracket is – while for $\theta > 90$, the sign is +.

According to the equation and published results, maximum interfacial attachment is achieved when the contact angle of the adsorbed particle is 90°[63]. Any deviation from this angle, indicating preferential localization of the particle into one phase over the other, results in a greater chance of detachment into the corresponding bulk phase[73]. By the same equation, the interfacial tension, γ_{ow}, can also be seen to influence the energy of attachment.

Nikolaides combines the three components to total energy within the system with the geometry of a particle adsorbed at an oil-water interface[84]. His equations, derived from previous investigations of colloid organization upon a two-dimensional interface[86], equate the energetic favorability of particle adsorption with the observed penetration of the particle into the secondary phase. Although Nikolaides' investigation involved particle flux from an oil continuum to an oil-water interface, the applicability of the above equations to situations in which the particle (i.e. flexo ink) initially diffuses from the aqueous phase is presumed unconditional. In **Figure 48**, the extent of particle penetration is denoted by z. A normalized version of this value, z_o, obtained by dividing z by R, is then used to determine the three separate contributions to total interfacial energy by the equations:

$$E_{po} = \gamma_{po} 2\pi R^2 \left(1 - z_o\right)$$
$$E_{pw} = \gamma_{pw} 2\pi R^2 \left(1 + z_o\right)$$
$$E_{ow} = -\gamma_{ow} \pi R^2 \left(1 - z_o^{\,2}\right)$$

Equation 10: The three contributions to total energy of a system following the isolation of a model colloidal particle at an oil-water interface.

The first two contributions stem from the interfacial energy of the ink particle upon complete immersion in the bulk PDMS or water phase. The magnitude of the contribution when the particle is adsorbed at the interface is dictated by z_o. The third equation is negative to account for the loss of interfacial energy that occurs as some of the PDMS-water interface is lost to accommodate the particle. With these values, the magnitude of the energy barrier associated with detachment of the particle from the

interface into either the PDMS or the pressate phase can be determined. Although the concept of energy barriers is an attractive premise to account for the sequestering of a flexo ink particle at the PDMS-pressate interface without actually measuring contact angles, the inability to measure the penetration depth of the particle into the oil phase limits the effectiveness of these equations.

A possible means to bypass the shortcomings of equations based on contact angles and penetration depths of a single flexo ink particle involves data taken from films prepared from pressate and calcium chloride. An additional benefit to this approach is that the flexo ink particles are not treated as ideal colloids. In other words, analysis of the data does not have to contend with the variation of the actual flexo ink particle and/or aggregate from the spherical model colloid for which the former equations were designed[s]. Once again, three contributions to total free energy of the interfacial system, γ_{ow}, γ_{op}, and γ_{wp}, are required to determine the efficiency of particle adsorption to the interface. Since $\Delta\gamma_{ow}$ as a function of calcium chloride concentration is expected to be negligible, adsorption of flexo ink to the PDMS-pressate interface was expected to depend on the remaining factors, γ_{op} and γ_{wp}. Since calcium chloride has previously been determined to change the contact angle taken from films formed from

---

[s] The morphology of a typical dispersed flexo ink particle is expected to be far from spherical. In fact, at higher calcium chloride concentrations, the "particle" is possibly an aggregate of many particles.

pressate (**Figure 34**), the Young equation can be used to infer comparable change in γ_{wp}:

$$\gamma_{ap} - \gamma_{wp} = \gamma_{wa} \cos \theta_{aw}$$

Equation 11: Young equation in which w corresponds to the aqueous pressate phase measured against air (a).

Clearly, calcium ions, complexing with dispersed flexo inks, can be presumed to increase γ_{wp} through screening-mediated reduction of the surface charge of the ink particle (i.e. the flexo ink particles lose hydrophilicity and, therefore, wettability). When the air phase is replaced by oil within the Young equation (**Equation 11**), the predicted higher γ_{wp} corresponds to a greater contact angle, measured through water, of the particle at the oil-water interface.

$$\gamma_{op} - \gamma_{wp} = \gamma_{ow} \cos \theta_{ow}$$

Equation 12: Young equation corresponding to a solid (p) adsorbed at an oil (o)-water (w) interface. Once again, the w value corresponds to the pressate phase.

Accordingly, the contact angle measurements taken from films prepared from pressate at various calcium chloride concentrations may be used as an approximation of the contact angle of a flexo ink particle adsorbed at the TDA-32-aqueous phase interface. Unfortunately, the relatively low contact angles determined for the film, even at the empirically determined optimal calcium chloride concentration of 100 ppm ($\theta \approx$ 45-80°), do not lead one to believe that the depth of penetration of flexo ink particles

167

into the oil phase will be significant. However, there is evidence to suggest that the contact angle of a solid adsorbed at a liquid-liquid interface may actually be different than the calculated value depending on the polarity of the oil phase. Point-in-case, oils of increasing polarity were found to yield higher-than-predicted contact angles at the surface of an adsorbed colloidal solid when measured through the water phase[63] [69] [71]. This may, in part, be due to the tendency of interfacially adsorbed particles to be slightly more hydrophobic than they would be in the bulk medium.

Recent work in the area of nanoparticle assembly on liquid-liquid interfaces suggests that, in some cases, a particle must form aggregates with similar particles prior to adsorption[85]. This theory is based on the ability of adsorbed particles to minimize the Helmholtz free energy, E. The equation, referenced previously (**Equation 8**), underscores the direct relationship between the change in free energy and particle size. Particles with small radii, although capable of adsorbing to the interface, do not significantly reduce the free energy of the system. As a result, detachment of these particles from the interface due to thermal energetic fluctuations does not increase the total free energy by any significant amount. This equation, combined with the equation to calculate the work of attachment of the particle while at the surface (**Equation 9**) suggests that successful adsorption of flexo ink at the interface may involve limited particle aggregation within the bulk aqueous phase. At a specific hydrodynamic radius, stable adsorption of the aggregate onto the interface will be both thermodynamically favorable and stable against detachment via thermal energy and physical shear. This may facilitate an explanation of the calcium chloride-dependent *in situ* collecting

behavior of TDA-32 droplets during the trials and at the PDMS-pressate interface during observations of the model system. Above the optimal calcium chloride concentration, the individual ink particles may become saturated with calcium ion and consequently resist aggregation. On the other hand, the resulting aggregates may be so large as to prevent their permanent retention at the oil-pressate interface of a passing emulsion droplet. Shearing forces may promptly detach the aggregate and return it to the bulk medium.

Inter-Particle Interactions at the Liquid-Liquid Interface

Collection of the ink particles by simple adsorption at the interface of an emulsified droplet is a feasible means by which the pulp brightness may be improved. Concluding this to be the only means for flexo collection, however, does not explain the results from the mimetic interfacial trials (**Figure 47**). The presence of the "dark bodies" suggests that the adsorbed ink particles are assembled, at or near the interface, into visible, supra-particle structures as a function of calcium chloride concentration. Since the calcium chloride concentration at which these structures appear coincides with that found to enhance the floatability of flexo ink during actual trials, three mechanisms for ink collection, stemming from confirmed inter-particle interactions are envisioned. In all instances, the ability of calcium ion to steer the course of the interactions will be addressed.

Colloidal particles, adsorbed at two-dimensional interfaces, are subject the same forces of interaction that exist between particles dispersed in a three-dimensional bulk solvent[69][84]. These include the attractive Van der Waals and repulsive electrostatic

forces that define the energetic primary minima and barriers, respectively, represented by the DLVO theory. However, the similarities end there as dispersed particles are defined by one solvent whereas interfacially adsorbed particles are exposed to two unique solvents. Moreover, the ultimate physicochemistry of the particle varies with depth of penetration into either phase. This leads to some interesting properties associated with particles sequestered at liquid-liquid interfaces that are absent within the bulk medium.

Although much work has been conducted to elucidate inter-particle interactions at a liquid-liquid interface, the overall scheme has yet to be conclusively defined. Fortunately, research into the assembly of colloidal particles into two-dimensional crystalline monolayers has yielded a generally accepted model (**Figure 49**) that is expected to apply to flexo ink particles and aggregates as well.

Regardless of the uniformity of charge around the perimeter of the particle, when adsorbed at an interface between two solvents (e.g. water-air, water-oil) of differing dielectric constant, the distribution of counterions around the particle will be asymmetric. Due to the asymmetry of charge across the particle, a dipole (p) is established that will largely determine subsequent inter-particle interactions. Because the counterions largely remain within the aqueous phase, this portion of the particle solvated within this phase can have varying charge depending on the concentration of counterion. The intrinsic charge at the surface of the fraction immersed within the oil remains relatively unaffected by electrolytic strength within the aqueous phase. For

similar reasons, the magnitude of the dipole is also contingent upon counterion concentration within the aqueous phase.
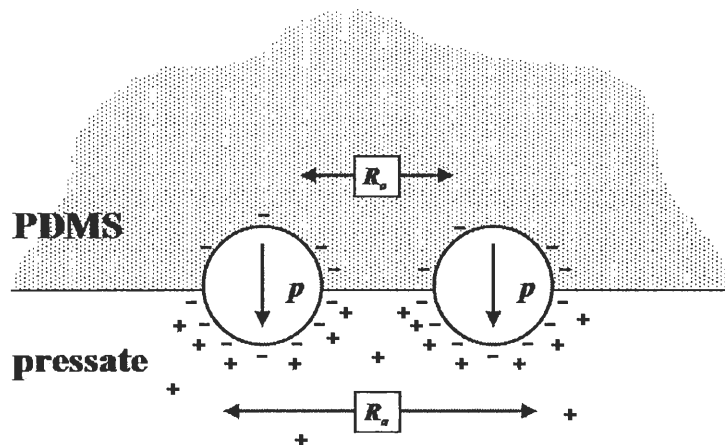
Figure 49: Long range inter-particle repulsion at a liquid-liquid interface is partially related to aligned dipole interactions.

Just as counterion screening effects and the resultant dipoles define the status of a single particle adsorbed at an interface, the interactions between two such particles are a function of the electrolytic strength of the system. Approach of the two particles is, in effect, an approach of two aligned dipoles. The end result of this is long range electrostatic repulsion between the similarly charged regions of the ink particles. Depending upon the magnitude of the charge and the medium through which the charge is carried, the overall electrostatic repulsion will vary from one side of the interface to the other. In the case of a flexo ink particle adsorbed at the PDMS-pressate interface, the repulsion (...) is expected ... g water through the aqueous phase with a higher dielectric constant, ε, at low, monovalent counterion concentrations. This repulsion,

combined with the slightly less repulsion through the PDMS phase (R_o), provides an electrostatic barrier to resist particle aggregation on the interface.

However, when counterion concentration is increased, electrostatic repulsion through the aqueous phase will tend to be reduced via charge screening action. The consequent lowering of the electrostatic repulsion barrier may enable particles to approach one another close enough to enter a primary minimum at which the particles may even aggregate. Investigators have found that, due to the induced dipole across the particle, the concentration of salt required to aggregate interfacially adsorbed particles can be up to two orders of magnitude less than that required to aggregate the same particles in bulk[68][69][74]. This may explain the ability of 100 ppm calcium chloride to forms aggregates at the PDMS-pressate interface but not within the bulk pressate (**Figure 24**).

However, when the counterion is divalent (i.e. calcium), there is expected to be a concentration at which the particle-aqueous phase begins to gain a cationic charge. Although flexo ink particles did not gain a cationic charge when dispersed in the bulk pressate phase at any of the calcium chloride concentrations assayed, the situation becomes much different when the particles are adsorbed at the oil-water interface. As a result of the increasing cationicity of the particle, the magnitude of the dipole increases and, once again, long range electrostatic repulsion prevents neighboring particles from interfacial aggregation. The tendency for flexo ink particles to reduce and then gain hydrophilicity as calcium chloride concentrations increase was revealed during contact angle measurements of pressate films (**Figure 33**).

172

As mentioned earlier, during the trials, before air was introduced into the flotation unit, the defoamer was observed to begin accumulating within eddies at the surface of the agitated pulp. The general color and texture of the exhausted defoamer suggested that the ink was sequestered within a continuous oil phase formed from the coalescence of numerous emulsion droplets. To this end, the requisite for effective "collection" of flexo ink particles was anticipated to depend solely on the presence of an oil-water interface. In other words, mass transfer of dispersed flexo into PDMS can occur at the surface of a TDA-32 droplet or across a thin film or lens of oil spread across a rising air bubble. Bearing in mind the boundary conditions governing the rate of adsorption of a colloidal particle to a liquid-liquid interface and the subsequent inter-particle interactions at the two-dimensional interface, three potential mechanisms for interfacial adsorption of flexo ink at and translocation across the PDMS-pressate interface are envisioned.
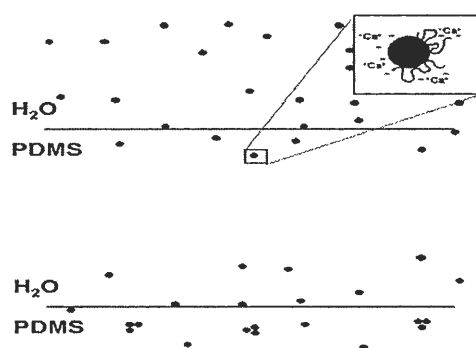
Figure 50: Schematic in which flexo ink is effectively "salted into" the oil phase as a function of calcium chloride levels within the aqueous phase.

In **Figure 50**, the interfacially-adsorbed ink particles continue to adsorb calcium until their surface energy with water is high enough to permit detachment into the oil phase. In this example, particles do not necessarily have to interact at the interface. Rather, at a certain concentration within the PDMS, $c\mu c_{oil}$, the particles may form the visible aggregates. This model is in accordance with the observed sudden appearance of dark bodies, with time, at the 100 ppm calcium chloride concentration. Above this concentration, the interfacially adsorbed particles may actually acquire a cationic charge that precludes biphasic transfer and actually sequesters the ink at the interface and/or returns the particle to the aqueous bulk phase. This would account for the observations recorded during the emulsion trials in which calcium concentrations greater than those found optimal during the flotation trials, would stabilize emulsions (**Figure 45**). The ability to adsorb at an oil-water interface and, thereby, stabilize an emulsion created from the two phases, it would seem, is not indicative of biphasic mass transfer.
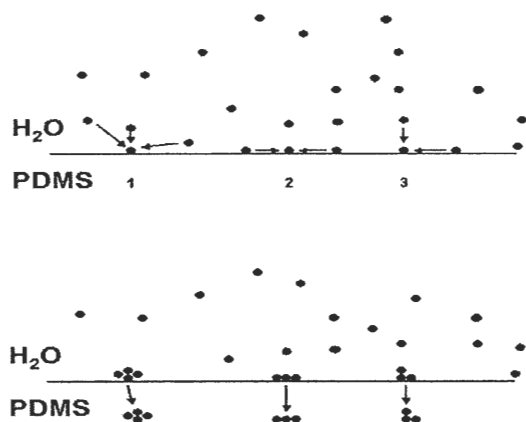
Figure 51: Supra-particle assembly at the interface as a function of calcium chloride concentration. The resultant flexo ink aggregates, upon reaching optimal sizes and/or surface chemistries, diffuse into the PDMS continuum.

In **Figure 51**, adsorbed particles may act as seeds upon which aggregates form as additional particles diffuse from the bulk suspension (1). Lateral diffusion of adsorbed particles at the interface in response to calcium-mediated reduction of long range electrostatic repulsion may also lead to interface-bound aggregate formation (2). Aggregates may also form from a combination of bulk and lateral diffusion (3). This latter phenomenon is well-documented in studies conducted to elucidate two dimensional crystal formation at liquid-liquid interfaces. At a specific size and/or morphology, the interface-bound aggregates may diffuse into the bulk oil continuum.

175
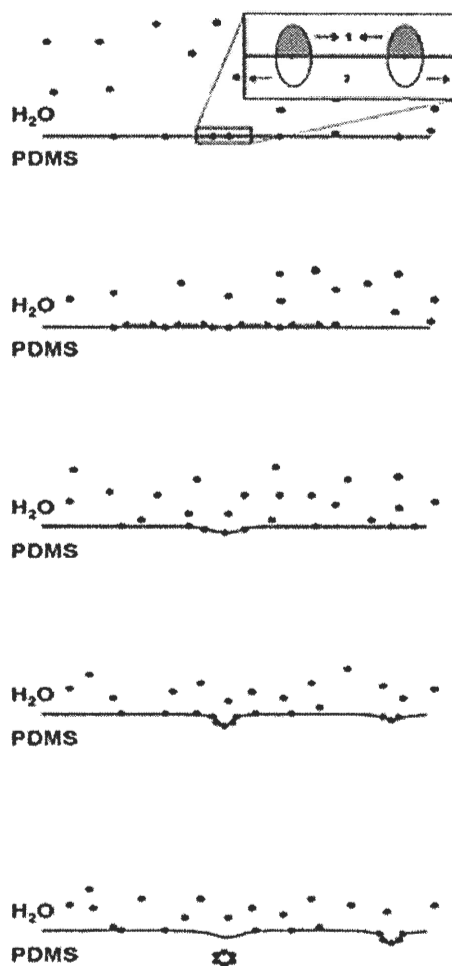
Figure 52: Inter-particle interactions may actually lead to the formation of a water-in-oil vesicle stabilized by adsorbed ink particles.

Another schematic, **Figure 84**, may correlate the appearance of dark flexo "supra-particle" assemblies within PDMS at a specific calcium chloride concentration with the ability of adsorbed particles to participate in spontaneous emulsion inversion interactions. As alluded to previously, particles adsorbed at the interface will develop a

"dipole" due to a charge screening disparity within the two phases. As a result, the nature of inter-particle interactive forces within the aqueous phase will differ from those within the oil phase. Since calcium ion directly influences these inter-particle interactions (especially within the aqueous phase), the magnitude and direction of the resulting interfacial curvature is expected to be a function of electrolyte concentration. The relationship between the curvature of a surfactant stabilized interface and ionic strength has previously been established[Error! Bookmark not defined.][69].

Supra-particle assembly at the interface may be driven by a disparity in inter-particle repulsion across the interface. Inter-particle repulsion within the oil phase, greater than that occurring within the aqueous phase at certain calcium chloride concentrations, will lead to curvature of the interface towards the oil phase. Likewise, inter-particle attraction within the global primary minima within the aqueous phase greater than that of the oil phase will also promote curvature towards the oil phase. Increasing calcium concentrations simultaneously promotes densification of the adsorbed flexo monolayer and reduces repulsion between the aqueous phase-bound fractions of the adsorbed particles relative to that within the oil. Eventually, specific regions of the interface with high concentrations of adsorbed ink may undergo a localized spontaneous curvature of the interface. As the density of the ink monolayer increases via further adsorption or lateral transport of ink particles from neighboring interface, a cavity may form within the bulk oil phase. At a critical compaction of the monolayer, the cavity may detach from the interface to yield an ink-stabilized vesicle within the oil phase. The presence of macro-vesicles within the TDA-32 droplets allows

for such an event to be speculated. Such local, spontaneous emulsion inversion events have been observed previously[62].

An explanation for the observed optimum calcium concentration for flexo flotation may stem from the aggregation behavior of colloids at interfaces relative to bulk suspensions. Increasing calcium chloride concentrations above 100 ppm, although capable of reducing the surface charge of dispersed flexo ink particles, may actually promote charge reversal of particles adsorbed at the interface. High calcium concentrations may also result in the improper orientation of adsorbed particles for vesicle formation (e.g. the particle is completely immersed in the oil phase and does not stimulate interfacial curvature).

A major advantage of these three postulated mechanisms, partitioning, interface assembly followed by diffusion and vesicle formation, is the constant regeneration of the oil-water interface for continued adsorption of flexo particles. Collection is not limited by the surface area available for adsorption. In addition, ink aggregates or ink-lined vesicles, sequestered within the emulsion droplets, are impervious to hydrodynamic shear forces generated within the flotation cell that would otherwise detach particles adsorbed at air bubble-water or oil-water interfaces before they can be retained within the foam layer.

CONCLUSIONS

Surfactant spray flotation incorporating conventional defoamer has been shown to be capable of enhancing the removal of ink from furnishes consisting of 100% flexographic ONP. The capacity of the defoamer emulsion to interact with the colloidally stable dispersed flexo ink particles is a direct function of calcium chloride concentration within the aerated furnish. At low levels of calcium chloride, the ability of the defoamer to enhance post-flotation pulp brightness is proportional to electrolytic strength. However, this relationship appears finite given that an empirically determined concentration of 100 ppm was found to yield the greatest brightness gains (up to 8 ISO points). Beyond this concentration, the brightness gains were found to diminish considerably. Conventional calcium-soap and commercial deinking additives failed to elicit brightness gains comparable to the novel mechanism when operated within optimized conditions. In addition to improving pulp brightness, the ability of surfactant spray technology to reduce yield losses across a flotation unit was retained within the defoamer-calcium chloride system.

Investigations into the fundamental mechanism of this electrolyte-dependent phenomenon indicate that the apparent collection of suspended flexo ink is not the result of specific chemical interactions between calcium and the ink particles. A systematic approach to identify specific interactions between calcium chloride and the defoamer yielded the following conclusions:

179

o Conductivity trials indicate that TDA-32, although capable of gaining an anionic charge within alkaline conditions, does not significantly consume calcium ion.

o Moreover, the cationic demand of the anionic TDA-32 emulsion droplets, although extremely low, was not influenced by increasing levels of calcium chloride.

o Calcium does not influence the rate at which the defoamer diffuses to the air-water interface of an air-bubble.

o Neither does calcium affect the affinity of the defoamer for the air-water interface.

o The spreading coefficient of the defoamer across the air-water interface is independent of calcium concentration with the proviso that the "water phase" is actually fiber-free pressate.

o FT-IR absorption spectra reveal that the chemical structure of the dispersed phase of TDA-32, polydimethylsiloxane, is not modified by the presence of calcium chloride.

o The demonstrated ability of a non-siloxane defoamer to replicate the brightness gains afforded through the use of TDA-32 indicates that the collective behavior of the emulsion drops is relatively independent of the nature of the oil. This also suggests

that the mechanism of "collection" involves physical rather than chemical interactions.

Trials designed to elucidate the influence of increasing concentrations of calcium chloride on the physicochemistry of flexo ink particles suggest that flexo ink particles are not simply made "more floatable" through the addition of calcium ions:

o When suspended within the bulk aqueous phase, flexo ink particles do not aggregate into more floatable dimensions by the addition of calcium chloride (at least at levels employed during the flotation trials).

o In addition, the particles tend to retain significant surface charge at all calcium chloride concentrations assayed.

o Contact angles taken from films prepared from dispersed flexo ink with various calcium chloride levels revealed the ink to be extremely hydrophilic at both low and high divalent electrolyte concentrations. The highest contact angle, recorded from films prepared with intermediate calcium chloride concentrations, was still too low to suggest particle aggregation within the aqueous phase.

Rather, than specific chemical interactions between calcium chloride and defoamer or calcium chloride and ink particles, the mechanism requires interplay

between all three components to enhance flotation efficiency. Trials designed to quantify the relationship between the three provided the following observations:

- o As calcium chloride concentrations increase, flexo ink particles are imparted with the ability to stabilize water-in-polydimethylsiloxane emulsions (indicating calcium chloride-mediated particle adsorption at the oil-water interface).

- o In addition, at specific calcium chloride concentrations, flexo ink particles diffuse into the oil continuum (above these concentrations, the phenomenon discontinues). The significance of this observation resides in the fact that the maximum diffusion occurs at calcium chloride concentrations found to yield the greatest brightness gains during actual flotation trials.

From these results the mechanism by which dispersed flexo ink particles are "collected" by the defoamer droplets has been determined to involve interfacial adsorption followed by biphasic transfer of the adsorbed particles into the oil continuum. Potential models by which this occurs are supported by published research defining inter-particle interactions at liquid-liquid interfaces. The most significant revelation maintains that interfacially-bound particles tend to aggregate at salt concentrations of up to two orders of magnitude less than that those required to promote aggregation within the aqueous bulk phase[68][69][74]. This would explain the formation of aggregates at the siloxane-water interface at 100 ppm calcium chloride while the same level of electrolyte could not aggregate ink particles in bulk.

Although the bulk of the trials were conducted with a furnish consisting of 100% flexo ONP (not likely to be found in any RCF mill today), applicability of the system to contend with pulps containing small portions of flexo-printed material is anticipated. In fact, as the weight percentage of flexo-printed material within the feed deviates from the 100% used throughout the trials, the reported brightness gain is expected to increase. Rather than necessitate the of inclusion of an entirely new chemistry within the deinking mill, the system exploits the presence of defoaming agent within the patented surfactant spray technology developed to minimize yield losses across the flotation unit[12]. To this end, in addition to improving yield, defoamer-mediated collection of flexo ink can be considered an additional benefit afforded by the technology.

INTRODUCTION TO EXPANSIN

Molecular manipulation of the fundamental polysaccharide scaffold within a pulp wood fiber typically ceases beyond bleaching operations. Any modification to the integrity of the cell wall subsequent to this event is largely of the mechanical variety as shear forces generated at the refiner randomly impart cracks, local compressions and microfissures within the fiber. Recently, structural modification of the fiber in excess of that afforded by conventional chemical and mechanical means has been accomplished through biological measures. Commercially available fiber "conditioning" enzyme systems rely on the degradative ability of exogenously applied proteins to increase pulp drainage rates, adjust surface charge, remove persistent lignin complexes and eliminate problematic extractives.

Unfortunately, application usually amounts to a loss in yield as valuable polysaccharides are hydrolyzed into fines and soluble monosaccharides to be lost at the forming table. Additionally, the specificity of this enzymatic hydrolysis is poor and biotechnological systems designed to augment specific virgin fiber properties can actually cleave load-bearing polymers within the cell wall. As a result, the tensile strength of the final product suffers. Compounding the disadvantages of current enzymatic systems is a general limitation to partial recovery of one or two desirable properties within secondary fibers at the expense of others. Consequently, paper products derived from such enzyme-treated pulps may possess limited physical and optical characteristics.

A recently isolated plant cell wall protein restores expansion within heat-killed seedling walls following exogenous delivery[87]. Since the protein appears to induce this phenomenon in a non-enzymatic manner, it is provided the noncommittal label "expansin". The exact physiological mechanism by which the protein stimulates extension is currently burdened with speculation. However, results generated from experiments designed to expose the intricacies of *in vivo* expansin physiology indicate a potential for controlled industrial application. The advantage of a single protein system over the costly enzymatic "cocktail" combination approach is immediately evident. However, expansin may generate the most industrial interest for an unprecedented biotechnological capacity: the ability to alter wood fiber dimensions in a fashion previously reserved for natural cell growth. The interaction between expansin and bleached wood fiber may impart the same benefits of the current biotechnologies without affecting fiber quality or yield. The value added to end-product quality as a consequence of manipulated fiber dimensions is clear (e.g. enhanced strengths, surface charge, conformability, etc.). Numerous processes involving expansin-mediated fiber manipulation are also envisioned (e.g. facilitated repulping and deinking regimes, enhanced biofuel production, novel conversion techniques, etc.). However, the primary goal of this investigation is to assay the capacity for exogenous expansin systems to reconstitute load-driven elongation of chemical wood pulp fibers.

SECONDARY FIBER

Before attempting to elucidate the mechanisms employed to recover secondary fiber, a basic comprehension of the morphological changes associated with pre-dried cell walls is essential. These alterations are largely responsible for the loss of papermaking efficiency and product quality with pulps containing substantial secondary furnish. The two primary causes of detriment to secondary fibers are hornification and surface inactivation.

Hornification is a holistic term given to the tendency of recycled fiber to become increasingly dense after the consecutive rewetting, dewatering, and drying steps associated with secondary fiber papermaking. **Figure 53** details a possible mechanism whereby the lamellae of the fiber wall undergo radial contraction during drying. In a hydrated virgin fiber, relatively devoid of lignin and residual extractives (i.e., chemically bleached kraft), water fills the voids between concentric lamellae to impart a robustness associated with maximal swelling. The consequential hydraulic strain within the fiber may continue to disrupt noncovalent interactions between wall polymers that were formed as lignin and wall proteins were extracted during bleaching. Although the bleaching sequence alone is responsible for enhancing the surface charge of the fiber, this water-mediated disruption of late-forming bonds may increase ionized functional groups at the newly exposed fiber surface and contribute to the overall charge. As long as the fiber remains hydrated, the buffering water layer serves to discourage the formation of noncovalent interactions between the hydroxyl groups of neighboring

lamellae thereby maintaining the maximum hydraulic volume. The fully swollen fiber diameter ensures a maximum surface area. This, combined with the enhanced availability of ionized groups increases the surface energy to promote optimal dispersion and interfiber bonding during papermaking. In addition, this hydraulic separation enables the lamellae to slide relative to one another within the cell wall. The consequential wall flexibility is essential for paper formation on the wire. In brief, the hydratability of the virgin fiber is directly proportional to the quality of the end product.
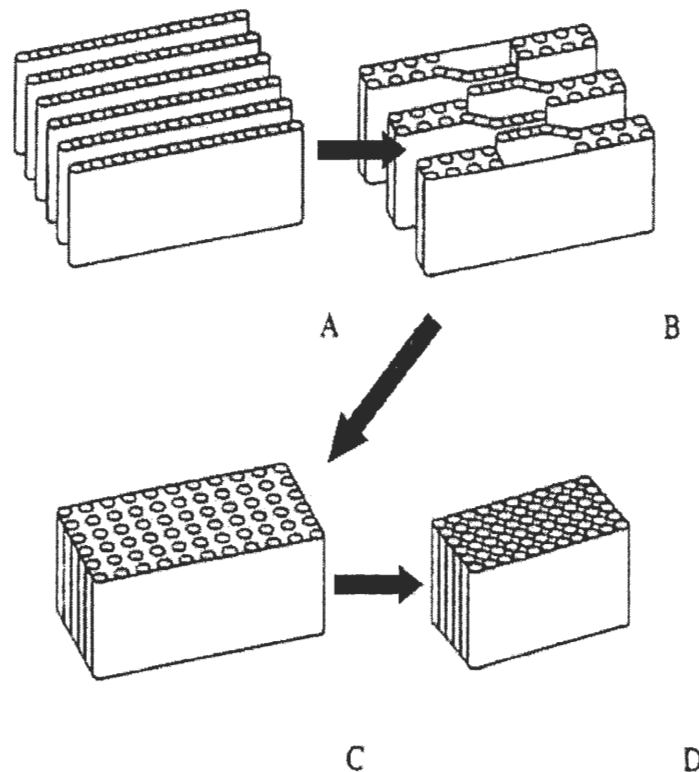
Figure 53: The lamination of lamellae during fiber drying. A. When fully hydrated, the concentric lamellae maintain complete separation. B. As water is removed from the wall, lamellae are pulled close together so that hydrogen bonds may form. C. Eventually, sufficient hydrogen bonds form to condense the entire cell wall. D. Further water removal results in densification of the wall.

Once incorporated into the forming web, the fiber begins to lose water during the drying process. Once interfiber moisture is effectively removed from the nascent paper sheet, interluminal and cell wall water are drawn from the individual fibers. As the buffering water layer becomes thinner, the lamellae are pulled together via capillary forces. At a specific proximity, the hydroxyl groups of adjacent lamellae interact to form a network of noncovalent bonds as seen in **Figure 53**. This is the same mechanism by which strong bonds are formed between individual fibers during papermaking. Fibers within the finished product, although tightly bound to neighboring fibers within the paper matrix, are much denser due to the internal lamination of coaxial lamellae. In addition, fiber pores decrease in size on account of the newly compacted cell wall. These phenomena, of extremely benefit to paper composed of virgin stock, prove rather disadvantageous to reuse of the fiber[88].

During recycling operations, the paper substrate of choice is repulped to separate individual fibers for subsequent cleaning and reconditioning prior to reintroduction into the paper machine. Unfortunately, the sheer number of hydrogen bonds created during the previous round of dewatering and drying prevent the separation of lamellae. This densification of the cell wall does not allow the fiber to accommodate the original volume of water upon hydration. The state in which the network of interlamellar bonds adversely affects hydration is referred to as hornification. Both fiber swelling and pore distension are retarded consequently decreasing the extent of accessible surface area and surface activation. Excessive internal hornification within the secondary fiber obviates

the limited sliding mobility between adjacent lamellae to reduce fiber flexibility. Fibers become stiff and brittle as a result and become less conformable at the forming table.

The coaxial compression of the cell wall decreases the fiber diameter during compaction. This effectively decreases the surface area of the fiber available for inter-fiber interactions within a nascent web. The densified fiber obscures functional groups at the fiber surface to adversely affect the extent of inter-fiber bonding. External fibrillation introduced during refining of the virgin pulp to augment interfiber bond strengths is also diminished as the fiber dries. As water is removed, the fibrils eventually collapse onto another cellulosic entity and form hydrogen bonds. This can occur between the fibrils and other fibrils, other fibers and/or the parent fiber. Simple hydration of the fiber during repulping operations is not sufficient to disrupt this interaction and the fibrils generally remain affixed to the fiber surface. This further limits the ability of the fibers to form strong external bonds on the wire[89][90]. This combination of hornification-related characteristics of post-consumer fiber effectively reduces the strength properties that can be expected from paper products containing recycled furnish.

To counteract the problematic nature of secondary pulps, refining regimes are often implemented to partially restore fiber flexibility and fibrillation. Beating recycled pulps introduces cracks and microfissures within the cell wall increasing the range of motion, increasing surface area and revealing internal functional groups. However, significant delamination is not obtainable by this method and the fiber retains considerable hornified density. Furthermore, the inherent brittleness of the secondary

fibers results in a renewed fines generation as mechanically imposed stresses within the refiner promote complete intra-fiber failure. In most instances, the liberated fines retain the hornified nature of the parent fiber which ensures a relatively small hydrodynamic volume (i.e. the fines are as compact as the original fiber with relatively few fibrils projecting from the surface). The hornified fines are more likely to be lost at the forming table in the whitewater filtrate.

As mentioned previously, refining imparts discontinuities within the cell wall as stress-relieving cracks and fissures appear[88] [t]. This effectively shears wall polymers thereby reducing the tensile strength of the individual fibers. This combination of hornification-related events involving reductions in fiber strength and inter-fiber bond strengths and frequency corresponds with a decrease in desirable physical properties of papers containing recycled fiber. Considering that this weakness is compounded by a loss in yield and an expensive supplementary step within recycling regimes, a sound

---

[t] Interestingly, lamination in the radial direction increases tangential stresses that eventually lead to the formation of radial cracks and fissures in the fiber wall. This could compensate for some of the loss in surface activation in recycled fiber due to pore closure by increasing the specific surface area and exposing internal cavities isolated during lamination. In addition, numerous rounds of rewetting, dewatering and drying decrease the amount of crystalline cellulose within the microfibrils. This may potentially introduce extra void space for water uptake and/or advance defibrillation at the fiber surface. Unfortunately, the alleviative contributions of these phenomena are negligible since experimental evidence has shown that recycling inevitably leads to irreversible loss of surface activity [3, 4].

method of secondary fiber reconditioning is a prerequisite to recovery of high-value fiber for low-cost manufacture of quality products.

ENZYMATIC FIBER CONDITIONING AND RECYCLING

The degree of reconditioning required to salvage desirable qualities within recycled fiber is contingent upon the history of the fiber prior to repulping. Recycling of waste streams containing high-value chemical pulps must contend with the detriments of hornification and surface deactivation as well as the presence of resilient coating components, sizing agents, dirt and ink particles. Although additional mechanical refining and chemical bleaching treatments may recover some conformability and optical properties, respectively, paper strengths and fiber yield may suffer. Moreover, additional expenses are required to cover the associated increase in energy and chemical consumption. An alternative to traditional reconditioning of the secondary fiber without additional steps or significant expenditure is to incorporate specific enzymes into the repulping and/or contaminant removal procedure. An industry may choose from a spectrum of pulp modifying enzymes to enhance drainage rates, increase paper strengths, reduce pitch problems, increase fiber wettability, facilitate ink removal, etc[91]. This may usually be accomplished with minimal capital investment as enzymatic technologies generally dovetail with current recycling practices and, in many instances, prove to be more efficient than conventional procedures[92]. Sufficient enzymatic activity can often be achieved with very small amounts of exogenous protein[93][94]. A summary of the more popular enzymes within the recycling industry is provided below along with the pros and cons of each application.

Cellulase

Cellulases have proven to have universal application within the papermaking industry. For recycling purposes, commercial preparations of these enzymes have been advanced for a range of fiber modification including strength augmentation, deinking, and increasing drainage rates[91][92][95][96]. Cellulases act by hydrolyzing the glycosidic linkage between neighboring glucose residues within cellulosic chains. Endo- and exo-cellulases are capable of chain cleavage from the middle or the ends of the molecule, respectively. This catalytic action theoretically releases numerous short-chained oligosaccharides and monomeric glucose units from the fiber wall as the enzyme glides along the surface[97]. A sort of peeling action takes place as the exo-cellulases systematically travel along the length of the cellulose strand releasing soluble reduced glucosyl residues in their wake. A notable consequence of the release of water soluble mono- and disaccharides is a general increase in the COD of the effluent[98]. Endo-celluloses, randomly cleaving the chain at internal sites, introduce new ends for exo-cellulase activity. It is this capacity for depolymerization that is exploited within fiber reconditioning procedures as an alternative to refining[91].

Virgin pulps are refined to impart conformability and, to some extent, generate fibrils at the fiber surface. Unfortunately, beating times required to ensure optimal flexibility may lead to surplus fibrillation. The newly exposed microfibrils increase the specific surface area of the fiber available to interact with water. This has the taxing tendency to decrease drainage rates which manifests as a reduction in paper machine runnability[95][96][97][99]. Cellulases are able to depolymerize these microfibril fragments thus

192

removing them from the fiber surface and recovering target drainage rates. Fines released during refining are also partially hydrolyzed to enhance dewatering[100]. In addition, the individual fibers are less prone to form agglomerations enabling greater head box consistencies. This may increase the quality of sheet formation and ultimately benefit the mechanical properties of the end product[96].

Recently, cellulases have been demonstrated to enhance flotation deinking of mixed office waste[91][96]. This discovery served as the impetus for global enzyme companies to tailor their current cellulase marketing campaigns to include references to deinking proficiency. Thermophilic cellulases with optimal activity within alkaline environments have been earmarked for deinking purposes[94][101]. Exact mechanisms by which most of the toner particles are removed from the fiber surface remain somewhat ambiguous. Current consensus maintains that the cellulases, during typical non-specific peeling hydrolytic activity, release the microfibrils or individual cellulose chains that serve as anchors to the ink particles[93]. This may involve gradually undermining the particle bound to the fiber surface or simple release of a particle tethered to the fiber surface by exposed microfibrils[102]. Another possible explanation is that some microfibrils bordering micropores and fissures providing footholds for physical attachment of toner to the fiber surface may be degraded by the cellulase. This serves to widen the depression and favor particle diffusion away from the fiber[96]. Other explanations hold that the cellulose binding domain of the cellulase enzyme has a large enough affinity for the fiber surface that it actually overcomes ink/fiber interactions and dislodges the ink by sheer force[103].

Once free from the fiber surface, the ink particles may still not adhere to the air bubbles on account of the hydrodynamic drag, increase in surface area and change in surface activity imposed by the attached microfibril fragments. The remarkable increase in floatability attributed to cellulase deinking may occur as the enzymes remove the protruding microfibrils from the ink particle surface thereby reducing drag and increasing particle hydrophobicity[92] [96]. For reasons as yet conclusively defined, the toner particles demonstratively shrink during enzymatic deinking. The consequent decrease in surface area favors adhesion to the air/liquid interface. However, should the particle shrink too much, this flotation efficiency suffers and brightness values of the final product are affected[103]. The enhanced release of toner particles and subsequent particle surface restoration combine to make cellulase-mediated flotation deinking of MOW a practical technology.

Like most deinking enzymes, the cellulase is added to the repulper operating at relatively high consistencies (~10-16%). The necessary mechanical agitation during fiberization generates the shear forces needed to facilitate detachment of partially loosened ink particles from the fiber surface. This critical prerequisite to effective enzymatic technology is universal and ensures that the enzyme maintains a uniform dispersion while promoting maximum productive catalytic interactions. In the end, cellulase treated pulp is both deinked and exhibits an increase in drainage rates.

Unfortunately, since cellulase is a degradative enzyme with specificity for cellulose, excessive use during reconditioning or deinking practices tends to reduce pulp viscosity. At this point, cellulose chain depolymerization and internal cleavage may

actually reduce the final strength of paper derived from the secondary pulp[95 97]. Another factor limiting the proficiency of cellulase is the presence of lignin during recycling. Secondary pulps containing substantial amounts of lignin (e.g. CTMP, TMP) are less susceptible to cellulase activity since the phenolic polymer physically obstructs enzyme binding sites and may affect ink detachment rates[94].

Cellulase, currently the enzyme of choice during flotation deinking, also reduces secondary fiber yield[103]. Although the enzyme does remove cellulosic fragments from toner surfaces, this is accomplished by dissolving the exposed regions of entrapped microfibrils. In effect, this process leaves significant portions of fiber within the toner particles that are subsequently lost during flotation. Possibly, the most notable deficiency of cellulase is the inability to reverse hornification within the once-dried fiber. Water retention values remain inferior and fibrils introduced during the original refining stage remain affixed to the fiber surface. Clearly, the role played by cellulase in recycling operations is limited.

Hemicellulase

Reconditioning of secondary fiber may incorporate alternate enzymes into the process with notable results. Drainage enhancement by cellulase application may be further improved by addition of hemicellulases. Typically xylanases, these hydrolyzing enzymes further reduce the fines within the pulp, dissolve lignin/carbohydrate complexes (LCCs), and expose cellulose microfibrils for cellulase activity[100].

Hemicellulases can be employed to augment the actions of cellulase. The ability to hydrolyze hemicellulosic components of the fiber cell wall provides these enzymes with the ability to disrupt some toner/microfibril interactions and contribute to the increase in hydrophobicity of the liberated ink particles. Xylanase is usually introduced prior to the high consistency repulper in conjunction with cellulase to control fines concentrations and enhance overall deinking efficiency.

However, the ability to increase ink removal and drainage rates occurs to the detriment of yield and end product properties in the same manner as cellulases. Overuse may lead to uncontrolled hemicellulose depolymerization that may both directly decrease viscosity and paper strength or expose more cellulose to cellulase with similar, although indirect, consequences. A synergetic hemicellulase/cellulase mixture may actually decrease the final fiber yield below that obtainable by pure cellulase.

Amylase, Lipase, Pectinase and Esterase

Amylases have proven to be effective starch modifying agents within the recycling industry. Internal and external sizes added to the original paper to impart a certain degree of hydrophobicity often carry over into the recycling process. The size residue decreases the wettability of the secondary fiber surface thereby hindering surfactant and/or enzyme accessibility. In addition, the sizes may have a bridging effect within the original paper product that resists separation of individual fibers within the repulper. Residual size adhering to the secondary fiber surface tends to neutralize surface charge and/or physically discourage inter-fiber bonding. This effectively reduces the number and strength of bonds within the final paper. Amylases are

introduced prior to the repulper to hydrolyze the starch into manageable monomeric sugar residues. Consequently, the hydrophilicity of the fiber surface increases and fiberization proceeds at a greater rate with less input of energy[96 102].

In addition to disrupting inter-fiber interactions, starch sizes may physically entrap ink, dirt, and lignin particles within or onto the fiber cell wall matrix. Dissolution of the polysaccharide chain by an amylase treatment allows the particles to diffuse into the surrounding aqueous phase for flotation removal. Residual starch, clinging to the particle surface, may be removed by the amylase to increase surface hydrophobicity and facilitate removal during flotation operations. Because this enzyme maintains specificity for β-cellulose (starch), pulp viscosity is not affected as no microfibril cellulose is hydrolyzed[96].

Other enzymes employed for secondary fiber modification include lipases to control pitch that has either avoided removal during production of the original pulp or been introduced during normal use of the paper prior to repulping[91 103]. Resins are degraded to triglycerides that may be further reduced into fatty acids via the action of exogenous lipases and esterases. Once pitch is removed, the fiber surface becomes less hydrophobic. Additionally, the problems associated with excessive pitch within the papermachine such as vessel picking and sticky deposition on high-energy surfaces become less frequent.

Lipase and esterase addition to the deinking process is primarily a means to dissolve oil-based organics such as ink vehicles and fiber-derived triglycerides. Often

used in concert, these hydrolases actively reduce the triglycerides of the carrier oil into fatty acids in a comparable fashion to resin dissolution. By this mechanism, the ink particles are readily dissolved and release the pigments for dispersion and subsequent removal[91 100 102]. Via a mechanism analogous to the removal of resins prior to paper manufacture, the hydrophobic character of the fiber decreases as the oil-based ink vehicle is dissolved.

Pectinases have been used as well to aid in fiberization procedures in much the same fashion as the amylases[103]. Popular ligninolytic enzymes used during pulping and bleaching operations such as oxidoreductases may be applied to the secondary furnish to remove any residual lignin that may have loosened or become exposed during the lifetime of the original paper product. These enzymes outlined above may be combined to recover a significant portion of the physical characteristics of the virgin fiber. Unfortunately, the high concentration of synthetic polymers within current papermaking practices precludes the use of these enzymes for extensive fiber reconditioning and cleaning purposes.

In summation, the enzymes that are currently available for secondary fiber recovery purposes have variable potencies when dealing with high-value, post-consumer chemical furnishes. A variety of enzymatic cocktails may be custom-made to address specific furnishes in a multi-pronged fashion. These are usually built upon a cellulase/hemicellulase base accompanied by a collection of accessory enzymes depending on contaminants within the furnish. Often, this results in satisfactory gains in brightness values, an increase in paper machine runnability and recovery of the certain

mechanical properties of the original product at considerable monetary savings. However, one drawback when using these degradative enzymes during traditional recycling operations remains the significant decrease in secondary fiber yield. Another is the requirement that the enzymatic cocktail be continuously modified to accommodate the heterogeneous flow of paper waste input to avoid over- or under-saturation of the enzyme. Clearly, an enzyme able to promote the recovery of virgin fiber attributes to an acceptable degree without the benefit of a cellulosic hydrolytic capacity would avoid the risk of pulp viscosity reductions and loss of fiber yield. At this point, the benefits of using a recently discovered enzyme, expansin, in the stead of degradative cellulases and/or hemicellulases are postulated.

EXPANSIN

Discovery

In 1992, two endogenous proteins were isolated from cucumber hypocotyls (*Cucumis sativus* cv Burpee Pickler) that displayed the ability to stimulate prolonged elongation of heat-inactivated cell walls immersed within an acidic suspension[87]. Cell wall loosening and turgor-driven expansion and elongation under acidic conditions has been well established although the exact biochemical mechanisms for such remained elusive preceding this discovery. Simon McQueen-Mason, Daniel Durachko and Daniel Cosgrove labeled these enzymes "expansins" and began a series of experiments to elucidate the underlying physiology of growth-related plant cell wall expansion and elongation with this newfound information. Before attempting to provide potential

mechanisms of expansion activity, the plant cell wall architecture in which the protein exists will be defined.

The Extensible Plant Cell Wall

The typical dicotyledonous primary plant cell wall can be loosely defined as a concentric assemblage of laterally aligned cellulose microfibril layers. Adjacent microfibrils within a layer are connected to one another by noncovalent interactions between heteroglycan sheaths or by way of a bridging wall protein. These interactions form a two-dimensional sheet of one microfibril thickness that extends around the circumference of the cell in sheath-like fashion. Continuous deposition of cellulose microfibrils and associated matrix polysaccharides during cell growth thickens the wall with a series of successive laminations. These laminations were referred to earlier in the discussion of fiber wall modification during drying.

Recently, nuclear magnetic resonance relaxation data has suggested that adjacent microfibrils within each layer are cross-linked through a network of hemicellulosic chains and that these chains do not actually form bridges to microfibrils of neighboring layers[104]. Traditionally, xyloglucan bridges were presumed to anchor one microfibril layer to the next and collectively resist stresses imposed normal to the cell wall. Instead, structural integrity across the thickness of the cell wall is maintained by a semi-heterogenous layer of galactan-rich pectin between each microfibril layer. **Figure 54** illustrates a recent model of the anatomy of major polymers within the plant cell wall proposed by Ha *et al* and Fenwick *et al* based upon NMR magnetic relaxation studies[105].

200
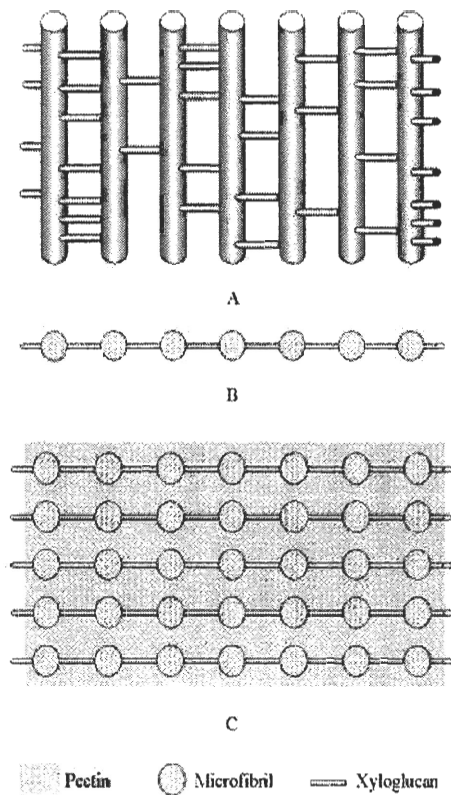
Figure 54: An extremely simplified version of the hydrated, *in vivo* plant cell wall as suggested by NMR relaxation assays. A. A tangential view of the cellulose microfibrils within a single layer and the bridging hemicellulosic elements. B. A cross-sectional view of the same layer. C. A hydrated pectin "gel" maintains separation between concentric microfibril layers.

Within the hydrated cell wall, the cellulosic microfibrils, by far the most rigid of the wall components, resist stresses imposed in directions relatively parallel to microfibril angle. Xyloglucan bridges between adjacent microfibrils within an individual lamella resist perpendicular tangential stresses and prevent separation of microfibrils. Pectins flow in and around these load-bearing components of the cell wall and are presumed to paradoxically provide both flexibility and rigidity to the cell wall in a time-dependent fashion. According to Fenwick *et al*, a significant portion of the pectin

component within an actively growing cell exhibits notable mobility during periods of applied stress (i.e. turgor)[105]. This mobility may indicate that these polymers are not forming the motion-limiting hydrogen bonds with the structural polysaccharide matrix of microfibril layers necessary to bridge the gap between layers. The lack of bridging between concentric layers enables the microfibril layers to slide relative to one another as they react on an individual basis to tensile forces. At this point, the pectin layer is essentially a fluid lubricant that relieves inter-microfibril layer shearing stresses imposed within the expanding cell wall. However, as the cell matures, the pectins begin to show less mobility. A drop in pectin component mobility closely corresponds with stiffening of the cell wall. Ha suggests that a reduction in the methyl-esterification of nascent pectins is directly related to this phenomenon[105]. A potential explanation is that the reduction in esterified methyl groups within the pectin may enable the protein to form hydrogen bonds to the hemicellulose and cellulose matrix within the microfibril layer and between adjacent pectins. In this manner, bridges begin to form between the layers thereby restricting the shearing movement. Now instead of serving as a molecular lubricant, the pectin layer assumes a slight structural role.

Within the thickening cell wall, the collective effort of the microfibrils, hemicellulose and pectin imparts an inherent multidirectional mechanical strength that counteracts the expansive forces imposed by intracellular turgor pressure. Controlled growth occurs as this load-bearing polymer matrix undergoes molecular relaxation by some physiological means. At this point, the cell wall can be considered a viscoelastic fluid material with inherent strain and failure properties under applied stress[106]. This

stress is provided in the form of a hydraulic pressure gradient generated across the cell wall in response to turgor. In response to the stress, the high-strain plasticity of the wall allows the cell to expand in all directions. As the pressure difference returns to zero with an increase in interluminal volume, the rate of expansion slows and eventually ceases.

The exact physiology by which the cell wall expands remained primarily conjectural until recently. Obviously, during growth, the cell will need to expand and lengthen while simultaneously strengthening the load-bearing properties of its wall. The slight strain allowed by the inherent viscoelastic properties of the wall is not sufficient to account for total cell growth. To overcome this limitation, microfibrils are presumed to slide relative to one another within and between individual lamellae[107]. To avoid a consequential thinning effect in the elongating cell wall, new compensatory matrix polysaccharides and proteins must be continuously deposited into the growing wall. Therefore, the wall may elongate while retaining the thickness required for structural soundness. Furthermore, as the cell grows it will tend to widen in a radial direction. To accommodate the increasing diameter, adjacent microfibrils must overcome the polysaccharide tethers and separate to enable integration of *de novo* produced microfibril between them[106 108 109]. This ability of the growing cell wall to extend in the x and y plane is referred to as "reptation". As the wall matures, the concentration of wall pectin and lignin becomes great enough to hamper microfibril sliding possibly through cross-linking, noncovalent and covalent interactions with adjacent microfibrils.

Once fully, mature, the wall is said to be inactive and does not undergo further expansion. The cell wall of the newly inactive plant cell is considered the fiber.

Although the exact physiology and cellular control of this complex sequence remains largely ambiguous, the tendency for auxin or fusicoccin to stimulate growth is well-documented[87][110]. The hormones are not generally thought themselves to be directly involved with extension but rather stimulate protein pumps within the cell to pack protons into cell membrane-bound Golgi vesicles for release into the growing wall matrix. By this process, known as "acid-growth", the local pH drops within the wall and the wall becomes noticeably pliant as the interactions between matrix polymers begin to weaken[106][111][112]. As a result, the aforementioned turgor pressure within the cell is able to force the cell wall outward as wall polymers slide past one another. Once the intra- and extra-cellular pressure difference has been obviated, the wall polymers may reestablish the noncovalent linkages and recover wall strength.

Previous to the finding of McQueen-Mason and Cosgrove, the drop in pH was thought to have a deionizing effect within the cell wall that triggered the loosening of the neutral and acidic polysaccharides and proteins. Deionized heteroglycans and/or pectins forming the bridge between microfibrils were suggested to disassociate from the cellulose thereby enabling the turgor-driven sliding action within the cell wall. Recent experiments have demonstrated that heat-inactivated cell walls do not maintain the ability to expand when exposed to acidic conditions. Therefore, the lower pH, although certainly a stimulant of expansion, is not completely responsible for the phenomenon.

The tendency for the cell wall to lose activity when exposed to heat is indicative of an essential protein within the cell wall for proper expansion. Until the discovery by McQueen-Mason and Cosgrove, this protein remained elusive. The suspect enzymes were endo- and exo-glucanases and xyloglucan transglycosylases[107]. Today, expansin has assumed the role of the chief protein mediator of cell wall expansion during acid growth[110]. Once the cell begins to mature and covalent interactions within the wall begin to accumulate, the resident expansins lose proficiency and the cell wall stabilizes. At this point, the cell wall becomes the familiar viscoelastic material encountered in paper grade fiber.

Mechanism of Expansin Action

The exact mechanism by which expansins facilitate cell wall extension and elongation remains vague[107]. Numerous experiments conducted to determine the preferred binding site of the protein within the wall matrix have indicated that the actual mechanism of cell wall expansion involves an expansin-mediated change in glycan-glycan interactions. In brief, under certain conditions, the presence of expansin, of either endogenous or exogenous origin[u], causes cellulose microfibrils and matrix

---

[u] In general, α-expansins have not been demonstrated to exhibit species specificity. This is probably due to > 75% homology between all currently available α-expansin primary amino acid sequences. Consequently, most plant physiological investigations, regardless of species, have used purified cucumber expansin with notable results. This may indicate an amenability of a standard exogenous expansin to fibers of various origin.

polymers to slide relative to one another when subjected to load-stress. The entire process appears to involve little more than mechanical disruption of secondary bonding between the polysaccharide framework components. This reptation is exclusively observed within living plant cells. As the cell matures, lignin deposition introduces interfibrillar covalent bonds that prevent reptation. Since fibril sliding is no longer an option to relieve axial stress, fiber deformation in response to the load is a function of the axial elastic modulus of the mature fiber. A stressed mature fiber undergoes a time-dependent change in molecular configuration as wall polymers align in the load direction in an attempt to reach a metastable equilibrium state. This rearrangement occurs through distortion of bonds and valence angles as the wall components assume a more crystalline form. However, significant elongation by virtue of the viscoelastic properties alone is negligible and complete failure is a real eventuality. Within a sheet of stressed paper, the slight fiber elongation combines with mobility between bonded fibers. The resulting elongation is collectively labeled "creep". Conversely, disruption of interfibrillar hydrogen bonds by expansin enables the viscous flow-like reptation in which wall polymers do not alter intramolecular bond length or angles in response to the load. Elongation proceeds without introducing shearing forces or breaking and distorting primary bonds and valence angles. The molecular fidelity of the fiber is effectively preserved without storing energy. It is the author's opinion that creep and reptation represent two separate, unique phenomena. Although traditional procedures designed to plot fiber stress-strain curves may still be used to measure elongation, the treatment of results must discriminate fiber viscoelastic properties from reconstituted "growth" (i.e. reptation).

The actual site of expansin binding within the wall matrix is unclear. Recent experiments have concluded that expansin binds at the interface between the cellulose microfibril and the sheath of hemicellulosic bridging elements[108]. **Figure 55** provides a simplified schematic of presumed expansin activity within the nascent wall matrix. In response to axial tension conferred by turgor pressure or artificial longitudinal stress, the release of short stretches of hemicellulose glycan tethers enables limited sliding movement of the cellulose microfibrils[109].
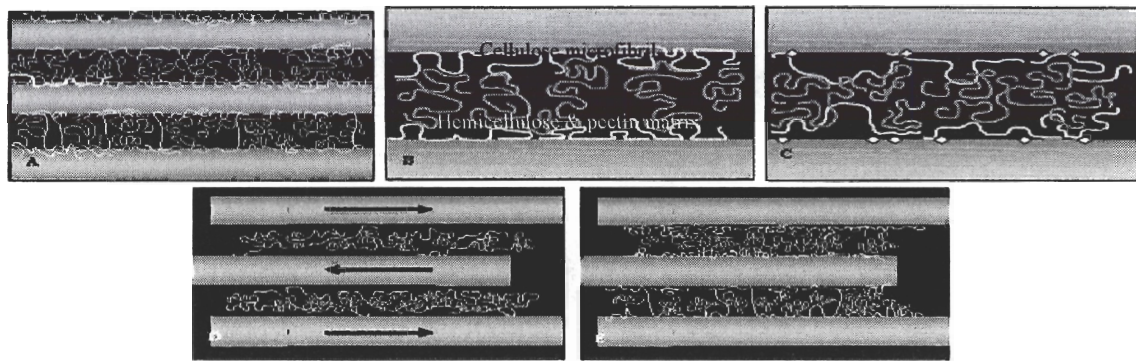
Figure 55: A generic schematic of a young cell wall under axial tension: A. Cellulose microfibrils embedded in a sheath of matrix polymers. Polysaccharide bridges resist microfibril movement. B. An enlarged view of the microfibril-hemicellulose interface. C. Expansin proteins (white diamonds) effectively disrupt hydrogen bonds at the interface thereby liberating short stretches of matrix polymer. D. With a reduced density of connected bridging elements, the fibrils are able to slide relative to one another in response to an imposed force and the cell wall lengthens. E. Physiological signals (e.g. a local increase in pH) deactivate expansin and bonds reform.

As mentioned previously, cell wall maturation is coupled with lignin deposition. The complex phenylpropanoid network introduces numerous covalent linkages between wall components. From an external perspective, the wall loses pliancy and reverts to

the viscoelastic solid characteristic of pulp wood fiber[112]. At this point, expansin activity is not perceptible. Isolated mature cell walls are not sensitive to the application of exogenous expansin at any pH or tensile force[87]. Covalent bonds are, therefore, expected to resist expansin activity within lignified wood fiber. In addition, deposition of lignin and extractives during maturation may shield the sites for expansin binding. These factors combine to preclude expansin activity and wall growth ceases. Fortunately, chemical wood pulp fibers, in which the covalent linkages of lignin are replaced by hydrogen bonding between structural polysaccharides, appear amenable to expansin activity.

ANTICIPATED BENEFITS OF FIBER MODIFICATION

Although potential obstacles remain, no decisive factor exists to refute transition of expansin-mediated fiber modifying physiologies to certain industrial applications. Exogenous application of expansin to chemical pulp wood fibers is projected to enhance conventional papermaking qualities, give rise to a generation of specialty papers and promote development of processes contingent upon fiber dimensional modification. Directly or indirectly, an expansin-based system is speculated to:

1. Alter wood fiber dimensions

2. Increase conformability

3. Increase and/or maintain refiner-imparted fibrillation

4.	Reduce bleaching costs[v]

5.	Minimize refiner energy requirements

6.	Increase dirt removal efficiency

7.	Reduce capital investment

8.	Make end-product more amenable to converting operations

9.	Augment operations dependent upon efficient cellulose degradation

10.	Facilitate deinking operations

All investigations involving expansin to date have been exclusively academic. To this end, no information is available to dispute or support any or all of the above claims. Thus, the capabilities and limitations provided as physiological evidence are extrapolated to industrial procedures pending experimental contradiction. Since all forecasted benefits can be logically deduced from reconstitution of interfibril mobility, this particular investigation will focus on the ability of expansin to reconstitute juvenile-like cell wall elongation in mature wood fiber.

------

[v] By "loosening" the cell wall matrix, expansin may facilitate bleaching chemical/agent penetration.

Perhaps the most outstanding feature of expansin will be a demonstrated ability to facilitate secondary fiber elongation. Periods of mechanical fiber agitation (e.g. refining, repulping, washing, etc.) should impose significant longitudinal loads along the length of the fiber to encourage expansin-mediated fibril sliding. Even a slight increase in fiber length will have immediate industrial significance. Should fibers elongate, a general thinning of the cell wall and a decreased diameter is expected as shifting wall material is not replaced by compensatory polysaccharides as would be the case if the cell was biologically active. The immediate results of fiber modification in the above manner are:

1. Increased specific surface area

2. Enhanced surface charge

3. Increased conformability

4. Reduced coarseness

The predicted increase in surface area and charge as a result of newly exposed cellulosic fibrils will directly increase the relative bonded area (RBA) of expansin treated sheets. Consequently, paper strength properties are improved. Fibers bearing the amended total surface charge will impart maximum retention of both fines and filler and enhance wet-strength within the forming web. Increased collapsibility as a function of thinning walls will compliment the amended RBA and contribute to paper strengths and

210

densities. In addition, the thinner fibers are expected to provide a smoother, denser sheet by means of tight packing and reduced coarseness.

ARTIFICIAL FIBER ELONGATION

A force not unlike the mechanical stresses generated within papermaking operations will be imposed to promote realignment of macromolecules (i.e. fibrils) within the lignin-free cell wall. A subsequent load-deformation curve will enable quantification of expansin-induced elongation. Current equations derived to distinguish and quantify short-term viscoelastic behavior from primary, recoverable creep and secondary, irrecoverable creep within the loaded fiber will be amended to account for expansin-mediated deformation. Results indicative of a significant fiber-lengthening capacity will serve as an impetus for further investigation within particular industries.

EXPERIMENTAL PROCEDURE

ISOLATION OF EXPANSIN

Over the past decade, the original procedure established by McQueen-Mason *et al* to isolate the expansin protein from cucumber hypocotyls has been extensively and continuously modified to accommodate a spectrum of published investigations[87]. Although the cucumber seedling remains the primary source of expansin-rich cell walls, investigators are performing isolations from alternate sources (e.g. mung bean, tobacco, tomato, etc.) on a routine basis. To increase the amount of expansin isolated per unit wet weight of starting plant mass, recombinant species expressing the original cucumber expansin genes are even being used[108]. Although the chemistry employed to coax the water-insoluble cell wall proteins from the cell wall is relatively constant, regimes designed to separate expansin from the resulting crude extract can be complex, time consuming and/or economically intensive. A completely unprecedented experiment, such as the addition of expansin to a mature wood fiber in tension, should be initially conducted with a whole cell wall extract to quickly and inexpensively expose deviations, if any, from the controls. In the event that a significant change is triggered by the whole extract application, further purification techniques may be employed to isolate expansin-mediated affects from those of the whole extract. To this end, initial fiber elongation trials were performed with fibers submerged in volumes of total wall protein extracts from the original cucumber hypocotyls. The actual extraction procedure varied slightly from the original of McQueen et al. and is presented below.

212

Cucumber Growth

Approximately 200 g of cucumber seeds (*Cucumis sativus* cv Burpee Pickler) were carefully poured onto the paper-side of a 1 meter section of a plastic film-backed, disposable laboratory bench-top cover. By keeping the seeds in a rough line ~5 cm from one edge of the cover, the entire piece could be rolled into a cylinder with the plastic backing facing outwards. Once secured with rubber bands, the cylinder was lowered into a container filled with distilled water to a depth of 3 cm (the end of the cylinder containing the seeds was submerged in the water). In this fashion, capillary movement of the water upwards through the paper side of the bench-top cover provided the seeds with continuous moisture. The entire container was then placed in a dark laboratory incubator preset to 25°C and allowed to incubate for 4 days. At the end of this period, the cylinders were removed and unrolled to reveal a line of cucumber seedlings. Taking care to collect only the upper 2 cm of each four-day old hypocotyl[w], approximately 200 g of wet mass was collected and placed in an ice bath to avoid excessive protein denaturation and tissue oxidation. Extraction of this biomass proceeded immediately.

Biomass Homogenization and Extraction

A detailed description of the extraction reagent chemistry and preparation is presented in appendix A. The total amount of hypocotyls harvested was then placed in a

---

[w] The most actively growing portion of the seedling by the 4th day of growth. Presumed to contain most of the expansin activity in the seedling.

standard blender. To this mass, 500 ml of chilled homogenization buffer (25 mM HEPES, 2 mM sodium metabisulfite, 2mM EDTA, pH 7.0) was added and then pureed for 40 seconds. The resulting pulp was then poured into a funnel lined with Miracloth and the filtrate, containing soluble proteins, discarded. To remove most of the homogenization buffer and cytoplasmic components released during cell rupture, the Miracloth was lifted from the funnel and squeezed with a gloved hand. Once returned to the funnel, 500 ml of chilled distilled water was added to the pulp. Again the filtrate was squeezed from the cell wall pulp and the wash repeated a second time. The washed pulp was then suspended in 500 ml homogenization buffer and allowed to sit at room temperature for an hour and a half. This incubation period was found to enhance total wall protein isolation. The pulp was again filtered to remove any soluble proteins liberated during the incubation period.

The cell wall fraction was then combined with 250 ml of extraction buffer (1 M NaCl, 25 mM HEPES, 2 mM EDTA, 2 mM sodium metabisulfite, pH 7.0). The suspension was then placed on ice and agitated slowly for one hour to allow wall proteins to diffuse from the cell wall into the surrounding medium. If the agitation proceeded too quickly, foam, indicative of protein denaturation, would form on the surface of the suspension. At the end of the agitation period, the wall fragments were filtered across the Miracloth once more. This time, however, the filtrate, containing salt-precipitated wall proteins, was recovered and placed on ice. The wall fragments removed during filtration were again suspended in 250 ml of extraction buffer and

agitated for 1 hour, filtered and the filtrate recovered. This second extraction served to recover even more protein from the wall fragments.

After combining the filtrates within a 500 ml flask, ammonium sulfate was slowly added to the suspension while the flask was rotated on ice. The total amount of ammonium sulfate added amounted to 0.4 grams per ml of total wall protein extract. As the salt precipitated the wall proteins, the filtrate acquired a milky appearance. After completely dissolving the salt in the filtrate, the flask was allowed to sit for 1 hour at 4°C to permit further precipitation of wall proteins.

After the precipitation period, the wall protein extract was divided into 50 ml Falcon centrifuge tubes. Centrifugation for 10 minutes at 5000 G and 4°C effectively concentrated the precipitated proteinaceous mass in each tube. After decanting the supernatant, each pellet was reconstituted with the minimum amount of 50 mM sodium acetate buffer required to completely dissolve the pellet. The dissolved pellets were combined. Five ml aliquots of the suspended wall protein were injected into Slide-A-Lyzer cassettes (Pierce). The cassettes were then submerged into dialysis buffer (50 mM sodium acetate, pH 4.5) and allowed to dialyze at 4°C overnight. During the dialysis, the buffer was exchanged once.

After dialysis, the aliquots of total cell wall protein, were removed from the cassettes, combined and the protein concentration determined by the standard Bradford assay using bovine serum albumin for calibration. From the assay, it was determined that the extraction procedure could provide roughly 1 mg of total extractable wall

protein per gram of hydrated cucumber hypocotyl. This crude extract was presumed to contain substantial amounts of expansin and was used in preliminary investigations designed to determine the impact, if any, of the protein when added to isolated fibers.

FIBER SELECTION, PREPARATION, AND CHARACTERIZATION

Selection of a model wood fiber for the extension measurements proceeded with respect to six fundamental fiber characteristics: length, width, cell wall thickness, ring location, and microfibril angle. In the interest of obtaining a relatively long fiber to facilitate mounting within the extensometer, a 4 foot cross-section of a recently felled (4 day old) 49 year-old loblolly (*Pinus taeda*) was acquired from a natural growth forest (Big Trees Forest Preserve, North Fulton County, Atlanta, Georgia). One inch thick cross-sections of the larger log were cut and the sections quartered with hacksaw. This particular section of the tree happened to contain enormous amounts of tension wood which was viewed as beneficial to the experiment at hand[x]. From each wedge of pine, early wood from both the 23rd and 24th ring was sliced away with a razor blade. Fibers contained within these rings were presumed to be completely mature and, therefore, devoid of cellular function including residual expansin activity. The isolated rings were further cut into ~2"X2" chips for bleaching.

The chips were then submitted to 72 hours of soxhlet extraction with a 1:1 mixture of ethanol and chloroform. This pre-bleaching stage served to solubilize some

---

[x] Fibers isolated from tension wood tend to have thinner cell walls and longer total lengths.

amount of the organic residuals from the chips. At the end of the extraction period, the chips were solvent exchanged with 100% methanol for 24 hours. After this time, the solvent was exchanged for 75% methanol for another 24 hours. This procedure was repeated over the next 72 hours with 50, 25, and 0% methanol solvents. At this point, the chips were ready for delignification via an acid chlorite holopulping procedure[113] [114]. The chlorite pulping procedure presents as a gentle means by which to delignify softwood fibers without considerable detriment to the structural integrity of the fibers themselves. As the name implies, the holopulping procedure allows both cellulose and hemicellulose to remain remarkably intact as a cell wall devoid of phenylpropanoid residues. Considering that expansin appears to require the presence of both wall polysaccharides for activity and that the activity is suppressed in the presence of lignin, holopulping of this design was an extremely attractive concept.

The chips were transferred to a 250 ml Erlenmeyer filter flask. To the flask, 200 ml of a buffered chlorite solution (12 g sodium chlorite and 8 g sodium acetate brought to 200 ml with dH_2O^y) was added. Within the fume hood, 13 ml of glacial acetic acid was added to the flask and the neck of the flask immediately closed with a rubber stopper. A vacuum was pulled into the flask via the aspiration tube within the flask neck for 1 hour. The vacuum is considered essential to assist penetration of the chlorite liquor into the chips. After the penetration period, the vacuum was released and the aspiration

---

outlet sealed with parafilm. A green-yellow gas forming within the flask was indicative of the generation of ClO_2. To minimize photoinactivation of the ClO_2, the entire flask was wrapped in aluminum foil thereby preventing ambient illumination of the bleaching chips. Over the course of the next 4 weeks, the buffering solution and acetic acid charge were changed whenever the presence of the greenish gas could not be detected. Near the end of the month long bleaching process, the chips appeared bright white and individual fibers could be seen diffusing away from the chip surface. At this time, the chips were removed and washed with generous amounts of distilled water to dilute and displace adsorbed bleaching chemicals. The chips were then easily defibered within a laboratory disintegrator and stored at 40°C until further use. For a complete description of the chipping, extraction and delignification of the loblolly chips, refer to appendix B.

Microfibril Angle Measurements

Transfer of a load imparted along the longitudinal axis of an isolated wood fiber depends, to a great extent, on the microfibril angle within the S2 layer of the cell wall. In short, the lower the microfibril angle, the greater the elastic modulus of the fiber along this axis. Fibers characterized by high microfibril angles tend to stretch and elongate in response to an applied stress as the fibrils attempt to arrange themselves parallel to the longitudinal axis. A mature wood fiber with a low microfibril angle does not undergo this rearrangement of wall components. Rather, the fiber will tend to resist elongation to the extent that the viscoelastic properties imparted by its collective microfibrils allow. To this end, the selection of the loblolly pine fiber as a model for expansin trials was greatly influenced by the low microfibril angles purported to occur

218

within the species. Elongation owing to fiber viscoelasticity recorded during the expansin trials would be minimal and any significant elongation would be much easier to attribute to expansin activity within the fiber wall.

To determine microfibril angles, bleached fibers were suspended in dH_2O and a drop of the resulting suspension applied to a standard microscopic slide. The water within the drop was allowed to evaporate at room temperature. A compound microscope enabled visualization of the fiber and the cell wall morphology. An attached CCD would provide photomicrographs of the fiber (**Figure 56**) that were analyzed via Scion imaging to ascertain microfibril angles.
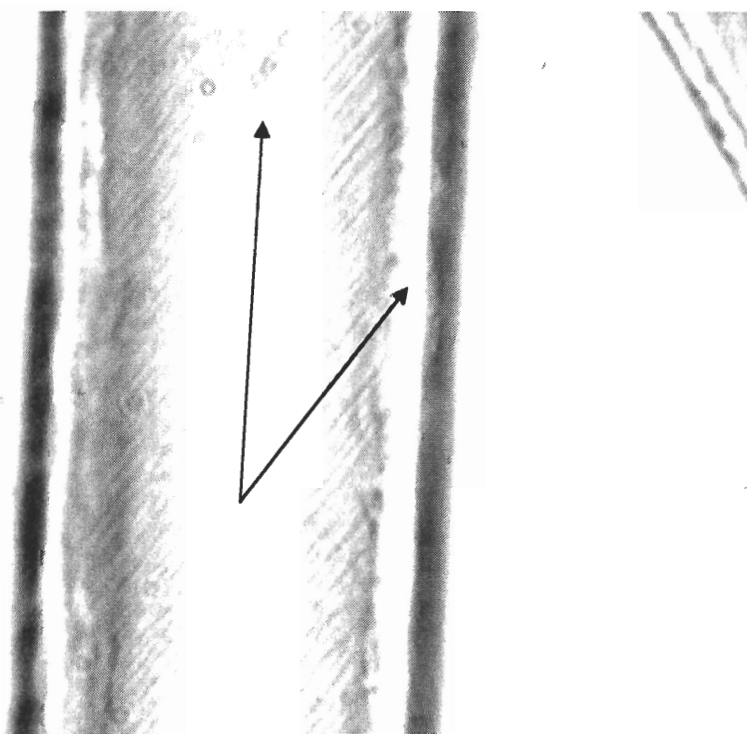

Figure 56: A magnified image of a holopulped loblolly fiber clearly showing microfibril angle. Pictures, such as this, were analyzed via imaging software to provide an average microfibril angle.

SINGLE FIBER EXTENSION

Single Fiber Extensometer

Development of an apparatus capable of detecting and recording the elongation of a solitary wood fiber was central to this investigation. Unfortunately, this would prove to be the most difficult stage since an entire spectrum of considerations would have to be addressed before the design was considered acceptable. On the most fundamental of levels, heterogeneity within the bleached fiber itself (e.g. length, width, cell wall thickness and morphology, etc.) necessitated a device in which the testing of numerous fibers could be conducted with relative ease to ensure significance. Extending this requirement, a system would have to be in place in which the fibers could be mounted without physically manipulating the fiber in such a way as to influence the results of an extension trial. An effectual means to maintain a fiber mounted within the extensometer submerged within an aqueous buffer containing expansin would also have to be developed. Moreover, a technique to apply a longitudinal load to the mounted, buffer immersed fiber would have to be devised. Even having accomplished these objectives, a system would have to be in place whereby the elongation of the loaded fiber, however slight, could be effectively gauged.

Extensometer Platform and Mount Support

A platform was constructed out of 3/4" thick aluminum plate (**Figure 57**). The weight of the construction was considered necessary to minimize vibration during elongation trials. Adjustable feet allowed the stage to be maintained level (monitored

with an attached leveling bubble). A system upon which to suspend a mounted fiber

with minimal contact to any other part of the extensometer was constructed upon the

3/4" x 3/4" vertical supports and crossbar. In the event that the loaded fiber would tend

to torque as a function of the microfibrils aligning with the load direction, bar magnets

were mounted on the inner walls of the support bars. Inclusion of a ferrous body (e.g.

wire) within the fiber mount and/or other constituents attached to the fiber mounts,

would be simultaneously drawn to both magnets on the support bars thereby resisting
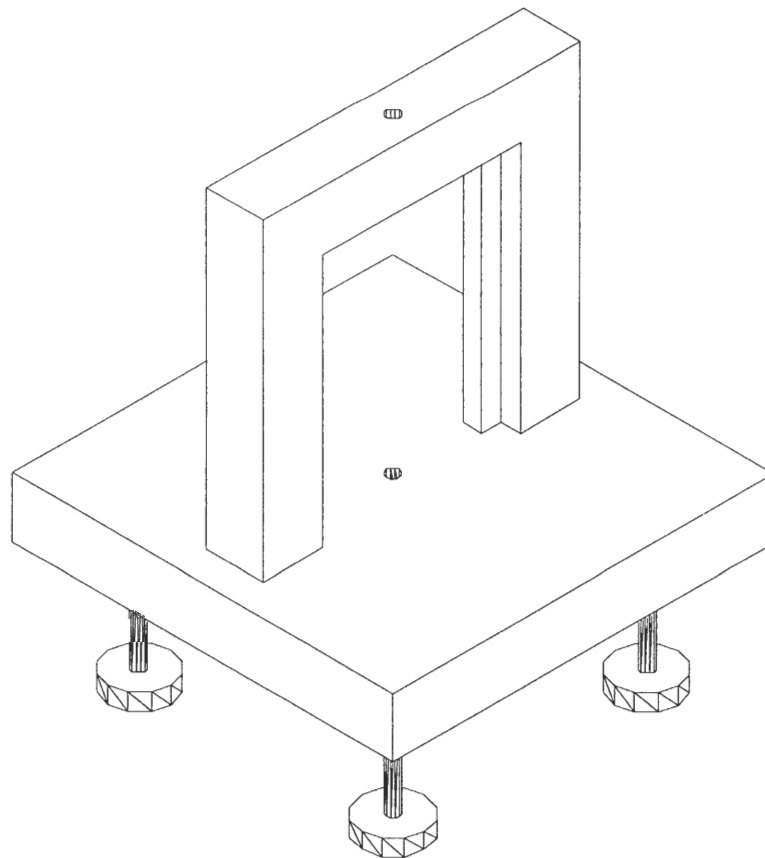
any rotation of the mount during a trial.

Figure 57: The single fiber extensometer frame was constructed from ¾" thick aluminum sheet. The bar magnets mounted along the inside of the vertical, aluminum supports prevented rotation of the mounted fiber in response to a uniaxial load during elongation trials.
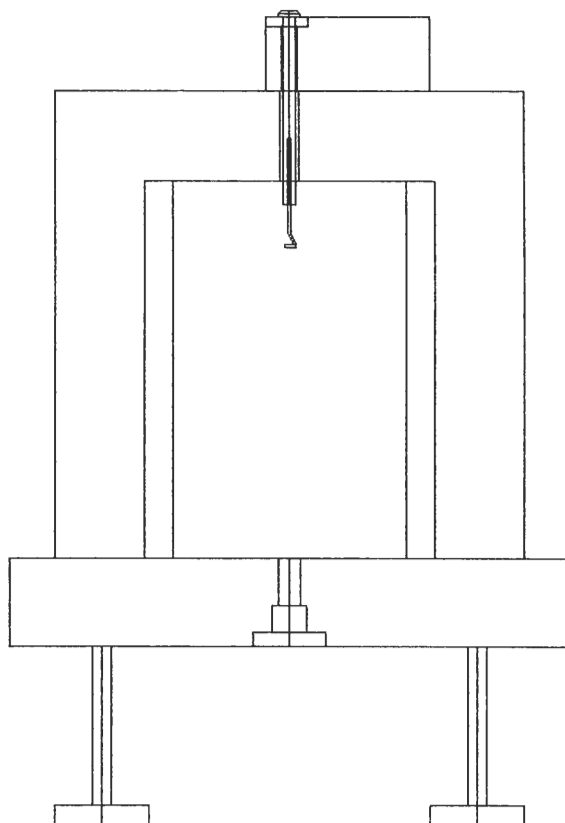
Figure 58: A load cell mounted on top of the frame provided a point upon which to suspend the mounted fiber assembly.

Load Cell

As will be seen, a load was applied to the mounted fiber even before immersion within the buffer. Various components of the mounting system were actually suspended from the dry fiber in addition to any weight purposely added to impart load. To accurately gauge the load applied to a single fiber during the elongation trial, including the mount assembly, a load cell (GSO-100, Transducer Techniques) was affixed to the top of the platform crossbar (**Figure 58**). A screw threaded through the load cell eyelet

was attached to a small hook fashioned from copper wire. This wire would provide a convenient tool upon which to suspend the mounted fiber. To this end, the only point of contact between the mounted fiber assembly and the extensometer platform would be through this thin wire hook affixed to the load cell.

Fiber Mounts

Evolution of a system by which a single wood fiber could be mounted for elongation trials would require continuous prototypical modification. The final technique, used during all subsequent elongation trials, will be covered within this thesis. The following technique describes a manner to mount fibers in which the central 2-3 mm of the fiber length are not physically contacted. This avoids introducing defects within the fiber that may lead to exaggerated strain or premature failure during elongation trials.

An extremely dilute suspension of the bleached fibers was dropped onto a black glass plate. Before the water could evaporate from the suspension, a needle was used to pull individual fibers by their ends from the aqueous phase onto the dry area of the plate. Most fibers tended to adhere to the plate while they dried. Other fibers would release from the plate surface and vigorously curl while drying. Fibers to be mounted were selected from the former group.

To construct fiber mounts, two 1 cm long segments of copper wire were gripped within the jaws of a modified brass electrical clip (**Figure 59**)[z]. The distance between the ends of the wire mounts was maintained at 2 mm. A small amount of epoxy (Epoxi-Patch, Dexter Corporation, NH) prepared from 1:1 mixing of resin to hardener was applied to the wire ends on both sides of the gap. Care was taken to avoid excessive use of the epoxy since additional curing time would be required before a mounted fiber would be considered secure. Using needle-tipped forceps, a dried fiber was carefully lifted from the black glass surface by one end and gently positioned across the epoxy droplets on either side of the gap. To ensure that the epoxy completely surrounded the ends of the fiber, the forceps were used to push the fiber ends into the epoxy.
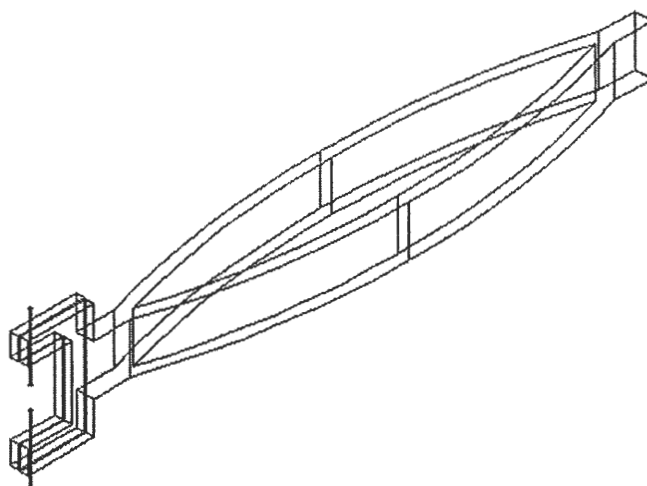

Figure 59: A modified electric clamp holding two wire mounts. A single fiber was placed across epoxy droplets placed at the inner ends of the mounts.

---

[z] The copper wire mounts would eventually be replaced by stainless steel to avoid the possibility of copper ions released into the acidic buffer solution intercalating and inactivating expansin.

Using a separate needle, the remaining epoxy was pushed to the edge of each plastic mount to generate a well-defined edge from which the fiber extends out over the gap and into the other defined edge. Any mounted fibers upon which epoxy could be seen to extend or wick out into the gap were discarded. The fiber mounts were allowed to dry for at least 24 hours before being placed into the extensometer.

Mounting Procedure

To begin the actual installation of a mounted fiber into the extensometer, a small stainless steel microvessel/arterial clip (cat #14-1030, Biomedical Research Instruments, Inc.) was affixed to the end of one wire mount protruding from the jaws of the modified electrical clip (**Figure 60**). Fortunately, the design of the arterial clips included a circular loop. By holding the electrical clip, the loop of the arterial clip could be slipped over the copper wire hook affixed to the load cell. By opening the electrical clip, the plastic mounts and attached fiber would be released and freely suspended from the arterial clip.

Immersing the fiber (at least the gap length of the fiber to be tested) would prove to be a source of difficulty. The original intention was to place a 3 µl drop of either buffer or buffer containing protein directly onto the fiber between the mounts. The cohesive properties of the liquid were expected to hold the bead onto the fiber. Unfortunately, the bead would evaporate before a 30-minute trial could be completed, both minimizing the time that the fiber is actually wet and increasing the concentration of protein, if applicable, as the drop evaporates.
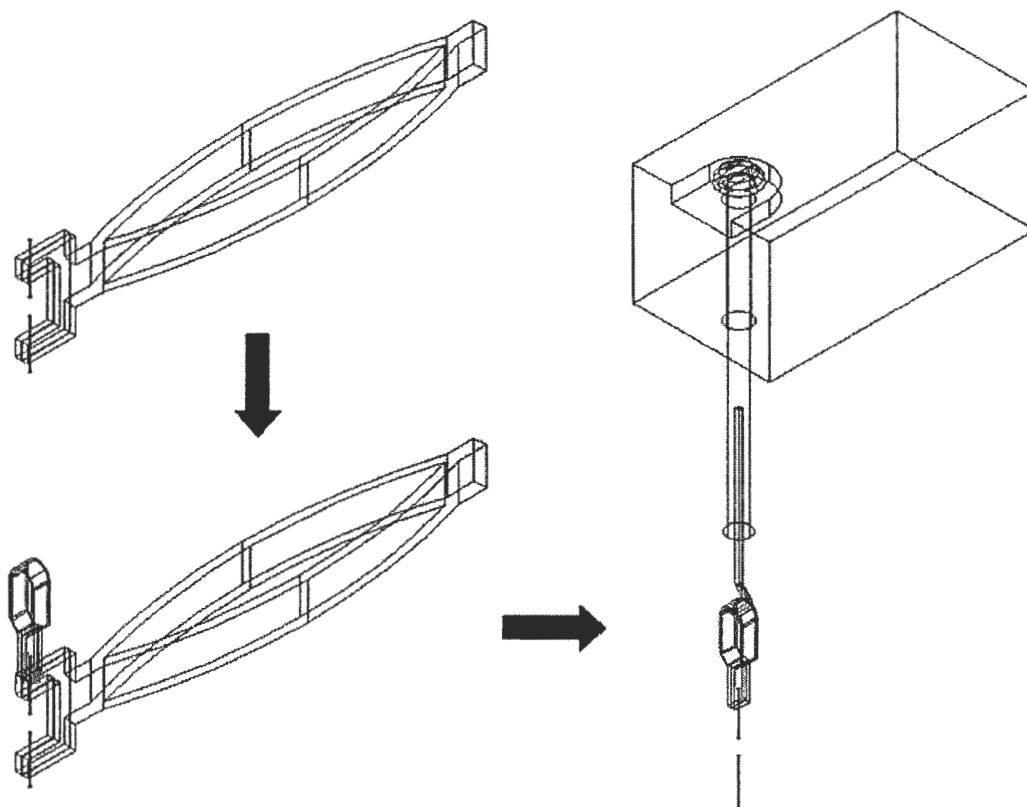
Figure 60: After 24 hours of drying, the jaws of the upper artery clip were fastened onto the exposed portion of the upper plastic tab. Using the electric clamp as a handle, the loop-like portion of the artery clip was placed over the wire hook attached to the load cell. When the jaws of the electric clip were opened, the mounted fiber was allowed to swing free.

The liquid drop had a tendency to slip down onto the mount during application and/or the tip of the pipette would brush the mounts thereby disturbing the mounted fiber. Building a chamber around the entire single fiber extensometer to shield the unit from air currents and physical insult would require the use of additional equipment (requiring both intensive capital and even more valuable time). Maintaining a high relative humidity in this manner could lower the rate of evaporation. A more cost-effective alternative was to develop a mechanism for shielding the submerged fiber

from the environmental influence via a more intimate approach that would only involve the fiber mounting unit. This was accomplished by clipping the narrow end from a 3 ml plastic disposable laboratory dropper and slipping the "tube" over the jaws of the lower artery clip (**Figure 61**). Vacuum grease was applied via a syringe to seal the lower end of the tube around the clip jaws. The lower wire mount, suspended from the fiber, was gently lowered into the large end of the tube until resting between the open jaws of the lower clamp. Relaxing the lower clip allowed the jaws to fasten upon the lower mount thereby effectively mounting the fiber within the cassette.
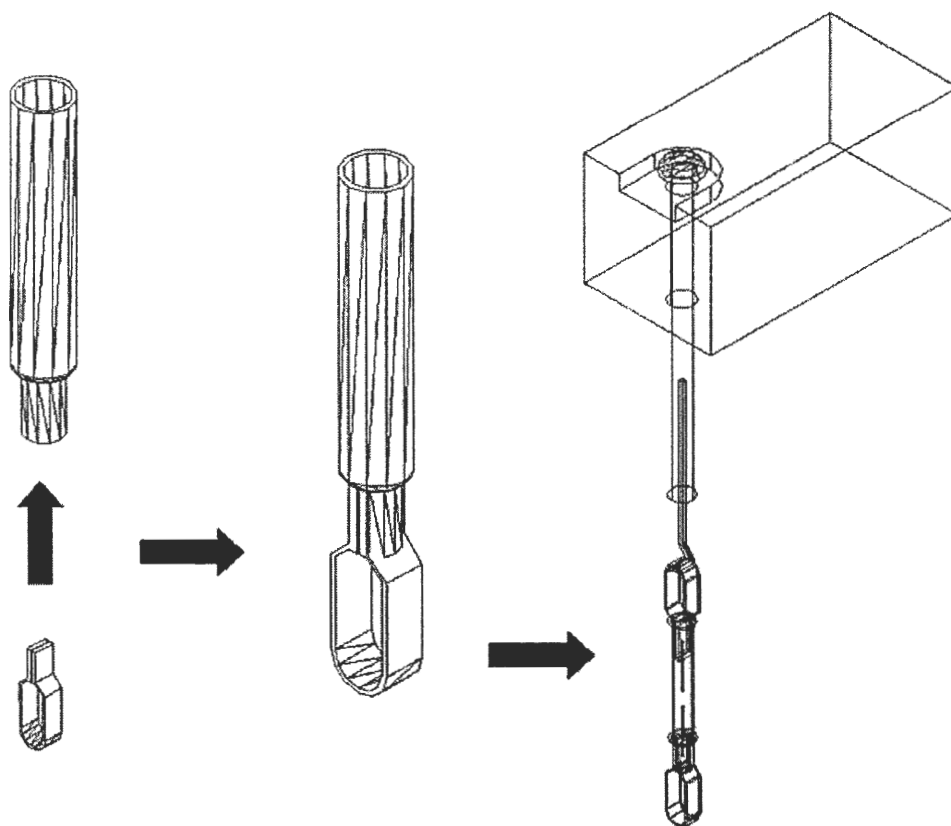

Figure 61: The lower artery clip was inserted up through the bottom of the plastic "chamber". After sealing the connection with vacuum grease, the jaws of the lower clip were carefully fastened to the lower plastic tab suspended from the fiber.

Load Assembly

To enable rapid variation of the load applied to an individual mounted fiber, a system was designed by which a "stirrup" would accommodate 0.5 to 20 gram standard brass calibration weights (sto-A-weigh, Ohaus Scale Corporation, NJ). This stirrup, constructed from copper wire with a thin platinum stage, was topped with a hook that could slip into the loop of the lower artery clip (**Figure 62**). Weights could be placed upon the stage within the stirrup either before or during an elongation trial. On the opposite side of the stage, a rare earth magnet was affixed to facilitate the measurement of fiber elongation.
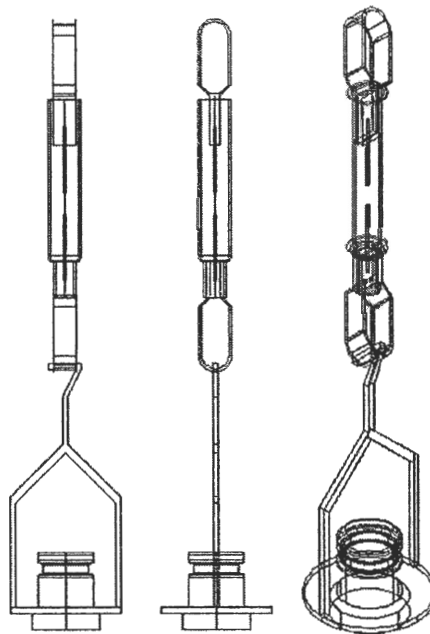
Figure 62: Three views of the weight stirrup (with weight) suspended from the lower artery clip. The rare earth magnet is attached to the underside of the stage.

Elongation of a small, 2 mm section of fiber under load within the extensometer was expected to be extremely minute. Effective means to detect and quantitatively record this event necessitated the incorporation of an ultra-sensitive sensor system into the extensometer. Currently, extensometers designed to quantify the elongation of an isolated plant cell wall are based on electronic position transducer technology[87 108 115 116 117]. However, the apparatus designed for similar performance with single fibers would incorporate a single Hall Effect sensor (HAL 805, Micronas) below the mounted fiber in order to maintain the fiber mount assembly, the actual fiber and the applied load suspended directly over the sensor (**Figure 63**).

The linear Hall voltage is generated within an integrated circuit in response to the presence of magnetic flux perpendicular to the circuit itself. The initial voltage of the circuit can be subtracted from the final voltage to reveal the magnitude of the Hall voltage. The output voltage generated in this manner is proportional to both the intensity of the magnetic flux across the circuit and the initial voltage within the circuit. This analog voltage can be rendered digital for conversion to meaningful data within a digital signal processing unit (DSP). The programmable linear Hall effect IC sensor was positioned directly below the strong magnet affixed to the bottom of the load assembly. In this manner, elongation of the fiber would lower the magnet towards the sensor thereby generating a Hall voltage proportional to the increased magnetic field. The voltage increase was then processed via a data acquisition card and accompanying software (E series Multifunction DAQ System, National Instruments).
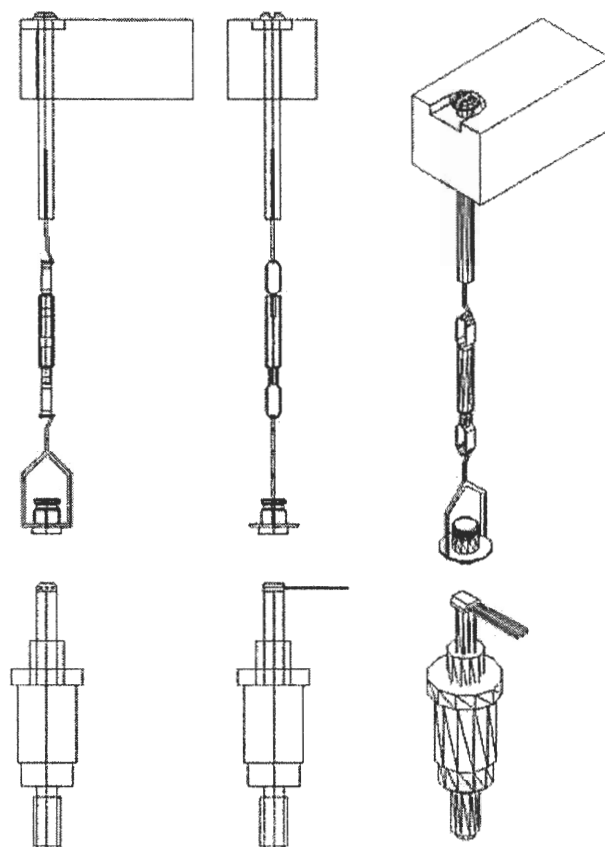
Figure 63: Three views of the load cell, mount assembly, weight stirrup, Hall Effect IC, and micrometer.

SINGLE FIBER EXTENSOMETER CALIBRATION

Calibration of the single fiber extensometer (SFE) involved programming the Hall Effect Sensor to gauge time-dependent displacement of a fiber under constant load. Considering that the gap distance between fiber mounts was 2 mm, the IC was programmed for optimum sensitivity over a 2 mm span representative of 100% elongation of the fiber within the gap. This degree of elongation within a 2 mm section of fiber was not expected but could allow for the SFE to be used for measuring displacement within thin sections of paper or cellulose/hemicellulose *Acetobacter*

230

xylinum derived composite. Once the output voltages at both end-point positions were recorded and programmed into the IC[aa], the SFE was connected to a separate computer with system DAQ capacity. A Lab View program enabled the simultaneous monitoring of both load applied to a mounted fiber and the displacement of the fiber in response to the load. After considerable trial and error, the program was customized to recognize and amplify the unexpectedly low output voltages provided by both the load cell and the sensor.

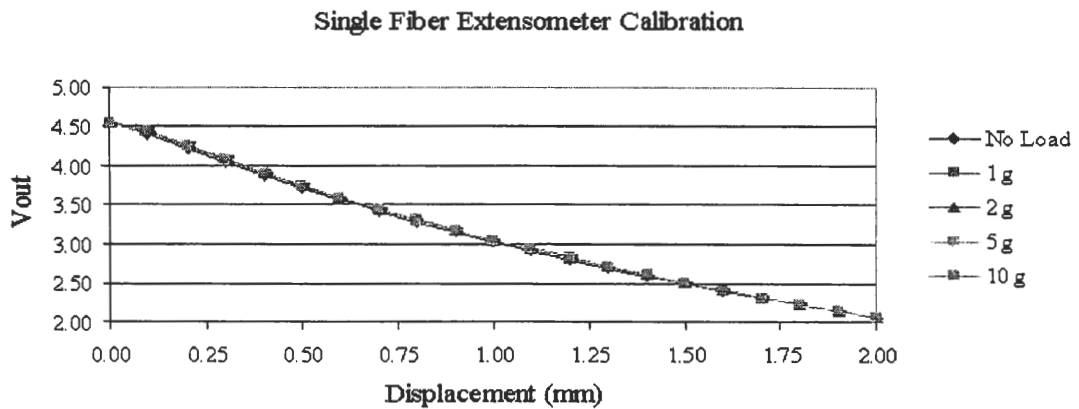**Single Fiber Extensometer Calibration**

Figure 64: The single fiber extensometer was calibrated with a number of different loads and the output voltage determined for each 0.1 mm increment across a total displacement of 2mm.

[aa] Before the sensor could be used in the extensometer, the background voltages within the Hall plate were recorded to normalize the actual Hall voltage output during actual trials.

Having yet to determine the maximum uniaxial load that a holopulped fiber could tolerate, a series of calibration curves were obtained from the SFE with loads of 0, 1, 2, 5 and 10 g (**Figure 64**). In these trials, the load cell was directly connected to the weight stirrup hook via a single copper wire hooked at both ends. Any deviation between the curves would reveal the existence of a potential source of error somewhere within the mounting assembly other than at the clip-mount interface. Fortunately, the curves were extremely similar. An exponential curve fit to averaged data provided a load-dependent equation that would be used to determine the displacement of a fiber during an actual elongation trial.

APPLICATION OF UNIAXIAL LOAD

In addition to serving as an effective means to enable calibration of the extensometer, the micrometer stage would serve another purpose. During subsequent elongation trials involving dry fibers, pellicle strips, fibers immersed in buffer and fibers immersed in protein extract, application of the load would need to be as consistent and gentle as possible. To minimize the physical impact of an extreme rate of loading, which often occurred while attempting the manually place a weight into the stirrup suspended from the lower mount, the micrometer stage would serve as a means of relatively smooth load transfer. The weight stirrup with the appropriate load was placed onto the top of the Hall Effect sensor. By raising the stage, the hook of the stirrup could be slowly fed through the lower artery clip loop without actually touching the clip. At a given time, the stage was slowly lowered. At a specific height, the stirrup

hook would contact the clip loop. Continuing to lower the stage would gradually transfer load of the stirrup and weight (if any) to the mount assembly. The point at which the transfer of load initiates was easily discernable by monitoring the output voltage from the load cell. Once the load was completely placed upon the mount, the Hall Effect sensor would be rapidly lowered a position characterized by a predetermined Hall voltage within 10 seconds. In this fashion, all substrates within the extensometer would generate the same voltage at T_0.

Considering that the fiber mounts are short lengths (1 cm) of copper wire, slippage between the clamps and the wire during testing was a distinct possibility. The extent of slippage was assumed to increase with load. To differentiate slippage between the clamps and the mounts from actual fiber elongation, another series of 30-minute trials were completed with loaded "blanks" (i.e. 1 cm sections of copper wire) and the apparent elongation (actually slippage) recorded (**Figure 65**). If considered a significant source of error, this pseudo-elongation would be subtracted from the total elongation during actual trials.

Blank (no fiber)
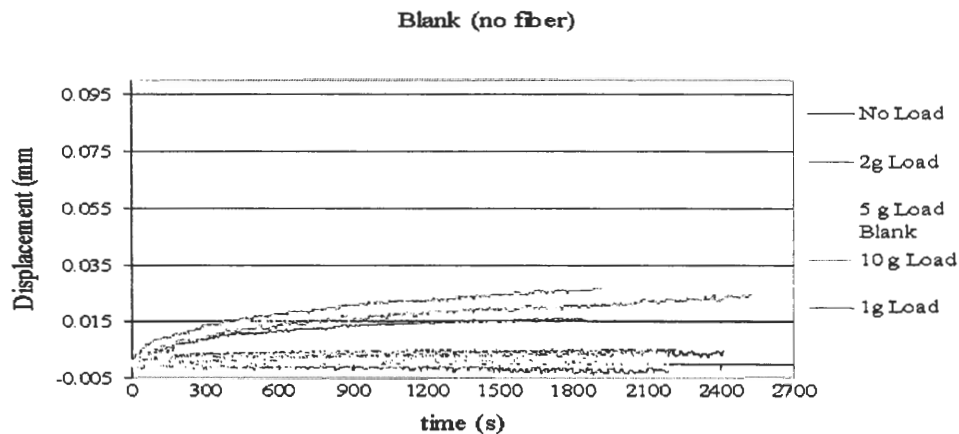
Figure 65: Displacement as a result of slippage between clamps and the copper wire blank. The earlier trials had more slippage (2 and 5g loads) due to poor contact between the clamp jaws and the wire. Modification of the clamp jaws (i.e. cutting them in half) minimized slippage in later trials.

Dry fibers were tested within the SFE to determine the amount of extension that can be presumed a function of the material properties of the fiber. This inherent

viscoelastic behavior would have to be taken into consideration when quantifying expansin-mediated elongation. The mounted fibers showed very little displacement when subjected to loads of 0, 1 and 2 g. Fibers loaded with 5 g began to show more extension but were also prone to fracture when the rate of load was too extreme. Loads of 10 g resulted in immediate rupture of the fiber. To minimize the insult to the fiber as a result of loading rate and the instances of shortened testing time due to fiber failure, the initial tests with actual expansin protein would be conducted with the minimum load (i.e. the rare earth magnet, the wire weight stirrup, the lower clamp upon which the stirrup is supported and the lower fiber mount to which the clamp is connected for a total of 1.5 g). Dry fibers loaded only with the stirrup and magnet exhibited negligible extension relative to heavier loaded fibers. The variation in displacements provided by each fiber was expected to be insignificant in comparison to values obtained by similarly loaded fibers in buffer solution and in buffer solution with protein.

Confirmation of Expansin Activity

Before a single fiber could be mounted within the extensometer and submerged within the crude extract, the extract would have to be assayed for expansin activity. Since no effective colorimetric or substrate-based assay has been designed to quantify expansin activity within an extract regardless of purity, units of expansin activity are indirectly determined by the percent elongation of an isolated substrate. In the earliest investigations, this meant isolated hypocotyl walls. Unfortunately, this process is highly subject to wide-value swings on account of the extreme variation in substrates employed during the trials. Units of expansin activity varied relative to the actual

experimental parameters employed during the trials (i.e. substrate type, width, thickness, inter-clamp gap length, uniaxial load selected, etc.). Even when a single plant species (e.g. 4-day old cucumber hypocotyls) was selected as the model substrate and the gap distance and substrate pretreatment leading up to the actual trial kept constant, the percent elongation, when subjected to identical loads, would vary significantly between trials. This variation has been attributed to irregularities within the isolated plant wall. Plant walls exhibit notorious heterogeneity with significant morphological deviation from one place to another within a single wall. To this end, another composite containing the structural elements of the primary cell wall was generated based upon a recent technique outlined by Whitney *et al*[108]. The relatively homogenous substrate provides relatively small deviation from one sample to the next. By including cellulose and xyloglucan within the composite, the presumed sites at which expansin exerts its activity should be readily available. A load placed upon an isolated portion of this composite submerged within a suspension of expansin should promote quantifiable elongation within the current extensometer. This composite substrate was used to as a means to confirm expansin activity within the crude extract.

Acetobacter xylinum Strain and Culture Propagation

An extremely pure strain of *Acetobacter xylinum* was obtained as a gift from Dr. Malcolm Brown, Jr. at the University of Texas at Austin. His culture, deemed NQ-5, is a 20 year-old strain with a robust stability and an inherent resistance to genetic drift and the accompanied generation of sub-species. NQ-5 is readily grown on liquid and solid unmodified Hestrin-Schramm media[118] (Appendix D - Hestrin-Schramm Media) which

facilitated the maintenance of the pure culture. To keep the bacteria within a state of continuous growth phase, fresh solid H-S plates were streaked once a week and kept under incubation at 30°C.

To prepare a liquid culture of the bacteria, 100 ml of the liquid H-S media was transferred to a 250 ml Erlenmeyer flask and autoclaved. Glass wool placed within the neck of the flask prevented contamination during transit of the flask between the autoclave, the fume hood and the incubator. Once the liquid media cooled, an inoculating loop was used to lift a single 4-day old colony from a solid media plate and stir it into the liquid phase. Inoculations were conducted within the fume hood at all times to minimize the possibility of contamination. The flask was then plugged with sterile glass wool and placed under slow agitation within the incubator set at 30°C. The liquid culture was allowed to grow for 4 days (a longer incubation could allow the bacteria to exhaust the glucose and/or generate excessive metabolites within the media and, thereby, affect the ability of the bacteria to multiply when used as an inoculant).

Cellulose Pellicle Preparation

Generation of bacterial pellicles both with and without tamarind xyloglucan was conducted in standard, sterilized plastic 100 mm x 15 mm Petri dishes. The 100 ml liquid culture, incubated under agitation for 4 days, was diluted 1:10 with fresh, sterile liquid H-S media (either with or without xyloglucan depending on the desired pellicle to be formed). After ensuring sufficient mixing of the fresh and initial liquid media, 15 ml of the media was metered into 12 individual plastic Petri plates. After pouring the

plates, they were carefully transferred to the 30°C incubator and allowed to remain motionless for the next 72 hours. This particular approach to *Acetobacter* pellicle growth is referred to as the shallow-layer quiescent-culture technique. The presence of oxygen is absolutely essential for pellicle formation thereby ensuring that a pellicle of uniform thickness will form only at the air-media interface within each plate (**Figure 66**). After the incubation period, the pellicles were "harvested" from the plates and then washed extensively in deionized water to remove any traces of media and cellular material (**Figure 67**). The final pellicles were then stored in a preserving solution of 0.02% NaN_2 at 40°C until use.
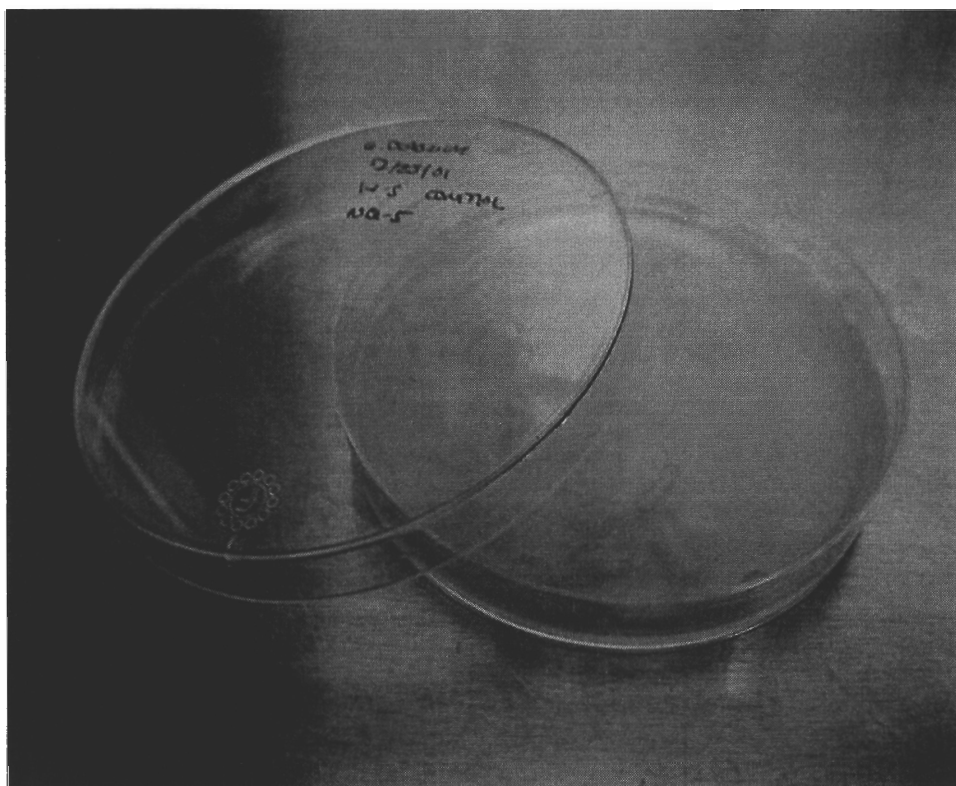
Figure 66: *Acetobacter xylinum* pellicle after 72 hours of incubation at 30°C. The pellicle only tends to form at the media-air interface.
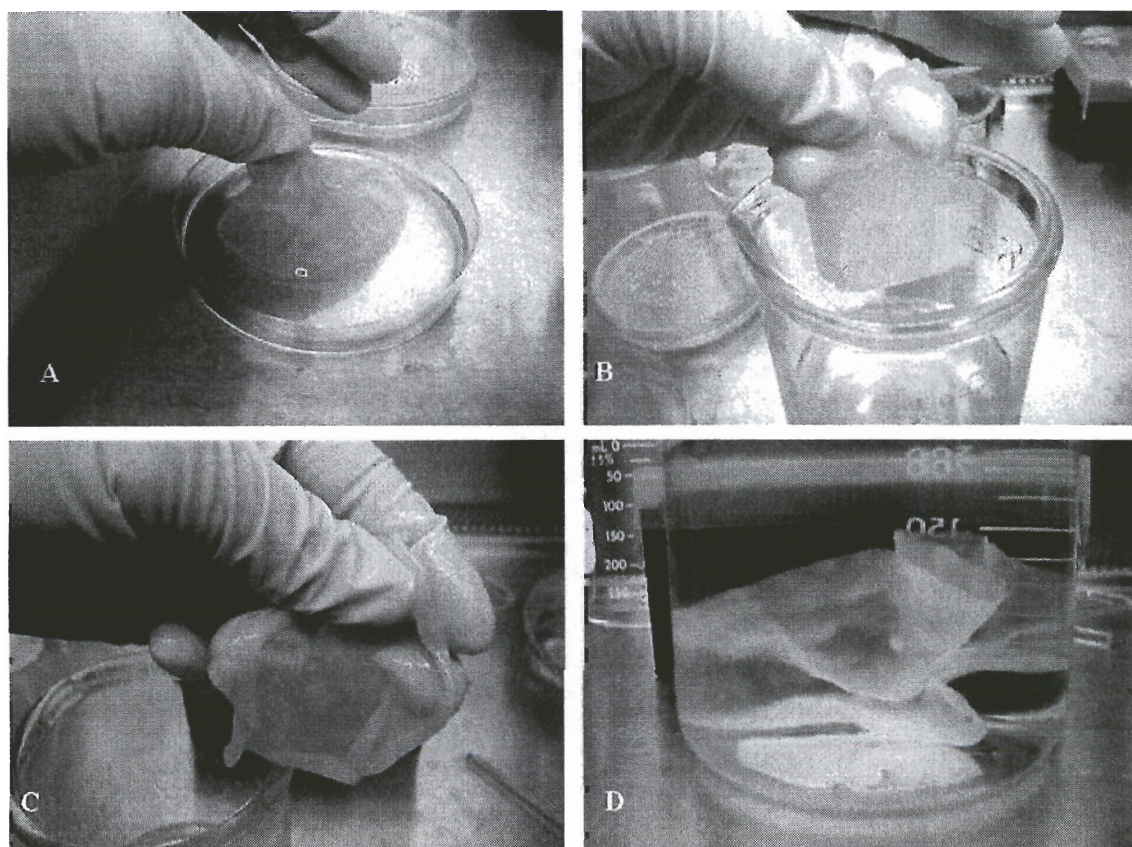
Figure 67: A. *Acetobacter xylinum* pellicle removed from Petri Dish. B & C. Pellicle is thoroughly washed in Millipore pure water to remove all bacterial debris, live cells, and entrained media. D. Pellicle is then stored in water at 4°C until use.

Pellicle Mounting and Elongation

Preparation of a composite sample to be mounted into the extensometer involved using a razor to cut a small 6 mm x 2 mm section from the thoroughly washed pellicle. It was found that this particular phase of the procedure could be facilitated by placing the hydrated pellicle between two sheets of copy paper and cutting the paper-composite-paper sandwich into 2 mm wide strips with an office paper cutter. The resulting strips could be placed in an airtight plastic bag and refrigerated for the

duration of time required to perform a single day of trials. The strips, now slightly dehydrated as a consequence of absorption into the copy paper, were hydrated in a 250 ml beaker containing 50 mM sodium acetate buffer. The hydration allowed the copy paper to be gently pulled from the pellicle strip. The strips were slowly pulled from the buffer with needle-tipped forceps and allowed to hang over the top of the beaker. Using a razor, 6 mm sections of the pellicle strip could be obtained by pinching the strip between the edge of the blade and the side of the glass beaker. The final segments were then placed between two glass coverslips which were then placed between two layers of tissue. A 500 g brass weight was then placed on top of the tissue/coverslip/pellicle segment stack to press buffer from the pellicle and facilitate handling of the segment during mounting procedures. Pellicle strips both with and without xyloglucan were prepared in this manner.

Mounting a 6 mm x 2 mm pellicle strip within the extensometer was as simple as gripping both ends of the strip between the jaws of the upper and lower arterial clip. Again, the jaws of lower clip were previously threaded through the bottom of the disposable dropper section before being fastened to the lower end of the pellicle strip. Once again, the bottom of the dropper section was sealed with vacuum grease to prevent leakage when buffer was added to the "cassette". Care was taken to maintain the gap distance between the two clip jaws constant throughout the course of the trials. The upper clip was then suspended from the copper wire hook. The load stirrup was suspended from the lower clip. 150 µl of 50 mM sodium acetate buffer, the buffer plus

crude extract, or the buffer plus boiled crude extract[bb] were pipetted into the cassette and the pellicle segment allowed to acclimate to the surrounding solution for 5 minutes. After the acclimatization period, a 20 g brass weight was placed in the stirrup and the resulting elongation recorded as a function of time. A typical trial would take 30 minutes and would be conducted at room temperature.

Fiber Extension Trials

Having confirmed the presence of active expansin within the crude extract with the composite substrate, elongation trials involving fibers submerged within the crude plant cell wall extract were initiated. By this time, potential sources of error during fiber extension within the extensometer were completely resolved or minimized to insignificancy. All trials at this stage were conducted with crude extract from a single extraction. This extract was kept at 4°C to prevent premature denaturation of the protein.

Fibers were mounted in the same manner used to mount fibers for the viscoelastic yield measurements. Once the cassette containing a mounted fiber was suspended from the load cell, the weight stirrup would be placed on top of the IC sensor. By slowly moving the spindle stage of the micrometer upwards, the hook at the top of the stirrup could be threaded through the lower arterial clip. At this point, the stirrup hook was slightly above the clip loop and did not place any load onto the fiber.

[bb] Boiling the crude extract serves to deactivate proteins.

A 150 µl aliquot of either the crude extract or the 50 mM sodium acetate buffer in which the extracted proteins were suspended, was gently pipetted into the chamber portion of the cassette. The resulting submerged fiber was allowed to equilibrate within the cassette for five minutes. The load placed upon the fiber by the 150 µl of liquid, the lower clip, the plastic chamber and the vacuum grease did not cause any significant extension during this acclimatization period. At the end of the period, the micrometer spindle was slowly lowered. The load of the weight stirrup was gently transferred to the lower clip. The point at which the load shifted from the spindle to the clip was easily discernible by monitoring the output from the load cell. Upon transfer of the load, the spindle was quickly lowered (< 10 s) to a position at which the Hall voltage was of a predetermined magnitude. By transferring the load in this fashion, all single fiber trials would begin at an equivalent Hall voltage. Over the course of the next 30 minutes, the displacement of the lower clip towards the IC sensor was recorded as a function of time. Ten fibers submerged in buffer and ten fibers submerged in extract were tested. Unfortunately, the fibers tended to fail in less than 30 minutes when the uniaxial load became excessive (i.e. greater than 3.5 g). To minimize the instances of fiber failure (and the accompanying loss of time spent preparing the mount), weight placed into the stirrup would not exceed 2 g. In combination with the stirrup, a load of 3.5 g was placed on the submerged fiber.

ARTIFACTS INHERENT TO EXTENSOMETER

Artery Clamp Slippage

Figure 68 presents the results from trials in which wire blanks were placed in the mounting assembly and displacement monitored as a function of time. Various weights were placed on the stirrup stage to simulate different uniaxial loads on a mounted fiber.
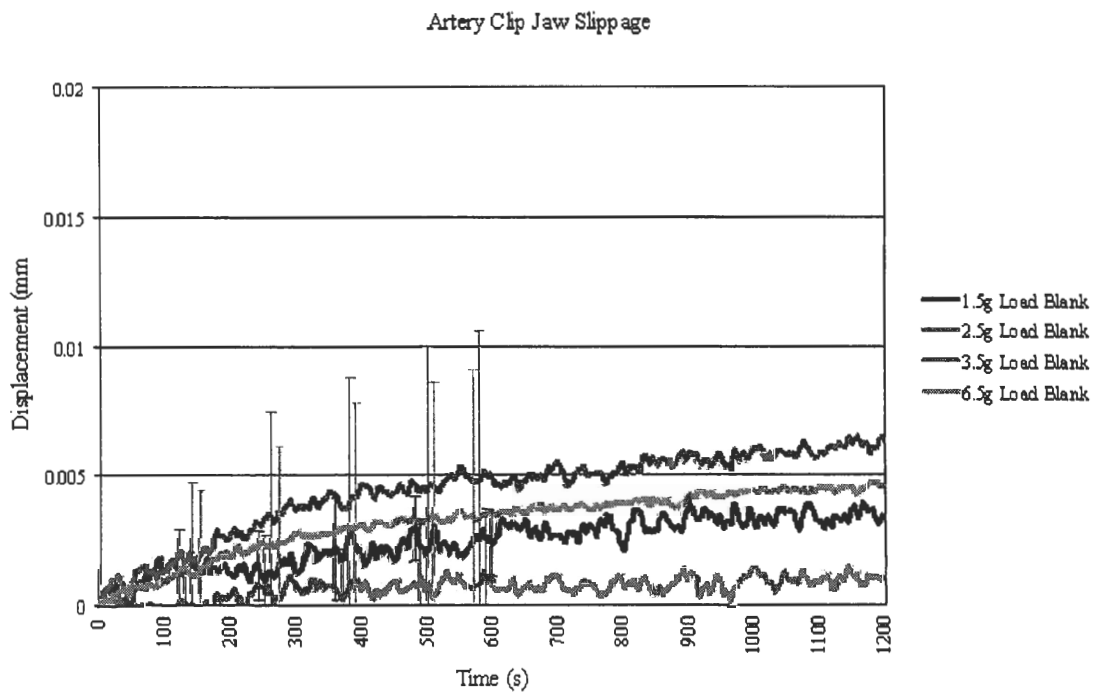

Figure 68: Time-dependent displacement curves generated as displacement within the fiber mount assembly occurs at the artery clip jaw-wire blank contact area. Voltages out have been converted to actual displacement.

Evidently, slippage did occur between the clip jaws and the wire mount. At low loadings (e.g. 1.5 and 2.5 g), this displacement appeared negligible. Loading the wire with 1.5 g promoted a displacement of 0.0015 mm after 20 minutes of trial time. This corresponds to an increase in length of 0.0075% within a 2 mm section of the wire blank. A total displacement after 20 minutes of trial time with 2.5 g of load corresponds to 0.0064 mm displacement or 0.32 % elongation. The finite sensitivity of the Hall Effect IC was not considered capable of discerning such small differences in displacement as a function of load as evidenced by the high deviation within the results. The significance of the deviation and the extent to which it would influence the results of actual trials would not be known until the percent elongation of actual fibers could be ascertained. If displacements provided during the fiber trials proved to be much greater than the displacement due to clip slippage, contribution from the latter would be disregarded as insignificant. The take home point from the trials presented in **Figure 68** is that slippage-mediated displacement between the jaws and the wire blank was responsible for up to 0.0064 mm or 0.32% of the observed elongation after 20 minutes. At ten minutes into the trial, these values were 0.0048 mm and 0.24% respectively.

Fiber Yield Properties and/or Fiber-Epoxy Bond Failure

The significance of the displacement due to clip slippage cannot be properly considered without gauging the magnitude of displacement that occurs when an actual fiber is placed under a similar load. Load-induced strain within the epoxy anchoring the fiber across the 2 mm gap was determined to be virtually non-existent (at least under

dry conditions). However, any failure between the fiber and the epoxy end mounts may contribute to the elongation attributed to the viscoelastic properties of the fiber. **Figure 69** presents the results from the series of trials designed to elucidate the elongation of the fiber primarily due to the inherent viscoelastic properties of the fiber itself and possibly the aforementioned fiber-epoxy bond failure.

Blank & Dry Fiber
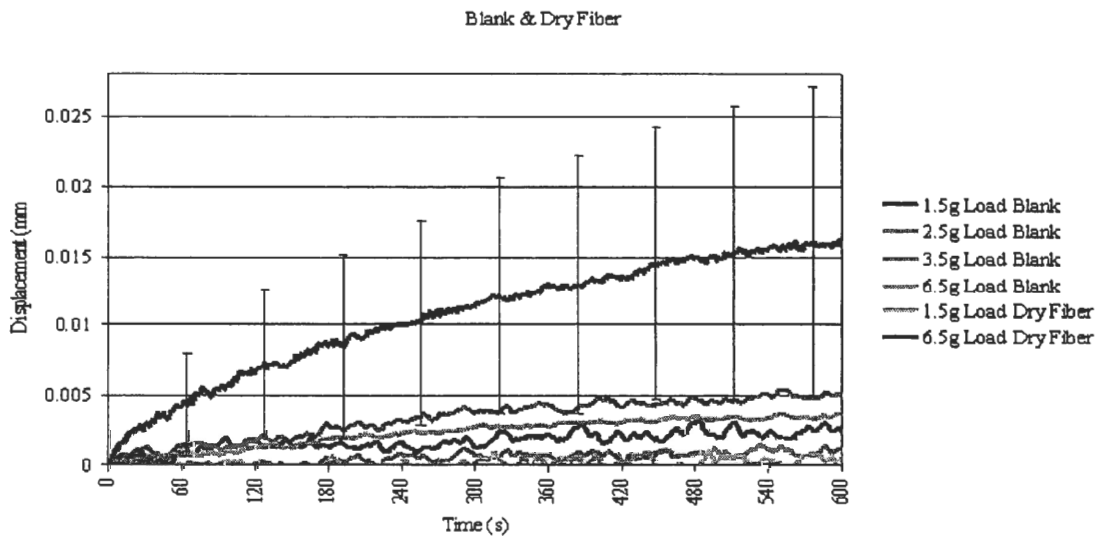
Figure 69: Elongation of a mounted dry fiber in response to uniaxial load. Displacement is considered to primarily represent the viscoelastic strain properties of the fiber although failure within the epoxy-fiber bond may also have occurred.

The variation in response to the 6.5 g loading was immediately evident whereas variation during elongation due to the 1.5 g loading was practically nonexistent even though 10 individual fibers were assayed at each weight. The percent elongation of the 2 mm segment of fiber held between the two epoxy anchors exhibited an upper

displacement of 1.89% and a low displacement of 0.23% after 10 minutes. From these results, it was concluded that the variation in fiber elongation was amplified by increasing the magnitude of the uniaxial load. In other words, the inherent heterogeneity of individual fibers becomes more of an influential factor as the load is increased. Based on this assumption, reducing the load should decrease the variability within the rate and extent of displacement due to fiber heterogeneity. To this end, actual fiber elongation trials would be conducted with a weight of 3.5 g to minimize variability in results.

ACETOBACTER PELLICLE TRIALS

Elongation trials conducted with strips of *Acetobacter xylinum* pellicles gripped between the artery clips in place of the wire fiber mounts provided the data presented in **Figure 70**.

Xyloglucan/Cellulose Composite (20g load)
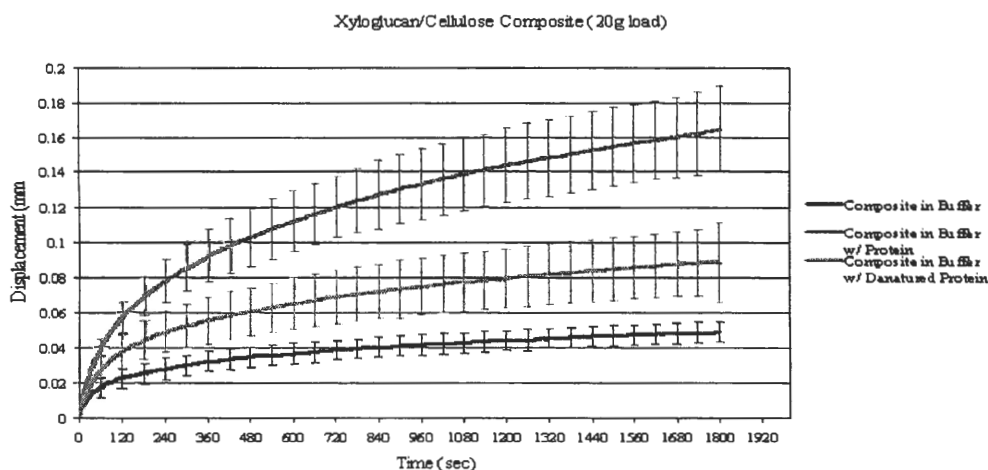
Figure 70: Elongation of *Acetobacter* pellicle strips as a function of time. The load was maintained at 20 g over the course of 30 minutes.

From the graph, it was immediately evident that the pellicle strip immersed within the buffer containing undenatured total wall protein elongated more than either of the other two treatments. After 30 minutes, the 2 mm gap held between the clips extended by 8% whereas the extension was only 2.5% in the absence of protein. Apparently, the attempted denaturation of the total protein extract failed to completely inactivate all protein within the aliquot since a certain amount of extension is evident.

From these trials, the total wall protein extract was assumed to contain a certain amount of expansin activity which would allow the next stage of the investigation, single fiber elongation, to proceed.

SINGLE FIBER TRIALS

Indisputably the most tedious phase of the investigation, 10 fibers were assayed within buffer and 1.5g or 3.5g loadings or buffer with protein and 1.5g or 3.5g loadings. The elongation over a 10 minute trial duration for each condition is presented in **Figure 71**. Results from fibers that would fail before the 10 minute trial period were not recorded. Again, a great deal of variation exists in the data due to the heterogeneity of the fibers assayed. Fibers immersed within the crude extract and placed under a 3.5g load would elongate an average of 2.3%. Elongation of fibers immersed within the protein-free buffer under similar load would extend by an average of 1.5%. When the load was lowered to 1.5g, fibers in contact with the protein extract extended by an average of 1.2% while fibers in simple buffer extended by 0.8%.
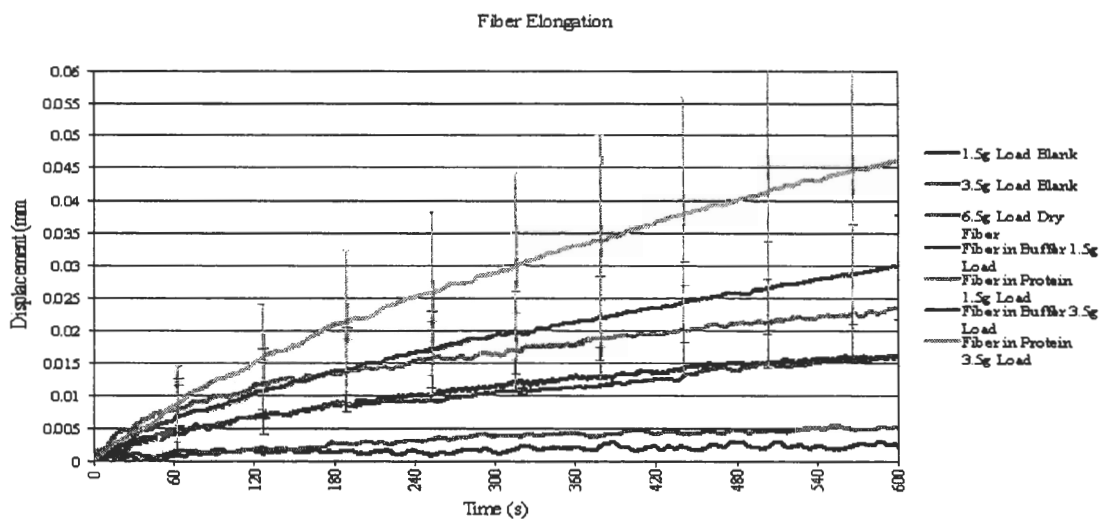

Figure 71: Fiber elongation in the absence and presence of crude total wall protein extract.

DISCUSSION AND CONCLUSIONS

Although, in each case, the addition of protein to the buffer appears to influence elongation rates, the results were highly variable. This is probably a direct function of the inherent variability between individual fibers (e.g. microfibril angle, morphology, cell wall thickness, etc.). Increasing the load did increase the extent of fiber elongation within the crude total wall protein extract relative to buffer alone. Unfortunately, even the fiber with the greatest degree of elongation is only capable of displacement of roughly 2.3% excluding the contribution of clamp slippage, epoxy effects, and inherent fiber plasticity within the buffer. Not only is such a small modification to the fiber unattractive to the papermaker, the magnitude of the load (3.5 g) and the duration of the constant stress applied to a single fiber (10 minutes) are not likely to be encountered within conventional operations involving virgin or secondary fiber (e.g. refining, deflaking, disintegrating, etc.).

It is entirely possible that the amount of expansin within the crude extract was insufficient to promote greater fiber elongation. In support of this, electrophoretic separation of the proteins contained within the crude extract reveal extremely faint bands at the molecular weight position previously identified as expansin. Unfortunately, extraction of large quantities protein at this time is both cost-prohibitive and time consuming. Perhaps amplified expression of recombinant expansin will facilitate similar trials conducted in the future.

Penetration of the protein into the cell wall may also be the limiting factor. In addition to a molecular weight (29 – 30 kD) that may physically prevent expansin from

penetrating a hornified cell wall, the protein is characterized by a cellulose binding site that may actually tether the protein to the periphery of the cell wall. In either scenario, expansin will be prevented from accessing targeted sites of activity within the polysaccharide matrix. The small amount of single fiber extension that was recorded during the trials may be attributed to the loosening of fiber wall components within this outer layer.

Although immediate industrial-scale implementation of biotechnologies involving exogenous expansin application cannot be envisioned through the results of this investigation, the protein does appear to have the capacity to modify fiber dimensions.

APPENDICES

Appendix A - Total Wall Protein Extraction Reagents

Stock Solutions:

1L 0.1 M sodium acetate – (8.203 g / 1000 ml dH$_2$O)

1L 0.1 M MES – (19.52 g / 1000 ml DI H$_2$O)

1L 0.2 M HEPES – (47.66 g / 1000 ml DI H$_2$O)

0.5 L 0.1 M sodium metabisulfite – (9.505 g / 500 ml DI H$_2$O)

L 0.5 M EDTA – (Sigma)

1L 2 M NaCl – (116.88 g / 1000 ml DI H$_2$O)

Homogenization   Buffer

(25 mM HEPES, 3 mM sodium metabisulfite, 1 mM EDTA, 1% polyvinylpyrolidone 40, 0.1% Triton X-100, 2mM DTT (dithiothreitol), pH 7.0 w/ NaOH)

1. 851 ml of DI H$_2$O

2. 125 ml of 0.2 M HEPES

3. 30 ml of 0.1 M sodium metabisulfite

4. 2 ml of 0.5 M EDTA

5. 10 g PVP-40

6. 1 ml Triton X-100

7. Adjusted to pH 7.0 w/ NaOH

8. Chilled before use

9. Added 0.3084 g of DTT immediately before homogenization

Extraction Buffer

(1 M NaCl, 25 mM HEPES, 1 mM EDTA, 3 mM sodium metabisulfite, pH 7.0 w/ NaOH)

1. 351 ml of DI H_2O

2. 500 ml of 2 M NaCl

3. 125 ml of 0.2 M HEPES

4. 30 ml of 0.1 M sodium metabisulfite

5. 2 ml of 0.5 M EDTA

6. Adjusted to pH 7.0 w/ NaOH

7. Added 0.3084 g of DTT immediately before extraction

Resuspension Buffer

(15 mM MES, pH 6.5)

1. 150 ml of 0.1 M MES

2. 850 ml DI H_2O

3. Adjusted to pH 6.5 w/ 1 M acetic acid

Dialysis Buffer

(15 mM MES, pH 6.5)

Reconditioning Buffer

(50 mM NaAc, pH 4.5)

1. 50 ml of 100 mM NaAc

2. 50 ml of DI H_2O

3. Adjusted to pH 4.5 w/ 1 M acetic acid

Appendix B - Holopulping Procedure

Chipping

1. Cut 1" discs from loblolly pine log (~49 years old)

2. With band saw, cut discs into pie-shaped wedges

3. With razor, cut the 23rd and 24th earlywood growth ring from each of the wedges

Soxhlet Extraction

1. Weighed out approximately 10 grams of chips

2. Prepared ~500 ml of 1:1 EtOH-chloroform extraction solution

3. Poured approximately 300 ml of the extraction solution into Florence flask

4. Connected a distillation tube to the top of the flask

5. Curled a filter paper into the top of the soxhlet distillation tube such that the bottom of the tube covers the effluent port of the tube (restricts small chips and released fibers from clogging the effluent tube)

6. Added the chips to the soxhlet distillation tube

7. Connected a condensation tube to the top of the distillation tube and began water flow

8. Turn heating mantle to 60 volts and observed to determine whether sufficient extraction solvent was added

9. Colored effluent removed from the percolating chips indicated the extraction process was not been completed

10. Continued extraction for 72 hours

Solvent Exchange

1. Removed chips from Soxhlet extraction assembly and transferred to 200 ml of 100 % methanol and left for 24 hours

2. Transferred chips to 200 ml of 75% methanol and left for another 24 hours

3. Continued to transfer chips for 24 hours at a time to 50 and 25% methanol

4. Finally, soaked chips for 24 hours in distilled water.

Delignification

1. Prepared a buffered chlorite solution (12 g sodium chlorite, 8 g sodium acetate, fill to 200 ml with DI H_2O, should be buffered at pH 4)

2. Placed the extracted chips (now water-wet) into a 250-ml Erlenmeyer filter flask.

3. Added 200 ml of the buffered chlorite solution and 13 ml of glacial acetic acid

4. Sealed flask with stopper and applied a vacuum for one hour

5. Released vacuum and observed evolution of ClO_2

6. Sealed the flask with parafilm and wrapped in aluminum foil to ensure complete darkness for the reaction (light degrades ClO_2)

7. Placed flask into a dark fume hood during the delignification process

8. Once ClO_2 evolution discontinued, replaced the exhausted buffer with fresh chlorite (200 ml of buffered chlorite, 13 ml of glacial acetic acid)

9. Over the course of 3 weeks, this buffer replacement was conducted 5 times in total.
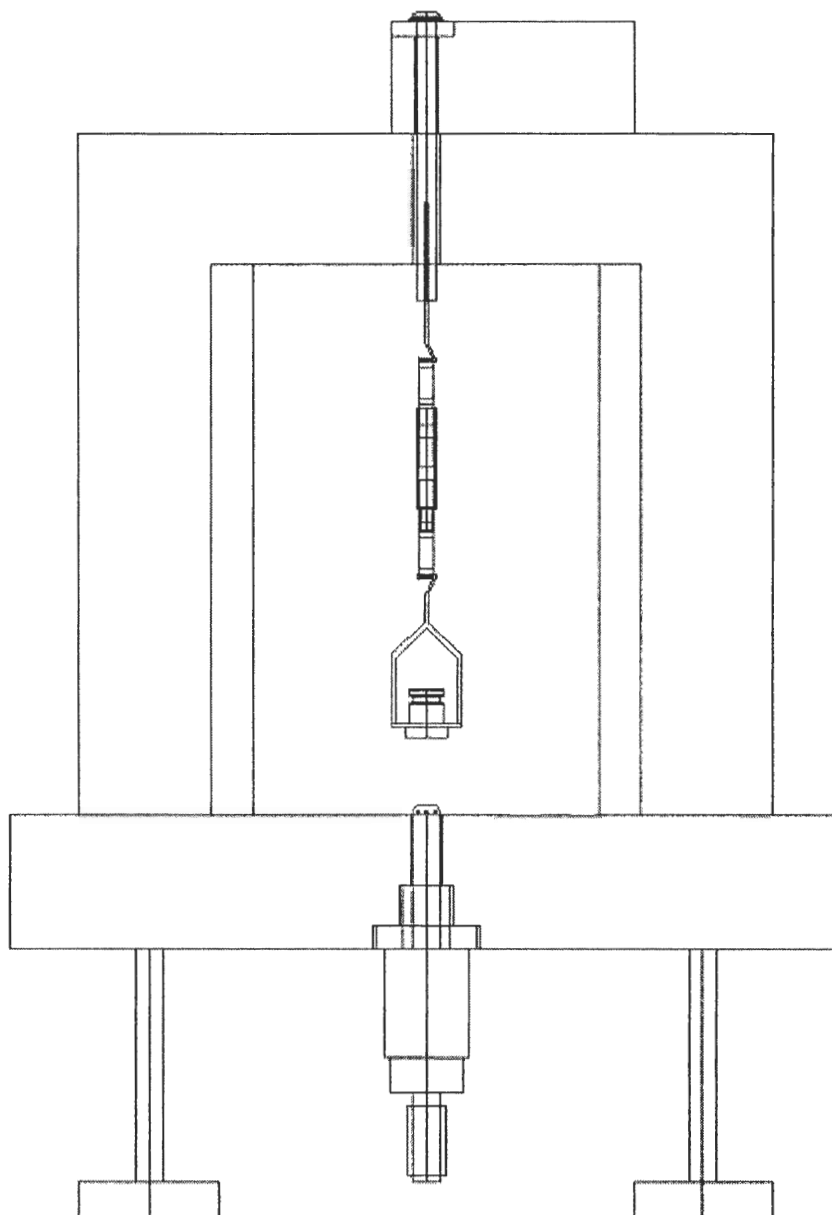
Front View

Side View

258
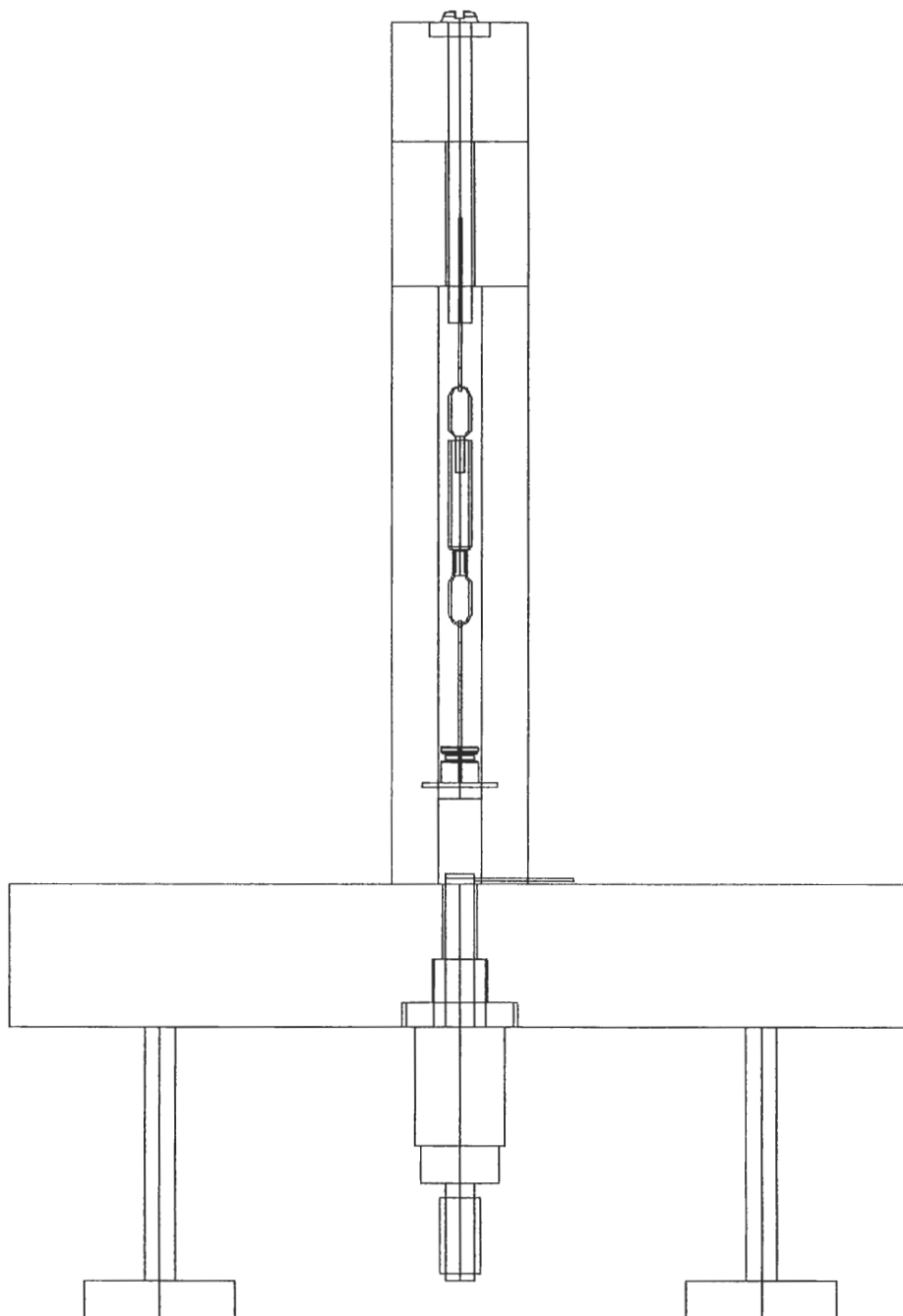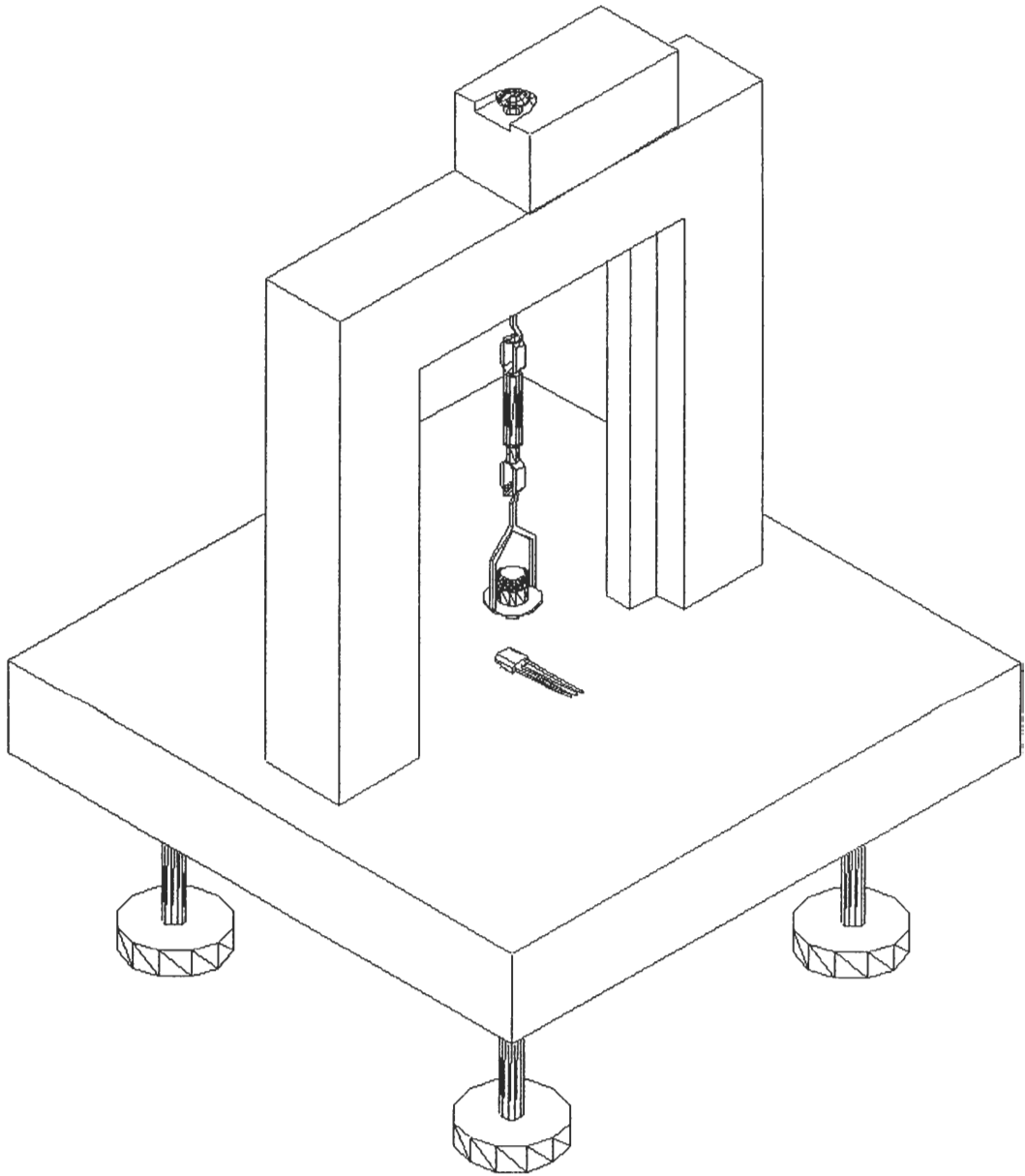
Isometric View

Appendix D - Hestrin-Schramm Media

Liquid Culture Media

1 liter of liquid culture media (2% w/v glucose, 0.5% w/v peptone, 0.5% w/v yeast extract, 0.27% anhydrous disodium phosphate, 0.15% w/v citric acid monohydrate, pH 5.0)

To a one liter Erlenmeyer flask added:

-20 g glucose

-5 g bactopeptone

-5 g yeast extract

-2.7 g disodium phosphate

-1.5 g citric acid monohydrate

1. Brought to 1 liter with dH_2O

2. Adjusted pH to 5.0 using 1 N acetic acid

3. Sterilized solution by autoclaving

4. Stored liquid culture media in refrigerator until use

5. Used liquid culture media to amplify NQ-5 from original plate (make (3) 100 ml liquid cultures)

Solid Culture Media

1. Prepared 500 ml of the liquid culture media.

2. Before adding dH_2O, added 7.5 g of bacto agar.

3. Autoclaved media for 15 minutes @ 15 lb/ in^2 pressure.

4. Allowed media to cool slightly.

5. Poured into 100 mm x 15 mm petri dishes (~ 40 ml per dish)

6. Sealed with Parafilm and stored in refrigerator until ready for use

*After streaking with liquid cultures, plates were incubated at 30ºC

Liquid Culture Media with Tamarind Xyloglucan

1. Prepared liquid culture media as described above (1/5th the quantities) without adding dH_2O.

2. Added 1.0 g of tamarind xyloglucan.

3. Added dH_2O until 200 ml.

4. Sterilized solution by autoclaving.

REFERENCES

1 Fernandez, E.O. and Hodgson, K.T., "Colloidal stability of flexographic newsprint deinking dispersions" *Pulp & Paper Canada*, vol. 99, no. 11, pp. T382-385, 1998.

2 Bennington, C.P.J, "Mills can expect even more variability in recovered paper quality" *Pulp & Paper Canada*, vol. 100, no. 12, pp. 23-28, 1999.

3 Anthony, F., "Newspapers: Advertising, economics will determine growth in 2002" *Flexo*, vol. 26, no. 12, pp. 61-63, 2001.

4 Galland, G., Vernac, Y. and Carré, B., "The advantages of combining neutral and alkaline deinking: Part I: Comparison of deinking of offset and flexo printed paper" *Pulp & Paper Canada*, vol. 98, no. 6, pp. T182-185, 1997.

5 Galland, G., Vernac, Y. and Carré, B., "The advantages of combining neutral and alkaline deinking: Part II: Comparison of various processes for deinking mixtures containing water-based printed paper in the CTP pilot plant" *Pulp & Paper Canada*, vol. 98, no. 7, pp. T254-257, 1997.

6 Sain, M.M., Marchildon, L., Lapointe, M. and Daneault, C., "A novel chemistry to ink separation from mixed paper waste contaminated with flexo ink" *Nordic Pulp Paper Res. J.*, vol. 3, pp. 157-163, 1996.

7 Philippe, I.J., "Effective flotation deinking of ONP with increasing levels of flexographic print" TAPPI Pulping Conference, Nashville, Oct. 27-31, vol. 2, pp. 805-810, 1996.

8 Cody, C.A. and Magauran, E.D., "Process for deinking wastepaper with organically modified smectite clay" U.S. pat. 5,151,155 (1992).

9 Cody, C.A. and Magauran, E.D., "Process for deinking wastepaper utilizing organoclays formed *in situ*" U.S. pat. 5,336,372 (1994).

10 Heise, O.U., Schriver, K.E. and Horng, A.J., "A novel flotation deinking chemistry to remove flexo inks: 30 tons/day pilot-plant results" *Tappi J.*, vol. 82, no. 3, pp. 131-136, 1999.

11 Alesse, V., Belardi, G., Cozza, C., Shehu, N. and Koch, V., "Deinking recycled paper with a high flexographic ink content" *Tappi J.*, vol. 84, no. 8, pp. 44, 2001.

12 Deng, Y. and Zhu, J.Y., "Froth flotation deinking process for paper recycling" U.S. pat. 5,876,558 (1999).

13 Deng, Y., "Effect of fiber surface chemistry on the fiber loss in flotation deinking" *Tappi J.*, vol. 83, no.6, pp. 1-8, 2000.

14 Ajersch, M. and Pelton, R., "Mechanisms of pulp loss in flotation deinking" *J. Pulp Paper Sci.*, vol. 22, no. 9, pp. J338-345, 1996.

15 Roth, J., "Web offset outlook 2001" *American Printer*, December 2001.

16 Sain, M.M., Daneault, C. & Marchildon, L., "A study on the ink-fiber interfacial interaction in waste printed paper I. The effect of a custom-designed polymeric additive on flotation de-Inking of solvent-treated wastepapers" *Cellulose*, vol. 1, pp. 221-235, 1994.

17 Wickman, M., Beadle, A., Sebring, T., Gurrera I Magrané, L. and Larsson, A., "The effect of alkyd resin composition on the adsorption on calcium carbonate" *Nordic Pulp Paper Res. J.*, vol. 2, pp. 94-100, 1994.

18 Wickman, M., Hallstensson, K. and Ström, G., "Adsorption behaviour of alkyd resins on surfaces present in offset printing inks", 4th Paper in Doctoral Thesis series, Institute for Surface Chemistry, Dept. of Pulp and Paper Technology and Chemistry, Stockholm, Sweden.

19 Zang, Y., "A new approach for modeling ink transfer" *Tappi J.*, vol. 76, no. 7, pp. 97-103, 1993.

20 Rosinski, J., "Aging and deinking of soy printed newsprint" *Progress in Paper Recycling*, pp. 55-62, May 1995.

21 Johansson, B., Wickman, M. and Ström, G., "The mechanism of offset ink particles agglomeration in a calcium-fatty acid collector system", *J. of Pulp and Paper Science*, vol. 22, no. 10, pp. J381-J385, October 1996.

22 Borchardt, J.K., "Ink types: The role of ink in deinking", *Paper Recycling Challenge-Deinking and Bleaching*, pp.13-17, Appleton, WI : Doshi & Associates, Inc., , c1997.

23 Bennington, C.P.J., Sui, O.S. and Smith, J.D., "The effect of mechanical action on waste paper defibering and ink removal in repulping operations", *4th Research Forum on Recycling*, CPPA, Quebec, PQ, Canada, pp. 1-9, Oct. 7-9, 1997.

24 Pirttinen, E. and Stenius, P., "The effects of chemical conditions on newsprint ink detachment and fragmentation", *Tappi J.*, Peer Reviewed Paper, pp. 1-14, November 2000.

25 Somasundaran, P., Zhang, L., Krishnakumar, S. and Slepetys, R., "Flotation deinking – A review of the principles and techniques", *Progress in Paper Recycling*, pp. 24-36, May 1999.

26 Krauthauf, E., "Deinking in a large deinking pulp mill", *Tappi 99 Proceedings*, pp. 519-529, 1999.

27 Rao, R.N. and Stenius, P., "Mechanisms of ink release from model surfaces and fibre", *J. of Pulp and Paper Science*, vol. 24, no. 6, pp. 183-187, June 1998.

28 Moe, S. and Røring, A., "Theory and practice of flotation deinking", *6th Research Forum on Recycling*, pp. 55-60, 2001.

29 Carré, B., Magnin, L., Galland, G. and Vernac, Y., "Deinking difficulties related to ink formulation, printing process, and type of paper", *Tappi J.*, vol. 83, no. 6, pp. 60-88, 2000.

30 Sain, M.M., Daneault, C. and Marchildon, L., "A study on the ink-fiber interfacial interaction in waste printed paper I. The effect of a custom-designed polymeric additive on flotation de-inking of solvent-treated wastepapers", *Cellulose*, vol. 1, pp. 221-235, 1994.

31 Røring, A. and Santos, A., "Pulper chemistry is a key to successful deinking", *4th Research Forum on Recycling*, CPPA, Quebec, PQ, Canada, pp. 249-255, Oct. 7-9, 1997.

32 Haynes, R.D., "The impact of the summer effect on ink detachment and removal", *Tappi J.*, vol. 83, no. 3, pp. 56-65, March 2000.

33 Beneventi, D. and Carré, B., "The mechanisms of Flotation Deinking and the Role of Fillers", *Progress in Paper Recycling*, pp. 77-85, February 2000.

34 Read, B.R., "The chemistry of flotation deinking", *Tappi Proc. Pulping Conf.*, pp. 851-856, 1991.

35 Ferguson, L.D., "Deinking chemistry: part 2", *Tappi J.*, pp. 49-58, August 1992.

36 Larsson, A., Stenius, P. and Ödberg, L., *Svensk Papperstidning*, no. 18, pp. 158-164, 1984.

37 Putz, H.J., Schaffrath, H.J. and Göttsching, L., "Deinking of oil- and water-borne printing inks: a new flotation deinking model", *Preprints 1st Research Forum on Recycling,* Technical Section CPPA, Toronto, ON, Canada, pp. 183-190, 1991.

38 Hodgson, K.T., "Deinking considerations with flexographic wastepaper", *Progress in Paper Recycling*, pp. 71-74, May 1996.

39 Upton, B.H. and Krishnagopalan, G.A., "Characterization of ultrafiltration for flexographic newsprint deinking", *Pulping, Papermaking and Chemical Preparation, AIChE Symposium Series*, vol. 92, no. 311, pp. 152-159, 1996.

40 Upton, B.H., Krishnagopalan, G.A. and Abubakr, S., "Deinking flexographic newsprint: Using ultrafiltration to close the water loop", *Tappi J.*, vol. 80, no. 2, pp. 155-164, February 1997.

41 Chabot, B., Krishnagopalan, G.A. and Abubakr, S., "Effect of ultrafiltration permeate recycling on deinking efficiency of flexo-printed newspapers", *Progress in Paper Recycling*, pp. 28-38, August 1998.

42 Ackermann, C., Putz, H.-J. and Göttsching, L., "Deinkability of waterborne flexo inks by flotation", *Pulp & Paper Canada*, vol. 95, no. 8, pp. T307-T312, 1994.

43 Chabot, B., Daneault, C. and Dorris, G.M., "Entrapment of water-based inks in fibre mats", *J. of Pulp and Paper Science*, vol. 21, no. 9, pp. J296-J301, September 1995.

44 McLennan, I.J. and Pelton, R., "Some factors affecting flexo ink calcium soap particle morphology in flotation deinking", *Preprints, 3rd Research Forum on Recycling*, CPPA, Vancouver, pp.77-90, 1995.

45 Dorris, G.M. and Nguyen, N., "Flotation of model inks. Part II. Flexo ink dispersions without fibers", *J. of Pulp and Paper Science*, vol. 21, no. 2, pp. J55-J62, February 1995.

46 Chabot, B., Daneault, C., Sain, M.M. and Dorris, G.M., "The adverse role of fibres during the flotation of flexographic inks", *Pulp & Paper Canada*, vol. 98, no. 12, pp. 115-121, 1997.

47 Vernac, Y., Carre, B., Rousset, X., Guillet, F. and Galland, G., "Process solutions to handle small amounts of flexo in wood containing raw material", *TAPPI Fall Technical Conference and Trade Fair*, San Diego, CA, United States, September 8-11, 2002.

48 Popson, S. J. and Malthouse, D. D., "Measurement and control of the optical properties of paper. Technidyne Corp., New Albany, IN, (©1991)

49 TAPPI Standard T 525, "Diffuse brightness of pulp (d/0°)"

50 TAPPI Standard T 452, "Brightness of pulp, paper, and paperboard (directional reflectance at 457 nm)"

51 Griesser, R., "Whiteness not brightness: A new way of measuring and controlling production of paper", *Appita*, vol. 46, no. 6, pp. 439-444, November 1993.

52 Bristow, J. A., "Brightness and whiteness- Definition and measurement". IARIGAI, 20th International Research Conference, Moscow, pp. 1-29, 1989.

53 Robertson, N., Patton, M. and Pelton, R., "Washing the fibers from foams for higher yields in flotation deinking", *Tappi J.*, vol. 81, no. 6, pp. 138-142, 1998.

54 Zhu, J.Y., Wu, G.H. and Deng, Y., "Flotation deinking of toner-printed papers using frother spray", *J. of Pulp and Paper Science*, vol. 24, no. 9, pp. 295-299, September 1998.

55 "News International may upset recovered paper market with switch to flexo printing", paperloop.com, November 20, 2002.

56 Jordan, B.D. and Popson, S.J., "Measuring the concentration of residual ink in recycled newsprint", *J. of Pulp and Paper Science*, vol. 20, no. 6, pp. J161-J167, June 1994.

57 Ben, X. and Dorris, G.M., "Handsheet and pulp pad preparation procedures for measurement of total and bound ink in ONP/OMG furnishes", *Progress in Paper Recycling*, pp. 34-41, February 1999.

58 Marinova, K.G., Alargova, R.G., Denkov, N.D., Velev, O.D., Petsev, D.N., Ivanov, I.B. and Borwankar, R.P., "Charging of oil-water interfaces due to spontaneous adsorption of hydroxyl ions", *Langmuir*, vol. 12, pp. 2045-2051, 1996.

59 Harkins, W.D., The Physical Chemistry of Surface Films, New York, NY: Reinhold, 1952.

60 Shaw, D.J., Colloid & Surface Chemistry, 4th Ed., Woburn, MA: Butterworth-Heinemann, pg. 77, 2000.

61 Binks, B.P. and Dong, J., "Emulsions and equilibrium phase behaviour in silicone oil + water + nonionic surfactant mixtures", *Colloids and Surfaces, A. Physicochemical and Engineering Aspects*, vol. 132, pp. 289-301, 1998.

62 Obey, T.M. and Vincent, B., "Novel monodisperse "silicone oil"/water emulsions", *J. Colloid Interface Sci.*, vol. 163, pp. 454-463, 1994.

63 Binks, B.P. and Clint, J.H., "Solid wettability from surface energy components: relevance to Pickering emulsions", *Langmuir*, vol. 18, pp. 1270-1273, 2002.

64 Fowkes, F.M., "Dispersion force contributions to surface and interfacial tensions, contact angles, and heats of immersion", *A.C.S. Advances in Chemistry Series*, vol. 43, pp. 99-111, 1964.

65 Moore, W.C., "Emulsification of water and of ammonium chloride solutions by means of lamp black", *J. Am. Chem. Soc.*, vol. 41, pp. 940-946, 1919.

66 Leodidis, E.B., Bommarius, A.S. and Hatton, T.A., "Amino acids in reverse micelles. 3. Dependence of the interfacial partition coefficient on excess phase salinity and interfacial curvature", *J. Phys. Chem.*, vol. 95, pp. 5943-5956, 1991.

67 Binks, B.P., "Relationship between microemulsion phase behavior and macroemulsion type in systems containing nonionic surfactant", *Langmuir*, vol. 9, pp. 25-28, 1993.

68 Williams, D.F. and Berg, J.C., "The aggregation of colloidal particles at the air-water interface", *J. Colloid Interface Sci.*, vol. 152, no. 1, pp. 218-229, 1992.

69 Aveyard, R., Clint, J.H., Nees, D., and Paunov, V.N., "Compression and structure of monolayers of charged latex particles at air/water and octane/water interfaces", *Langmuir*, vol. 16, pp. 1969-1979, 2000.

70 Pickering, S.U., "Emulsions", *J. Chem. Soc.*, vol. 91, pp. 2001-2021, 1907.

71 Binks, B.P. and Lumsdon, S.O., "Effects of oil type and aqueous phase composition on oil-water mixtures containing particles of intermediate hydrophobicity", *Phys. Chem. Chem. Phys.*, vol. 2, pp. 2959-2967, 2000.

72 Binks, B.P. and Lumsdon, S.O., "Transitional Phase Inversion of solid-stabilized emulsions using particle mixtures", *Langmuir*, vol. 16, pp. 3748-3756, 2000.

73 Binks, B.P. and Lumsdon, S.O., "Influence of particle wettability on the type and stability of surfactant-free emulsions", *Langmuir*, vol. 16, pp. 8622-8631, 2000.

74 Binks, B.P. and Lumsdon, S.O., "Pickering emulsions stabilized by monodisperse latex particles: effects of particle size", *Langmuir*, vol. 17, pp. 4540-4547, 2001.

75 Kabalnov, A. and Wennerström, H., "Macroemulsion stability: The oriented wedge theory revisited", *Langmuir*, vol. 12, pp. 276-292, 1996.

76 Velev, O.D., Furusawa, K. and Nagayama, K., "Assembly of latex particles by using emulsion droplets as templates. 1. Microstructured hollow spheres", *Langmuir*, vol. 12, pp. 2374-2384, 1996.

77 Caruso, F., Caruso, A.R., and Möhwald, H., "Nanoengineering of inorganic and hybrid hollow spheres by colloidal templating", *Science*, vol. 282, pp. 1111-1114, 1998.

78 Möhwald, H., "From langmuir monolayers to nanocapsules", *Colloids and Surfaces, A. Physicochemical and Engineering Aspects*, vol. 171, pp. 33-45, 2000.

79 Binks, B.P. and Lumsdon, S.O., "Catastrophic phase inversion of water-in-oil emulsions stabilized by hydrophobic silica", *Langmuir*, vol. 16, pp. 2539-2547, 2000.

80 Ashby, N.P. and Binks, B.P., "Pickering emulsions stabilized by Laponite clay particles", *Phys. Chem. Chem. Phys.*, vol. 2, pp. 5640-5646, 2000.

81 Gelot, A., Friesen, W., and Hamza, H.A., *Colloids Surf.*, vol. 12, pp. 271, 1984.

82 Tambe, D.E. and Sharma, M.M., "Factors controlling the stability of colloid-stabilized emulsions", *J. Colloid Interface Sci.*, vol. 157, pp. 244-253, 1993.

83 Binks, B.P. and Lumsdon, S.O., "Pickering emulsions stabilized by monodisperse latex particles: effects of particle size", *Langmuir*, vol. 17, pp. 4540-4547, 2001.

84 Nikolaides, M.G., "Colloids at liquid-liquid interfaces, Diploma Thesis, TU München, 2001.

85 Lin, Y., Skaff, H., Emrick, T., Dinsmore, A.D. and Russell, T.P., "Nanoparticle assembly and transport at liquid-liquid interfaces", *Science*, vol. 299, pp. 226-229, 2003.

86 Pieranski, P., "Two-dimensional interfacial colloidal crystals", *Physical Review Letters*, vol. 45, pp. 569-572, 1980.

87 McQueen-Mason, S., Durachko, D.M. and Cosgrove, D.J., "Two endogenous proteins that induce cell wall extension in plants," *Plant Cell*, vol. 4, pp. 1425-1433, November 1992.

88 Weise, U. and Paulapuro, H., "Changes of fibre dimensions during drying," International Paper Physics Conference, Niagara-on-the-Lake, Ontario, Canada, pp. 121-124, 1995.

89 Nazhad, M.M. and Paszner, L., "Fundamentals of strength loss in recycled paper" *Tappi J.*, vol. 77, no. 9, pp. 171-179, September 1994.

90 Oye, R., Okayama, T., Yamazaki, Y. and Yoshinaga, N., "Changes of pulp fibre cell wall by recycling." Forum Recherche sur le Recyclage, Toronto, Ontario, Canada, pp. 191-195, 1991.

91 Dykstra, G.M. and Stoner, M.T., "Enzymes & biodispersants in papermaking." Biological Sciences Symposium, San Francisco, California USA, pp. 117-124, 1997.

92   Jeffries, T. "Enzyme technologies for pulp bleaching and deinking." http://www.biotech.wisc.edu/jeffries/enztech/enztech.html.

93 Jeffries, T., Klungness, J.H., Sykes, M.S. and Rutledge, K., "Preliminary results of enzyme-enhanced versus conventional deinking of xerographic printed paper." Recycling Symposium, New Orleans, Louisiana USA, pp. 183-188, 1993.

94 Sreenath, H.K., Yang, V.W., Burdsall, H.H. and Jeffries, T, "Toner removal by alkaline-active cellulases from desert basidiomycetes." Recycled Fiber and Deinking. Fapet Oy, Helsinki, Finland, pp. 267-279, 2000.

95 Jeffries, T.W., "Enzymatic treatments of pulps: Opportunities for the enzyme industry in pulp and paper manufacture."
http://www2.biotech.wisc.edu/jeffries/wolnak/wolnak.html

96 Gehlhoff, W.S., "The benefits of using enzymes to improve flotation deinking of office paper furnishes." Recycling Symposium, New Orleans, Louisiana USA, pp. 277-289, 1997.

97 Rutledge-Cropsey, K., Klungness, J.H. and Abubakr, S.M., "Performance of enzymatically deinked recovered paper on paper machine runnability." *Tappi J.*, vol. 81, no. 2, pp. 148-151, February 1998.

98 Magnin, L., Lantto, R. and Delpech, P., "Use of enzymes for deinking of wood-free and wood-containing recovered papers." *Progress in Paper Recycling*, pp. 13-20, August 2002.

99 Sarkar, J.M., "Recycle paper mill trial using enzyme and polymer for upgrading recycled fibre." *Appita J.*, vol. 50, no. 1, pp. 57-60, 1996.

100 Moerkbak, A.L. and Zimmermann, W., "Applications of enzymes in paper deinking processes." Recycled Fiber and Deinking. Fapet Oy, Helsinki, Finland, pp. 133-141, 2000.

101 Jobbins, J.M. and Franks, N.E., "Enzymatic deinking of mixed office waste: Process condition optimization." *Tappi J.*, vol. 80, no. 9, pp. 73-78, September 1997.

102 Wong, K.Y. and Mansfield, S.D., "Enzymatic processing for pulp and paper manufacture – A review", *Appita J.*, vol. 52, no. 6, pp. 409-418, 1999.

103 Bajpai, P. and Bajpai, P., "Deinking with enzymes: A review." *Tappi J.*, vol. 81, no. 12, pp. 111-117, December 1998.

104 Fenwick, K.M., Jarvis, M.C. and Apperly, D.C., "Estimation of polymer rigidity in cell walls of growing and nongrowing celery collenchyma by solid-state nuclear magnetic resonance *in vivo*" *Plant Physiol.*, vol. 115, pp. 587-592, 1997.

105 Ha, M., Apperly, D.C. and Jarvis, M.C., "Molecular rigidity in dry and hydrated onion cell walls" *Plant Physiol.*, no. 115, pp. 593-598, 1997.

106 Cosgrove, D.J., "Enzymes and other agents that enhance cell wall extensibility" *Annu. Rev. Plant Physiol. Plant Mol. Biol.*, vol. 50, pp. 391-417, 1999.

107 Cosgrove, D.J., "Expansive growth of plant cell walls" *Plant Physiol. Biochem.*, vol. 38(1/2), pp. 109-124, 2000.

108 Whitney, S.E.C., Gidley, M.J. and McQueen-Mason, S.J., "Probing expansin action using cellulose/ hemicellulose composites" *Plant J.*, vol. 22, no. 4, pp. 327-334, 2000.

109 Cosgrove, D.J., "Cell wall loosening by expansins" *Plant Physiology*, vol. 118, pp. 333-339, 1998.

110 Hutchinson, K.W., Singer, P.B., McInnis, S., Diaz-Sala, C. and Greenwood, M.S., "Expansins are conserved in conifers and expressed in hypocotyls in response to exogenous auxin" *Plant Physiology*, vol. 120, pp. 827-831, July 1999.

111 Link, B.M. and Cosgrove, D.J., "Acid-growth response and α-expansin in suspension cultures of bright yellow 2 tobacco" *Plant Physiology*, vol. 118, pp. 907-916, 1998.

112 Cosgrove, D.J., "Creeping walls, softening fruit, and penetrating pollen tubes: The growing roles of expansins." *Proc. Natl. Acad. Sci.*, USA vol. 94, pp. 5504-5505, May 1997.

113 Thompson, N.S. and Kaustinen, O.A., "Some chemical and physical properties of pulps prepared by mild oxidative action", *Tappi J.*, vol. 47, no. 3, pp. 157-161, March 1964.

114 Wise, Murphey, and D'Appieco: *Tappi J.*, vol. 122, no. 2, pp. 35-43, January 1946.

115 Rose, J.K.C., Cosgrove, D.J., Albersheim, P. Darvill, A.G. and Bennett, "Detection of expansin proteins and activity during tomato fruit ontogeny" *Plant Physiology*, vol. 123, pp. 1583-1592, August 2000.

116 Li, Z., Durachko, D.M. and Cosgrove, D.J., "An oat coleoptile wall protein that induces wall extension *in vitro* and that is antigenically related to a similar protein from cucumber hypocotyls" *Planta*, vol. 191, pp. 349-356, 1993.

117 Wu, Y., Sharp, R.E., Durachko, D.M. and Cosgrove, D.J., "Growth maintenance of the maize primary root at low water potentials involves increases in cell-wall extension properties, expansin activity, and wall susceptibility to expansins" *Plant Physiology*, vol. 111, pp. 765-772, 1996.

118 Hestrin, S. and Schramm, M., "Synthesis of cellulose by *Acetobacter xylinum*: 2. Preparation of freeze-dried cells capable of polymerizing glucose to cellulose" *Biochem. J.*, vol. 58, pp. 345-352, 1954.